ISSN 2686-7575 (Online)

МИТХТ

ТОНКИЕ ХИМИЧЕСКИЕ ТЕХНОЛОГИИ

Fine Chemical Technologies

- Theoretical Bases of Chemical Technology
- Chemistry and Technology of Organic Substances
- Chemistry and Technology of Medicinal Compounds and Biologically Active Substances
- Synthesis and Processing of Polymers and Polymeric Compounds
- Chemistry and Technology of Inorganic Materials
- Analytical Methods in Chemistry and Chemical Technology
- Mathematical Methods and Information Systems in Chemical Technology

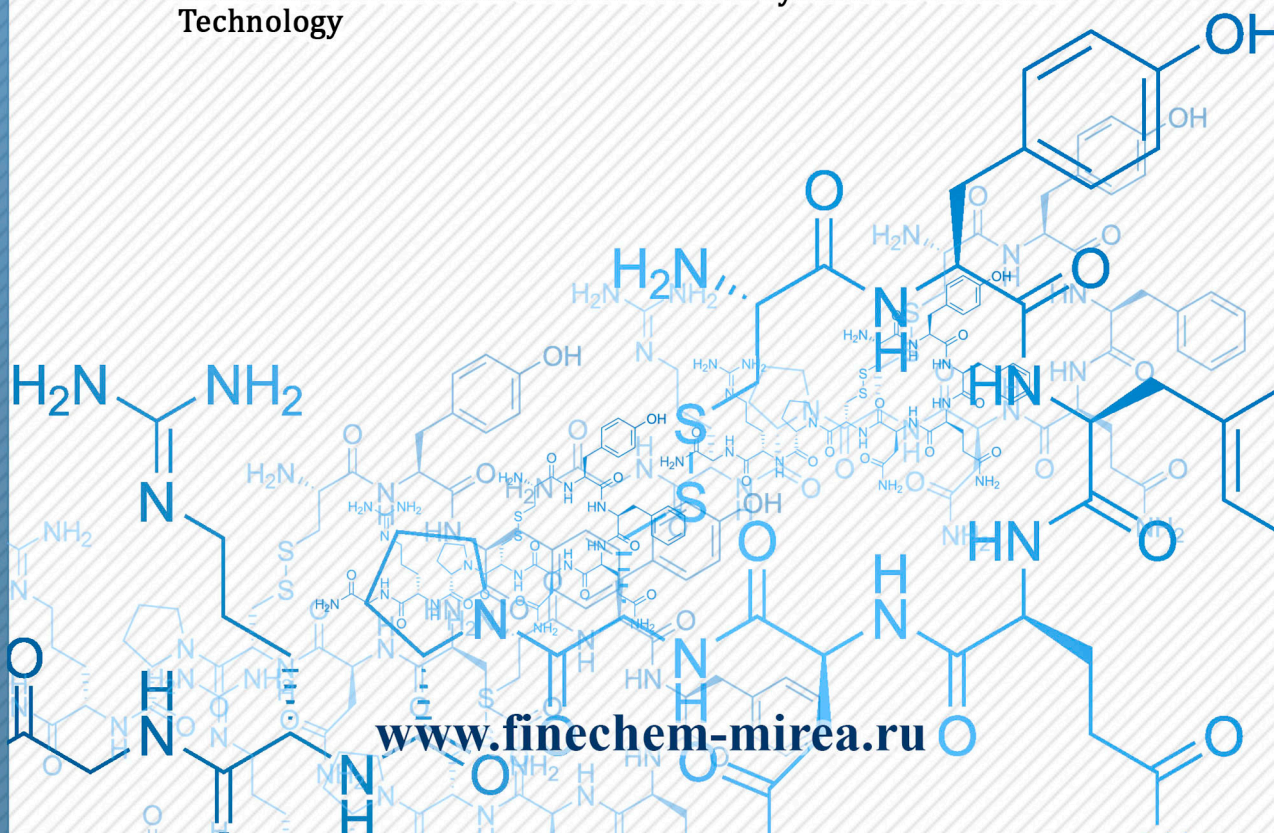

16(4)
2021

www.finechem-mirea.ru

ISSN 2686-7575 (Online)

ТОНКИЕ ХИМИЧЕСКИЕ ТЕХНОЛОГИИ

Fine Chemical Technologies

- Theoretical Bases of Chemical Technology
- Chemistry and Technology of Organic Substances
- Chemistry and Technology of Medicinal Compounds and Biologically Active Substances
- Synthesis and Processing of Polymers and Polymeric Composites
- Chemistry and Technology of Inorganic Materials
- Analytical Methods in Chemistry and Chemical Technology
- Mathematical Methods and Information Systems in Chemical Technology

Tonkie Khimicheskie Tekhnologii = Fine Chemical Technologies
Vol. 16, No. 4, 2021

Тонкие химические технологии = Fine Chemical Technologies
Том 16, № 4, 2021

https://doi.org/10.32362/2410-6593-2021-16-4
www.finechem-mirea.ru

https://doi.org/10.32362/2410-6593 ***www.finechem-mirea.ru***

Tonkie Khimicheskie Tekhnologii =
Fine Chemical Technologies
2021, Vol. 16, No. 4

The peer-reviewed scientific and technical journal Fine Chemical Technologies highlights the modern achievements of fundamental and applied research in the field of fine chemical technologies, including theoretical bases of chemical technology, chemistry and technology of medicinal compounds and biologically active substances, organic substances and inorganic materials, synthesis and processing of polymers and polymeric composites, analytical and mathematical methods and information systems in chemistry and chemical technology.

Founder and Publisher

Federal State Budget
Educational Institution
of Higher Education
"MIREA – Russian Technological University"
78, Vernadskogo pr., Moscow, 119454, Russian Federation.

Publication frequency: bimonthly.
The journal was founded in 2006. The name was Vestnik MITHT until 2015 (ISSN 1819-1487).

The journal is included into the List of peer-reviewed science press of the State Commission for Academic Degrees and Titles of the Russian Federation.
The journal is indexed:
DOAJ, Chemical Abstracts, Science Index, RSCI, Ulrich's International Periodicals Directory

86, Vernadskogo pr., Moscow, 119571, Russian Federation.
Phone: +7(495) 246-05-55 (#2-88)
E-mail: *seredina@mirea.ru*

Registration Certificate ПИ № ФС 77–74580, issued on December 14, 2018 by the Federal Service for Supervision of Communications, Information Technology, and Mass Media of Russia

The subscription index of *Pressa Rossii*: **36924**

Тонкие химические технологии =
Fine Chemical Technologies
2021, том 16, № 4

Научно-технический рецензируемый журнал «Тонкие химические технологии» освещает современные достижения фундаментальных и прикладных исследований в области тонких химических технологий, включая теоретические основы химической технологии, химию и технологию лекарственных препаратов и биологически активных соединений, органических веществ и неорганических материалов, синтез и переработку полимеров и композитов на их основе, аналитические и математические методы и информационные системы в химии и химической технологии.

Учредитель и издатель

федеральное государственное бюджетное
образовательное учреждение
высшего образования
«МИРЭА – Российский технологический университет»
119454, РФ, Москва, пр-кт Вернадского, д. 78.

Периодичность: один раз в два месяца.
Журнал основан в 2006 году. До 2015 года издавался под названием «Вестник МИТХТ» (ISSN 1819-1487).

Журнал входит в Перечень ведущих рецензируемых научных журналов ВАК РФ.
Индексируется:
DOAJ, Chemical Abstracts, РИНЦ (Science Index), RSCI, Ulrich's International Periodicals Directory

119571, Москва, пр. Вернадского, 86, оф. Л-119.
Тел.: +7(495) 246-05-55 (#2-88)
E-mail: *seredina@mirea.ru*

Свидетельство о регистрации СМИ: ПИ № ФС 77-74580 от 14.12.2018 г. выдано Федеральной службой по надзору в сфере связи, информационных технологий и массовых коммуникаций (Роскомнадзор)

Индекс по Объединенному каталогу «Пресса России»: **36924**

ТОНКИЕ ХИМИЧЕСКИЕ ТЕХНОЛОГИИ
Fine Chemical Technologies
16(4)
2021

CONTENTS

СОДЕРЖАНИЕ

THEORETICAL BASES OF CHEMICAL TECHNOLOGY

ТЕОРЕТИЧЕСКИЕ ОСНОВЫ ХИМИЧЕСКОЙ ТЕХНОЛОГИИ

ISSN 2686-7575 (Online)

https://doi.org/10.32362/2410-6593-2021-16-4-273-286

UDC 544.31:[665.753.2+546.26]

RESEARCH ARTICLE

Energy intensity of hydrocarbons in liquid and solid states

Gennady J. Kabo, Lubov A. Kabo, Larisa S. Karpushenkava[@], Andrey V. Blokhin

Belarusian State University, Minsk, 220030 Belarus
[@]Corresponding author, e-mail: karpushenkava@bsu.by

Abstract

Objectives. *The increased use of unmanned aerial vehicles necessitates the search for jet fuels based on hydrocarbon materials with high energy intensity and physical density. The purpose of the work was to analyze the influence of various factors on the mass energy intensity of hydrocarbons. This analysis is required to substantiate the algorithm for locating energy-intensive C_nH_m structures.*

Methods. *Combustion energy was calculated using additive procedures. The calculations were performed using Microsoft Excel.*

Results. *During the analysis of the mass energy intensity of C_nH_m hydrocarbons, the m/n ratio was discovered to be the decisive factor for achieving high values of the mass energy intensity of hydrocarbons. The energy intensity decreases when moving from alicyclic to cyclic hydrocarbons, and this decrease is not compensated by the production of strain energy. An additive scheme that allows the molar volume of hydrocarbons to be predicted with sufficient accuracy is proposed for calculating the volumetric enthalpies of combustion.*

Conclusions. *According to the thermodynamic analysis, n-alkanes have the highest mass energy intensities. The technology for extracting n-alkanes from oil fractions is well developed, and a decrease in the hydrogen content in the fuel results in a decrease in the mass energy intensity. It appears improbable that the mass and volumetric energy intensities of hydrocarbons seem will reach their maximum values simultaneously. Hydrocarbons that have a high m/n value, 2, 3, 4, 5, 6-membered rings, and phenyl fragments may have relatively high mass and volumetric energy intensities at the same time.*

Keywords: *hydrocarbon fuel, energy intensity, polycyclic hydrocarbons, mass enthalpy of combustion, volumetric enthalpy of combustion, additive calculations*

For citation: Kabo G.J., Kabo L.A., Karpushenkava L.S., Blokhin A.V. Energy intensity of hydrocarbons in liquid and solid states. *Tonk. Khim. Tekhnol. = Fine Chem. Technol.* 2021;16(4):273–286 (Russ., Eng.). https://doi.org/10.32362/2410-6593-2021-16-4-273-286

НАУЧНАЯ СТАТЬЯ

Энергоемкость углеводородов в жидком и твердом состояниях

Г.Я. Кабо, Л.А. Кабо, Л.С. Карпушенкова[@], А.В. Блохин

Белорусский государственный университет, Минск, 220030 Беларусь
[@]Автор для переписки, e-mail: karpushenkava@bsu.by

Аннотация

Цели. *Расширение сфер использования беспилотных летательных аппаратов требует поиска реактивных топлив с высокой энергоемкостью и физической плотностью на основе углеводородных материалов. Цель работы заключалась в проведении анализа влияния различных факторов на массовую энергоемкость углеводородов, необходимого для обоснования алгоритма поиска энергоемких структур C_nH_m.*

Методы. *Энергия сгорания рассчитывались с использованием аддитивных процедур. Расчеты проводились в программе MS Excel.*

Результаты. *В ходе проведенного анализа массовой энергоемкости углеводородов C_nH_m было установлено, что решающим фактором для достижения высоких значений массовой энергоемкости углеводородов является отношение m/n. При переходе от алициклических углеводородов к циклическим энергоемкость снижается, и данное снижение не компенсируется возникающей энергией напряжения. Предложена аддитивная схема, позволяющая с достаточной точностью предсказать молярный объем углеводородов для расчета объемных энтальпий сгорания.*

Заключение. *Термодинамический анализ показал, что максимальной массовой энергоемкостью обладают н-алканы, технология извлечения которых из нефтяных фракций хорошо отработана, уменьшение же содержания водорода в топливе приводит к снижению массовой энергоемкости. Одновременное достижение максимальных значений массовых и объемных энергоемкостей углеводородов представляется маловероятным. Возможно, одновременно более высокой массовой и объемной энергоемкостью будут обладать углеводороды с высоким значением m/n, содержащие 2, 3, 4, 5, 6-ти членные циклы и фенильные фрагменты.*

Ключевые слова: *углеводородное топливо, энергоемкость, полициклические углеводороды, массовая энтальпия сгорания, объемная энтальпия сгорания, аддитивные расчеты*

Для цитирования: Кабо Г.Я., Кабо Л.А., Карпушенкова Л.С., Блохин А.В. Энергоемкость углеводородов в жидком и твердом состояниях. *Тонкие химические технологии.* 2021;16(4):273–286. https://doi.org/10.32362/2410-6593-2021-16-4-273-286

C_nH_m hydrocarbons in condensed states (liquid and crystal) are effective fuels for jet engines because of their high energy intensity and a set of other physical and technical characteristics [1]. The mass and volumetric enthalpies of combustion of hydrocarbons (Δ_cH (C_nH_m) MJ·kg^{-1}, Δ_cH (C_nH_m) MJ·dm^{-3}) are the key parameters for assessing the prospects of using hydrocarbons as fuel for air-jet engines. Technically, rocket engines that use fuels based on T-1 and T-6 petroleum fractions and synthetic hydrocarbons containing three- and four-membered cycles in the molecular structure have been implemented [2, 3]. The energy of strained C_3 and C_4 cycles in hydrocarbon molecules is generally accepted [2] to be released in the form of additional energy upon their combustion.

There are established methods for predicting the physicochemical properties of hydrocarbons based on the classical theory of molecular structure [4, 5]. However, there are no clearly formulated rules or algorithms for finding energy-intensive compounds. Therefore, the search for energy-intensive substances is carried out intuitively, and some commercially produced hydrocarbons, such as syntin (1-methyl-1,2-dicyclopropylcyclopropane) and bicyclobutane [6], do

not have maximum energy intensities although their synthesis methods and technologies are complex and expensive [3].

This paper presents an analysis of the influence of various factors on the mass energy intensity of hydrocarbons, which is necessary for substantiating a possible search algorithm for energy-intensive C_nH_m structures.

INFLUENCE OF DIFFERENT FACTORS ON THE MASS ENERGY INTENSITY OF C_nH_m HYDROCARBONS

It can be assumed a priori that the following, not in order of their importance, are the main factors that determine the energy intensity of fuels:

1. The state of hydrocarbons (crystal (cr.) or liquid (liq.)).

2. The elemental composition of C_nH_m, that is, the m/n ratio, or the mass fraction of hydrogen in the hydrocarbon.

3. The structural features of the C_nH_m molecules: the presence of double bonds and cycles of various sizes.

To study the influence of these factors on the mass energy intensity of C_nH_m we used the values of $\Delta_c H^{\text{gross}}$ (298.15 K, liq., cr.) of the gross (higher, standard) enthalpy of combustion of 95 C_6H_m–$C_{12}H_m$ hydrocarbons of various compositions and structures from the National Institute of Standards and Technology database (NIST, USA)[1] and their enthalpies of melting from reference books [7, 8]. The net (lower) heats of combustion were calculated using the following equation:

$$\Delta_c H^{\text{net}}(298.15\,\text{K}, C_nH_m, \text{liq., cr.}) = \Delta_c H^{\text{gross}}(298.15\,\text{K}, C_nH_m, \text{liq., cr.}) + \frac{m}{2}\Delta_{\text{vap}} H^{\circ}(298.15\,\text{K}, H_2O), \quad (1)$$

where the enthalpy of vaporization of water[1] $\Delta_{\text{vap}}H^0(298.15\text{ K}, H_2O) = 44.0\text{ kJ·mol}^{-1}$.

To determine the fraction of melting enthalpy in the enthalpy of combustion, the difference between the enthalpies of combustion of various hydrocarbons in the crystalline and liquid states was analyzed. The enthalpies of melting of hydrocarbons are significantly irregular, varying by a factor of 2–5 even among related compounds. This is largely determined by the existence of solid-phase transitions, including those associated with the formation of plastic crystals, in which the reorientation of molecules at the sites of crystal lattices is not excluded [9–11]. There are no simple correlations between the melting enthalpies and the melting point (T_{fus}) values such as Trouton's rule: $\frac{\Delta_{\text{fus}}H^{\circ}(T_{\text{fus}})}{T_{\text{fus}}} \neq \text{const}$. Estimates of the ratios $\frac{\Delta_{\text{fus}}H^{\circ}(T_{\text{fus}})}{\Delta_c H^{\circ}(298.15\text{ K})}$ for C_nH_m suggest that this value is within 0.1–0.5% in most cases and is comparable with the values of possible deviations $\Delta_c H^{\text{gross}}(C_nH_m)$ in measurements for samples of the same type from different authors. Thus, the mass energy intensity of C_nH_m can be assumed to be practically independent of the condensed state of the hydrocarbon: liquid or solid. However, the density of hydrocarbons, the volumetric energy intensity of fuels, and many other properties that influence the design of jet engines as well as their tactical and technical characteristics are all influenced by the state of substances.

The influence of the composition of C_nH_m hydrocarbons on the mass energy intensity was investigated based on the classical theory of molecular structure [4, 5]. It is worth noting that the value of the standard enthalpy of combustion increases as the mass fraction of hydrogen in molecules increases (Fig. 1). According to the Tatevskii principles of

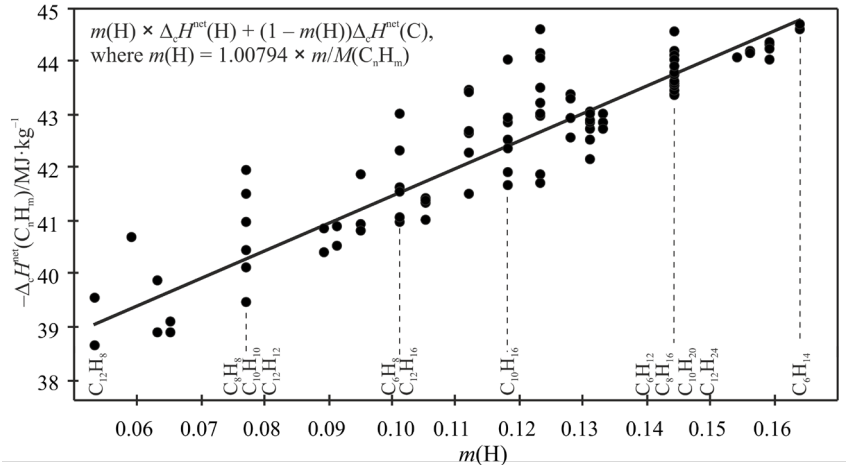

Fig. 1. Dependence of the mass enthalpy of combustion of hydrocarbons, $\Delta_c H^{\text{net}}(C_nH_m, 298.15\text{ K})$ MJ·kg^{-1}, on the mass fraction of hydrogen m(H) in the compound.

[1] NIST Chemistry Webbook. https://webbook.nist.gov/chemistry/. Accessed May 20, 2021.

classification of effective atoms [4, 5] the chemical individuality, i.e., the charge of nuclei determines the genus of atoms. Therefore, in a first approximation, the gross and net molar enthalpies of combustion of hydrocarbons can be represented as equation (2):

$$\Delta_c H^{\text{gross,net}}(C_nH_m, 298.15\ \text{K}, \text{kJ}\cdot\text{mol}^{-1}) = \\ = n\Delta_c H^{\text{gross,net}}(\text{C}) + m\Delta_c H^{\text{gross,net}}(\text{H}), \quad (2)$$

where n and m are the numbers of carbon and hydrogen atoms in the molecules, respectively; $\Delta_c H^{\text{gross,net}}(\text{C})$ and $\Delta_c H^{\text{gross,net}}(\text{H})$ are the fractions of the enthalpies of combustion attributed to the corresponding effective atoms. The numerical values of the additive contributions, $\Delta_c H^{\text{gross,net}}(\text{C})$ and $\Delta_c H^{\text{gross,net}}(\text{H})$ (kJ·mol^{-1}), were calculated using the least squares method from a system of 95 equations for $\Delta_c H°$ (C_nH_m, 298.15 K) borrowed from the NIST Chemistry Webbook of C_nH_m hydrocarbons (n = 6, 8, 10, and 12) with various m/n ratios, which suggests a variety of structural features of various classes of hydrocarbons, such as alkanes, alkenes, cycloalkanes, polycycloalkanes, and aromatic compounds. Although the choice of substances was rather arbitrary, substances with the smallest declared experimental error $\Delta_c H°$ (C_nH_m, 298.15 K) were shown preferences.

For mass enthalpies of combustion, the following equation is valid:

$$\Delta_c H^{\text{gross,net}}(C_nH_m, 298.15\text{K}) = m_C\Delta_c H^{\text{gross,net}}(\text{C})\ \text{MJ}\cdot\text{kg}^{-1} + \\ + m_H\Delta_c H^{\text{gross,net}}(\text{H})\ \text{MJ}\cdot\text{kg}^{-1}, \quad (3)$$

where m_C and m_H are the masses of the corresponding atoms in 1 kg (g) of the C_nH_m hydrocarbon, i.e., $m_C + m_H = 1$ kg (1 g).

The values of the additive contributions for the molar and mass enthalpies of combustion are presented in Table 1.

The deviation of the calculated $\Delta_c H^{\text{gross,net}}$ (C_nH_m) from the experimental values is $|\delta|_{\text{mean}} \approx 1.1\%$ on average. This difference exceeds $3 \times |\delta|_{\text{mean}}$ for 6 out of 95 hydrocarbons.

This indicates that predicting $\Delta_c H^{\text{gross,net}}$ (C_nH_m) based on the simplest qualification by the genus of effective atom is satisfactory. A comparison of the net mass enthalpies of combustion of well-characterized hydrocarbon fuels (Table 2) can provide additional confirmation of the efficiency of forecasting $\Delta_c H^{\text{gross,net}}$ (C_nH_m) based on equations (1) and (2).

Since the ratio of the atom contributions to the net mass enthalpy of combustion $\Delta_c H^{\text{net}}$ (C_nH_m, MJ·kg^{-1}) is $\Delta_c H^{\text{net}}(\text{H}) : \Delta_c H^{\text{net}}(\text{C}) = 87.977 : 36.275$, hydrocarbons with the highest values $\frac{m_H}{m_C}$ (with a larger mass fraction of hydrogen) should have the highest energy intensity (Fig. 1). This parameter varies from 0.335 for methane to 2.77×10^{-3} for fullerene hydride, $C_{60}H_2$.

All the noted regularities are practically independent of the state (liquid or crystal) of hydrocarbons, and no noticeable systematic deviation of C_nH_m in the solid state was observed in the calculations.

The influence of the molecular structure on the mass energy intensity of substances was determined according to the classical theory of molecular structure [4, 5]. According to the Tatevskii principles [4, 5], effective atoms in molecules are classified into species based on their valence states and nearest environment.

There are four species of effective carbon atoms in alkanes, depending on the first environment:

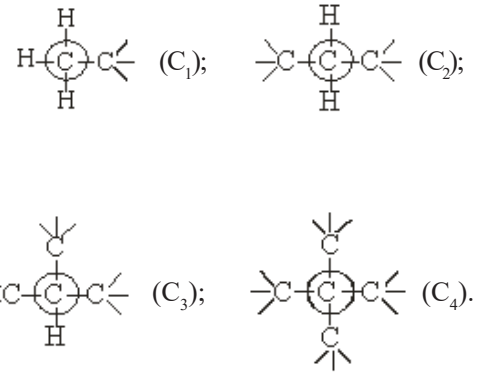

Table 1. Increments of the enthalpies of combustion of C and H atoms in C_nH_m hydrocarbons

$-\Delta_c H^{\text{gross}}$ (C), kJ·mol^{-1}	$-\Delta_c H^{\text{gross}}$ (H), kJ·mol^{-1}	$-\Delta_c H^{\text{net}}$ (C), kJ·mol^{-1}	$-\Delta_c H^{\text{net}}$ (H), kJ·mol^{-1}
435.687	110.675	435.687	88.675
$-\Delta_c H^{\text{gross}}$ (C), MJ·mol^{-1}	$-\Delta_c H^{\text{gross}}$ (H), MJ·mol^{-1}	$-\Delta_c H^{\text{net}}$ (C), MJ·mol^{-1}	$-\Delta_c H^{\text{net}}$ (H), MJ·mol^{-1}
36.275	109.83	36.275	87.977

Table 2. The net mass enthalpies of combustion of some hydrocarbon fuels

No.	Combustible C_nH_m	M, g·mol^{-1}	$\frac{m_H}{m_C}$	$-\Delta_c H^{net}$, MJ·kg^{-1}, exp.	$-\Delta_c H^{net}$, MJ·kg^{-1}, calc.
1	T-6 $C_{13.51}H_{25.34}$	187.5057	$\frac{0.136}{0.864}$	43.15*	43.30
2	α-Methylstyrene dimer $C_{18}H_{20}$	236.3514	$\frac{0.0853}{0.9147}$	40.2*	40.7
3	Anthracene $C_{14}H_{10}$	178.2292	$\frac{0.0566}{0.9434}$	39.9*	39.2
4	Toluene C_7H_8	92.1354	$\frac{0.0875}{0.9125}$	40.96*	40.8

* NIST Chemistry Webbook.

For calculating the gross enthalpies of combustion of alkanes (Table 3), Yarovoi [5] calculated the numerical values of the contributions $\Delta\Delta_c H^{gross}(C_i)$ of four species of effective atoms, C_i (i = 1–4). Table 3 also shows the values of similar additive increments calculated based on the results of this work using the following equation:

$$-\Delta\Delta_c H^{gross*}(C_i) = \Delta_c H^{gross}(C) + \\ +(4-i)\Delta_c H^{gross}(H), \quad (4)$$

where i is the species of effective atom (i = 1–4); $\Delta_c H^{gross}(C)$ is the increment of the enthalpy of combustion of the C atom (Table 1), and $\Delta_c H^{gross}(H)$ is the increment of the enthalpy of combustion of the H atom (Table 1).

The results of $\Delta\Delta_c H^{gross*}(C_i)$ calculations using equation (4) are in satisfactory agreement with the corresponding values obtained by Yarovoi [5] (Table 3).

This implies that the difference in the enthalpies of combustion of alkane isomers should be small. Indeed, the maximum values of the ratios of the enthalpy of isomerization to the enthalpy of combustion in condensed states are 0.43, 0.38, and 0.29% for hexane isomers, heptane, and octane, respectively [12]. In this case, *n*-alkanes are almost always characterized by the maximum enthalpy of combustion. Exceptions may exist for highly branched hydrocarbons with additional steric effects. For example, according to NIST, $\Delta_c H^{gross}$ (*n*-$C_{14}H_{30}$) = −9399.83 kJ·mol^{-1} and $\Delta_c H^{gross}$ (2,2,3,3,5,5,6-heptamethylheptane) = −9413.60 kJ·mol^{-1} ($\Delta\Delta_c H^{gross}$ ~0.15%).

Thus, it is worth noting that the isomerism in alkanes and alkyl groups has a minor effect on the mass energy intensity of hydrocarbons.

The valence states and the "cyclicity" of effective carbon atoms affect the value of the enthalpy of combustion of hydrocarbons. We have shown [9, 13, 14] that introducing the "cyclicity" parameter of the effective atom, which is determined by the size and method of joining the cycles, results in the versatility of additive calculations of physicochemical properties. In this case, the number of types of effective carbon atoms increases to six:

Table 3. Contributions of $\Delta\Delta_c H^{gross}(C_i)$ and $\Delta\Delta_c H^{gross*}(C_i)$ of the effective atoms to the enthalpy of combustion of alkanes

No.	Atom	$-\Delta\Delta_c H^{gross}(C_i)$, kJ·mol^{-1} [5]	$-\Delta\Delta_c H^{gross*}(C_i)$, kJ·mol^{-1}, this work	$\lvert\delta\rvert_{mean}$, %
1	C_1	770.45	767.71	0.36
2	C_2	645.98	657.04	0.31
3	C_3	535.51	546.36	1.27
4	C_4	421.32	435.69	3.4

C – acyclic

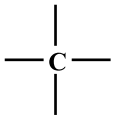

$C^{C^{I}}$ – monocyclic

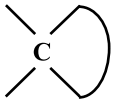

$C^{C^{I},C^{II}}$ – bicyclic

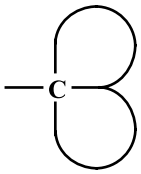

$C^{C^{I},C^{II},C^{III}}$ – tricyclic

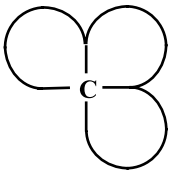

$C^{C^{I},C^{II},C^{III},C^{IV}}$ – tetracyclic

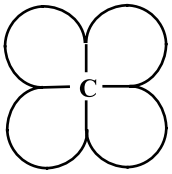

$C^{S-C^{I},C^{II}}$ – spirocyclic

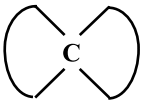

Conventionally, double bonds are considered two-membered cycles. Naturally, such a classification of effective atoms significantly increases the number of required additive constants. The possibility of predicting the enthalpy of combustion $\Delta_c H^{gross}$ (C_nH_m, 298.15 K) can be simplified using the generalized parameters of cycle strain energy, which are determined for monocyclic compounds as

$$E_i = \Delta_c H^{gross}(C_nH_m)_{exp.} - \Delta_c H^{gross}(C_nH_m)_{calc.} \quad (5)$$

In this ratio, $\Delta_c H^{gross}(C_nH_m)_{calc.}$ is calculated using the corresponding contributions for unstrained compounds in the state of ideal gas according to Benson [15] or Tatevskii and Yarovoi [4, 5]. Kozina [16] and Kolesov [17] studied the strain energies of cyclic hydrocarbons in detail. In [16], the conditionality of the E_i value was rightly noted, and in [17], E_i was demonstrated to be less dependent on the number of alkyl substituents in cyclic compounds. Table 4 presents the numerical values of E_i in cyclic compounds in the state of ideal gases.

We used equations similar to equation (5) to calculate the conditional strain energy (E_i^*) for monocyclic hydrocarbons in the liquid state:

$$E_i^*(kJ\cdot mol^{-1}) = \Delta_c H^{gross}(C_nH_m)_{liq.,\,exp.} - \Delta_c H^{gross}(C_nH_m)_{liq.,\,calc.} \quad (6)$$

Using the data in Table 1, the calculated value of the enthalpy of combustion of liquid hydrocarbons $\Delta_c H^{gross}(C_nH_m)_{liq.,\,calc.}$ was determined using equation (7). The fact that the increments for the liquid and crystalline states are practically indistinguishable in magnitude was considered:

$$\Delta_c H^{gross}(C_nH_m, kJ\cdot mol^{-1})_{liq.,\,calc.} = n\Delta_c H^{gross}(C)_{liq.} + m\Delta_c H^{gross}(H)_{liq.} \quad (7)$$

The results of E_i^* calculation and the change in the strain energy of the cycle during the transition from liquid to gaseous state are provided in Table 4.

The effective strain energies of the liquid hydrocarbon cycles are 35–45 kJ·mol^{-1} lower than those of the compounds in the ideal gas state. Five- and six-membered compounds are even more stable than their acyclic counterparts. The notable effects of energy stabilization of cyclic compounds in the liquid state are most likely associated with processes that result in an increase in the density of liquids due to a decrease in the intrinsic volume of molecules and an increase in intermolecular interaction.

As each new cycle or double bond is formed, the compound loses two hydrogen atoms. This causes a 2 × (–110.675) kJ·mol^{-1} (Table 1) decrease in the molar energy intensity, which is not compensated by the cycle strain energy even in the case of the most strained cyclopropane hydrocarbons (Table 4).

The strain energy of cycles for polycyclic compounds (E_i^{**}, Table 5) can differ significantly from that for monocyclic compounds (Table 4).

For polycyclic C_nH_m compounds, the number of cycles can be determined as

$$n_{i,cycle} = \frac{2n+2-m}{2}, \quad (8)$$

and the molar gross heat of combustion can be calculated as

$$\Delta_c H^{gross}(C_nH_m) = n\Delta_c H^{gross}(C) + m\Delta_c H^{gross}(H) + \sum_{i=2}^{6} n_{i,\,cycle} \times E_i^{**}, \quad (9)$$

where E_i^{**} is the effective strain energy for cycles i = 2, 4, 5, and 6 in the liquid state. The net heat of combustion is calculated in a similar manner.

Based on equation (9), new values of the additive constants, $\Delta_c H^{gross,net}(C)$ and $\Delta_c H^{gross,net}(H)$, $E_i^{**gross,net}$,

Table 4. E_i strain energies and E_i* effective (conventional) strain energies of cyclic hydrocarbons [13, 16]

No.	Cycle type	E_i, id. gas, kJ·mol^{-1}	E_i^*, liquid, kJ·mol^{-1}	$\Delta_{gas}^{liq}E_i$, kJ·mol^{-1}
1		−93.5	−47.9	45.6
2		−115.5	−80.1	35.4
3		−111.3	−67.5	43.8
4		−25.1	9.3	34.4
5	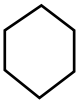	−0.8	34.3	35.1

Table 5. Increments for $\Delta_c H^{gross,net}$ (298.15 K) values calculation

$\Delta_c H^{gross,net}$ (298.15 K)	kJ·mol^{-1}		MJ·kg^{-1}	
	gross	net	gross	net
$-\Delta_C H$(C)	432.57	432.57	36.87	36.87
$-\Delta_C H$(H)	111.69	89.69	106.16	84.33
E_2^{**}	−50.67	−50.67	−1.81	−1.81
E_3^{**}	−79.87	−79.87	−1.90	−1.90
E_4^{**}	−76.87	−76.87	−1.37	−1.37
E_5^{**}	1.63	1.63	0.023	0.023
E_6^{**}	31.50	31.50	0.374	0.374
$E_{benz.}^{**}$	35.37	35.37	0.453	0.453

(Table 5) were calculated using the least squares method. This allowed the calculation error to be reduced on average to $|\delta|_{mean}$ = 0.4% for all 95 compounds in the working database.

When calculating additive constants E_i^{**}, MJ·kg^{-1} (kJ·g^{-1}), it was assumed that

$$E_i^{**}(\text{MJ}\cdot\text{kg}^{-1}) = \frac{E_i^{**}(\text{kJ}\cdot\text{mol}^{-1})}{M(\text{CH}_2)\cdot i}, \quad (10)$$

and thus, for the benzene (phenyl) ring, it was determined as

$$E_{benz.}^{**}(\text{MJ}\cdot\text{kg}^{-1}) = \frac{E_{benz.}^{**}(\text{kJ}\cdot\text{mol}^{-1})}{M(\text{C}_6\text{H}_6)}. \quad (11)$$

The effectiveness of Equation (9) is illustrated by the calculation of the energy intensity of 11 $C_{10}H_{16}$ substances (Table 6). The calculated values of enthalpies of combustion were obtained using the data from Table 5. The mean calculation error was 0.34%, which is considered a good result for a simple additive procedure.

Equation (9) can also be used to calculate $\Delta_c H^{gross}(C_nH_m)$ of cage hydrocarbons with convex polyhedron structures using the Euler formula for calculating the number of facet cycles:

$$n_{cycle} = n_{ij} - n + 2, \quad (12)$$

where n_{ij} is the number of C–C bonds (edges), n is the number of atoms (vertices), and n_{cycle} is the number of cycles (faces).

Table 6. Experimental and calculated values of the gross enthalpy of combustion ($-\Delta_c H^{gross}$, kJ·mol^{-1}) of $C_{10}H_{16}$ hydrocarbons

No.	Compounds		$-\Delta_c H^{gross}$, exp.[1]	Calculations		$-\Delta_c\Delta^{calc.}_{exp.} H^{gross}$	
				Equation	$-\Delta_c H^{gross}$	kJ·mol^{-1}	|δ|, %
1	*trans*-1-Methyl-1,2 dicyclopropyl-cyclopropane (syntin), liq.		6353.7 [18]	$10\Delta_c H^B(C)+16\Delta_c H^B(H)+3E_3^{**}$	6352.4	1.4	0.02
2	Adamantane, cr.		6033.1	$10\Delta_c H^B(C)+16\Delta_c H^B(H)+3E_6^{**}$	6018.2	14.9	0.25
3	Limonene, liq.	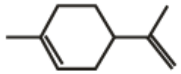	6128.3	$10\Delta_c H^B(C)+16\Delta_c H^B(H)+2E_2^{**}+E_6^{**}$	6182.6	−54.3	0.89
4	α-Pinene, liq.	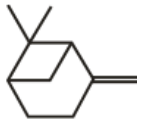	6205.0	$10\Delta_c H^B(C)+16\Delta_c H^B(H)+E_2^{**}+E_4^{**}+E_6^{**}$	6208.8	−3.8	0.06
5	β-Pinene, liq.	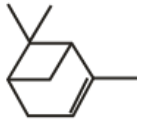	6214.1	$10\Delta_c H^B(C)+16\Delta_c H^B(H)+E_2^{**}+E_4^{**}+E_6^{**}$	6208.8	5.3	0.09
6	Camphene, cr.	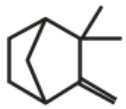	6146	$10\Delta_c H^B(C)+16\Delta_c H^B(H)+E_2^{**}+2E_5^{**}$	6160.2	−14.2	0.23

Table 6. Continued

No.	Compounds		$-\Delta_c H^{gross}$, exp.[1]	Calculations		$-\Delta_c\Delta^{calc.}_{exp.} H^{gross}$	
				Equation	$-\Delta_c H^{gross}$	kJ·mol^{-1}	|δ|, %
7	3-Carene, cr.	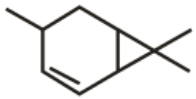	6192.2	$10\Delta_c H^B(C)+16\Delta_c H^B(H)+E_2^{**}+E_3^{**}+E_6^{**}$	6211.8	−19.6	0.32
8	Tricyclene, cr.		6146.7	$10\Delta_c H^B(C)+16\Delta_c H^B(H)+E_3^{**}+2E_5^{**}$	6189.4	−42.7	0.69
9	Perhydrotriquinacene, cr.		6062.8	$10\Delta_c H^B(C)+16\Delta_c H^B(H)+3E_5^{**}$	6107.9	−45.1	0.74
10	Tricyclopropylmethane, liq.	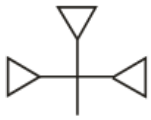	6380.8	$10\Delta_c H^B(C)+16\Delta_c H^B(H)+3E_3^{**}$	6352.4	28.5	0.45
11	4,7-Methano-1H-indene, octahydro-, cr.	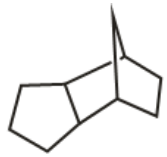	6109	$10\Delta_c H^B(C)+16\Delta_c H^B(H)+3E_5^{**}$	6107.9	1.1	0.02
$\|\delta\|_{mean}$							0.34

[1] NIST Chemistry Webbook.

For example:

1. Cubane (C_8H_8) is a set of 6 four-membered cycles ($n_{cycle} = 12 - 8 + 2 = 6$). Then

$$\Delta_c H^{gross}(C_8H_8,cr.) = 8\Delta_c H^{gross}(C) + 8\Delta_c H^{gross}(H) + 6E_4^{**} = -4815.3 \text{ kJ·mol}^{-1}, \quad (13)$$

which is 17.97 kJ·mol^{-1} (~0.4%) less than the experimental value (NIST value) for the crystal.

2. The C_{60} fullerene structure consists of 12 five-membered and 20 benzene rings (see below). Thus,

$$\Delta_c H^{gross}(C_{60},cr.) = 60\Delta_c H^{gross}(C) + 12E_5^{**} + 20E_{benz.}^{**} = -25277 \text{ kJ·mol}^{-1}, \quad (14)$$

which differs by about 2.8 % from the experimental value of the enthalpy of combustion for C_{60} fullerite = −25956 kJ·mol^{-1} [19]. Naturally, cage strain energy should be an individual characteristic of hydrocarbons such as tetrahedranes, prismanes, and icosahedranes [20], but the cage strain will most likely not exceed ~1% of the $\Delta_c H^{gross}(C_nH_m,cond.)$ kJ·mol^{-1} value.

Benzene derivatives are a special group of hydrocarbons. Conjugation effects increase the energy stability of liquid benzene. This is accompanied by a decrease in the molecule geometrical dimensions and an increase in the liquid density. Thus, *n*-hexane, cyclohexane, benzene have densities of 0.655, 0.7785, and 0.8790 g·cm^{-3}, respectively [7]. According to our estimations, the mean value of the stabilization energy of the phenyl fragment is 35.37 kJ·mol^{-1}. Thus, the final formula for calculating the mass (molar) energy of combustion is

$$\Delta_c H^{gross}(C_nH_m) = n\Delta_c H^{gross}(C) + m\Delta_c H^{gross}(H) + \sum n_{i,cycle}E_i^{**} + n_{benz.}E_{benz.}^{**}, \quad (15)$$

where $n_{benz.}$ is the number of benzene rings in the C_nH_m molecule.

VOLUMETRIC ENERGY INTENSITY OF C_nH_m HYDROCARBONS $\Delta_c H(C_nH_m)$ MJ·dm^{-3} (kJ·cm^{-3})

The volumetric energy intensity of hydrocarbons is also one of the most important characteristics of reactive fuels. Various theoretically substantiated procedures for calculating the densities or molecular volumes of substances in condensed phases can be used to predict it [5, 21–24]. To implement the main task of this work, it is most likely advisable to use simple additive procedures similar to those previously used for calculating mass energy intensities. The proposition about the additivity of the molecular volumes of hydrocarbons appears to be physically justified. It can be approximately represented as equation (16):

$$V_m(C_nH_m) \text{ см}^3\text{·моль}^{-1} = nV_m(C) + mV_m(H) + \sum n_{i,cycle}V_i + n_{benz.}V_{benz.}, \quad (16)$$

where $V_m(C)$ and $V_m(H)$ are the molar volumes of the C and H atoms in hydrocarbons, and V_i is the parameter that accounts for the influence of cycles (double bonds) in molecules on $V_m(C_nH_m)$.

Thus, the volumetric energy intensity of hydrocarbons can be calculated using equations (17) or (18):

$$\frac{\Delta_c H^{gross,net}(C_nH_m) \text{ kJ·mol}^{-1}}{V_m(C_nH_m) \text{ cm}^3\text{·mol}^{-1}} = \Delta_c H^{gross,net}(C_nH_m) \text{ kJ·cm}^{-3}, \quad (17)$$

$$\frac{n\Delta_c H(C) + m\Delta_c H(H) + \sum n_{i,cycle}E_i^{**} + n_{benz.}E_{benz.}^{**}}{nV_m(C) + mV_m(H) + \sum n_{i,cycle}V_i + n_{benz.}V_{benz.}} = \Delta_c H(C_nH_m) \text{ kJ·cm}^{-3}. \quad (18)$$

The additive constants of molecular volumes for 75 liquid C_nH_m hydrocarbons with n = 6–16 and different molecular structures were calculated using the d^{20} values (g·cm^{-3}) found in the data from [7]. The $V_m(C)$, $V_m(H)$ and V_i values (Table 7) were obtained in the first version of calculations using the least squares method. They reproduced the experimental values with a mean absolute error of $|\delta|_{mean}$ = 0.89%. However, it is difficult to explain the physical meaning of the obtained constants, particularly $V_m(C)$ = −16.618 cm^3·mol^{-1}.

In the second version of the calculation, we used the value of the hydrogen atom volume, $V(H) = (2.0 \times 10^{-8})^3$ cm^3, obtained by Askadskii and Matveev [21]. This value corresponds to $V_m^{'}(H)$ = 1.205 cm^3·mol^{-1}. If we assume that the packing density of molecular liquids is $K \approx 0.6$, then $V_m(H) \approx 2.0$ cm^3·mol^{-1}. Table 7 shows other $V_m(C)$ and V_i values that reproduce the values of $V_m(C_nH_m)$ with a relative mean deviation of $|\delta|_{mean}$ = 3.79%. As a cycle forms due to the loss of two H atoms, the molar volume decreases by about $-2V_m(H) = 4$ cm^3·mol^{-1} for each cycle.

For the monocyclic C_nH_{2n} hydrocarbons, the larger the cycle size at i = 2–6, the larger the decrease in the molecular volume, and accordingly, the increase in the density since $V_2 > V_3 > V_4 > V_5 > V_6$.

Figure 2 is a comparison of the densities (d, g·cm^{-3}) of C_nH_m hydrocarbons at n = 6. As shown in the figure, the loss of each pair of hydrogen atoms increases the density of the hydrocarbons.

Table 7. Additive constants for calculating molecular volumes $V_m(C_nH_m)$

V_m, cm^3·mol^{-1}	V_m(C)	V_m(H)	V_2	V_3	V_4	V_5	V_6	$V_{benz.}$	$\|\delta\|_{mean}$
I	−16.62	16.41	24.74	22.89	20.00	15.17	12.08	91.90	0.89
II	15.34	2.0	1.7	−0.13	−1.65	−11.42	−26.06	−26.57	3.79

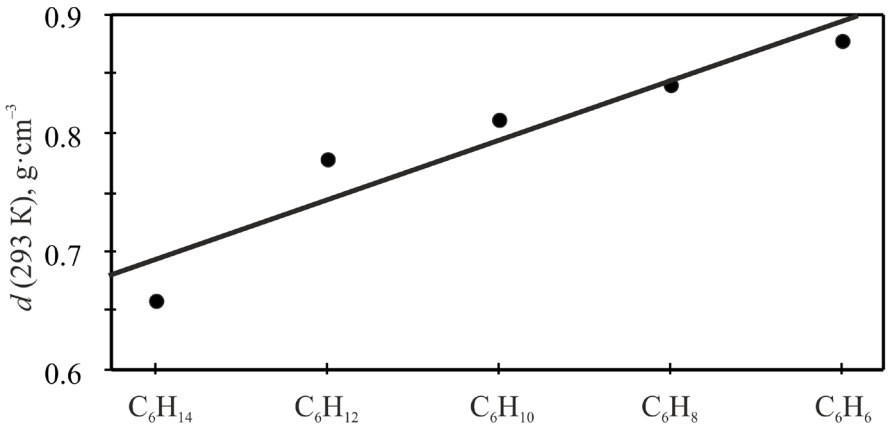

Fig. 2. Dependence of the density of hydrocarbons (hexane, cyclohexane, cyclohexene, 1,3-cyclohexadiene, and benzene) on the composition at n = 6 according to [7].

Thus, simultaneously achieving the maximum values of the mass and volumetric energy intensities of hydrocarbons appears improbable, and the optimization procedure is difficult. C_nH_m hydrocarbons with high m/n values and 4,5,6-membered rings in their molecular structures may have relatively high mass and volumetric energy intensities simultaneously.

The volumetric energy intensity of fuels with high mass energy intensity can be increased by adding high-density carbon substances to them. We have demonstrated [25] that using nanotubes significantly increases the volumetric energy intensity of hydrocarbon fuels.

CONCLUSIONS

The above analysis of the molar and mass enthalpy of combustion (energy intensity) of C_nH_m hydrocarbons suggests that the following statements are true:

1. The m/n ratio, not the presence of a large number of small carbon cycles in the molecules, is the decisive factor for achieving high values of molar and mass energy intensity of C_nH_m hydrocarbons (kJ·mol^{-1}, MJ·kg^{-1}).

2. As the cycles in C_nH_m molecules occur, the number of hydrogen atoms by two atoms per cycle. This results in a decrease of $2\Delta_cH^{gross}(H) = -223.38$ kJ·mol^{-1} in the energy intensity, and in condensed hydrocarbons, this decrease is not compensated by the arising strain energy.

3. The highest mass energy intensity is found in n-alkanes, which are extracted from oil fractions using well-developed technology.

4. For quick estimates of the values of the molar and mass energy intensity of hydrocarbons at 298.15 K with an error of about 1%, it is logical to use simple relations:

$$\Delta_cH^{net,gross}(C_nH_m)_{liq.,cr.} = \left[n\Delta_cH^{net,gross}(C) + m\Delta_cH^{net,gross}(H)\right], \text{kJ}\cdot\text{mol}^{-1}$$

$$\Delta_cH^{net,gross}(C_nH_m)_{liq.,cr.} = \left[m_C\Delta_cH^{net,gross}(C) + m_H\Delta_cH^{net,gross}(H)\right], \text{MJ}\cdot\text{kg}^{-1}$$

5. Owing to the unique nature of these properties, a separate analysis is required to justify the method for predicting molar volumes (V_m (dm^3·mol^{-1})), densities (d (kg·dm^{-3})), and volumetric combustion energies (MJ·dm^{-3}).

Acknowledgments

The study was supported by the State Research Program, project 2.1.1 "Chemical processes, reagents and technologies, bioregulators and bioorganic chemistry," 2021–2025.

Authors' contribution

G.J. Кабо – developing the scientific work concept, writing the text of the article;

L.A. Kabo – collecting and processing the material, making calculations;

L.S. Karpushenkava – making calculations, writing the text of the article;

A.V. Blokhin – writing the text of the article, offering consultations on methodology and research.

The authors declare no conflicts of interest.

REFERENCES

1. Bakulin V.N., Dubovkin N.F., Kotova V.N., Sorokin V.A., Frantskevich V.P., Yanovskii L.S. *Energoemkie goryuchie dlya aviatsionnykh i raketnykh dvigatelei* (*Energy-intensive fuels for aircraft and rocket engines*). Moscow: Fizmatlit; 2009.400 p. (in Russ.). ISBN 978-5-9221-1091-4

2. Azov V., Vorontsov D. The last fight of hydrocarbons? *Novosti Kosmonavtiki = Cosmonautics News*. 2008;18(2):44–46 (in Russ.).

3. Grigoriev A.A. Synthetic hydrocarbon rocket fuels (ways of synthine price decreasing). *Kataliz i Neftekhimiya = Catalysis and Petrochemistry*. 2005;(13):44–52 (in Russ.).

4. Tatevskii V.M. *Klassicheskaya teoriya stroeniya molekul i kvantovaya mekhanika* (*Classical theory of molecular structure and quantum mechanics*). Moscow: Khimiya; 1973. 520 p. (in Russ.).

5. Yarovoi S.S. *Metody rascheta fiziko-khimicheskikh svoistv uglevodorodov* (*Methods for calculating the physical and chemical properties of hydrocarbons*). Moscow: Khimiya; 1978. 256 p. (in Russ.).

6. Averkov I.S., Demskaya I.A., Katkov R.E., Raznoschikov V.V., Samsonov D.A., Tupitsyn N.N., Yanovskii L.S. Analysis of energy performance of composite hydrocarbon fuels for oxygen engines of space rocket stages. *Kosmicheskaya Tekhnika i Tekhnologii* (*Space engineering and technology*). 2017;(4):46–51. (in Russ.).

7. Tatevskii V.M. (Ed.). *Fiziko-khimicheskie svoistva individual'nykh uglevodorodov*: *Spravochnik* (*Physical and chemical properties of individual hydrocarbons: A Handbook*). Moscow: Gostoptekhizdat; 1960. 412 p. (in Russ.).

8. Zhang Z.-Y., Frenkel M., Marsh K.N., Wilhoit R.C. Enthalpies of Fusion and Transition of Organic Compounds. In: *Part of Subvolume A* "*Enthalpies of Fusion and Transition of Organic Compounds*" *of Volume 8* "*Thermodynamic Properties of Organic Compounds and Mixtures*" of Landolt-Börnstein – Group IV Physical Chemistry. Springer; 1995. 588 p. https://doi.org/10.1007/b55145

9. Kabo G.J., Blokhin A.V., Paulechka E. Roganov G.N., Frenkel M., Yursha I.A., Diky V., Zaitsau D., Bazyleva A., Simirsky V.V., Karpushenkava L.S., Sevruk V.M. Thermodynamic properties of organic substances: Experiment, modeling, and technological applications. *J. Chem. Thermodyn*. 2019;131:225–246. https://doi.org/10.1016/j.jct.2018.10.025

10. Blokhin A.V. Energy states of molecules in plastic crystals of organic substances. In: *Chemical problems of creating new materials and technologies*: Coll. of articles. 2nd ed. Ivashkevich O.A. (Ed.). Minsk: BSU; 2003:200–229 (in Russ.). http://elib.bsu.by/handle/123456789/31676

11. Kabo G., Paulechka E., Frenkel M. Heat Capacities and Phase Transitions for the Dynamic Chemical Systems: Conformers, Tautomers, Plastic Crystals, and Ionic Liquids. In: Letcher T., Wilhelm E. (Eds.). *Heat Capacities of Liquids and Vapours*. Cambridge, UK: RSC; 2010. P. 390–420. https://www.nist.gov/publications/heat-capacities-and-phase-transitions-dynamic-chemical-systems-conformers-tautomers

12. Kabo G.Ya., Roganov G.N., Frenkel M.L., Thermodynamics and Equilibria of Isomers. In: Frenkel M. (Ed.). *Thermochemistry and Equilibria of Organic Compounds*. New York: VCH; 1993. 602 p.

13. Kabo G.Ya., Roganov G.N., Fenkel M.L. *Termodinamika i ravnovesiya izomerov* (*Thermodynamics and equilibrium of isomers*). Minsk: Universitetskoe; 1986. 224 p. (in Russ.).

14. Kabo G.Ya., Roganov G.N. Principles of additivity of enthalpies of cyclic hydrocarbons. *Doklady AN BSSR = Reports of the Academy of Sciences of the BSSR*. 1986;30(9):832–835 (in Russ.).

СПИСОК ЛИТЕРАТУРЫ

1. Бакулин В.Н., Дубовкин Н.Ф., Котова В.Н., Сорокин В.А., Францкевич В.П., Яновский Л.С. *Энергоемкие горючие для авиационных и ракетных двигателей*. М.: Физматлит; 2009. 400 с. ISBN 978-5-9221-1091-4

2. Азов В., Воронцов Д. Последний бой углеводородов? *Новости космонавтики*. 2008;18(2):44–46.

3. Григорьев А.А. Синтетические углеводородные ракетные горючие (пути снижения стоимости синтина). *Катализ и нефтехимия*. 2005;(13):44–52.

4. Татевский В.М. *Классическая теория строения молекул и квантовая механика*. М.: Химия; 1973. 520 с.

5. Яровой С.С. *Методы расчета физико-химических свойств углеводородов*. М.: Химия, 1978. 256 с.

6. Аверьков И.С., Демская И.А., Катков Р.Э., Разносчиков В.В., Самсонов Д.А., Тупицын Н.Н., Яновский Л.С. Анализ энергетических возможностей составных углеводородных горючих для кислородных двигателей космических ракетных ступеней. *Космическая техника и технологии*. 2017;19(4):46–51.

7. Татевский В.М. (под ред.). *Физико-химические свойства индивидуальных углеводородов: Справочник*. М.: Гостоптехиздат; 1960. 412 с.

8. Zhang Z.-Y., Frenkel M., Marsh K.N., Wilhoit R.C. Enthalpies of Fusion and Transition of Organic Compounds. In: *Part of Subvolume A «Enthalpies of Fusion and Transition of Organic Compounds» of Volume 8* «*Thermodynamic Properties of Organic Compounds and Mixtures*» of Landolt-Börnstein – Group IV Physical Chemistry. Springer; 1995. 588 p. https://doi.org/10.1007/b55145

9. Kabo G.J., Blokhin A.V., Paulechka E. Roganov G.N., Frenkel M., Yursha I.A., Diky V., Zaitsau D., Bazyleva A., Simirsky V.V., Karpushenkava L.S., Sevruk V.M. Thermodynamic properties of organic substances: Experiment, modeling, and technological applications. *J. Chem. Thermodyn*. 2019;131:225–246. https://doi.org/10.1016/j.jct.2018.10.025

10. Блохин А.В. Энергетические состояния молекул в пластических кристаллах органических веществ. *Химические проблемы создания новых материалов и технологий*: Сб. ст. Вып. 2; под ред. О.А. Ивашкевича. Минск: БГУ; 2003:200–229. http://elib.bsu.by/handle/123456789/31676

11. Kabo G., Paulechka E., Frenkel M. Heat Capacities and Phase Transitions for the Dynamic Chemical Systems: Conformers, Tautomers, Plastic Crystals, and Ionic Liquids. In: Letcher T., Wilhelm E. (Eds.). *Heat Capacities of Liquids and Vapours*. Cambridge, UK: RSC; 2010. P. 390–420. https://www.nist.gov/publications/heat-capacities-and-phase-transitions-dynamic-chemical-systems-conformers-tautomers

12. Kabo G.Ya., Roganov G.N., Frenkel M.L., Thermodynamics and Equilibria of Isomers. In: Frenkel M. (Ed.). *Thermochemistry and Equilibria of Organic Compounds*. New York: VCH; 1993. 602 p.

13. Кабо Г.Я., Роганов Г.Н., Фенкель М.Л. *Термодинамика и равновесия изомеров*. Минск: Университетское; 1986. 224 с.

14. Кабо Г.Я., Роганов Г.Н. Принципы аддитивности энтальпий циклических углеводородов. *Доклады АН БССР.* 1986;30(9):832–835.

15. Бенсон С. *Термохимическая кинетика*: пер. с англ. М.: Мир; 1971. 308 с.

16. Козина М.П., Мастрюков В.С., Мильвицкая Е.М. Энергия напряжения, геометрическое строение и константы спин-спинового взаимодействия циклических углеводородов. *Успехи химии*. 1982;51(8):1337–1373. https://doi.org/10.1070/RC1982v051n08ABEH002906

15. Benson S. *Termokhimicheskaya Kinetika* (*Thermochemical Kinetics*): transl. from Eng. Moscow: Mir; 1971. 308 p. (in Russ.).

[Benson S.W. Thermochemical Kinetics. Methods for the Estimation of Thermochemical Data and Rate Parameters. New York: John Wiley & Sons, Inc.; 1968. 320 p.]

16. Kozina M.P., Mastryukov V.S., Mil'vitskaya E.M. The Strain Energy, Geometrical Structure, and Spin–Spin Coupling Constants of Cyclic Hydrocarbons. *Russ. Chem. Rev.* 1982;51(8):765–787. https://doi.org/10.1070/RC1982v051n08ABEH002906

17. Kolesov V.P., Kozina M.P. Thermochemistry of Organic and Organohalogen Compounds. *Russ. Chem. Rev.* 1986;55(10):912–928. https://doi.org/10.1070/RC1986v055n10ABEH003231

18. Pimenova S.M., Lukyanova V.A., Ilin D.Y., Druzhinina A.I., Dorofeeva O.V., *et al*. Standard enthalpies of formation of dicyclopropyldinitromethane and tricyclopropylmethane. *J. Chem. Thermodyn*. 2019;132:316–321. https://doi.org/10.1016/j.jct.2018.12.040

19. Diky V.V., Kabo G.J. Thermodynamic properties of C_{60} and C_{70} fullerenes. *Russ. Chem. Rev.* 2000;69(2):95–104. https://doi.org/10.1070/RC2000v069n02ABEH000535

20. Karpushenkava L.S., Kabo G.J., Bazyleva A.B. Structure, frequencies of normal vibrations, thermodynamic properties, and strain energies of the cage hydrocarbons C_nH_n in the ideal-gas state. *J. Mol. Struct.: THEOCHEM*. 2009;913(1–3):43–49. https://doi.org/10.1016/j.theochem.2009.07.016

21. Askadskii A.A., Matveev Yu.I. *Khimicheskoe stroenie i fizicheskie svoistva polimerov* (*Chemical structure and physical properties of polymers*). Moscow: Khimiya; 1983.248 p. (in Russ.).

22. Tatevskii V.M., Grikina O.E., Abramchikov A.V., Tkachik Z.A. Molecular volumes and densities of hydrocarbons containing small rings and multiple bonds. *Vestnik Moskovskogo Universiteta, ser. 2: Khimiya = Moscow University Chemistry Bulletin*. 1983;(1):27–31 (in Russ.).

23. Grikina O.E., Tatevskii V.M. Calculation of enthalpies of formation, molecular volumes and densities of polycyclic hydrocarbons. *Vestnik Moskovskogo Universiteta, ser. 2: Khimiya = Moscow University Chemistry Bulletin*. 1988;29(1):22–26 (in Russ.).

24. Rukavishnikov V.V., Belik A.V. Prediction of the density of organic compounds in the framework of the new ANSAB approximation. *Izvestiya Chelyabinskogo Nauchnogo Tsentra UrO RAN*. 2006;33(3):16–19 (in Russ.).

25. Karpushenkava L.S., Kabo G.Ya., Blokhin A.V. Stacked-cup multiwall carbon nanotubes as components of energy-intensive suspension jet fuels. *Tonk. Khim. Tekhnol. = Fine Chem. Technol*. 2020;15(2):38–46 (in Russ.). https://doi.org/10.32362/2410-6593-2020-15-2-38-46

17. Колесов В.П., Козина М.П. Термохимия органических и галогенорганических соединений. *Успехи химии*. 1986;55(10):1603–1632. https://doi.org/10.1070/RC1986v055n10ABEH003231

18. Pimenova S.M., Lukyanova V.A., Ilin D.Y., Druzhinina A.I., Dorofeeva O.V., *et al*. Standard enthalpies of formation of dicyclopropyldinitromethane and tricyclopropylmethane. *J. Chem. Thermodyn*. 2019;132:316–321. https://doi.org/10.1016/j.jct.2018.12.040

19. Дикий В.В., Кабо Г.Я. Термодинамические свойства фуллеренов C_{60} и C_{70}. *Успехи химии*. 2000;69(2):107–117. https://doi.org/10.1070/RC2000v069n02ABEH000535

20. Karpushenkava L.S., Kabo G.J., Bazyleva A.B. Structure, frequencies of normal vibrations, thermodynamic properties, and strain energies of the cage hydrocarbons C_nH_n in the ideal-gas state. *J. Mol. Struct.: THEOCHEM.* 2009;913(1–3):43–49. https://doi.org/10.1016/j.theochem.2009.07.016

21. Аскадский А.А., Матвеев Ю.И. *Химическое строение и физические свойства полимеров*. М.: Химия; 1983. 248 с.

22. Татевский В.М., Грикина О.Е., Абрамчиков А.В., Ткачик З.А. Молекулярные объемы и плотности углеводородов, содержащих малые циклы и кратные связи. *Вестник Московского университета. Сер. 2: Химия.* 1983;24(1):27–31.

23. Грикина О.Е., Татевский В.М. Расчет энтальпий образования, молекулярных объемов и плотностей полициклических углеводородов. *Вестник Московского университета. Сер. 2: Химия.* 1988;29(1):22–26.

24. Рукавишников В.В., Белик А.В. Прогноз плотности органических соединений в рамках нового приближения ANSAB. *Известия Челябинского научного центра УрО РАН.* 2006;33(3):16–19.

25. Карпушенкова Л.С., Кабо Г.Я., Блохин А.В. Многослойные углеродные нанотрубки–компонент энергоемких суспензионных реактивных горючих. *Тонкие химические технологии.* 2020;15(2):38–46. https://doi.org/10.32362/2410-6593-2020-15-2-38-46

About the authors:

Gennady J. Kabo, Dr. Sci. (Chem.), Professor, Professor of the Department of Physical Chemistry, Belarusian State University (14, Leningradskaya ul., Minsk, 220030, Belarus). E-mail: kabo@bsu.by. Scopus Author ID 56261611100

Lubov A. Kabo, Student, Department of Functional Analysis and Analytical Economics, Belarusian State University (4, Nezavisimosti pr., Minsk, 220030, Belarus). E-mail: alvykabo@gmail.com. https://orcid.org/0000-0003-2620-3749

Larisa S. Karpushenkava, Cand. Sci. (Chem.), Associate Professor, Associate Professor of the Department of Physical Chemistry, Belarusian State University (14, Leningradskaya ul., Minsk, 220030, Belarus). E-mail: karpushenkava@bsu.by. Scopus Author ID 6504468775, ResearcherID AAB-8934-2020, https://orcid.org/0000-0002-8875-5568

Andrey V. Blokhin, Dr. Sci. (Chem.), Professor, Head of the Department of Physical Chemistry, Belarusian State University (14, Leningradskaya ul., Minsk, 220050, Belarus). E-mail: blokhin@bsu.by. Scopus Author ID 7101971167, ResearcherID AAF-8122-2019, https://orcid.org/0000-0003-4778-5872

Об авторах:

Кабо Геннадий Яковлевич, д.х.н., профессор, профессор кафедры физической химии Белорусского государственного университета (Беларусь, 220030, Минск, ул. Ленинградская, д. 14). E-mail: kabo@bsu.by. Scopus Author ID 56261611100

Кабо Любовь Андреевна, студентка кафедры функционального анализа и аналитической экономики Белорусского государственного университета (Беларусь, 220030, Минск, пр. Независимости, 4). E-mail: alvykabo@gmail.com. https://orcid.org/0000-0003-2620-3749

Карпушенкова Лариса Степановна, к.х.н., доцент, доцент кафедры физической химии Белорусского государственного университета (Беларусь, 220030, Минск, ул. Ленинградская, д. 14). E-mail: karpushenkava@bsu.by. Scopus Author ID 6504468775, ResearcherID AAB-8934-2020, https://orcid.org/0000-0002-8875-5568

Блохин Андрей Викторович, д.х.н., профессор, заведующий кафедрой физической химии Белорусского государственного университета (Беларусь, 220030, Минск, ул. Ленинградская, д. 14). E-mail: blokhin@bsu.by. Scopus Author ID 7101971167, ResearcherID AAF-8122-2019, https://orcid.org/0000-0003-4778-5872

The article was submitted: June 15, 2021; approved after reviewing: June 19, 2021; accepted for publication: August 10, 2021.

Translated from Russian into English by M. Povorin
Edited for English language and spelling by Enago, an editing brand of Crimson Interactive Inc.

CHEMISTRY AND TECHNOLOGY OF ORGANIC SUBSTANCES

ХИМИЯ И ТЕХНОЛОГИЯ ОРГАНИЧЕСКИХ ВЕЩЕСТВ

ISSN 2686-7575 (Online)

https://doi.org/10.32362/2410-6593-2021-16-4-287-306

UDC 577.1:547.415.1:547.415.5

REVIEW ARTICLE

Structure and biological action of analogs and derivatives of biogenic polyamines

Oleg S. Egorov[1,@], Nadezhda Yu. Borisova[1], Elena Ya. Borisova[1], Muzaffar L. Rezhabbaev[1], Elena Yu. Afanas'eva[2], Evgeny V. Arzamastsev[2]

[1]MIREA – Russian Technological University (M.V. Lomonosov Institute of Fine Chemical Technologies), Moscow, 119571 Russia
[2]National Medical Research Center of Cardiology, Ministry of Health of the Russian Federation, Moscow, 121552 Russia
[@]Corresponding author, e-mail: egorov1997@inbox.ru

Abstract

Objectives. *Biogenic polyamines are widely present in nature. They are characteristic of both protozoan cells and multicellular organisms. These compounds have a wide range of biological functions and are necessary for normal growth and development of cells. Violation of polyamine homeostasis can cause significant abnormalities in cell functioning, provoking various pathological processes, including oncological and neuropsychiatric diseases. The impact on the "polyamine pathway" is an attractive basis for the creation of many pharmacological agents with a diverse spectrum of action. The purpose of this review is to summarize the results of the studies devoted to understanding the biological activity of compounds of the polyamine series, comparing their biological action with action on certain molecular targets. Due to the structural diversity of this group of substances, it is impossible to fully reflect the currently available data in one review. Therefore, in this work, the main attention is paid to the derivatives, acyclic saturated polyamines.*

Results. *The following aspects are considered: biological functionality, biosynthesis and catabolism, cell transport, and localization of biogenic polyamines in the living systems. Structural analogs and derivatives of biogenic polyamines with antitumor, neuroprotective, antiarrhythmic, antiparasitic, antibacterial, and other biological activities are represented; the relationship between biological activity and the target of exposure is reflected. It was found that the nature of the substituent, the number of cationic centers, and the length of the polyamine chain have a great influence on the nature of the effect.*

Conclusions. *At present, the use of polyamine structures is restrained by cytotoxicity and nonspecific toxic effects on the central nervous system. Further research in the field of biochemistry, cell transport, and a deeper understanding of receptor interaction mechanisms will help making polyamines as the basis for potential drug formulation.*

Keywords: *polyamines, biogenic amines, putrescine, polyamine derivatives, spermine, spermidine, polyamine biosynthesis, polyamine catabolism, polyamine transport, antiarrhythmic activity, antibacterial activity, antitumor activity, polyamine analogs, neurodegenerative diseases*

For citation: Egorov O.S., Borisova N.Yu., Borisova E.Ya., Rezhabbaev M.L., Afanas'eva E.Yu., Arzamastsev E.V. Structure and biological action of analogs and derivatives of biogenic polyamines. *Tonk. Khim. Tekhnol. = Fine Chem. Technol.* 2021;16(4):287–306 (Russ., Eng.). https://doi.org/10.32362/2410-6593-2021-16-4-287-306

ОБЗОРНАЯ СТАТЬЯ

Структура и биологическое действие аналогов и производных биогенных полиаминов

О.С. Егоров[1,@], Н.Ю. Борисова[1], Е.Я. Борисова[1], М.Л. Режаббаев[1], Е.Ю. Афанасьева[2], Е.В. Арзамасцев[2]

[1]МИРЭА – Российский технологический университет (Институт тонких химических технологий им. М.В. Ломоносова), Москва, 119571, Россия
[2]Национальный медицинский исследовательский центр кардиологии Министерства здравоохранения РФ, Москва, 121552 Россия
[@]Автор для переписки, e-mail: egorov1997@inbox.ru

Аннотация

Цели. *Биогенные полиамины широко представлены в живой природе. Они характерны как для клеток простейших, так и для многоклеточных организмов. Данные соединения обладают широким спектром биологической активности и необходимы для нормального роста и развития клеток. Нарушение гомеостаза полиаминов может вызывать существенные отклонения в функционировании клетки, провоцируя протекание патологических процессов различного рода, включая онкологические и психоневрологические заболевания. Воздействие на «полиаминовый путь» является привлекательным базисом для создания ряда фармакологически активных веществ с различным спектром действия. Целью данного обзора является обобщение результатов исследований, посвященных изучению биологической активности соединений полиаминового ряда; сопоставление биологического действия с воздействием на определенные молекулярные мишени. В виду структурного многообразия данной группы веществ невозможно в полной мере отразить имеющиеся на сегодняшний момент данные в одном обзоре. Поэтому в настоящей работе основное внимание уделено производным насыщенных полиаминов ациклического строения.*

Результаты. *В общем виде рассмотрены следующие аспекты: биологическая активность, биосинтез и катаболизм, клеточный транспорт и локализация биогенных полиаминов в живых системах. Представлены структурные аналоги и производные биогенных полиаминов, обладающие противоопухолевой, нейропротекторной, антиаритмической, противопаразитарной, антибактериальной и некоторыми другими видами биологической активности; отражена взаимосвязь между биологической активностью и мишенями воздействия. Установлено, что на характер воздействия большое влияние оказывает природа заместителя, количество катионных центров, а также длина полиаминовой цепи.*

Выводы. *В настоящее время применение структур полиаминового ряда сдерживается наличием цитотоксичности, а также неспецифического токсического воздействия на ЦНС. Дальнейшие исследования в области биохимии, клеточного транспорта, а также более глубокое понимание механизмов рецепторного взаимодействия позволят использовать полиамины в качестве основы для создания потенциальных лекарственных препаратов.*

Ключевые слова: *полиамины, биогенные амины, путресцин, производные полиаминов, спермин, спермидин, биосинтез полиаминов, катаболизм полиаминов, транспорт полиаминов, антиаритмическая активность, антибактериальная активность, противоопухолевая активность, аналоги полиаминов, нейродегенеративные заболевания*

Для цитирования: Егоров О.С., Борисова Н.Ю., Борисова Е.Я., Режаббаев М.Л., Афанасьева Е.Ю., Арзамасцев Е.В. Структура и биологическое действие аналогов и производных биогенных полиаминов. *Тонкие химические технологии*. 2021;16(4):287–306. https://doi.org/10.32362/2410-6593-2021-16-4-287-306

INTRODUCTION

Polyamines (polymethylene polyamines) represent a large group of compounds that are widespread among biological entities. Structurally, polyamines are quite diverse, but the majority of their compounds are based on three biogenic polyamines: putrescine **1**, spermidine **4**, and spermine **7**. Cadaverine **2**, norspermidine **3**, homospermidine **5**, norspermine **6**, and homospermine **8** are similar to the three basic polyamines, but with different molecular chain length (Fig. 1).

Structural fragments of polyamines exist in several alkaloids and toxins [1, 2]. To date, many conjugates of polyamines with other biomolecules, such as amino acids, oligonucleotides, steroids, etc., have been isolated and characterized [3, 4].

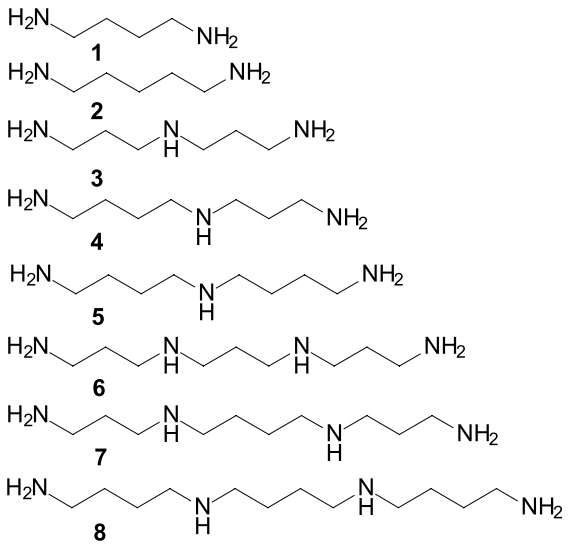

Fig. 1. Basic polyamines.

In living systems, at physiological pH values, these compounds exist in ionized form, representing organic polycations. The presence of a positive charge reflects a wide range of biological functionalities. Polyamines are involved in a variety of biological processes, such as cell growth, proliferation, and cell differentiation [5]. They are essential components of normal cell growth and development.

Polyamines can interact with negatively charged protein fragments, nucleic acids, and phospholipids [6]. The formation of conjugates, as well as "bridging" structures with high-molecular compounds such as RNA and DNA, has a stabilizing effect on their conformations, protecting them against denaturation, occurring under the influence of heat, chemical reagents, or radiation [7, 8]. Under oxidative stress, polyamines act as antioxidants, neutralizing reactive oxygen species [9].

The first mentions of polyamines are also associated with the name of the Dutch naturalist Leeuwenhoek, who isolated crystals of spermine phosphate in 1678. However, the correct structure of spermine was established only in 1926 by Rosenheim [10]. In 1898, Poehl proposed the use of spermine for the treatment of various diseases. In 1938, Zeller, in his works, described the enzyme—diamine oxidase (DAO), an impetus for the development of the polyamine biochemistry [11].

BIOSYNTHESIS AND CATABOLISM OF POLYAMINES

In all living systems, polyamines are formed from precursor amino acids, which are mainly L-arginine (Arg), L-ornithine (Orn), L-lysine (Lys), and L-methionine (Met). However, among bacteria and eukaryotes,

there are differences in the qualitative composition of polyamines, and in their biosynthesis and catabolism pathways [12]. Figure 2 shows the general scheme of biosynthesis of basic polyamines in living cells.

The initial stage in the polyamine biosynthesis is the decarboxylation of amino acid precursors. In plants and bacteria, putrescine can be formed in two ways: 1) directly from ornithine with the help of the enzyme ornithine decarboxylase (ODC); 2) indirectly, through the formation of agmatine from arginine with the help of arginine decarboxylase (ADC), followed by the conversion of agmatine to putrescine by the enzyme agmatinase [13].

In animal cells, putrescine is produced exclusively by the first pathway, i.e. from L-ornithine [14]. Putrescine formation is a limiting step in the polyamine biosynthesis [15].

Under the action of the enzyme S-adenosylmethionine synthase, also known as methionine adenosine transferase (MAT), and the ATP molecule, L-methionine is converted to S-adenosylmethionine (SAM), which is transformed by pyruvate-dependent S-adenosylmethionine decarboxylase (S-adenosylmethionine decarboxylase), deforming into S-AdoMet nosylmethioninamine (dsSAM). Spermidine and spermine are formed by transfer of an aminopropyl group from dsSAM via spermidine synthase (SpdSy) and spermine synthase (SpmSy), respectively [16].

Cadaverine is formed from L-lysine with the participation of the enzyme lysine decarboxylase (LDC) [17].

Notably, putrescine and cadaverine are more common among bacteria than other polyamines [18]. In mammals, putrescine is a source for the formation of higher polyamines, such as spermine and spermidine [19].

Initially, it was assumed that two main enzymes are responsible for the catabolism of polyamines in mammals: spermine/spermidine-N^1-acetyltransferase (SSAT) and acetylpolyamine oxidase (APAO) [20]. A recent study [21] has identified another enzyme responsible for the degradation of polyamines: spermine oxidase (SMO). It is a cytosolic enzyme that catalyzes the direct transformation of spermine to spermidine. The key difference between this enzyme and APAO is that the former does not require

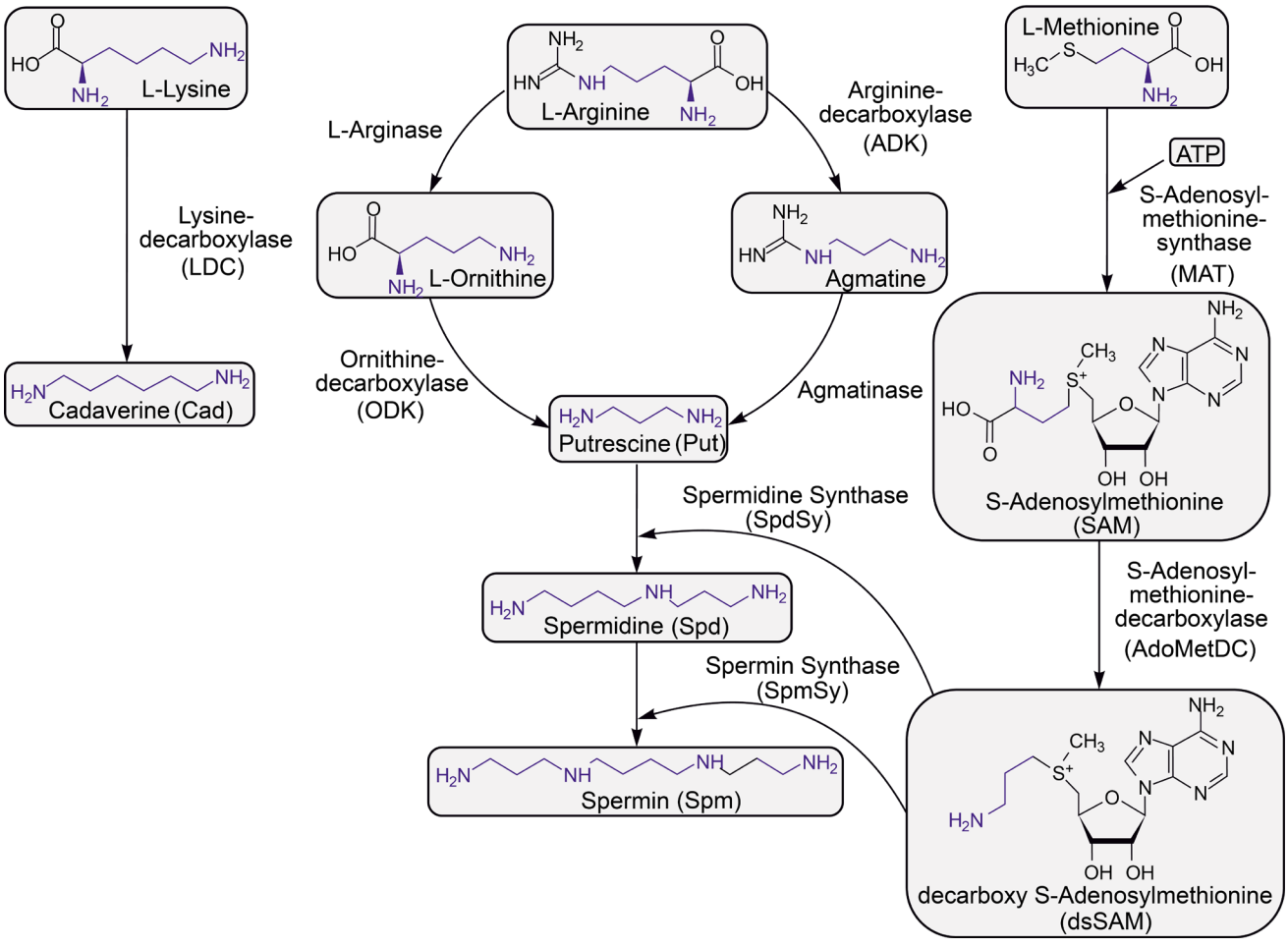

Fig. 2. General scheme of biosynthesis of basic polyamines.

preliminary acetylation of the substrate [22].

In general, the catabolism of polyamines in mammals is shown in Fig. 3.

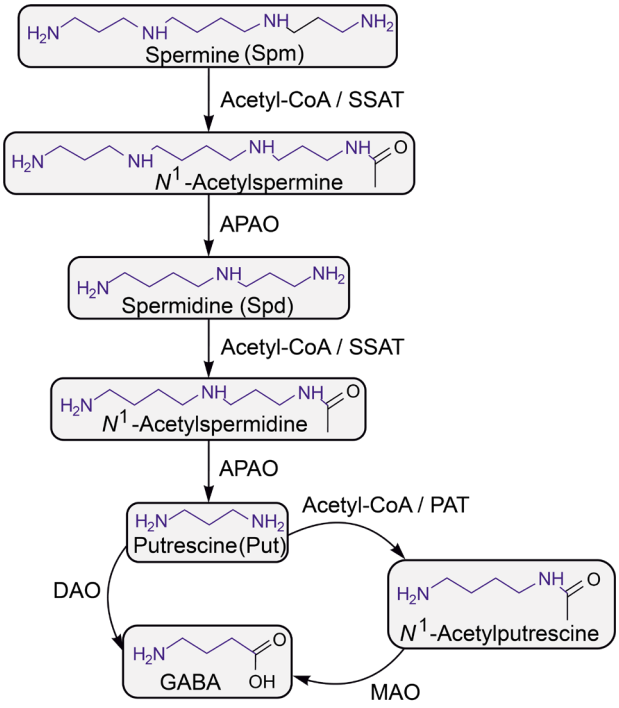

Fig. 3. General scheme of catabolic transformations of polyamines.

The degradation of higher polyamines is the SSAT-catalyzed acetylation of the substrate (Spd and Spm) acetyl-CoA. Acetylation is necessary because APAO exhibits extremely low activity with respect to nonacetylated polyamines [23]. Acetylpolyamine oxidase (APAO) catalyzes the degradation of N^1-acetylspermine and N^1-acetylspermidine to spermidine and putrescine, respectively. In this case, the formation of toxic products, hydrogen peroxide and unstable 3-acetamidopropanal, occurs.

Compared to spermidine and spermine, putrescine has a shorter biological half-life [24]. It is known that the catabolism of putrescine is not the same for all tissues of the mammalian body. The main enzyme catalyzing the decomposition of putrescine is diamine oxidase (DAO); however, in the mammalian brain, DAO activity is low [25]. It was shown in [26] that putrescine degradation in the mammalian brain, is catalyzed by monoamine oxidase (MAO) with the substrate, monoacetylputrescine, formed under the action of acetyl CoA and putrescine N^1-transferase [27]. Subsequently, it is oxidized to *N*-acetyl-4-aminobutyrate, which is converted to γ-aminobutyric acid (GABA) [28].

Another pathway of putrescine catabolism is associated with the copper-containing enzyme DAO, which catalyzes the degradation of 3–6 long-chain diamines, and histamine, by oxidative deamination. DAO is able to degrade putrescine to form γ-aminobutanal, which is then converted to GABA [29].

DAO is a rate-limiting enzyme in the terminal catabolism of polyamines since the oxidation products of putrescine are not involved in the polyamine interconversion cycle [30].

As reported [31], diamine oxidase (DAO) is largely responsible for the metabolism of cadaverine.

TRANSPORT AND LOCALIZATION OF POLYAMINES

While the presence of polyamines is typical for all living organisms, the level, ratio, and qualitative composition of these compounds are different for plants, animals, and bacteria. So, in the body of animals, the content of polyamines is heterogeneous. Not surprisingly, the highest concentration of polyamines is present in the tissues with active cell proliferation (hair follicles, mucosal epithelium, spinal cord, etc.) as they are necessary for cell division.

The level of extracellular polyamines is low. Thus, the content of spermidine in cerebrospinal fluid samples (0.12 ± 0.4 nmol/mL) is almost two orders of magnitude lower than in the white matter of the spinal cord (15.9 ± 1.25 nmol/mg), the content of spermine is 12 times lower (0.14 ± 0.01 nmol/mL and 1.69 ± 0.10 nmol/mg), and the content of putrescine is 4 times lower (0.23 ± 0.05 nmol/mL and 0.96 ± 0.19 nmol/mg) [32].

The homeostasis of polyamines is maintained via the regulation of their biosynthesis, catabolism, and transport in the body [33–34].

While the mammalian body synthesizes polyamines on its own, food products and intestinal microbiota act as additional sources [35]. A previous report investigated and confirmed the absorption of polyamines by cells [36]. Research showed that inhibition of polyamine biosynthesis by α-difluoromethylornithine (DFMO) stimulates the absorption of these compounds from the external environment.

Currently, the transport pathways of polyamines are well studied for unicellular organisms, such as *E. coli* [37]. However, for multicellular organisms, including mammals, the functioning of the polyamine transport system has not been fully understood. A comprehensive review [38] established three models describing the transport of polyamines in mammalian cells. In general, the transport of polyamines depends

on the carrier, temperature, pH-medium, time, concentrations of Na^+, Mn^{2+}, Ca^{2+}, Mg^{2+} ions, and is also dependent on potential.

The first model [39] includes two stages: transport of the substrate into the cytosol via a voltage-dependent membrane transporter, and vesicular sequestration requiring an H^+ gradient.

The second model describes glypican-mediated endocytosis. It is assumed that spermidine, binding to heparan sulfate fragments of glypican, enters the cell, where it is separated from glypican by oxidation of NO, which leads to the accumulation of polyamine in special vesicles [40].

According to the third model [41], endocytosis of polyamines is caveolin-mediated: by means of a certain "polyamine receptor" whose structure has not been established. As in the previous model, the secretion of polyamines into vesicles is mediated by NO.

Understanding the role of polyamines in the functioning of living systems, opens new ways of influencing physiological and pathological cellular processes. Creation of synthetic analogs and derivatives of biogenic polyamines will expand the arsenal of drugs.

ANTITUMOR ACTIVITY

As noted earlier, the concentration of polyamines is the highest in rapidly renewing tissues since these compounds are involved in the processes of cell differentiation and proliferation. The rate of synthesis and absorption of extracellular polyamines is noticeably higher in actively proliferating cells, including tumor cells [42]. Due to this fact, polyamines can be promising structures for the design of novel anticancer drugs. The first successful step in this direction was the study [43] devoted to the synthesis of mono- and dicyano-derivatives of biogenic polyamines—spermine and spermidine—with different chain lengths. Among several compounds, five exhibited antitumor activities, confirmed *in vivo* [44].

To date, many different biogenic polyamine derivatives have been developed, exhibiting an antitumor effect, including symmetric and asymmetric alkylated, heterofunctional, heterochain, sterically hindered, and even metal complex analogs [45, 46].

In general, targeting the enzymes of biosynthesis and catabolism, causes disruption of polyamine homeostasis in the tumor cell, leading to a cytostatic and/or apoptotic effect [47].

Alkylated analogs

Porter [48, 49] was one of the first to study the antitumor activity of *N*-alkyl and *N*-acyl derivatives of spermidine (Fig. 4). These compounds are able to compete with unmodified spermidine for cellular uptake, replacing it, and leading to inhibition of cell growth.

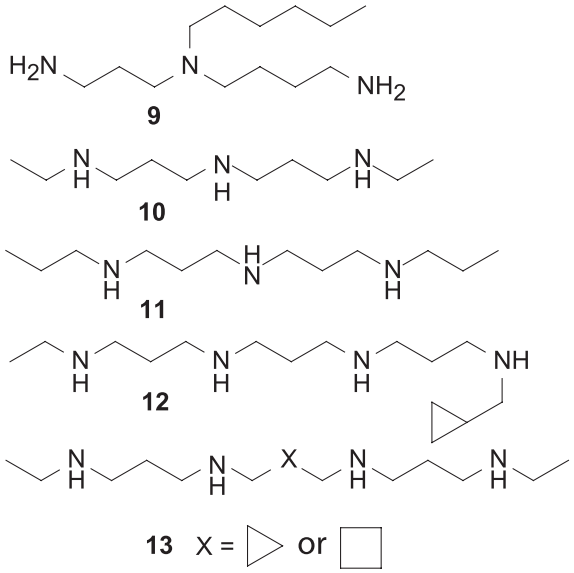

Fig. 4. *N*-alkyl and *N*-acyl derivatives of spermidine.

The best antiproliferative activity is exhibited by N^4- and N^1, N^8-alkyl substituted derivatives of spermidine, namely N^4-hexyl-, N^1, N^8-bis (ethyl) and N^1, N^8-bis (propyl) spermidines **9**–**11**.

Later, a wide variety of alkyl derivatives of biogenic polyamines were obtained and studied; among them, were asymmetric **12**, and conformationally hindered **13** derivatives of norspermine [50, 51].

Bis-alkylated, at the terminal amino groups, analogs of polyamines cause enhanced induction of the catabolytic enzyme SSAT, thereby depleting intracellular reserves of polyamines [52]. Moreover, methylated derivatives have a cytostatic effect, while ethyl and propyl analogs are characterized by a cytotoxic effect [53].

Also, in the context of structural analogy, it is worth mentioning the antidiarrheal activity of alkylated spermine analogs [54].

The greatest progress has been made for N^1N^{14}-diethylhomospermine (DENSpm); studies advanced to phase II clinical trials as an antineoplastic drug for patients with inoperable liver cancer, but clinical trials were stopped due to low efficacy and toxic effects on the central nervous system [55].

Heterochain analogs

Heterochain analogs of biogenic polyamines are structurally interesting since, in addition to methylene units and amino groups, atoms of oxygen, sulfur, silicon, etc. are included in the structure of the molecule (Fig. 5).

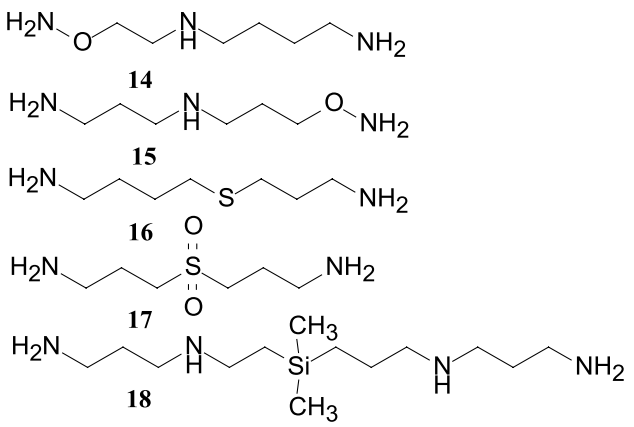

Fig. 5. Heterochain analogs of biogenic polyamines.

Khomutov and co-authors were among the first to demonstrate the inhibitory ability of the amino-hydroxy analogue of putrescine against ornithine decarboxylase (ODC), an enzyme of polyamine biosynthesis [56]. In their further studies, a series of amino-oxyanalogues of spermine and spermidine was synthesized, and it was found that analogs 1-Ao-Spd **14** and 8-Ao-Spd **15** compete with natural (unmodified) substrates to enter the cell. The study of the effect of **14** and **15** on the growth of the L1210 cell culture showed the absence of cytotoxicity and the presence of cytostatic effects IC_{50} = 70 and 100 μM for 1-Ao-Spd and 8-Ao-Spd, respectively. For the spermine analog (mono-Ao-Spm), the IC_{50} value was 500 μM [57–59].

Later [60], heterochain analogs containing sulfur **16**, oxygen, and sulfuryl group **17** were obtained. However, structures of this type were not widely used.

Organosilicon derivatives were obtained and investigated for antitumor activity on L1210 cancer lines and on transplanted Lewis lung carcinoma (DBA/2). The best results were achieved with the use of (6-amino-3-azagexyl), (7-amino-4-azageptyl)-dimethylsilane (AzhexAzhepSi) **18**, the introduction of two daily doses of 25 mmol/kg had a significant cytostatic effect. AzhexAzhepSi and difluoromethylornithine (DFMO) have a cumulative effect on tumor reduction. DFMO blocks putrescine synthesis from ornithine, while dimethylsilyl analogs inhibit the polyamine oxidase catabolic enzyme, thereby depleting the polyamine pool and accumulating "mimetics" in the cell [61].

ANTIBACTERIAL AND FUNGICIDAL ACTIVITY

Resistance development in bacterial pathogens to general antibiotics, is a big problem in modern medicine and pharmacology. To address the problem, immense research is aimed at formulating new antibacterial agents [62].

Potential antibacterial agents have been found in the metabolites of the sea sponge *Suberea ianthelliformis*, as reported by Xu in a study [63]. Structurally, these alkaloids are derivatives of polyamines—spermine and spermidine. According to [64], *Ianthelliformisamine A* **19** and *Ianthelliformisamine C* **20** (Fig. 6) demonstrate antibacterial activity against the gram-negative bacterium *P. aeruginosa*, the EC_{50} values are 7 μM and 9 μM, respectively.

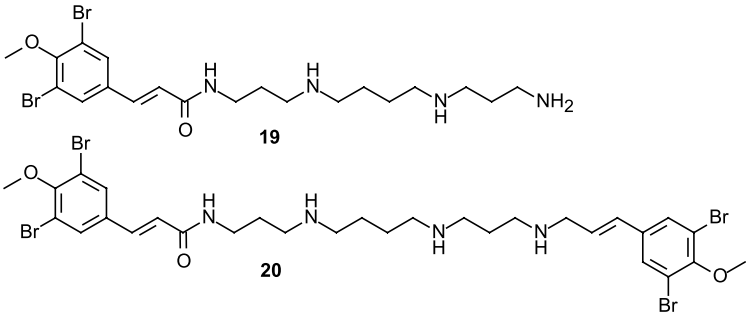

Fig. 6. *Ianthelliformisamine A* **19** and *Ianthelliformisamine C* **20**.

Khan [65] was the first to synthesize and study the antibacterial activity of several structural analogs of *Ianthelliformisamine A–C* (Fig. 7). The best results were demonstrated by samples **21** and **22**: the minimum inhibitory concentrations of MIC for *E. coli* are 1.2 and 0.15 μM, respectively; for *S. aureus* MIC = 0.12 and 0.15 μM, respectively.

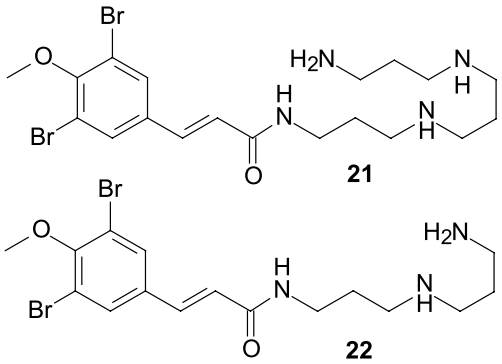

Fig. 7. Structural analogs of *Ianthelliformisamine A–C* (**21**, **22**).

Compounds **23**, **24** are similar analogs of the alkaloids of the sea sponge *Suberea ianthelliformis* (Fig. 8). They have good antibacterial activity against the gram-positive bacteria *S. intermedius* and *S. aureus*, the MIC values are 3.125 and 6.25 μM,

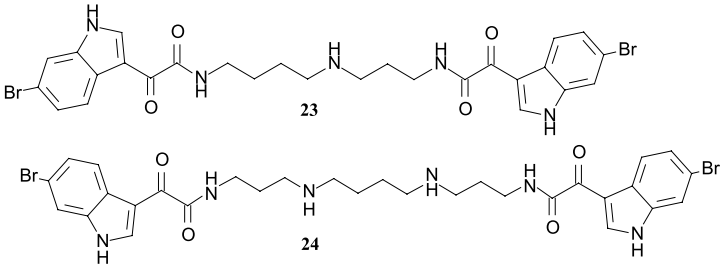

Fig. 8. Analogues **23**, **24** of the alkaloids of the sea sponge *Suberea ianthelliformis*.

respectively. Compound **23** has a strong fungicidal effect against *C. albicans* (MIC = 17.2 μM) and *C. neoformans* (MIC = 1.1 μM) [66].

Equally interesting antibacterial agents are analogs of motuporamine A (an alkaloid of the sea sponge *Xestosponga exigua*) containing a polyamine fragment (Fig. 9). Structures **25**, **26** have a strong antibacterial effect against staphylococci (*S. aureus* and *S. intermedius*), gram-positive enterococcus (*E. faecalis*), Escherichia coli (*E. coli*), and against gram-negative Pseudomonas aeruginosa (*P. aeruginosa*); MIC values are in the range from 1.56 to 12.5 μM [67].

It is also worth mentioning that bis-acetylated polyamines **29** have less pronounced antibacterial properties than previously described compounds. The authors note the possibility of using these structures as sensitizers of some bacterial pathogens, but their use is constrained by nonspecific toxicity [68].

Presumably, the mechanism of action of polyamine antibiotics is based on depolarization and/or disruption of the cell membrane integrity. The development of such structures might solve the problem of bacterial resistance [69].

ANTIPARASITIC ACTIVITY

A considerable danger, especially for the population of tropical and subtropical regions, is represented by vector-borne diseases, such as malaria and leishmaniosis, caused by the simplest parasitic organisms, including *P. falciparum*, *L. tropica*, *L. donovani*, *T. cruzi*, etc. Emergence of bacterial resistance to several conventional as well as modern drugs, such as solusurmin, chloroquine, primaquine, mefloquine, etc., has become a significant problem in medicine [70].

A new approach in the chemotherapy of such diseases may be the "polyamine pathway." Thus, unicellular parasites have an increased need for polyamines due to their tendency to proliferate. Interference with the metabolism of polyamines is likely to have a depressing effect on the vital activity of these microorganisms [71].

This was confirmed in [72]. Several bis(benzyl) polyamine analogs **30** with different chain lengths have been studied (Fig. 10), and the inhibitory effect (*in vivo*) on the growth of chloroquine-resistant *P. falciparum*.

According to the test results, the structure MDL 27695 (n = 7) has the best inhibitory effect against both chloroquine-resistant and chloroquine-sensitive *P. falciparum* strains. Later, the effectiveness of this compound against *L. donovani*, the causative agent of leishmaniasis, was confirmed [73]. A study [74] noted the possibility of using such analogs to combat African sleeping sickness caused by *T. cruzi* (Chagas disease).

In addition, the authors of a study [75] reported a similar antiparasitic activity of *N*, *N*-substituted analogs of biogenic diamines—putrescine and cadaverine.

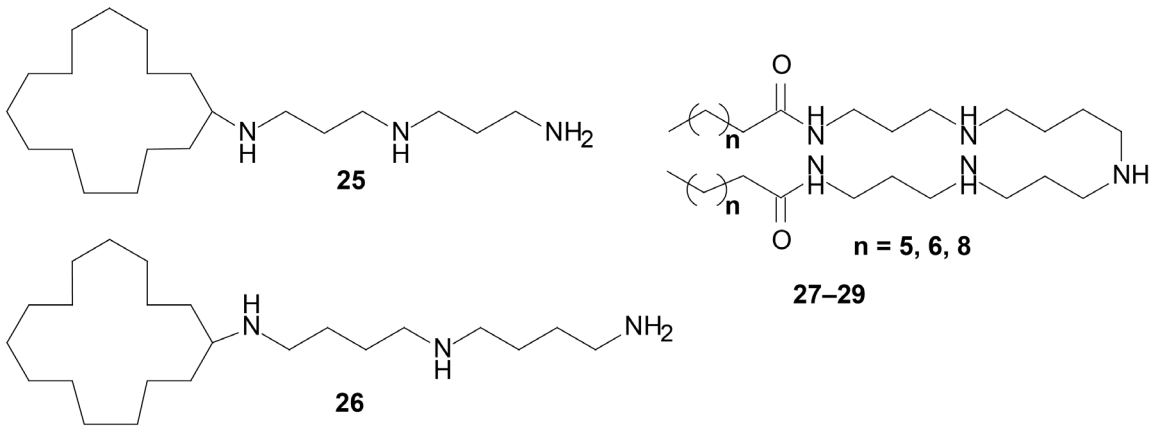

Fig. 9. Analogs of motuporamine A **25**, **26** and bis-acetylated polyamines **27**–**29**.

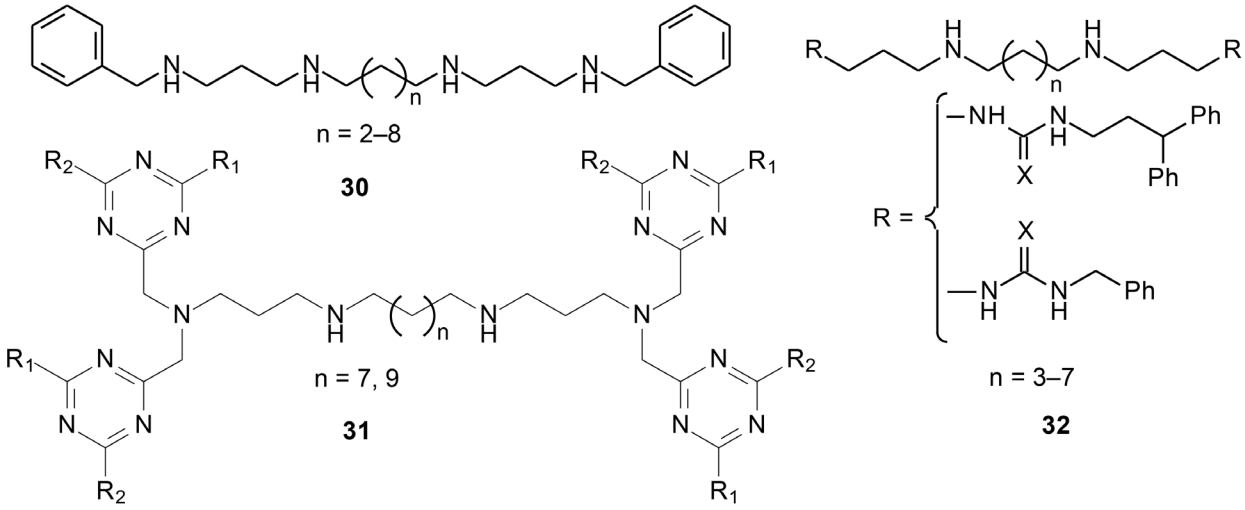

Fig. 10. Bis(benzyl)polyamine analogs **30**, 1,3,5-triazine-substituted polyamines **31**, bis(thiourea)derivatives of biogenic polyamines **32**.

1,3,5-triazine-substituted polyamines **31** exhibited antiplasmid activity against *P. falciparum*, as reported by Klenke [76]. Long-chain methylated structures (n = 9, R_1, R_2 = $NHCH_3$, $N(CH_3)_2$) showed the greatest antimalarial activity against *P. falciparum*; EC_{50} values are 0.0477 to 0.0698 for the NF54 line (wild type) and 0.0519 to 0.0622 for K1 (primaquine, chloroquine resistant), respectively. These structures also showed good activity against *T. cruzi* [77]. However, it is worth noting that the outstanding antiplasmid activity is weighed down by the presence of acute toxicity.

Another group of compounds for the suppression of vital activity of *P. falciparum*, includes bis(urea) and bis(thiourea) derivatives of biogenic polyamines **32**, the synthesis and biological tests of which are described in the work of Verlinden [78]. The best results were demonstrated by structures with a longer carbon chain (n = 6, 7), the EC_{50} value varied from 100 to 650 nM. In addition, the antimalarial effect was slightly higher in samples with diphenylpropylcarbamate fragments.

Niemand presented anthracene conjugates of biogenic polyamines (Fig. 11); investigated *in vitro* inhibitory effect on the growth of *P. falciparum* and some cancer cell lines. The best effect was demonstrated by N^1-[(anthracene-9-yl)methyl] butane-1,4-diamine **33**; the EC_{50} value for malaria plasmodium was 0.64 ± 0.04 mM [79].

The inhibitory effect on the development of *P. falciparum* is also exerted by 1,14-diphenylacetamide derivatives of spermine **34**, as reported previously [80].

What is also worth noting are the indoleglyoxamide analogs **35**, which have an aniplasmid effect, especially against *T. brucei*; EC_{50} values range from 0.18 to 0.27 mM [81].

In general, the antiparasitic effect of polyamine analogs is chemotherapeutic in nature. Disruption of metabolic processes caused by inhibition of enzymes of biosynthesis/catabolism of polyamines, as well as interaction with DNA/RNA, causes the death of pathogenic organisms [82].

ANTIARHYTHMIC ACTIVITY

In substances, structurally similar to biogenic polyamines, biological activities in relation to the cardiovascular system, can be explained based on the principle of structural similarity [83].

Thus, biogenic polyamines, localized in the cytoplasm, can modulate the activity of voltage-dependent sodium channels (Na_V), as reported by Huang and Moczydlowski in a study [84]. In the later work, the same authors compared the sensitivity of various isoforms of sodium channels (Na_V) in mammals and concluded that the cardiac canal (Na_V 1.5) is more sensitive to the blocking action of polyamines than other isoforms [85].

In addition to sodium channels, polyamines—spermine, spermidine along with Mg^{2+} cations, regulate the conductance of inward rectification potassium channels (Kir), eg. Kir 2.1 [86]. Modulation of these type of channels affects the heart rate, and the action potential of cardiomyocytes [87].

The hypothesis was confirmed in a study [88] wherein the antiarrhythmic activity of polyamine

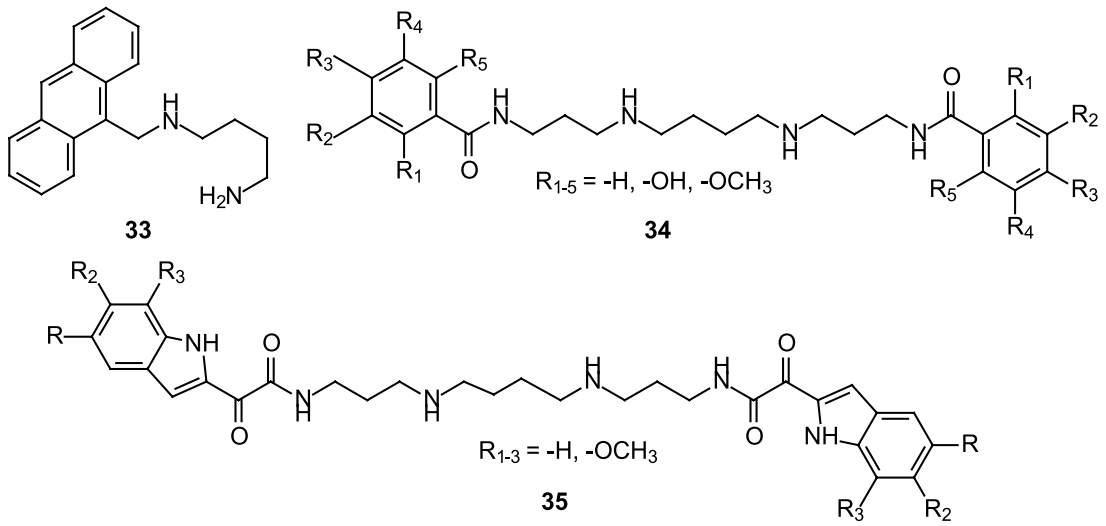

Fig. 11. N^1-[(anthracene-9-yl)methyl]butane-1,4-diamine **33**, 1,14-diphenylacetamide derivatives of spermine **34**, indoleglyoxamide analogs **35**.

analogs was studied in Wistar rats; ventricular fibrillation was provoked with isoprenaline. The highest antiarrhythmic activity was demonstrated by the structures PYR 3.3.3 and PYR 3.4.3 **36** (Fig. 12); when rats were administered a dose of 59 mmol/kg, the survival rate of the animals was 60%.

Another example of the antiarrhythmic effect of biogenic polyamine analogs is described in a study [89], in which the activity of linear methoxyphenyltriazaalkanes **37** was investigated.

Half-lethal doses (LD_{50}) for the intraperitoneal route of administration for the compounds ranged from 35.1 to 163.3 mg/kg. As per the aconite model of arrhythmia, structures containing two methylene units between amino groups (n = x = 2) were active, while for the calcium chloride model, molecules with three methylene units between nitrogen atoms (n = x = 3) were active, indicating different targets of impact. An exception is N^1-(2,3,4-trimethoxybenzyl)-N^2-{2-[(2,3,4-trimethoxybenzyl)amino]ethyl}-1,2-ethanediamine, which is active in all the studied models of arrhythmia. In addition, some compounds exhibited a statistically significant anti-ischemic effect, as confirmed in the isoprenaline model of ischemia.

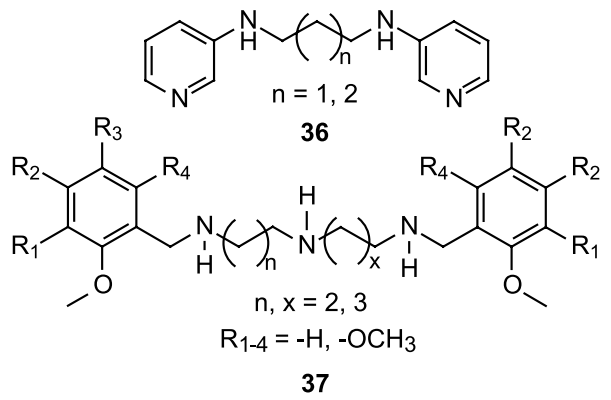

Fig. 12. PYR 3.3.3 and PYR 4.4.4 **36**, linear methoxyphenyltriazaalkanes **37**.

Several years of scientific research and a colossal amount of work have resulted in the development of a novel class of N-substituted aminoamides, potential new generation antiarrhythmic drugs.

These compounds **38** can be considered as derivatives of putrescine (n = 2), cadaverine (n = 3), or their analogs (n > 3) (Fig. 13) based on their structures.

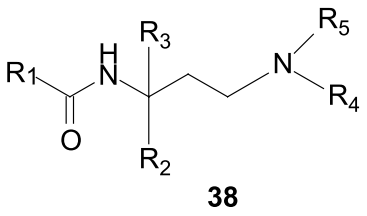

Fig. 13. Compounds **38**—derivatives of putrescine, cadaverine and their analogs.

Numerous works have aimed at developing and studying the biological action of a number of structures containing various substituents at the amine (NR_4R_5 = $N(CH_3)_2$, $N(C_2H_5)_2$, piperidyl, morpholino, $N(C_3H_7)_2$, $N(C_4H_9)_2$), amide (R_1 = CH_3, H, C_6H_5, $CH_2C_6H_5$, 1-adamantyl, cyclohexyl, etc.) groups and in the main chain of the molecule (R_2 = alkyl, C_6H_5, RC_6H_4; R_3 = H, alkyl) [90].

In the test results, it was found that these compounds are less toxic, highly active antiarrhythmic agents, as demonstrated in the aconite model of rat arrhythmia (the antiarrhythmic index values are an order of magnitude higher in comparison with novocainamide); half-lethal dose (LD_{50}) values for most compounds ranged from 110 to 940 mg/kg with the intraperitoneal administration [91].

NEUROPROTECTIVE ACTIVITY

Observing the effect of polyamines on ion channels, one cannot fail to note the ability of polyamines to modulate the *N*-methyl-D-aspartate receptor (NMDA receptor), one of the subtypes of ionotropic glutamate receptors (iGlu) [92], which plays an important role in neuronal communication, the mechanism of synaptic plasticity, and therefore, in the process of thinking and memory [93]. Disruption of the receptor function can lead to several pathological conditions, such as schizophrenia, neurodegenerative diseases, depressive disorders, etc. [94–96]. Since the discovery of the relationship between these disorders and iGlu receptors, several attempts have been made to develop pharmacological agents for the treatment and correction of such conditions.

Several studies [97–100] report the neuroprotective action of biogenic polyamines, such as putrescine, spermidine, and spermine, against various damages, including mechanical, neurotoxic, and ischemia. Thus, an ischemic stroke initiates excessive activation of excitatory synapses, accompanied with a steady influx of Ca^{2+} through glutamate receptors; an increase in the intracellular Ca^{2+} triggers neuronal death [101].

Polyamine analogs that can competitively bind to the NDMA receptor in comparison with glutamate are its antagonists and thus, may have a neuroprotective effect against some damages.

Sulfanyl derivatives of spermine (Fig. 14), N^1-dansylspermine (N^1-DnsSpm) **39** and N^1-(*n*-octosulfonyl) spermine (N^1-OsSpm) **40**, are able to inhibit NDMA NR1 and NR2A receptors several times stronger than spermine; this circumstance allows considering these compounds as potential neuroprotective agents [102, 103]. In addition, Kirby [104] reports that high doses of N^1-dansylspermine (N^1-DnsSpm) have an antiepileptic effect.

It is also worth mentioning anthracene **41** and anthraquinone **42** derivatives of spermine and homospermine, also potent antagonists, as demonstrated in [105] using recombinant NMDA receptors (NRs).

In addition to sulfanyl, anthracene, and anthraquinone derivatives, the literature also describes indane **43** [106], adamantane **44** [107], benzyl [108], and quinoline structures [109], based on fragments of biogenic polyamines.

Natural derivatives of polyamines—polyamine toxins—present in the venom of some insects and spiders deserve special attention (Fig. 15). Polyamine toxins **45** were first isolated from the venom of the spider *Argiope lobata* and characterized in a study [110]. Later, the ability of these compounds to act on the central nervous system of mammals was discovered. Polyamine toxins are generally non-selective (iGlu) receptor antagonists and the blocking effect is carried out by a non-competitive mechanism [111]. A similar mechanism is at the heart of the drug (Ebixa®) used for moderate to severe Alzheimer's dementia [112].

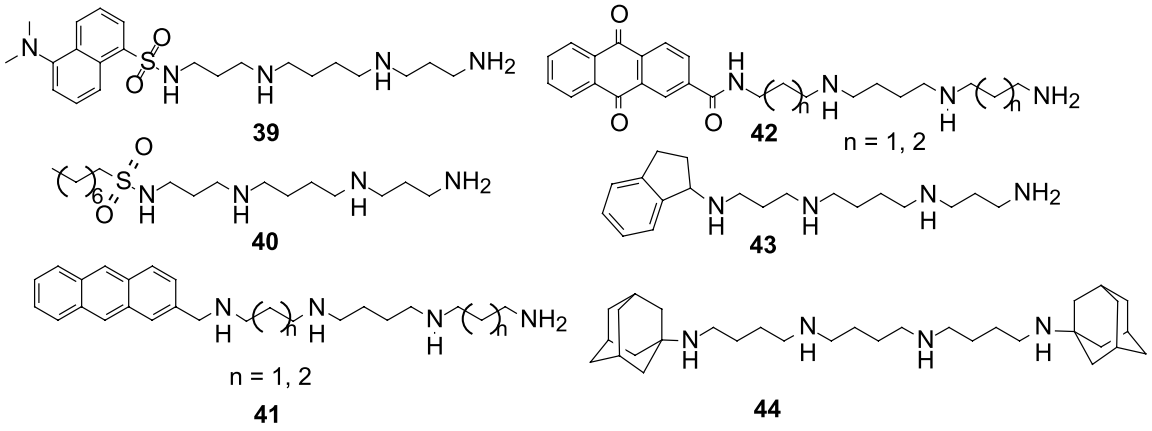

Fig. 14. Sulfanyl derivatives of spermine **39**, **40**, anthracene **41** and anthraquinone **42** derivatives of spermine and homospermine, indane **43**, adamantane **44** structures.

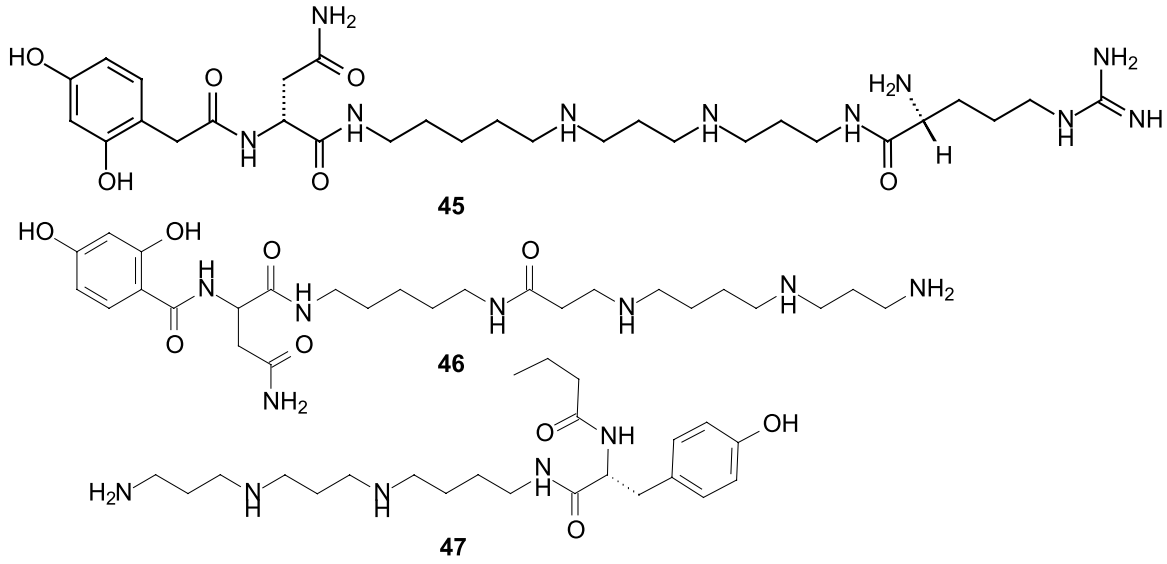

Fig. 15. Polyamine toxins found in spider **45**, **46** and wasp **47** venom.

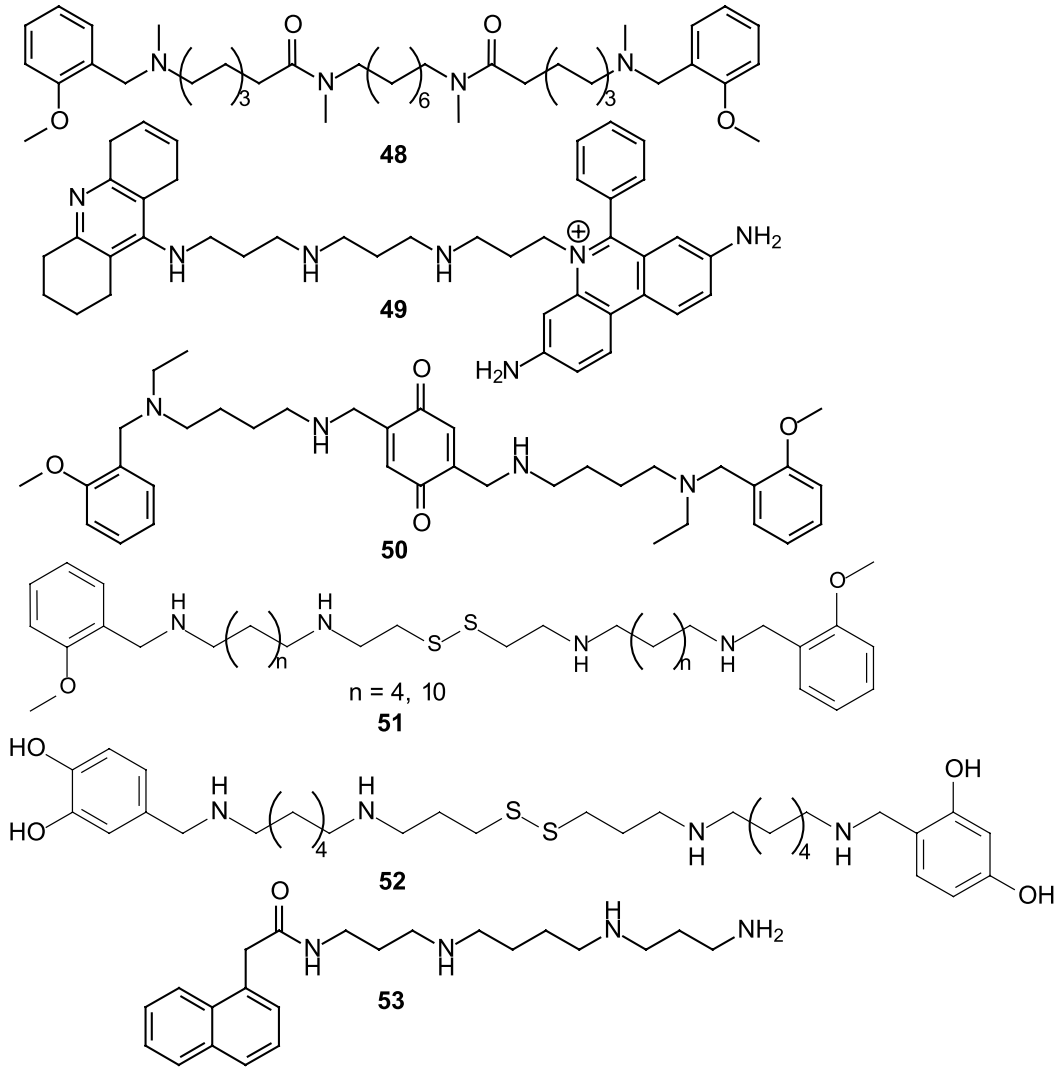

Fig. 16. Engineered structures to fight Alzheimer's disease.

Another example of a polyamine spider toxin is JSTX-3 **46**, isolated from the venom of *Nephila clavata*; JSTX-3 is able to noncompetitively block the AMPA glutamate receptor, providing neuroprotective effects [113]. In addition, the antiepileptic effect of this toxin was noted, as demonstrated *in vitro* on neurons of the human CA1 hippocampus [114].

The toxin PhTX-433 **47**, present in the venom of wasps of the species *Philanthus triangulum*, is a potent antagonist of AMPA and the kainate receptor [115]. Its strong blocking effect on nicotinic acetylcholine receptors (nACh) was also noted [116]. Their activity against iGlu receptors made it possible to use PhTX-433 to determine their subunit composition [117].

Interest in the structures and the associated biological action in the mammalian CNS were not limited to the natural polyamine toxins only. Attempts have been made to establish the structure-activity relationship [118], which led to the creation of several synthetic analogs—antagonists of glutamate [119, 120] and nicotinic acetylcholine [121, 122] receptors.

Moreover, it is necessary to consider compounds with potential therapeutic benefits in treating neurodegenerative diseases. A common feature for the diseases of this group is irreversible, progressive death of nerve cells with the onset of symptoms of impaired memory and motor functions. Currently, there are no drugs that can cure (prevent the pathological process) the patients suffering from diseases of this group. Moreover, the mechanisms underlying these disorders have not yet been established.

The pharmacology of neurodegenerative diseases is reduced to maintenance therapy. The main targets of exposure are ionotropic channels and conjugated enzymes of neurotransmitter degradation.

Below are the structures of the polyamine series that are of potential interest in the fight against these pathologies.

Based on the concept of multi-target-directed-ligands explained by Bolognesi [123], several structures **48**–**50** were designed to control the Alzheimer's disease (Fig. 16). All of them exhibited an inhibitory effect on acetylcholinesterase (AChE), slowing down the degradation of the main neurotransmitter, acetylcholine, with IC_{50} values ranging from 1.5 nM to 0.17 μM. In addition, the inhibitory effect of compounds **49**, **50**, and **53** was recorded [124] on the aggregation of amyloid protein (Aβ40), which has a destructive effect on the nervous tissue. The deposition of amyloid aggregates is among the main hypotheses regarding the mechanisms of Alzheimer's disease [125, 126].

Disulfide analogs of benextramine **51**, **52** (a known blocker of α-adrenergic receptors), have another target of action, different from the structures described above. Di Paolo demonstrated the ability of these compounds to inhibit human monoamine oxidase isoforms (MAO A and MAO B), one of the main enzymes of monoamine catabolism [127]. Biogenic monoamines—dopamine, serotonin, catecholamines—are the most important neurotransmitters, in the degradation of which MAO is involved.

Blocking the action of monoamine oxidase is an attractive target to fight neurodegenerative diseases, such as Parkinson's and Alzheimer's disease, as well as some neuropsychiatric disorders, including depression [128–130].

CONCLUSIONS

Research in the polyamine biochemistry will provide an in-depth understanding of the role of these compounds in the functioning of living systems—from primitive bacteria to humans. The study of the cellular transport of polyamines, their interactions with receptors, membranes, macromolecules of nucleic acids, and proteins, will significantly expand the arsenal of pharmacological agents to combat pathologies, such as oncological, cardiovascular and neuropsychiatric diseases.

Authors' contribution

The authors equally contributed to the research work, the arrangement of the materials and the technical design of the article were made by O.S. Egorov.

The authors declare no conflicts of interest.

REFERENCES

1. Shoji T., Hashimoto T. Polyamine-Derived Alkaloids in Plants: Molecular Elucidation of Biosynthesis. In: *Polyamines: A Universal Molecular Nexus for Growth, Survival, and Specialized Metabolism*. Tokyo, Japan: Springer; 2015. P. 189–200. https://doi.org/10.1007/978-4-431-55212-3_16

2. Kachel H.S., Buckingham S.D., Sattelle D.B. Insect toxins–selective pharmacological tools and drug/chemical leads. *Curr. Opin. Insect. Sci.* 2018;30:93–98. https://doi.org/10.1016/j.cois.2018.10.001

3. Fujiwara T., Hasegawa S., Hirashima N., Nakanishi M., Ohwada T. Gene transfection activities of amphiphilic steroid–polyamine conjugates. *Biochim. Biophys. Acta. Biomembr*. 2000;1468(1–2):396–402. https://doi.org/10.1016/S0005-2736(00)00278-9

4. Menzi M., Lightfoot H.L., Hall J. Polyamine–oligonucleotide conjugates: a promising direction for nucleic acid tools and therapeutics. *Future Med. Chem.* 2015;7(13):1733–1749. https://doi.org/10.4155/fmc.15.90

5. Pegg A.E. Functions of polyamines in mammals. *J. Biol. Chem.* 2016;291(29):14904–14912. https://doi.org/10.1074/jbc.r116.731661

6. Bachrach U. Naturally occurring polyamines: interaction with macromolecules. *Curr. Protein Pept. Sci.* 2005;6(6):559–566. https://doi.org/10.2174/138920305774933240

7. D'Agostino L., Di Pietro M., Di Luccia A. Nuclear aggregates of polyamines are supramolecular structures that play a crucial role in genomic DNA protection and conformation. *The FEBS J.* 2005;272(15):3777–3787. https://doi.org/10.1111/j.1742-4658.2005.04782.x

8. Douki T., Bretonniere Y., Cadet J. Protection against radiation-induced degradation of DNA bases by polyamines. *Radiat. Res.* 2000;153(1):29–35. https://doi.org/10.1667/0033-7587(2000)153[0029:PARIDO]2.0.CO;2

9. Rudolphi-Szydło E., Filek M., Dyba B., Miszalski Z., Zembala M. Antioxidative action of polyamines in protection of phospholipid membranes exposed to ozone stress. *Acta Biochim. Pol*. 2020;67(2):259–262. https://doi.org/10.18388/abp.2020_5230

10. Rosenheim O. The isolation of spermine phosphate from semen and testis. *Biochem. J.* 1924;18(6):1253–1262. https://doi.org/10.1042/bj0181253

11. Bachrach U. The early history of polyamine research. *Plant Physiol. Biochem.* 2010;48(7):490–495. https://doi.org/10.1016/j.plaphy.2010.02.003

12. Michael A.J. Polyamines in eukaryotes, bacteria, and archaea. *J. Biol. Chem.* 2016;291(29):14896–14903. https://doi.org/10.1074/jbc.R116.734780

13. Kuksa V., Buchan R., Lin P. K.T. Synthesis of polyamines, their derivatives, analogues and conjugates. *Synthesis.* 2000;2000(09):1189–1207. https://doi.org/10.1055/s-2000-6405

14. Gupta K., Dey A., Gupta B. Plant polyamines in abiotic stress responses. *Acta Physiol. Plant.* 2015;35(7):2015–2036. https://doi.org/10.1007/s11738-013-1239-4

15. Urdiales J.L., Medina M.A., Sanchez-Jimenez F. Polyamine metabolism revisited. *Eur. J. Gastroenterol. Hepatol.* 2001;13(9):1015–1019. https://doi.org/10.1097/00042737-200109000-00003

16. Mimitsuka T., Sawai H., Hatsu M., Yamada K. Metabolic engineering of Corynebacterium glutamicum for cadaverine fermentation. *Biosci. Biotechnol. Biochem.* 2007;71(9):2130–2135. https://doi.org/10.1271/bbb.60699

17. Chou, H.T., Li, J.Y., Peng, Y.C., Lu, C.D. Molecular characterization of PauR and its role in control of putrescine and cadaverine catabolism through the γ-glutamylation pathway in Pseudomonas aeruginosa PAO1. *J. Bacteriol.* 2013;195(17):3906–3913. https://doi.org/10.1128/jb.00275-13

18. Konishi H., Nakajima T., Sano I. Metabolism of putrescine in the central nervous system. *J. Biochem.* 1977;81(2):355–360. https://doi.org/10.1093/oxfordjournals.jbchem.a131466

19. Casero Jr R.A., Pegg A.E. Spermidine/spermine N^1-acetyltransferase—the turning point in polyamine metabolism. *Faseb J.* 1993;7(8):653–66. https://doi.org/10.1096/fasebj.7.8.8500690

20. Vujcic S., Diegelman P., Bacchi C.J., Kramer D.L., Porter C.W. Identification and characterization of a novel flavin-containing spermine oxidase of mammalian cell origin. *Biochem. J.* 2002;367(3):665–675. https://doi.org/10.1042/bj20020720

21. Takao K., Sugita Y. Pentamine as a Substrate for Measuring Spermine Oxidase Activity. In: *Polyamines: Methods and Protocols*. New York, USA: Humana Press; 2018. P. 149–154. https://doi.org/10.1007/978-1-4939-7398-9_15

22. Casero Jr R.A., Pegg A.E. Polyamine catabolism and disease. *Biochem. J.* 2009;421(3):323–338. https://doi.org/10.1042/bj20090598

23. Seiler N., Eichentopf B. 4-Aminobutyrate in mammalian putrescine catabolism. *Biochem. J.* 1975;152(2):201–210. https://doi.org/10.1042/bj1520201

24. Burkard W.P., Gey K.F., Pletscher A. Diamine oxidase in the brain of vertebrates. *J. Neurochem.* 1963;10(3):183–186. https://doi.org/10.1111/j.1471-4159.1963.tb09481.x

25. Seiler N., Schmidt-Glenewinkel T., Sarhan S. On the formation of γ-aminobutyric acid from putrescine in brain. *J. Biochem.* 1979;86(1):277–278.

26. Seiler N., Lamberty U., Al-Therib M.J. Acetyl-Coenzyme A:1, 4-diaminobutane *N*-acetyltransfetase: activity in rat brain during development, in experimental brain tumors and in brains of fish of different metabolic activity. *J. Neurochem.* 1975;24(4):797–800.

27. Seiler N., Al-Therib M.J. Acetyl-CoA:1, 4-diaminobutane *N*-acetyltransferase occurence in vertebrate organs and subcellular localization. *Biochim. Biophys. Acta. Gen. Subj.* 1974;354(2):206–212. https://doi.org/10.1016/0304-4165(74)90007-5

28. Sessa A., Perin A. Diamine oxidase in relation to diamine and polyamine metabolism. *Agents and Actions.* 1994;43(1–2):69–77. https://doi.org/10.1007/BF02005768

29. Missala K., Sourkes T.L., Putrescine catabolism in rats given heparin or aminoguanidine. *Eur. J. Pharmacol.* 1980;64(4):307–311. https://doi.org/10.1016/0014-2999(80)90238-1

30. Schayer R.W., Smiley R.L., Kennedy J. Diamine oxidase and cadaverine metabolism. *J. Biol. Chem.* 1954;206(1):461–464.

31. Ekegren T., Gomes-Trolin C., Nygren I., Askmark H. Maintained regulation of polyamines in spinal cord from patients with amyotrophic lateral sclerosis. *J. Neurol. Sci.* 2004;222(1–2):49–53. https://doi.org/10.1016/j.jns.2004.04.011

32. Ekegren T., Gomes-Trolin C. Determination of polyamines in human tissues by precolumn derivatization with 9-fluorenylmethyl chloroformate and high-performance liquid chromatography. *Anal. Biochem.* 2005;338(2):179–185. https://doi.org/10.1016/j.ab.2004.11.040

33. Wallace H.M., Fraser A.V. Inhibitors of polyamine metabolism. *Amino acids.* 2004;26(4):353–365. https://doi.org/10.1007/s00726-004-0092-6

34. Palmer A.J., Wallace H.M. The polyamine transport system as a target for anticancer drug development. *Amino acids.* 2010;38(2):415–422. https://doi.org/10.1007/s00726-009-0400-2

35. Bardocz S., Grant G., Brown D.S., Pusztai A. Polyamines in food—implications for growth and health. *J. Nutr. Biochem.* 1993;4(2):66–71. https://doi.org/10.1016/0955-2863(93)90001-D

36. Ask A., Persson L., Heby O. Increased survival of L1210 leukemic mice by prevention of the utilization of extracellular polyamines. Studies using a polyamineuptake mutant, antibiotics and a polyamine-deficient diet. *Cancer Lett.* 1992;66(1):29–34. https://doi.org/10.1016/0304-3835(92)90276-2

37. Igarashi K., Ito K., Kashiwagi K. Polyamine uptake systems in *Escherichia coli*. *Res. Microbiol.* 2001;152(3–4):271–278. https://doi.org/10.1016/S0923-2508(01)01198-6

38. Poulin R., Casero R.A., Soulet D. Recent advances in the molecular biology of metazoan polyamine transport. *Amino acids.* 2012;42(2–3):711–723. https://doi.org/10.1007/s00726-011-0987-y

39. Soulet D., Gagnon B., Rivest S., Audette M., Poulin R. A fluorescent probe of polyamine transport accumulates into intracellular acidic vesicles via a two-step mechanism. *J. Biol. Chem.* 2004;279(47):49355–49366. https://doi.org/10.1074/jbc.M401287200

40. Belting M., Mani K., Jönsson M., Cheng F., Sandgren S., Jonsson S., Ding K., Delcros J., Fransson L. Glypican-1 is a vehicle for polyamine uptake in mammalian cells a pivotal role for nitrosothiol-derived nitric oxide. *J. Biol. Chem.* 2003;278(47):47181–47189. https://doi.org/10.1074/jbc.M308325200

41. Uemura T., Yerushalmi H.F., Tsaprailis G., Stringer D.E., Pastorian K.E., Hawel L., Byus C.V., Gerner E.W. Identification and characterization of a diamine exporter in colon epithelial cells. *J. Biol. Chem.* 2008;283(39):26428–26435. https://doi.org/10.1074/jbc.M804714200

42. Bachrach U., Seiler N. Formation of acetylpolyamines and putrescine from spermidine by normal and transformed chick embryo fibroblasts. *Cancer Res.* 1981;41(3):1205–1208.

43. Israel M., Rosenfield J.S., Modest E.J. Analogs of Spermine and Spermidine. I. Synthesis of Polymethylenepolyamines by Reduction of Cyanoethylated α, ι-Alkylenediamines1,2. *J. Med. Chem.* 1964;7(6):710–716. https://doi.org/10.1021/jm00336a006

44. Maddock C. L., D'Angio G.J., Farber S., Handler A.H. Biological studies of Actinomycin D. *Ann. N. Y. Acad. Sci.* 1960;89(2):386–398. https://doi.org/10.1111/j.1749-6632.1960.tb20162.x

45. Serre D., Erbek S., Berthet N., Ronot X., Martel-Frachet V., Thomas F. Copper(II) complexes of N_3O tripodal ligands appended with pyrene and polyamine groups: anti-proliferative and nuclease activities. *J. Inorg. Biochem*. 2018;179:121–134. https://doi.org/10.1016/j.jinorgbio.2017.11.006

46. Silva T.M., Andersson S., Sukumaran S.K., Marques M.P., Persson L., Oredsson S. Norspermidine and novel Pd(II) and Pt(II) polynuclear complexes of norspermidine as potential antineoplastic agents against breast cancer. *PLoS One.* 2013;8(2):e55651. https://doi.org/10.1371/journal.pone.0055651

47. Seiler N. Thirty years of polyamine-related approaches to cancer therapy. Retrospect and prospect. Part 1. Selective enzyme inhibitors. *Curr. Drug. Targets*. 2003;4(7):537–564. https://doi.org/10.2174/1389450033490885

48. Porter C.W., Cavanaugh P.F., Stolowich N., Ganis B., Kelly E., Bergeron R.J. Biological properties of N^4-and N^1, N^8-spermidine derivatives in cultured L1210 leukemia cells. *Cancer Res.* 1985;45(5):2050–2057.

49. Porter C.W., Berger F.G., Pegg A.E., Ganis B., Bergeron R.J. Regulation of ornithine decarboxylase activity by spermidine and the spermidine analogue N^1,N^8-bis(ethyl)-spermidine. *Biochem. J.* 1987;242(2):433–440. https://doi.org/10.1042/bj2420433

50. Saab N.H., West E.E., Bieszk N.C., Preuss C.V., Mank A.R., Casero Jr R.A., Woster P.M. Synthesis and evaluation of unsymmetrically substituted polyamine analogs as modulators of human spermidine/spermine-N^1-acetyltransferase (SSAT) and as potential antitumor agents. *J. Med. Chem*. 1993;36(20):2998–3004. https://doi.org/10.1021/jm00072a020

51. Reddy V.K., Valasinas A., Sarkar A., Basu H.S., Marton L.J., Frydman B. Conformationally restricted analogues of ^1N,^{12}N-bisethylspermine:synthesis and growth inhibitory effects on human tumor cell lines. *J. Med. Chem.* 1998;41(24):4723–4732. https://doi.org/10.1021/jm980172v

52. Valasinas A., Sarkar A., Reddy V.K., Marton L.J., Basu H. S., Frydman, B. Conformationally restricted analogues of ^1N,^{14}N-bisethylhomospermine (BE-4-4-4): synthesis and growth inhibitory effects on human prostate cancer cells. *J. Med. Chem.* 2001;44(3):390–403. https://doi.org/10.1021/jm000309t

53. Zagaja G.P., Shrivastav M., Marton L.J., Rinker-Schaeffer C.W., Dolan M.E., Fleig M.F. Effects of polyamine analogues on prostatic adenocarcinoma cells *in vitro* and *in vivo*. *Cancer Chemother. Pharmacol.* 1998;41(6):505–512. https://doi.org/10.1007/s002800050774

54. Bergeron R.J., Wiegand J., McManis J.S., Weimar W.R., Smith R.E., Algee S.E., Fannin T.L., Slusher M.A., Snyder P.S. Polyamine analogue antidiarrheals: a structure-activity study. *J. Med. Chem*. 2001;44(2):232–244. https://doi.org/10.1021/jm000277+

55. Wolff A.C., Armstrong D.K., Fetting J.H., Carducci M.K., Riley C.D., Bender J.F., Casero Jr. R.A., Davidson N.E. A Phase II study of the polyamine analog N^1,N^{11}-diethylnorspermine (DENSpm) daily for five days every 21 days in patients with previously treated metastatic

breast cancer. *Clin. Cancer Res.* 2003;9(16):5922–5928.

56. Khomutov R.M., Denisova G.F., Khomutov A.R., Belostotskaya K.M., Shlosman R.B., Artamonova E.Yu. Aminooxypropylamine is an effective inhibitor of ornithine decarboxylase *in vitro* and *in vivo*. *Bioorganicheskya Khimiya = Russian Journal of Bioorganic Chemistry*. 1985;11(11):1574–1576 (in Russ.).

57. Khomutov A.R., Shvetsov A.S., Vepsalainen J., Kramer D.L., Porter C.W., Hyvonen T., Keinanen T., Eloranta T.O., Khomutov R.M. New aminooxy analogs of biogenic polyamines. *Russ. J. Bioorganic Chem*. 1996;22(7):476–478.

58. Eloranta T.O., Khomutov A.R., Khomutov R.M., Hyvönen T. Aminooxy analogues of spermidine as inhibitors of spermine synthase and substrates of hepatic polyamine acetylating activity. *J. Biochem*. 1990;108(4):593–598.

59. Khomutov M.A., Weisell J., Hyvönen M., Keinänen T.A., Vepsäläinen J., Alhonen L., Khomutov A.R., Kochetkov S.N. Hydroxylamine derivatives for regulation of spermine and spermidine metabolism. *Biochemistry* (*Moscow*). 2013;78(13):1431–1446 https://doi.org/10.1134/S0006297913130051

60. Edwards M.L., Prakash N.J., Stemerick D.M., Sunkara S.P., Bitonti A.J., Davis G.F., Dumont J.A., Bey P. Polyamine analogs with antitumor activity. *J. Med. Chem*. 1990;33(5):1369–1375. https://doi.org/10.1021/jm00167a014

61. Seiler N., Douaud F., Havouis R., LeRoch N., Renault J., Vaultier M., Moulinoux J. Dimethylsilane polyamines, a new class of potential anticancer drugs. *Int. J. Oncol*. 1997;11(4):835–841. https://doi.org/10.3892/ijo.11.4.835

62. Levy S. B. Antibiotic resistance—the problem intensifies. *Adv. Drug Deliv. Rev.* 2005;57(10):1446–1450. https://doi.org/10.1016/j.addr.2005.04.001

63. Xu M., Davis R.A., Feng Y., Sykes M.L., Shelper T., Avery V.M., Camp D., Quinn R.J. Ianthelliformisamines A–C, antibacterial bromotyrosine-derived metabolites from the marine sponge Suberea ianthelliformis. *J. Nat. Prod*. 2012;75(5):1001–1005. https://doi.org/10.1021/np300147d

64. Choudhary A., Naughton L.M., Montánchez I., Dobson A.D., Rai D.K. Current status and future prospects of marine natural products (MNPs) as antimicrobials. *Mar. Drugs.* 2017;15(9):272. https://doi.org/10.3390/md15090272

65. Khan F.A., Ahmad S., Kodipelli N., Shivange G., Anindya R. Syntheses of a library of molecules on the marine natural product ianthelliformisamines platform and their biological evaluation. *Org. Biomol. Chem*. 2014;12(23):3847–3865. https://doi.org/10.1039/C3OB42537A

66. Li S.A., Cadelis M.M., Sue K., Blanchet M., Vidal N., Brunel J.M., Bourguet-Kondracki M., Copp B.R. 6-Bromoindolglyoxylamido derivatives as antimicrobial agents and antibiotic enhancers. *Bioorg. Med. Chem.* 2019;27(10):2090–2099. https://doi.org/10.1016/j.bmc.2019.04.004

67. Borselli D., Blanchet M., Bolla J.M., Muth A., Skruber K., Phanstiel IV, O., Brunel J.M. Motuporamine Derivatives as Antimicrobial Agents and Antibiotic Enhancers against Resistant Gram-Negative Bacteria. *ChemBioChem*. 2017;18(3):276–283. https://doi.org/10.1002/cbic.201600532

68. Balakrishna R., Wood S.J., Nguyen T.B., Miller K.A., Kumar E.S., Datta A., David S.A. Structural correlates of antibacterial and membrane-permeabilizing activities in acylpolyamines. *Antimicrob. Agents Chemother.* 2006;50(3):852–861. https://doi.org/10.1128/aac.50.3.852-861.2006

69. Blanchet M., Borselli D., Brunel J.M. Polyamine derivatives: a revival of an old neglected scaffold to fight resistant Gram-negative bacteria? *Future. Med. Chem.* 2016;8(9):963–973. https://doi.org/10.4155/fmc-2016-0011

70. Laurence D.R., Bennett P.N. *Clinical Pharmacology.* Edinburgh, London, and New York: Churchill Livingstone; 1987. V. 1. 788 p.

71. Marton L.J., Pegg A.E. Polyamines as targets for therapeutic intervention. *Annu. Rev. Pharmacol. Toxicol.* 1995;35(1):55–91. https://doi.org/10.1146/annurev.pa.35.040195.000415

72. Bitonti A.J., Dumont J.A., Bush T.L., Edwards M.L., Stemerick D.M., McCann P.P., Sjoerdsma A. Bis(benzyl)polyamine analogs inhibit the growth of chloroquine-resistant human malaria parasites (*Plasmodium falciparum*) *in vitro* and in combination with alpha-difluoromethylornithine cure murine malaria. *PNAS USA.* 1989;86(2):651–655. https://doi.org/10.1073/pnas.86.2.651

73. Baumann R.J., Hanson W.L., McCann P.P., Sjoerdsma A., Bitonti A.J. Suppression of both antimony-susceptible and antimony-resistant *Leishmania donovani* by a bis(benzyl)polyamine analog. *Antimicrob. Agents Chemother.* 1990;34(5):722–727. https://doi.org/10.1128/aac.34.5.722

74. Baumann R.J., McCann P.P., Bitonti A.J. Suppression of *Leishmania donovani* by oral administration of a bis(benzyl)polyamine analog. *Antimicrob. Agents Chemother.* 1991;35(7):1403–1407. https://doi.org/10.1128/aac.35.7.1403

75. Majumder S., Kierszenbaum F. Inhibition of host cell invasion and intracellular replication of *Trypanosoma cruzi* by *N*,*N*'-bis(benzyl)-substituted polyamine analogs. *Antimicrob. Agents Chemother.* 1993;37(10):2235–2238. https://doi.org/10.1128/AAC.37.10.2235

76. Labadie G.R., Choi S.R., Avery M.A. Diamine derivatives with antiparasitic activities. *Bioorganic Med. Chem. Lett.* 2004;14(3):615-619. https://doi.org/10.1016/j.bmcl.2003.11.055

77. Klenke B., Barrett M.P., Brun R., Gilbert I.H. Antiplasmodial activity of a series of 1,3,5-triazine-substituted polyamines. *J. Antimicrob. Chemother.* 2003;52(2):290–293. https://doi.org/10.1093/jac/dkg307

78. Verlinden B.K., De Beer M., Pachaiyappan B., Besaans E., Andayi W.A., Reader J., Niemand J., Biljon R., Guy K., Egan T., Woster P.M., Birkholtz L.M. Interrogating alkyl and arylalkylpolyamino (bis)urea and (bis)thiourea isosteres as potent antimalarial chemotypes against multiple lifecycle forms of *Plasmodium falciparum* parasites. *Bioorg. Med. Chem.* 2015;23(16):5131–5143. https://doi.org/10.1016/j.bmc.2015.01.036

79. Niemand J., Burger P., Verlinden B.K., Reader J., Joubert A.M., Kaiser A., Louw A.I., Kirk K., Phanstiel IV O., Brikholtz L. Anthracene-polyamine conjugates inhibit *in vitro* proliferation of intraerythrocytic *Plasmodium falciparum* parasites. *Antimicrob. Agents Chemother*. 2013;57(6):2874–2877. https://doi.org/10.1128/aac.00106-13

80. Liew L.P., Pearce A.N., Kaiser M., Copp B.R. Synthesis and *in vitro* and *in vivo* evaluation of antimalarial polyamines. *Eur. J. Med. Chem.* 2013;69:22–31. https://doi.org/10.1016/j.ejmech.2013.07.055

81. Wang J., Kaiser M., Copp B.R. Investigation of indolglyoxamide and indolacetamide analogues of polyamines as antimalarial and antitrypanosomal agents. *Mar. Drugs.* 2014;12(6):3138–3160. https://doi.org/10.3390/md12063138

82. El Bissati K., Redel H., Ting L.M., Lykins J.D., McPhillie M.J., Upadhya R., Woster P.M., Yarlett N., Kim K., Weiss L.M. Novel synthetic polyamines have potent antimalarial activities *in vitro* and *in vivo* by decreasing intracellular spermidine and spermine concentrations. *Front. Cell. Infect. Microbiol*. 2019;9:9. https://doi.org/10.3389/fcimb.2019.00009

83. Eckert H., Bajorath J. Molecular similarity analysis in virtual screening: foundations, limitations and novel approaches. *Drug Discov. Today.* 2007;12(5–6):225–233. https://doi.org/10.1016/j.drudis.2007.01.011

84. Huang C.J., Moczydlowski E. Cytoplasmic polyamines as permeant blockers and modulators of the voltage-gated sodium channel. *Biophys. J.* 2001;80(3):1262–1279. https://doi.org/10.1016/S0006-3495(01)76102-4

85. Fu L.Y., Cummins T.R., Moczydlowski E.G. Sensitivity of cloned muscle, heart and neuronal voltage-gated sodium channels to block by polyamines: a possible basis for modulation of excitability *in vivo*. *Channels*. 2012;6(1):41–49. https://doi.org/10.4161/chan.19001

86. Nichols C.G., Lee S. Polyamines and potassium channels: A 25-year romance. *J. Biol. Chem.* 2018;293(48):18779–18788. https://doi.org/10.1074/jbc.tm118.003344

87. Melnikov K.N., Vislobokov A.I., Kolpakova M.E., Borisova V.A., Ignatov Yu.D. Potassium of ionic channels of cellular membranes. *Obzory po klinicheskoy farmakologii i lekarstvennoy terapii = Reviews on clinical pharmacology and drug therapy.* 2009;7(1):3–27 (in Russ.).

88. Bergeron R.J., Wiegand J., Weimar W.R., Snyder P.S. Polyamine analogue antiarrhythmics. *Pharmacol. Res.* 1998;38(5):367–380. https://doi.org/10.1006/phrs.1998.0384

89. Mokrov G.V., Likhosherstov A.M., Barchukov V.V., Stolyaruk V.N., Tsorin I.B., Vititnova M.B., Kryzhanovskii S.A., Gudasheva T.A., Seredenin S.B. Synthesis and Cardiotropic Activity of Linear Methoxyphenyltriazaalkanes. *Pharm. Chem. J.* 2019;53(6):500–506. https://doi.org/10.1007/s11094-019-02027-7

90. Borisova E.Ya., Afanas'eva E.Yu., Borisova N.Yu., Arzamastsev E.V., Cherkashin M.I. New generation antiarrhythmic remedies of the *N*-substituted amidoamines class. *Drug design. Mikroelementy v meditsine = Trace elements in medicine* (*Moscow*). 2005;6(3):56–61 (in Russ.).

91. Afanas'eva E.Yu., Borisova E.Ya., Arzamastsev E.V., Borisova N.Yu., Cherkashin M.I. Toxicity of novel functionally substituted amines. *Mikroelementy v meditsine = Trace elements in medicine* (*Moscow*). 2005;6(3):74–77 (in Russ.).

92. Williams K., Zappia A.M., Pritchett D.B., Shen Y.M., Molinoff P.B. Sensitivity of the *N*-methyl-d-aspartate receptor to polyamines is controlled by NR_2 subunits. *Mol. Pharmacol.* 1994;45(5):803–809.

93. Hansen K.B., Yi F., Perszyk R.E., Furukawa H., Wollmuth L.P., Gibb A.J., Traynelis S.F. Structure, function, and allosteric modulation of NMDA receptors. *J. Gen. Physiol.* 2018;150(8):1081–1105. https://doi.org/10.1085/jgp.201812032

94. Kristiansen L.V., Huerta I., Beneyto M., Meador-Woodruff J.H. NMDA receptors and schizophrenia. *Curr. Opin. Pharmacol*. 2007;7(1):48–55. https://doi.org/10.1016/j.coph.2006.08.013

95. Wang R., Reddy P.H. Role of glutamate and NMDA receptors in Alzheimer's disease. *J. Alzheimer's Dis.* 2017;57(4):1041–1048. https://doi.org/10.3233/JAD-160763

96. Massey P.V., Johnson B.E., Moult P.R., Auberson Y.P., Brown M.W., Molnar E., Collingridge G.L., Bashir Z.I. Differential roles of NR_2A and NR_2B-containing NMDA receptors in cortical long-term potentiation and long-term depression. *J. Neurosci*. 2004;24(36):7821–7828. https://doi.org/10.1523/jneurosci.1697-04.2004

97. Adibhatla R.M., Hatcher J.F., Sailor K., Dempsey R.J. Polyamines and central nervous system injury: spermine and spermidine decrease following transient focal cerebral ischemia in spontaneously hypertensive rats. *Brain Res.* 2002;938(1–2):81–86. https://doi.org/10.1016/s0006-8993(02)02447-2

98. Harada J., Sugimoto M. Polyamines prevent apoptotic cell death in cultured cerebellar granule neurons. *Brain Res.* 1997;753(2):251–259. https://doi.org/10.1016/S0006-8993(97)00011-5

99. Kish S.J., Wilson J.M., Fletcher P.J. The polyamine synthesis inhibitor α-difluoromethylornithine is neuroprotective against *N*-methyl-D-aspartate-induced brain damage *in vivo*. *Eur. J. Pharmacol.* 1991;209(1–2):101–103. https://doi.org/10.1016/0014-2999(91)90017-k

100. Sparapani M., Dall'Olio R., Gandolfi O., Ciani E., Contestabile A. Neurotoxicity of polyamines and pharmacological neuroprotection in cultures of rat cerebellar granule cells. *Exp. Neurol.* 1997;148(1):157–166. https://doi.org/10.1006/exnr.1997.6627

101. Benveniste H., Jørgensen M.B., Diemer N.H., Hansen A.J. Calcium accumulation by glutamate receptor activation is involved in hippocampal cell damage after ischemia. *Acta Neurol. Scand.* 1988;78(6):529–536. https://doi.org/10.1111/j.1600-0404.1988.tb03697.x

102. Chao J., Seiler N., Renault J., Kashiwagi K., Masuko T., Igarashi K., Williams K. N^1-Dansyl-Spermine and N^1-(*n*-Octanesulfonyl)-Spermine, Novel Glutamate Receptor Antagonists: Block and Permeation of *N*-Methyl-D-Aspartate Receptors. *Mol. Pharmacol.* 1997;51(5):861–871. https://doi.org/10.1124/mol.51.5.861

103. Seiler N., Douaud F., Renault J., Delcros J.G., Havouis R., Uriac P., Moulinoux J.P. Polyamine sulfonamides with NMDA antagonist properties are potent calmodulin antagonists and cytotoxic agents. *Int. J. Biochem. Cell Biol.* 1998;30(3):393–406. https://doi.org/10.1016/s1357-2725(97)00150-7

104. Kirby B.P., Shaw G.G. Effect of spermine and N^1-dansyl-spermine on epileptiform activity in mouse cortical slices. *Eur. J. Pharmacol*. 2005;524(1–3):53–59. https://doi.org/10.1016/j.ejphar.2005.09.009

105. Jin L., Sugiyama H., Takigawa M., Katagiri D., Tomitori H., Nishimura K., Kaur N., Phanstiel O., Kitajima M., Takayama H., Okawara T., Williams K., Kashiwagi K., Igarashi K. Comparative studies of anthraquinone- and anthracene-tetraamines as blockers of *N*-methyl-D-aspartate receptors. *J. Pharmacol. Exp. Ther.* 2007;320(1):47–55. https://doi.org/10.1124/jpet.106.110528

106. Gilad G.M., Gilad V.H. Novel polyamine derivatives as neuroprotective agents. *J. Pharmacol. Exp. Ther.* 1999;291(1):39–43.

107. Kumamoto T., Nakajima M., Uga R., Ihayazaka N., Kashihara H., Katakawa K., Ishikawa T., Saiki R., Nishimura K., Igarashi K. Design, synthesis, and evaluation of polyamine-memantine hybrids as NMDA channel blockers. *Bioorg. Med. Chem*. 2018;26(3):603–608. https://doi.org/10.1016/j.bmc.2017.12.021

108. Igarashi K., Shirahata A., Pahk A.J., Kashiwagi K., Williams K. Benzyl-polyamines: Novel, Potent *N*-Methyl-D-aspartate Receptor Antagonists. *J. Pharmacol. Exp. Ther.* 1997;283(2):533–540.

109. Cen J., Liu L., He L., Liu M., Wang C.J., Ji B.S. N^1-(quinolin-2-ylmethyl)butane-1,4-diamine, a polyamine analogue, attenuated injury in *in vitro* and *in vivo* models of cerebral ischemia. *Int. J. Dev. Neurosci*. 2012;30(7):584–595. https://doi.org/10.1016/j.ijdevneu.2012.08.008

110. Grishin E.V., Volkova T.M., Arseniev A.S., Reshetova O.S., Onoprienko V.V., Magazanik L.G., Antonov S.M., Fedorova I.M. Structure-functional characteristics of argiopine—an ion channel blocker from the venom of spider *Argiope lobata*. *Bioorganicheskaya Khimiya = Russian Journal of Bioorganic Chemistry*. 1986;12 (8):1121–1124 (in Russ.).

111. Nelson J.K., Frølund S.U., Tikhonov D.B., Kristensen A.S., Strømgaard K. Inside Cover: Synthesis and Biological Activity of Argiotoxin 636 and Analogues: Selective Antagonists for Ionotropic Glutamate Receptors. *Angew. Chem. Int. Ed.* 2009;48(17):2994–2994. https://doi.org/10.1002/anie.200990085

112. Wimo A. Pharmacoeconomic aspects of memantine (Ebixa®) in the treatment of Alzheimer's disease. *Expert Rev. Pharmacoecon. Outcomes. Res.* 2003;3(6):675–680. https://doi.org/10.1586/14737167.3.6.675

113. Iino M., Koike M., Isa T., Ozawa S. Voltage-dependent blockage of Ca (2+)-permeable AMPA receptors by joro spider toxin in cultured rat hippocampal neurones. *J. Physiol.* 1996;496(2):431–437. https://doi.org/10.1113/jphysiol.1996.sp021696

114. Salamoni S.D., da Costa J.C., Palma M.S., Konno K., Nihei K.I., Azambuja N.A., Neto E.P., Venturin G.T., Tavares A.A., Abreu D.S., Breda R.V. The antiepileptic activity of JSTX-3 is mediated by *N*-methyl-D-aspartate receptors in human hippocampal neurons. *Neuroreport.* 2005;16(16):1869–1873. https://doi.org/10.1097/01.wnr.0000185012.98821.2b

115. Andersen T.F., Vogensen S.B., Jensen L.S., Knapp K.M., Strømgaard K. Design and synthesis of labeled analogs of PhTX-56, a potent and selective AMPA receptor antagonist. *Bioorg. Med. Chem.* 2005;13(17):5104–5112. https://doi.org/10.1016/j.bmc.2005.05.023

116. Nurowska E, Tumiatti V, Dworakowska B. Effect of polyamines on the nicotinic ACh receptor. *J. Pre-Clin. Clin. Res.* 2018;12(3):73–76. https://doi.org/10.26444/jpccr/93936

117. Harris J., Mundey M., Tomlinson S., Mellor I., Nakanishi K., Bell D., Usherwood P.N.R. Interaction of polyamide toxin Philanthotoxin-343 with cloned and mutant glutamate receptors expressed in Xenopus oocytes. *Toxicon*. 1996;7(34):730–731.

118. Karst H., Piek T. Structure-activity relationship of philanthotoxins—II. Effects on the glutamate gated ion channels of the locust muscle fibre membrane. Comp. Biochem. Physiol. C Toxicol. *Pharmacol.* 1991;98(2–3):479–489. https://doi.org/10.1016/0742-8413(91)90237-n

119. Jensen L.S., Bølcho U., Egebjerg J., Strømgaard K. Design, Synthesis, and Pharmacological Characterization of Polyamine Toxin Derivatives: Potent Ligands for the Pore-Forming Region of AMPA Receptors. *ChemMedChem*. 2006;1(4):419–428. https://doi.org/10.1002/cmdc.200500093

120. Strømgaard K., Mellor I. AMPA receptor ligands: synthetic and pharmacological studies of polyamines and polyamine toxins. *Med. Res. Rev*. 2004;24(5):589–620. https://doi.org/10.1002/med.20004

121. Olsen C.A., Mellor I.R., Wellendorph P., Usherwood P.N., Witt M., Franzyk H., Jaroszewski J.W. Tuning Wasp Toxin Structure for Nicotinic Receptor Antagonism: Cyclohexylalanine-Containing Analogues as Potent and Voltage-Dependent Blockers. *ChemMedChem*. 2006;1(3):303–305. https://doi.org/10.1002/cmdc.200500067

122. Strømgaard K., Mellor I.R., Andersen K., Neagoe I., Pluteanu F., Usherwood P.N., Krogsgaard-Larsen P., Jaroszewski J.W. Solid-Phase synthesis and pharmacological evaluation of analogues of PhTX-12—A potent and selective nicotinic acetylcholine receptor antagonist. *Bioorganic Med. Chem. Lett.* 2002;12(8):1159–1162. https://doi.org/10.1016/S0960-894X(02)00120-8

123. Bolognesi M.L., Rosini M., Andrisano V., Bartolini M., Minarini A., Tumiatti V., Melchiorre C. MTDL design strategy in the context of Alzheimer's disease: from lipocrine to memoquin and beyond. *Curr. Pharm. Des*. 2009;15(6):601–613. https://doi.org/10.2174/138161209787315585

124. Kabir A., Jash C., Payghan P.V., Ghoshal N., Kumar G.S. Polyamines and its analogue modulates amyloid fibrillation in lysozyme: A comparative investigation. *Biochim. Biophys. Acta. Gen. Subj.* 2020;1864(5):129557. https://doi.org/10.1016/j.bbagen.2020.129557

125. Selkoe D.J., Hardy J. The amyloid hypothesis of Alzheimer's disease at 25 years. *EMBO Mol. Med.* 2016;8(6):595–608. https://doi.org/10.15252/emmm.201606210

126. Blennow K., Mattsson N., Schöll M., Hansson O., Zetterberg H. Amyloid biomarkers in Alzheimer's disease. *Trends Pharmacol. Sci.* 2015;36(5):297–309. https://doi.org/10.1016/j.tips.2015.03.002

127. Di Paolo M.L., Cozza G., Milelli A., Zonta F., Sarno S., Minniti E., Ursini F., Rosini M., Minarini A. Benextramine and derivatives as novel human monoamine oxidases inhibitors: an integrated approach. *FEBS J.* 2019;286(24):4995–5015. https://doi.org/10.1111/febs.14994

128. Caslake R., Macleod A., Ives N., Stowe R., Counsell C. Monoamine oxidase B inhibitors versus other dopaminergic agents in early Parkinson's disease. *Cochrane Database Syst. Rev.* 2009;4.Art. No.:CD006661. https://doi.org/10.1002/14651858.cd006661.pub2

129. Riederer P., Müller T. Use of monoamine oxidase inhibitors in chronic neurodegeneration. *Expert Opin. Drug. Metab. Toxicol.* 2017;13(2):233–240. https://doi.org/10.1080/17425255.2017.1273901

130. Thomas S.J., Shin M., McInnis M.G., Bostwick J.R. Combination therapy with monoamine oxidase inhibitors and other antidepressants or stimulants: strategies for the management of treatment-resistant depression. *Pharmacotherapy.* 2015;35(4):433–449. https://doi.org/10.1002/phar.1576

About the authors:

Oleg S. Egorov, Master Student, N.A. Preobrazhensky Department of Chemistry and Technology of Biologically Active Compounds, Medical and Organic Chemistry, M.V. Lomonosov Institute of Fine Chemical Technologies, MIREA – Russian Technological University (86, Vernadskogo pr., Moscow, 119571, Russia). E-mail: egorov1997@inbox.ru. Scopus Author ID 8880163900, https://orcid.org/0000-0002-8122-3577

Nadezhda Yu. Borisova, Cand. Sci. (Chem.), Associate Professor, N.A. Preobrazhensky Department of Chemistry and Technology of Biologically Active Compounds, Medical and Organic Chemistry, M.V. Lomonosov Institute of Fine Chemical Technologies, MIREA – Russian Technological University (86, Vernadskogo pr., Moscow, 119571, Russia). E-mail: ladask714485@yandex.ru. Scopus Author ID 55780738100, https://orcid.org/0000-0002-7316-8109

Elena Ya. Borisova, Dr. Sci. (Chem.), Professor, N.A. Preobrazhensky Department of Chemistry and Technology of Biologically Active Compounds, Medical and Organic Chemistry, M.V. Lomonosov Institute of Fine Chemical Technologies, MIREA – Russian Technological University (86, Vernadskogo pr., Moscow, 119571, Russia). E-mail: helen-bor714485@yandex.ru. Scopus Author ID 8880163900, https://orcid.org/0000-0002-8122-3577

Muzaffar L. Rezhabbaev, Postgraduate Student, N.A. Preobrazhensky Department of Chemistry and Technology of Biologically Active Compounds, Medical and Organic Chemistry, M.V. Lomonosov Institute of Fine Chemical Technologies, MIREA – Russian Technological University (86, Vernadskogo pr., Moscow, 119571, Russia). E-mail: Rezhabbayev@gmail.com, https://orcid.org/0000-0002-5393-913X

Elena Yu. Afanas'eva, Cand. Sci. (Med.), Leading Researcher, National Medical Research Center of Cardiology, Ministry of Health of the Russian Federation (15a, 3 Cherepkovskaya ul., Moscow, 121552, Russia). E-mail: embroilment@gmail.com, https://orcid.org/0000-0002-5620-4649

Evgeny V. Arzamastsev, Dr. Sci. (Med.), Professor, Head of the Laboratory of Drug Toxicology, National Medical Research Center of Cardiology, Ministry of Health of the Russian Federation (15a, 3 Cherepkovskaya ul., Moscow, 121552, Russia). E-mail: arz4146931@yandex.ru, https://orcid.org/0000-0002-1270-3067

Об авторах:

Егоров Олег Сергеевич, магистр кафедры химии и технологии биологически активных соединений, медицинской и органической химии им. Н.А. Преображенского Института тонких химических технологий им. М.В. Ломоносова ФГБОУ ВО «МИРЭА – Российский технологический университет» (119571, Россия, Москва, пр-т Вернадского, д. 86). E-mail: egorov1997@inbox.ru. ResearcherID AAW-7636-2020, https://orcid.org/0000-0003-1930-8227

Борисова Надежда Юрьевна, к.х.н., доцент кафедры химии и технологии биологически активных соединений, медицинской и органической химии им. Н.А. Преображенского Института тонких химических технологий им. М.В. Ломоносова ФГБОУ ВО «МИРЭА – Российский технологический университет» (119571, Россия, Москва, пр-т Вернадского, д. 86). E-mail: ladask714485@yandex.ru. Scopus Author ID 55780738100, https://orcid.org/0000-0002-7316-8109

Борисова Елена Яковлевна, д.х.н., профессор кафедры химии и технологии биологически активных соединений, медицинской и органической химии им. Н.А. Преображенского Института тонких химических технологий им. М.В. Ломоносова ФГБОУ ВО «МИРЭА – Российский технологический университет» (119571, Россия, Москва, пр-т Вернадского, д. 86). E-mail: helen-bor714485@yandex.ru. Scopus Author ID 8880163900, https://orcid.org/0000-0002-8122-3577

Режаббаев Музаффар Латибжонович, аспирант кафедры химии и технологии биологически активных соединений, медицинской и органической химии им. Н.А. Преображенского Института тонких химических технологий им. М.В. Ломоносова ФГБОУ ВО «МИРЭА – Российский технологический университет» (119571, Россия, Москва, пр-т Вернадского, д. 86). E-mail: Rezhabbayev@gmail.com, https://orcid.org/0000-0002-5393-913X

Афанасьева Елена Юльевна, к.м.н., ведущий научный сотрудник, ФГБУ «Национальный медицинский исследовательский центр кардиологии» Минздрава РФ (121552, Россия, Москва, ул. 3-я Черепковская, д. 15а). E-mail: embroilment@gmail.com, https://orcid.org/0000-0002-5620-4649

Арзамасцев Евгений Вениаминович, д.м.н., профессор, заведующий лаборатории лекарственной токсикологии ФГБУ «Национальный медицинский исследовательский центр кардиологии» Минздрава РФ (121552, Россия, Москва, ул. 3-я Черепковская, д. 15а). E-mail: arz4146931@yandex.ru, https://orcid.org/0000-0002-1270-3067

The article was submitted: January 18, 2021; approved after reviewing: January 26, 2021; accepted for publication: August 13, 2021.

Translated from Russian into English by H. Moshkov
Edited for English language and spelling by Enago, an editing brand of Crimson Interactive Inc.

CHEMISTRY AND TECHNOLOGY OF MEDICINAL COMPOUNDS AND BIOLOGICALLY ACTIVE SUBSTANCES

ХИМИЯ И ТЕХНОЛОГИЯ ЛЕКАРСТВЕННЫХ ПРЕПАРАТОВ И БИОЛОГИЧЕСКИ АКТИВНЫХ СОЕДИНЕНИЙ

ISSN 2686-7575 (Online)

https://doi.org/10.32362/2410-6593-2021-16-4-307-317

UDC 54.052

RESEARCH ARTICLE

The use of microfluidic hardware in the synthesis of oligohexamethylene guanidine derivatives

Diana A. Akhmedova[1,2,@], Denis O. Shatalov[1], Ivan S. Ivanov[1], Anna V. Aydakova[1,2], Alexander Herbst[3], Lasse Greiner[4], Alexander P. Kaplun[1], Anton S. Zhurbenko[1], Stanislav A. Kedik[1]

[1]MIREA – Russian Technological University (M.V. Lomonosov Institute of Fine Chemical Technologies), Moscow, 119571 Russia
[2]Institute of Pharmaceutical Technologies, Moscow, 121353 Russia
[3]Wingflow AG, Frick AG, 5070 Switzerland
[4]Mannheim University of Applied Sciences, Mannheim, 68163 Germany
[@]Corresponding author, e-mail: akhmedova.diana.a@gmail.com

Abstract

Objectives. *To develop a method for the microfluidic synthesis of oligohexamethylene guanidine salts in a flow-type reactor and to evaluate its effectiveness in relation to the synthesis in a traditional capacitive reactor and compare the purities of products obtained by these methods.*
Methods. *The synthesis of oligohexamethylene guanidine bihydrocarbonate (OHMG-BHC) was done using microfluidic hardware and the classical approach in volume. The purity and structure of the resulting product were confirmed by ^{13}C NMR spectroscopy and high-performance liquid chromatography (HPLC).*
Results. *The ^{13}C NMR spectrum of OHMG-BHC in classical bulk synthesis demonstrates that the product is unbranched and contains additionally unidentifiable impurities, in contrast to the sample obtained by the microfluidic method. Furthermore, the HPLC analysis showed that the OHMG-BHC sample synthesized using microfluidic technology has a 1.5-fold lower content than the initial monomers.*
Conclusions. *The advantage of synthesizing OHMG-BHC in a flow-type reactor compared to the traditional method of synthesis in volume is demonstrated since a product with a higher degree of purity is obtained.*

Keywords: *antimicrobial resistance, oligohexamethylene guanidine, bihydrocarbonate, microfluidic synthesis*

For citation: Akhmedova D.A., Shatalov D.O., Ivanov I.S., Aydakova A.V., Herbst A., Greiner L., Kaplun A.P., Zhurbenko A.S., Kedik S.A. The use of microfluidic hardware in the synthesis of oligohexamethylene guanidine derivatives. *Tonk. Khim. Tekhnol. = Fine Chem. Technol.* 2021;16(4):307–317 (Russ., Eng.). https://doi.org/10.32362/2410-6593-2021-16-4-307-317

НАУЧНАЯ СТАТЬЯ

Применение микрофлюидного аппаратного оснащения в синтезе производных олигогексаметиленгуанидина

Д.А. Ахмедова[1,2,@], Д.О. Шаталов[1], И.С. Иванов[1], А.В. Айдакова[1,2], А. Гербст[3], Л. Грайнер[4], А.П. Каплун[1], А.С. Журбенко[1], С.А. Кедик[1]

[1]МИРЭА – Российский технологический университет, Москва, 119571 Россия
[2]Институт фармацевтических технологий, Москва, 121353 Россия
[3]Wingflow AG, Фрик АК 5070, Швейцария
[4]Манхеймский университет прикладных наук, Манхейм, 68163 Германия
[@]Автор для переписки, e-mail: akhmedova.diana.a@gmail.com

Аннотация

Цели. *Разработать методику микрофлюидного синтеза солей олигогексаметиленгуанидина в реакторе проточного типа и оценить ее эффективность по сравнению с синтезом в классическом емкостном реакторе, а также сравнить чистоту продуктов, полученных данными методами.*
Методы. *Синтез олигогексаметиленгуанидина дигидрокарбоната (ОГМГ-ДГК) проводили с применением микрофлюидного аппаратного оснащения и классическим методом в объеме. Подтверждение чистоты и структуры полученного продукта осуществляли с помощью ^{13}C ЯМР спектроскопии и высокоэффективной жидкостной хроматографии (ВЭЖХ).*
Результаты. *Спектр ^{13}C ЯМР ОГМГ-ДГК при классическом синтезе в объеме демонстрирует, что продукт является неразветвленным и содержит дополнительно неидентифицируемые примеси в отличие от образца, полученного микрофлюидным способом. Анализ методом ВЭЖХ показал, что образец ОГМГ-ДГК, синтезированный с помощью микрофлюидной технологии, имеет в 1.5 раза более низкое содержание исходных мономеров.*
Выводы. *Синтез ОГМГ-ДГК в проточном реакторе имеет преимущество по сравнению с классическим способом синтеза в объеме, поскольку выдает продукт с более высокой степенью чистоты.*

Ключевые слова: *резистентность к противомикробным препаратам, олигогексаметиленгуанидин, гидрокарбонат, микрофлюидный синтез*

Для цитирования: Ахмедова Д.А., Шаталов Д.О., Иванов И.С., Айдакова А.В., Гербст А., Грайнер Л., Каплун А.П., Журбенко А.С., Кедик С.А. Применение микрофлюидного аппаратного оснащения в синтезе производных олигогексаметиленгуанидина. *Тонкие химические технологии.* 2021;16(4):307–317. https://doi.org/10.32362/2410-6593-2021-16-4-307-317

INTRODUCTION

According to the World Health Organization, antimicrobial resistance is a global threat to humanity[1]. The development of effective antibiotics in the 20th century is a direct result of the significant breakthroughs in antimicrobial therapy. Yet, the widespread use of antimicrobial drugs has contributed to the emergence of resistant pathogenic microflora, making it challenging to treat emerging infections and increasingly complex and expensive. Thus, an important task is searching and synthesizing new substances that exhibit antimicrobial activity [1, 2]. In this regard, compounds of several alkylene guanidines, in particular, oligohexamethylene guanidine (OHMG), with a wide spectrum of activity, a low toxicity class, and having a prolonged effect are promising [3, 4]. No bacterial resistance was detected for this class of compounds, and therefore they can be recommended for use, for example, as active pharmaceutical substances in ready-made dosage forms [5].

[1]https://www.who.int/drugresistance/documents/surveillancereport/en/ (Accessed April 04, 2021).

In recent years, one of the foremost perspectives taken by development actions for antimicrobial compounds is the synthesis of analogs and derivatives and the replacement of functional groups or parts of a molecule of already studied drugs, provided these parts meet the requirements for antimicrobial action and biological safety [6]. According to this approach, such derivatives of oligoalkylene guanidine as OHMG hydrochloride and OHMG hydrosuccinate were synthesized and studied. The studies have proved their effectiveness in dealing with pathogenic and opportunistic microorganisms compared to chlorohexidine and miramistin [5, 7]. Moreover, it is assumed that the new compounds of the OHMG class will also be highly effective against a wide range of pathogenic microflora. In this regard, the task of finding ways to obtain new derivatives of OHMG, for example, hydrocitrate, hydrosulfosalicylate, and hydrosalicylate, is urgent.

Traditionally, OHMG salts are obtained in capacitance-type reactors by polycondensing the initial monomers-hexamethylenediamine and guanidine bicarbonate or guanidine hydrochloride. Then, depending on the preferred guanidine salts, OHMG dihydrocarbonate (OHMG-BHC) or OHMG hydrochloride (OHMG-HC) are obtained, which are subsequently converted into other salt forms of OHMG (Fig. 1). However, the bulk synthesis approach, which is the traditional method, has many disadvantages; for example, this process's turbulent mixing regimes resulting in an uneven flow leads to a high content of residual monomers and anisotropy of the molecular mass characteristics of the resulting product [8–10].

Currently, microfluidics is a rapidly developing field of chemical synthesis. The primary advantage of microfluidic technology is its high efficiency due to improved mass and heat exchange provided by laminar flow and the ability to accurately control process parameters [11–16].

Previous studies have worked out the technology of microfluidic synthesis of OHMG-GC [17, 18], used as a semi-product for the production of other derivatives of OHMG, the synthesis of which was carried out according to scheme 1 (Fig. 1). However, as a disadvantage, it can be noted that in this scheme, additional stages are required for the further reaction: first, the preparation of the base of OHMG and/or OHMG-BHC, and then its corresponding salt (Fig. 1, Scheme 1). Alternatively, the implementation of synthesis through a semi-product of OHMG-BHC (Fig. 1, Scheme 2) can be considered. This, together with the use of microfluidic hardware, will reduce the number of stages and enhance the quality criteria in reference to its analog synthesized in volume. Thus, this study compares the effectiveness of methods for obtaining OHMG salt and the purity of the resulting product, based on the approach used – synthesis by the classical method in a capacitive reactor or microfluidics in a flow-type reactor.

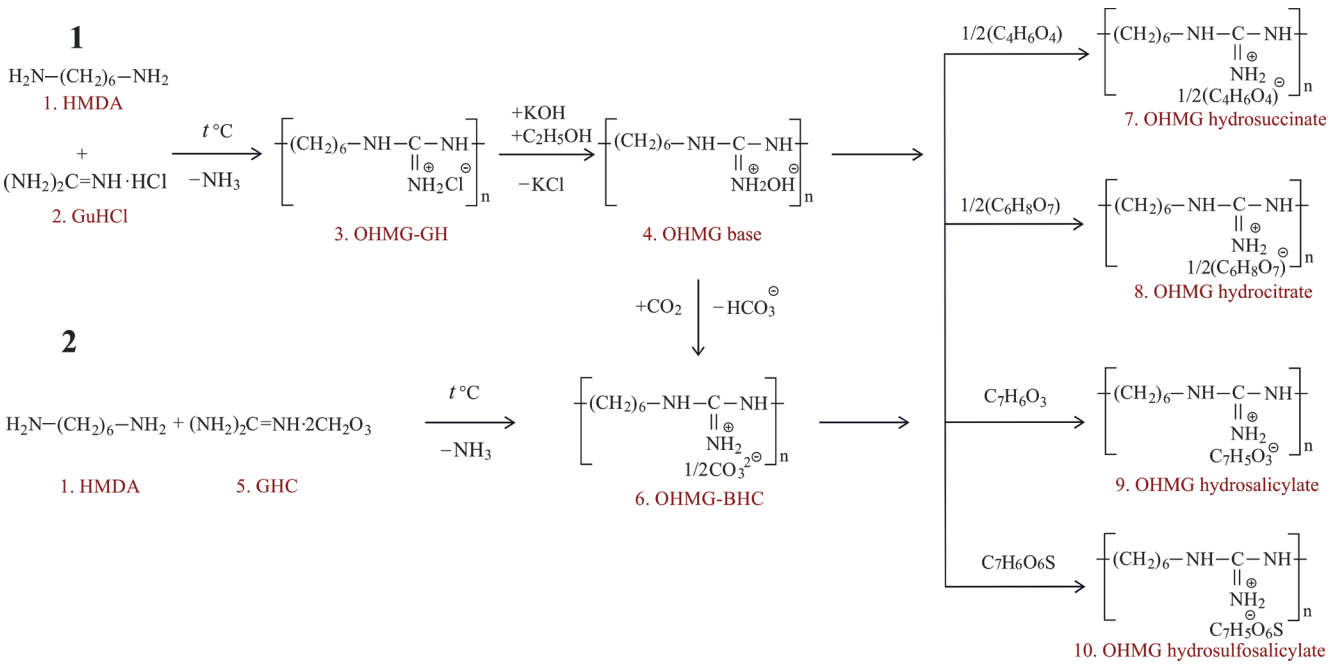

Fig. 1. Scheme synthesis of OHMG salts. HMDA – hexamethylenediamine; GuHCl – guanidine hydrochloride; OHMG base – the base of oligohexamethylene guanidine; GHC – guanidine hydrocarbonate.

EXPERIMENTAL

The following reagents were used in the experiment: Hexamethylenediamine (HMDA, *Acros Organics*, Belgium); guanidine hydrocarbonate (GHC, *Sigma-Aldrich*, USA). For microfluidic synthesis, a Qmix Pro Ext microreactor module from *Wingflow AG* (Switzerland) was used, consisting of syringe pumps (neMESYS MPM, Switzerland) and a capillary with a diameter of 1/8 inch (Qmix Q + HP flow, Switzerland) (Fig. 2). In addition, a rotary evaporator (IKA RV 10, Germany) was used to evaporate the water mixture.

OHMG-DHA was obtained in two ways—using traditional synthesis in volume and in a flow reactor.

Method 1-synthesis in a capacitive reactor. 1.55 g (1 mol) was mixed in a pre-weighed three-necked flask with a volume of 250 mL GHC and 1.0 g (1 mol) of HMDA. A flask with attachments of the initial components was installed on a heating plate, providing thermal insulation with asbestos cloth. Mixing the components was carried out using an upper-drive mixing device with a paddle stirrer immersed in the flask. The synthesis was started with simultaneous stirring and heating of the flask's contents at 90°C for 1 h. After that, the melt temperature was raised to 110°C, and polycondensation was carried out for 4 h. At the end of the process, the formed polymer was cooled to room temperature. A sample was taken for NMR analysis of the product and the quantitative content of related impurities [8].

Method 2-microfluidic synthesis in a flow reactor. In a pre-weighed glass, 1.55 g (1 mol) HHC, 1.0 g (1 mol) HMDA, and 11.5 g of water purified with a magnetic stirrer and an elliptical armature were mixed at room temperature until the substances were completely dissolved. The purified water acted as a solvent, which made it possible to avoid limiting the capillary throughput and, as a result, clogging it. The final concentration of the solution was 8.7% and 13.0% in the case of HMDA and GHC, respectively. The resulting mixture was continuously fed into the capillary using a syringe pump at about 0.01 mL/min rate. Polycondensation was carried out at 90°C for 1 h, after which the heating was increased to 110°C and the working mixture was maintained for 4 h. Thus, the OHMG salt was formed in the liquid flow as it moved along the length of the reactor at certain values of temperature and time. At the end of the synthesis, the working mixture was collected in a round-bottomed flask and transferred to the evaporation stage using a rotary evaporator at a temperature of 97°C. After the evaporation stage, a sample was taken from the formed polymer, which was subsequently analyzed by high-performance liquid chromatography (HPLC) and ^{13}C NMR.

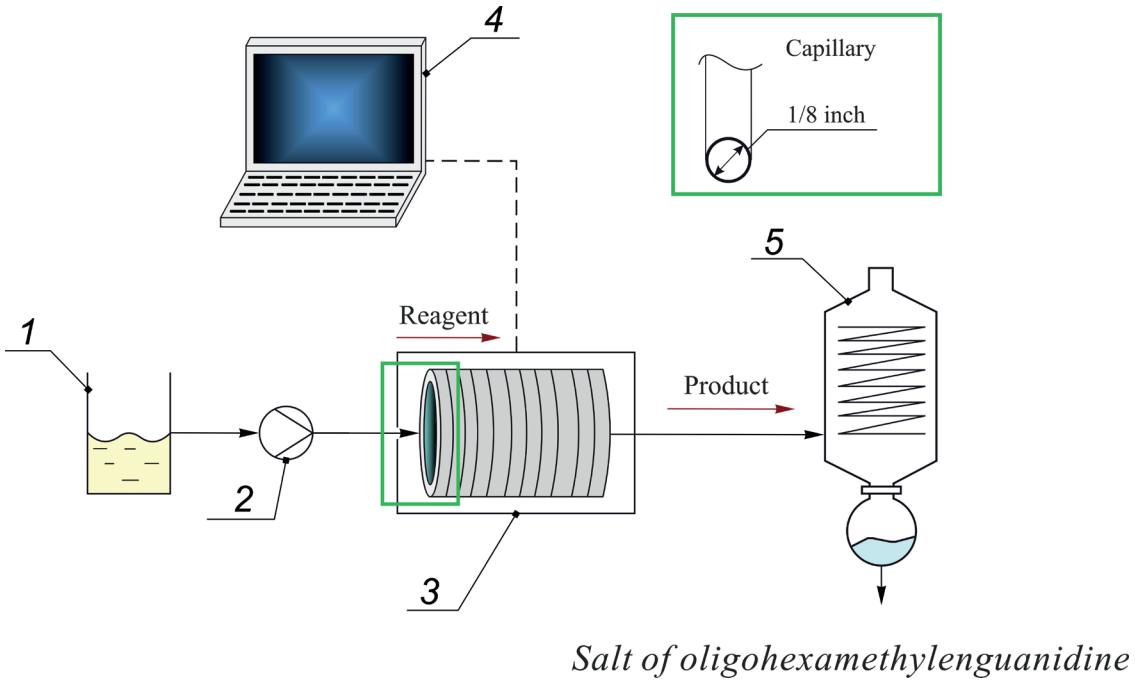

Fig. 2. Hardware diagram of microfluidic synthesis: *1* – an aqueous solution of GHC and HMDA; *2* – a syringe pump; *3* – a microreactor; *4* – a control computer; *5* – a rotary evaporator.

Spectra ^{13}C NMR samples of the synthesized compounds were recorded using the Bruker DPX NMR spectrometer (*Bruker*, Germany), deuterium oxide D_2O was used as a solvent, the resonant frequency was 75 MHz.

Quantitative determination of impurities in OHMG-BHC was carried out according to the State Pharmacopoeia of the Russian Federation of the 14th edition of the OFS.1.2.1.2.0005.15 "High-performance liquid chromatography" on the *Thermo Fisher Scientific* chromatograph (USA). The controlled limit of related impurities, namely HMDA and GHC, was determined according to the work of I.S. Ivanov[2] and amounted to 0.05 wt %. The concentrations of HMDA and GHC were determined chromatographically by external standards with UV detection at wavelengths of 205 nm and 264 nm, respectively[3].

The conditions for chromatographic determination of HMDA: column Luna C18(2) 5 µm, 150 × 4.6 mm; mobile phase A: water for chromatography; mobile phase B: acetonitrile; flow rate: 1 mL/min; temperature: 25°C; the volume of injected sample: 20.0 µL; analysis time: 30 min; gradient profile: 0–3 min, 0% B, 4–15 min, 90% B, 16–30 min, 0% B.

The conditions for chromatographic determination of GHC: column Luna C18(2) 5 µm, 250 × 4.6 mm; mobile phase A: water for chromatography; mobile phase B: acetonitrile; flow rate: 1 mL/min; temperature: 30°C; the volume loops – 100 µL; gradient profile: 0–1 min, 40% B, 10–16 min, 90% B, 17–20 min, 40% B.

RESULTS AND DISCUSSION

The authenticity of the synthesized compounds was confirmed by comparing the signals in a typical ^{13}C NMR spectrum of OHMG-BHC (according to the abovementioned work of Ivanov, Fig. 3) with signals in the spectra of the obtained samples (Fig. 4 and 5). The ^{13}C NMR spectrum analysis (Table 1) showed that in the case of a sample obtained by the classical method in volume, there is no signal at 156 ppm characterizing the branched structure of OHMG-BHC. In addition, signals from unidentifiable impurities were present in

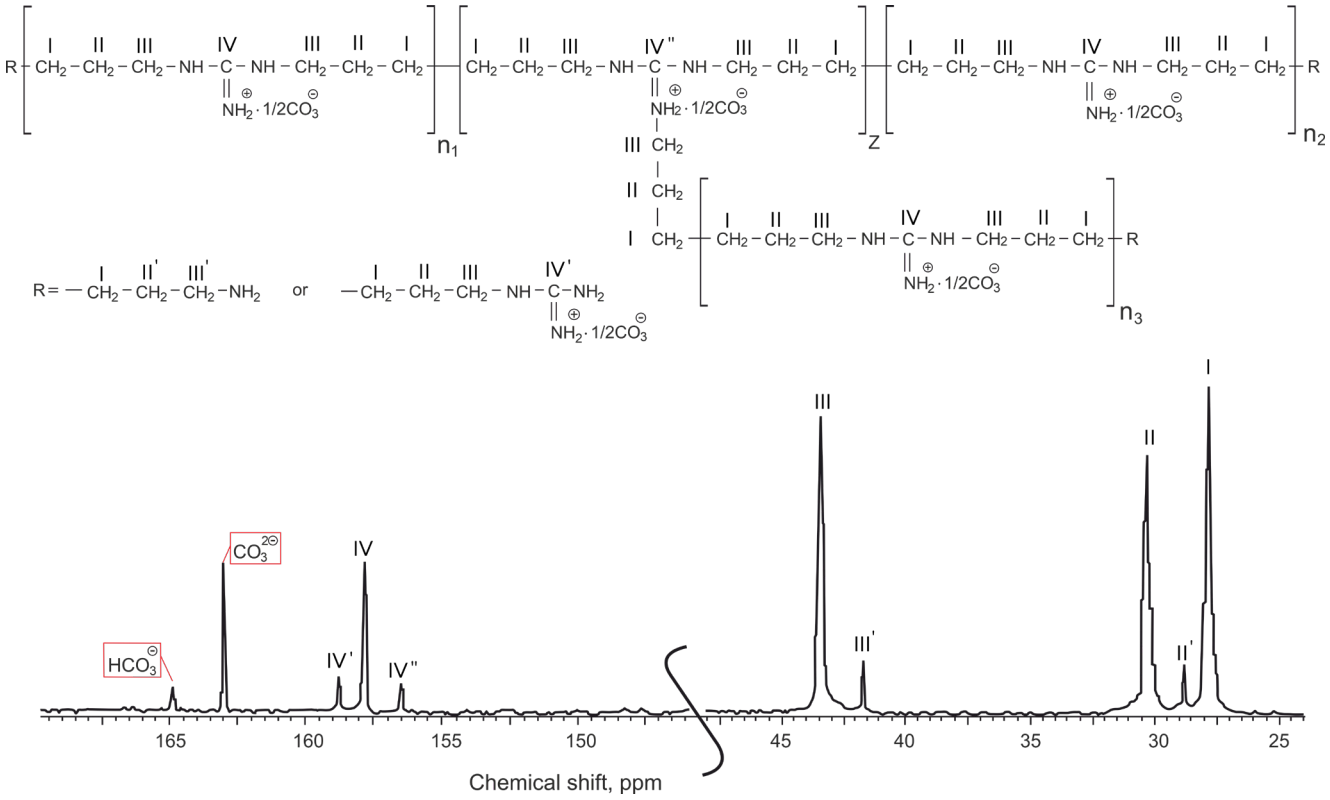

Fig. 3. Typical OHMG-BHC ^{13}C NMR spectrum (the signals in the spectrum are indicated according to the numbering of the atoms in the structural formula of the compound shown in the figure).

[2] Ivanov I.S. Microfluidic synthesis of the substance oligohexamethylene guanidine hydrosuccinate and the creation of an ophthalmic drug based on it. Cand. Thesis (Pharm.). Moscow: RTU MIREA; 2021. 118 p., 38–40.

[3] Shatalov D.O. Development and standardization of quality control methods for branched oligohexamethylene guanidine hydrochloride. Cand. Thesis (Pharm.). Samara: Sam. gos. med. un-t; 2015. 137 p., 67–70.

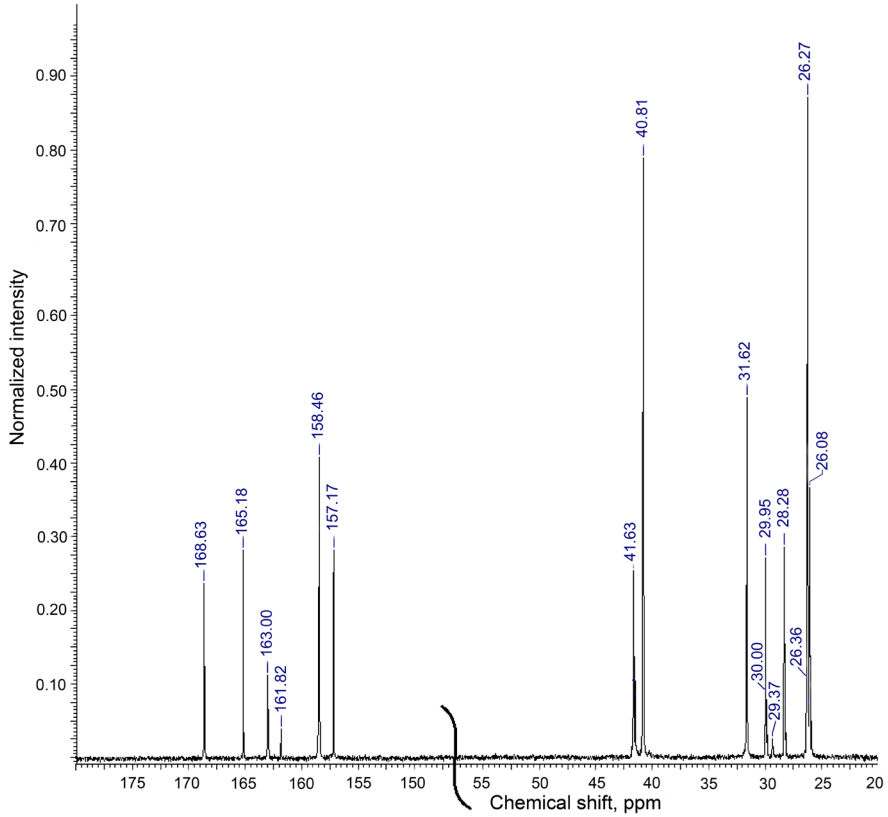

Fig. 4. ^{13}C NMR spectrum of OHMG-BHC obtained in volume.

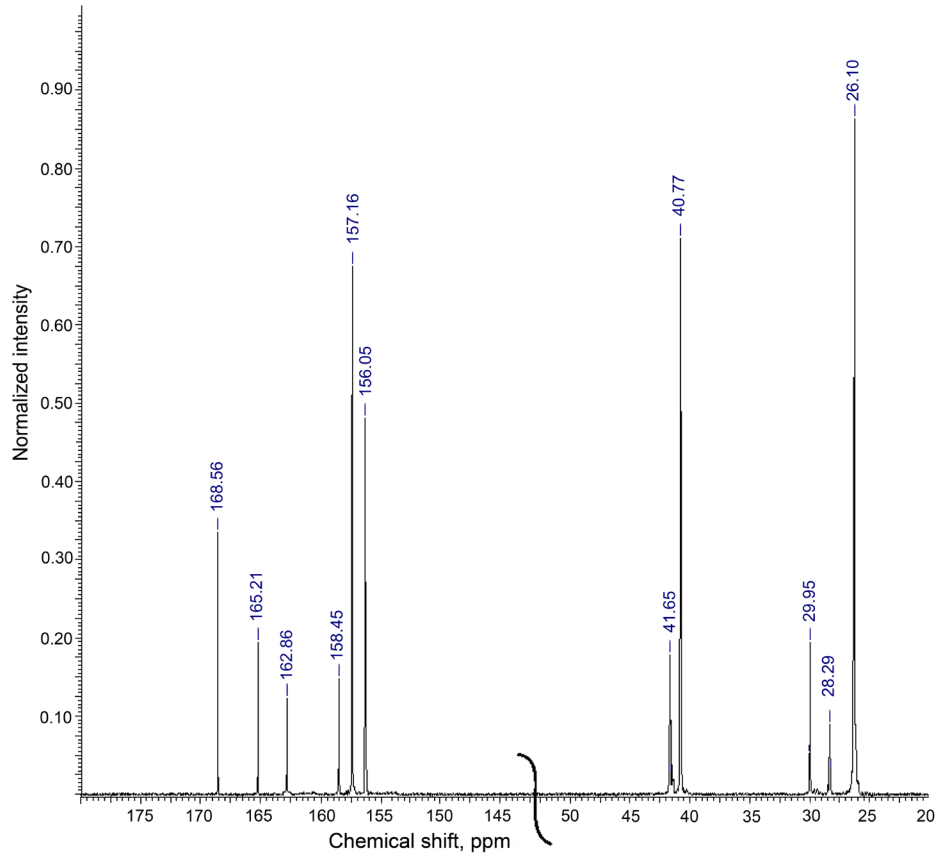

Fig. 5. ^{13}C NMR spectrum of OHMG-BHC obtained by microfluidic synthesis.

Table 1. Position of signals in the ^{13}C NMR spectrum of OHMG-BHC samples

Designation	Chemical shift, ppm		
	Typical spectrum	Volume synthesis	Microfluidic synthesis
I	26.0	26.27	26.10
II/	28.5	28.28	28.29
II	30.0	29.95	29.95
III/	40.0	40.81	40.77
III	41.5	41.63	41.65
IV//	156.0	–	156.05
IV	157.5	157.17	157.16
IV/	158.0	158.46	158.45
CO_3^{2-}	163.0	163.00	162.86
HCO_3	165.0	165.18	165.21
Impurity signals	–	168.63/161.82 31.82/30.00/29.37/26.36/26.08	168.56

the spectrum. However, microfluidic technology makes it possible to achieve branching of the OHMG-BHC oligomeric chain, which contributes to an increase in antimicrobial activity [19].

It could be seen from the HPLC analysis of samples of OHMG bicarbonate obtained by the two methods that the product contains the initial monomers GHC (Fig. 6) and HMDA (Fig. 7) with retention times of 14.38 min and 4.07 min, respectively. However, the analysis of results indicates (Table. 2) that OHMG-BHC, obtained from microfluidic technology, showed about 1.5 times lower content of the initial monomers—HMDA and GHC, thus indicating a more complete reaction the consumption of reagents. Nevertheless, the results show the need for further purification of the product, irrespective of the choice of the synthesis method.

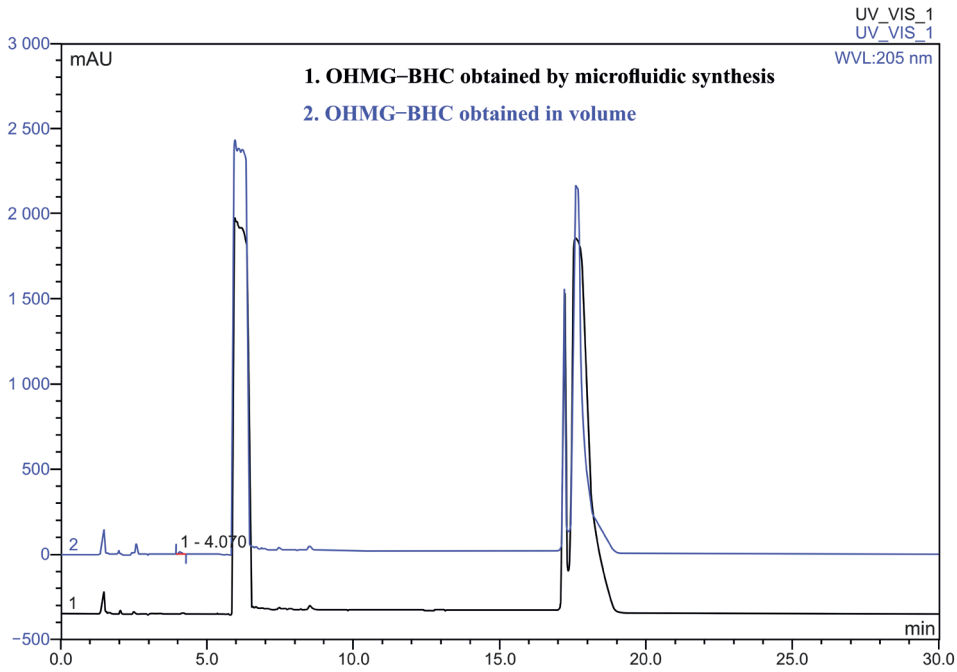

Fig. 6. Two methods obtained chromatograms for determining the quantitative content of GC in OHMG-BHC samples.

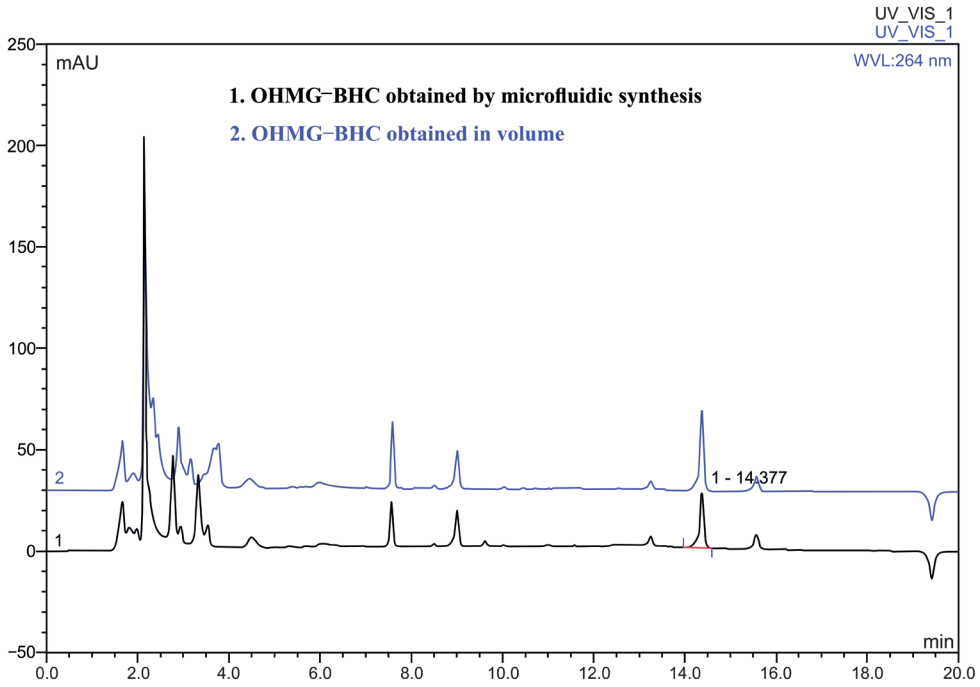

Fig. 7. Two methods obtained chromatograms for determining the quantitative content of HMDA in OHMG-BHC samples.

Table 2. The content of impurities in OHMG–BHC

Synthesis	GHC, wt %	HMDA, wt %
Voluminous	1.372	0.628
Microfluidic	0.821	0.451

CONCLUSIONS

The initial stages of the study showed the advantage of using microfluidic hardware in synthesizing OHMG-BHC compared to the classical method in volume. Therefore, the application of microfluidic technology results in higher purity products, which can be used as a semi-product for the production of other salts of OHMG, expanding the range of biologically active compounds with antimicrobial activity and the scope of their application.

Authors' contributions

D.A. Akhmedova – preparing the original project, conducting experiments, managing the project;

D.O. Shatalov – creating a research concept, implementation of the analytical stage in experimental studies;

I.S. Ivanov – methodology development, preparing the original project, conducting experiments;

A.V. Aydakova – conducting experiments;

A. Herbst – development of a technological base for conducting research; analysis of literary sources, writing and editing the text of the article;

L. Greiner – development of a technological base for conducting research; analysis of literary sources, writing and editing the text of the article;

A.P. Kaplun – processing experimental data, adjustment of experimental studies;

A.S. Zhurbenko – conducting experiments;

S.A. Kedik – creating a research concept, development of a technological base for conducting research.

The authors declare no conflicts of interest.

REFERENCES

1. Wanted: a reward for antibiotic development. Nat. Biotechnol. 2018;36(7):555. https://doi.org/10.1038/nbt.4193

2. Gil-Gil T., Laborda P., Sanz-García F., Hernando-Amado S., Blanco P., Martínez J.L. Antimicrobial resistance: A multifaceted problem with multipronged solutions. *Microbiologyopen.* 2019;8(11):e945. https://doi.org/10.1002/mbo3.945

СПИСОК ЛИТЕРАТУРЫ

1. Wanted: a reward for antibiotic development. *Nat. Biotechnol.* 2018;36(7):555. https://doi.org/10.1038/nbt.4193

2. Gil-Gil T., Laborda P., Sanz-García F., Hernando-Amado S., Blanco P., Martínez J.L. Antimicrobial resistance: A multifaceted problem with multipronged solutions. *Microbiologyopen*. 2019;8(11):e945. https://doi.org/10.1002/mbo3.945

3. Asyamova A.V., Gerunov V.I. Guanidine derivatives in medicine and agriculture. *Vestnik of Omsk SAU*. 2017:4(29):130–135 (in Russ.).

4. Pasero C., D'Agostino I., De Luca F., Zamperini C., Deodato D., Truglio G.I., Sannio F., Del Prete R., Ferraro T., Visaggio D., Mancini A., Guglielmi M.B, Visca P., Docquier J.-D., Botta M. Alkylguanidine Compounds as Potent Broad-Spectrum Antibacterial Agents: Chemical Library Extension and Biological Characterization. *J. Med. Chem.* 2018;61(20):9162–9176. https://doi.org/10.1021/acs.jmedchem.8b00619

5. Beliakov S.V., Shatalov D.O., Kedik S.A., Aydakova A.V., Zasypkina N.A. Preliminary *in vitro* and *in vivo* evaluation of specific activity of branched oligohexamethyleneguanidine hydrochloride. *Drug Dev. Ind. Pharm*. 2020;46(9):1517–1523. https://doi.org/10.1080/03639045.2020.1810267

6. Hua D., Hongtao Yu. New Antibiotics: Where Are They? Biomed. *J. Sci. & Tech. Res.* 2018;10(1):7629–7631. http://dx.doi.org/10.26717/BJSTR.2018.10.001909

7. Kovalenko A.V., Shatalov D.O., Kedik S.A., Gromakova A.I., Kaplun A.P., Ivanov I.S., Sterin I.V. The direction of development of drug therapy for infectious conjunctivitis (literature review). *Problems of biological, medical and pharmaceutical chemistry.* 2019;22(12):5−11 (in Russ.). https://doi.org/10.29296/25877313-2019-12-01

8. Vointseva, I.I., Gembitskiĭ P.A. *Poliguanidiny–dezinfektsionnye sredstva i polifunktsional'nye dobavki* (*Polyguanidines are disinfectants and multifunctional additives*). Moscow: LKM-press; 2009. 304 p. (in Russ.). ISBN 978-5-9901286-2-0

9. Weia D., Maa Q., Guana Y., Hua F., Zhenga A., Zhangb X., Tengb Z., Jiangb H. Structural characterization and antibacterial activity of oligoguanidine (polyhexamethylene guanidine hydrochloride). *Materials Science and Engineering.* 2009;29(6):1776–1780.

10. Bally F., Serra C. A., Brochon C., Hadziioannou G. Synthesis of Branched Polymers under Continuous-Flow Microprocess: An Improvement of the Control of Macromolecular Architectures. *Macromol. Rapid Commun.* 2011;32:1820−1825.

11. Manz A., Graber N., Widmer H.M. Miniaturized total chemical analysis systems: A novel concept for chemical sensing. *Sensors and Actuators B.* 1990;2(4):244–248.

12. Srinivasan R., Firebaugh S.L., Hsing I.-M., Ryley J., Harold M.P., Jensen K.F., Schmidt M.A. Chemical performance and high temperature characterization of micromachined chemical reactors. In: *Proceedings of International Solid State Sensors and Actuators Conference (Transducers 1997)*. 1997;1:163–166. https://doi.org/10.1109/SENSOR.1997.613608

13. Schwalbe T., Autze V., Wille G. Chemical synthesis in microreactors. *Chimia.* 2002;56(11):636–646.

14. Marre S., Roig Y., Aymonier C. Supercritical microfluidics: Opportunities in flow-through chemistry and materials science. *J. Supercrit. Fluids*. 2012;66:251–264.

15. Kockmann N., Gottsponer M., Zimmermann B., Roberge D.M. Enabling continuous-flow chemistry in microstructured devices for pharmaceutical and fine-chemical production. *Chem. Eur. J.* 2008;14:7470–7477. https://doi.org/10.1002/chem.200800707

16. Bally F., Serra C. A., Brochon C., Hadziioannou G. Synthesis of Branched Polymers under Continuous-Flow Microprocess: An Improvement of the Control of Macromolecular Architectures. *Macromol. Rapid Commun*. 2011;32:1820−1825.

3. Асямова А.В., Герунов В.И. Производные гуанидина в медицине и сельском хозяйстве. *Вестник Омского ГАУ.* 2017:4(29):130–135.

4. Pasero C., D'Agostino I., De Luca F., Zamperini C., Deodato D., Truglio G.I., Sannio F., Del Prete R., Ferraro T., Visaggio D., Mancini A., Guglielmi M.B, Visca P., Docquier J.-D., Botta M. Alkylguanidine Compounds as Potent Broad-Spectrum Antibacterial Agents: Chemical Library Extension and Biological Characterization. *J. Med. Chem.* 2018;61(20):9162–9176. https://doi.org/10.1021/acs.jmedchem.8b00619

5. Beliakov S.V., Shatalov D.O., Kedik S.A., Aydakova A.V., Zasypkina N.A. Preliminary *in vitro* and *in vivo* evaluation of specific activity of branched oligohexamethyleneguanidine hydrochloride. *Drug Dev. Ind. Pharm.* 2020;46(9):1517–1523. https://doi.org/10.1080/03639045.2020.1810267

6. Hua D., Hongtao Yu. New Antibiotics: Where Are They? Biomed. *J. Sci. & Tech. Res.* 2018;10(1):7629–7631. http://dx.doi.org/10.26717/BJSTR.2018.10.001909

7. Коваленко А.В., Шаталов Д.О., Кедик С.А., Громакова А.И., Каплун А.П., Иванов И.С., Стерин И.В. Направление развития медикаментозной терапии инфекционных конъюнктивитов (обзор литературы). *Вопросы биологической, медицинской и фармацевтической химии.* 2019;22(12):5−11. https://doi.org/10.29296/25877313-2019-12-01

8. Воинцева, И.И., Гембицкий П.А. *Полигуанидины–дезинфекционные средства и полифункциональные добавки*. М.: ЛКМ-пресс; 2009. 304 с. ISBN 978-5-9901286-2-0

9. Weia D., Maa Q., Guana Y., Hua F., Zhenga A., Zhangb X., Tengb Z., Jiangb H. Structural characterization and antibacterial activity of oligoguanidine (polyhexamethylene guanidine hydrochloride). *Materials Science and Engineering.* 2009;29(6):1776–1780

10. Bally F., Serra C. A., Brochon C., Hadziioannou G. Synthesis of Branched Polymers under Continuous-Flow Microprocess: An Improvement of the Control of Macromolecular Architectures. *Macromol. Rapid Commun.* 2011;32:1820−1825

11. Manz A., Graber N., Widmer H.M. Miniaturized total chemical analysis systems: A novel concept for chemical sensing. *Sensors and Actuators B*. 1990;2(4):244–248.

12. Srinivasan R., Firebaugh S.L., Hsing I.-M., Ryley J., Harold M.P., Jensen K.F., Schmidt M.A. Chemical performance and high temperature characterization of micromachined chemical reactors. In: *Proceedings of International Solid State Sensors and Actuators Conference (Transducers 1997)*. 1997;1:163–166. https://doi.org/10.1109/SENSOR.1997.613608

13. Schwalbe T., Autze V., Wille G. Chemical synthesis in microreactors. *Chimia.* 2002;56(11):636–646.

14. Marre S., Roig Y., Aymonier C. Supercritical microfluidics: Opportunities in flow-through chemistry and materials science. *J. Supercrit. Fluids*. 2012;66:251–264.

15. Kockmann N., Gottsponer M., Zimmermann B., Roberge D.M. Enabling continuous-flow chemistry in microstructured devices for pharmaceutical and fine-chemical production. *Chem. Eur. J.* 2008;14:7470–7477. https://doi.org/10.1002/chem.200800707

16. Bally F., Serra C. A., Brochon C., Hadziioannou G. Synthesis of Branched Polymers under Continuous-Flow Microprocess: An Improvement of the Control of Macromolecular Architectures. *Macromol. Rapid Commun.* 2011;32:1820−1825.

17. Ivanov I.S., Kedik S.A., Shatalov D.O., Legon'kova O.A., Aydakova A. V., Norin A.M., Khar'kovskaya M.D. Prospects for use of microfluidics for synthesis of alkylen guanidinetype compounds. *Polymer Science. Series D*. 2020;12:30–37 (in Russ.). https://doi.org/10.1134/S1995421221020088

18. Shatalov D.O., Kedik S.A., Beliakov S.V., Ivanov I.S., Aydakova A.V., Sedishev I.P. Method of producing branched oligohexamethylene guanidine salts having degree of purity sufficient for use thereof as pharmaceutical substance: RU Pat. 2729421. Publ. 06.08.2020. (in Russ.).

19. Kedik S.A., Sedishev I.P., Panov A.V., Zhavoronok E.S., Ha A.C. Branched oligomers based on a guanidine derivative and a disinfectant containing them: RU Pat. 2443684. Publ. 27.02.2012. (in Russ.).

17. Иванов И.С., Кедик С.А., Шаталов Д.О., Легонькова О.А., Айдакова А.В., Норин А.М., Харьковская М.Д. Перспективы применения микрофлюидики для синтеза соединений алкиленгуанидинового ряда. *Все материалы. Энциклопедический справочник.* 2020;12:30–37. https://doi.org/10.31044/1994-6260-2020-0-12-30-37

18. Шаталов Д.О., Кедик С.А., Беляков С.В., Иванов И.С., Айдакова А.В., Седишев И.П. Способ получения солей разветвленного олигогексаметиленгуанидина, имеющих степень чистоты, достаточную для их применения в качестве фармацевтической субстанции: пат. 2729421 РФ. Заявка № 2019122256; заявл. 15.07.2019; опубл. 06.08.2020. Бюл. № 22.

19. Кедик С.А., Седишев И.П., Панов А.В., Жаворонок Е.С., Ха А.К. Разветвленные олигомеры на основе производного гуанидина и содержащее их дезинфицирующее средство: пат. 2443684 РФ. Заявка № 2010150831/04; заявл. 13.12.2010; опубл. 27.02.2012. Бюл. № 6.

About the authors:

Diana A. Akhmedova, Master Student, Department of Biotechnology and Industrial Pharmacy, M.V. Lomonosov Institute of Fine Chemical Technologies, MIREA – Russian Technological University (86, Vernadskogo pr., Moscow, 119571, Russia); Researcher, Institute of Pharmaceutical Technologies (86, Vernadskogo pr., Moscow, 119571, Russia). E-mail: akhmedova.diana.a@gmail.com, https://orcid.org/0000-0002-0951-939X

Denis O. Shatalov, Cand. Sci. (Pharm.), Associate Professor, Department of Biotechnology and Industrial Pharmacy, M.V. Lomonosov Institute of Fine Chemical Technologies, MIREA – Russian Technological University (86, Vernadskogo pr., Moscow, 119571, Russia). E-mail: shat-05@mail.ru. https://orcid.org/0000-0003-4510-1721

Ivan S. Ivanov, Postgraduate Student, Department of Biotechnology and Industrial Pharmacy, M.V. Lomonosov Institute of Fine Chemical Technologies, MIREA – Russian Technological University (86, Vernadskogo pr., Moscow, 119571, Russia). E-mail: ivan.ivanov1994@gmail.com, https://orcid.org/0000-0002-1346-7588

Anna V. Aydakova, Postgraduate Student, Department of Biotechnology and Industrial Pharmacy, M.V. Lomonosov Institute of Fine Chemical Technologies, MIREA – Russian Technological University (86, Vernadskogo pr., Moscow, 119571, Russia); Researcher, Institute of Pharmaceutical Technologies (86, Vernadskogo pr., Moscow, 119571, Russia). E-mail: ann.reznikova2012@yandex.ru, https://orcid.org/0000-0002-2560-5028

Alexander Herbst, Dr. Sci. (Eng.), General Director, Wingflow AG (Gänsacker 5, Frico AG, 5070, Switzerland). E-mail: herbst@wingflow.ch. https://orcid.org/0000-0003-2706-6360

Lasse Greiner, Dr. Sci. (Eng.), Professor, Head of the Faculty of Biotechnology, Manheim University of Applied Sciences (10, Paul-Wittsack Street, Mannheim, 68163, Germany). E-mail: greiner@wingflow.ch, https://orcid.org/0000-0002-5427-0378

Alexander P. Kaplun, Dr. Sci. (Chem.), Professor, Department of Biotechnology and Industrial Pharmacy, M.V. Lomonosov Institute of Fine Chemical Technologies, MIREA – Russian Technological University (86, Vernadskogo pr., Moscow, 119571, Russia). E-mail: alexander.p.kaplun@gmail.com. Scopus Author ID 7006433250, https://orcid.org/0000-0002-5600-8648

Anton S. Zhurbenko, Student, Department of Biotechnology and Industrial Pharmacy, M.V. Lomonosov Institute of Fine Chemical Technologies, MIREA – Russian Technological University (86, Vernadskogo pr., Moscow, 119571, Russia). E-mail: Zhurbenko_anton@mail.ru. https://orcid.org/0000-0001-5572-0695

Stanislav A. Kedik, Dr. Sci. (Eng.), Professor, Head of the Department of Biotechnology and Industrial Pharmacy, M.V. Lomonosov Institute of Fine Chemical Technologies, MIREA – Russian Technological University (86, Vernadskogo pr., Moscow 119571, Russia). E-mail: doctorkedik@yandex.ru. Scopus Author ID 7801632547, https://orcid.org/0000-0003-2610-8493

Об авторах:

Ахмедова Диана Александровна, студентка кафедры биотехнологии и промышленной фармации Института тонких химических технологий им. М.В. Ломоносова ФГБОУ ВО «МИРЭА – Российский технологический университет» (119571, Россия, Москва, пр-т Вернадского, д. 86); исследователь, Институт фармацевтических технологий (119571, Россия, Москва, пр-т Вернадского, д. 86). E-mail: akhmedova.diana.a@gmail.com. https://orcid.org/0000-0002-0951-939X

Шаталов Денис Олегович, к.фарм.н., доцент кафедры биотехнологии и промышленной фармации Института тонких химических технологий им. М.В. Ломоносова ФГБОУ ВО «МИРЭА – Российский технологический университет» (119571, Россия, Москва, пр-т Вернадского, д. 86). E-mail: shat-05@mail.ru. https://orcid.org/0000-0003-4510-1721

Иванов Иван Сергеевич, аспирант кафедры биотехнологии и промышленной фармации Института тонких химических технологий им. М.В. Ломоносова ФГБОУ ВО «МИРЭА – Российский технологический университет» (119571, Россия, Москва, пр-т Вернадского, д. 86). E-mail: ivan.ivanov1994@gmail.com. https://orcid.org/0000-0002-1346-7588

Айдакова Анна Викторовна, аспирант кафедры биотехнологии и промышленной фармации Института тонких химических технологий им. М.В. Ломоносова ФГБОУ ВО «МИРЭА – Российский технологический университет» (119571, Россия, Москва, пр-т Вернадского, д. 86); исследователь, Институт фармацевтических технологий (119571, Россия, Москва, пр-т Вернадского, д. 86). E-mail: ann.reznikova2012@yandex.ru. https://orcid.org/0000-0002-2560-5028

Гербст Александр, д.т.н., генеральный директор «Wingflow AG» (5070, Швейцария, Frick AG, Gänsacker 5). E-mail: herbst@wingflow.ch, https://orcid.org/0000-0003-2706-6360

Грайнер Лассе, д.т.н., профессор, декан факультета биотехнологии «Манхеймский университет прикладных наук» (68163, Германия, Мангейм, ул. Пауля-Виттсака, 10). E-mail: greiner@wingflow.ch, https://orcid.org/0000-0002-5427-0378

Каплун Александр Петрович, д.х.н., профессор кафедры биотехнологии и промышленной фармации Института тонких химических технологий им. М.В. Ломоносова ФГБОУ ВО «МИРЭА – Российский технологический университет» (119571, Россия, Москва, пр-т Вернадского, д. 86). E-mail: alexander.p.kaplun@gmail.com, Scopus Author ID 7006433250, https://orcid.org/0000-0002-5600-8648

Журбенко Антон Станиславович, студент кафедры биотехнологии и промышленной фармации Института тонких химических технологий им. М.В. Ломоносова ФГБОУ ВО «МИРЭА – Российский технологический университет» (119571, Россия, Москва, пр-т Вернадского, д. 86). E-mail: Zhurbenko_anton@mail.ru, https://orcid.org/0000-0001-5572-0695

Кедик Станислав Анатольевич, д.т.н., профессор, зав. кафедрой биотехнологии и промышленной фармации Института тонких химических технологий им. М.В. Ломоносова ФГБОУ ВО «МИРЭА – Российский технологический университет» (119571, Россия, Москва, пр-т Вернадского, д. 86); генеральный директор АО «Институт фармацевтических технологий» (119571, Россия, Москва, пр-т Вернадского, д. 86). E-mail: doctorkedik@yandex.ru. Scopus Author ID 7801632547, https://orcid.org/0000-0003-2610-8493

The article was submitted: April 24, 2021; approved after reviewing: May 11, 2021; accepted for publication: August 02, 2021.

Translated from Russian into English by N. Isaeva
Edited for English language and spelling by Enago, an editing brand of Crimson Interactive Inc.

CHEMISTRY AND TECHNOLOGY OF MEDICINAL COMPOUNDS AND BIOLOGICALLY ACTIVE SUBSTANCES

ХИМИЯ И ТЕХНОЛОГИЯ ЛЕКАРСТВЕННЫХ ПРЕПАРАТОВ И БИОЛОГИЧЕСКИ АКТИВНЫХ СОЕДИНЕНИЙ

ISSN 2686-7575 (Online)

https://doi.org/10.32362/2410-6593-2021-16-4-318-336

UDC 543.06

REVIEW ARTICLE

Biological functions of cobalt and its toxicology and detection in anti-doping control

Irina V. Pronina[1,2,@a], Elena S. Mochalova[1], Yuliya A. Efimova[3], Pavel V. Postnikov[1,@b]

[1]National Anti-Doping Laboratory (Institute), Lomonosov Moscow State University, Moscow, 105005 Russia
[2]Institute of General Pathology and Pathophysiology, Moscow, 125315 Russia
[3]MIREA – Russian Technological University (M.V. Lomonosov Institute of Fine Chemical Technologies), Moscow, 119571 Russia
[@]Corresponding author, e-mail: [a]pronina@dopingtest.ru, [b]postnikov@dopingtest.ru

Abstract

Objectives. *Over the last decade, hematopoietic stimulants have grown increasingly popular in elite sports. This is supported by the growing number of high-profile doping scandals linked to their use. A group of these stimulants includes cobalt salts, which cause an increase in the oxygen capacity of the blood as well as a powerful stimulation of metabolic processes, resulting innoticeable competitive advantages. The use of cobalt salts is regulated according to the Prohibited List of the World Anti-Doping Agency (WADA). Currently, only a few works have been dedicated to solving the problem of detecting the abuse of cobalt salts in anti-doping control. Only a few laboratories have included cobalt salt determination in their methodological bases. The purpose of this review is to attract the attention of the scientific community to the toxicity of cobalt compounds, consequences of their intake, and pharmacokinetics, as well as the problems in their detection methods due to their widespread availability in the modern market and the growing number of abuse cases.*

Results. *The main biological functions of cobalt, cellular levels of exposure, toxicity, and symptoms of cobalt salt poisoning are presented in detail in this review article. The data from the literature on the main methods for detecting cobalt as a doping agent have been generalized and systematized. There is a major focus on the amount of cobalt in dietary supplements that could cause an athlete to test positive for cobalt when they are consumed.*

Conclusions. *After analyzing promising cobalt detection approaches and methods, it was determined that high-performance liquid chromatography in combination with inductively coupled plasma mass spectrometry has an undeniable advantage for detecting cobalt as a doping agent. The lack of explicit WADA requirements for detection methods and the lack of its obligation to determine cobalt make it tempting for unscrupulous athletes to use its salts. Therefore, anti-doping laboratories must implement the abovementioned method as soon as possible.*

Keywords: *hematopoietic stimulants, cobalt, biological functions, dietary supplements, HIF, anti-doping control, toxic effect, mass spectrometry*

For citation: Pronina I.V., Mochalova E.S., Efimova Yu.A., Postnikov P.V. Biological functions of cobalt and its toxicology and detection in anti-doping control. *Tonk. Khim. Tekhnol. = Fine Chem. Technol.* 2021;16(4):318–336 (Russ., Eng.). https://doi.org/10.32362/2410-6593-2021-16-4-318-336

ОБЗОРНАЯ СТАТЬЯ

Биологические функции кобальта, токсикология и обнаружение в антидопинговом контроле

И.В. Пронина[1,2,@a], Е.С. Мочалова[1], Ю.А. Ефимова[3], П.В. Постников[1,@b]

[1]Национальная антидопинговая лаборатория (Институт), Московский государственный университет им. М.В. Ломоносова, Москва, 105005 Россия
[2]Научно-исследовательский институт общей патологии и патофизиологии, Москва, 125315 Россия
[3]МИРЭА – Российский технологический университет (Институт тонких химических технологий им. М.В. Ломоносова), Москва, 119571 Россия
[@]Автор для переписки, e-mail: [a]pronina@dopingtest.ru, [b]postnikov@dopingtest.ru

Аннотация

Цели. *В последнее десятилетие чрезвычайную популярность в спорте высших достижений приобрели стимуляторы кроветворения. Этот факт подтверждают и участившиеся громкие допинговые скандалы, связанные с их употреблением. Соли кобальта относятся к данному классу веществ, их использование приводит к увеличению кислородной емкости крови и к мощной стимуляции обменных процессов, что дает несомненные конкурентные преимущества. Применение солей кобальта регламентировано в соответствии с Запрещенным списком Всемирного антидопингового агентства. В настоящее время проблематике выявления злоупотреблений солями кобальта в антидопинговом контроле посвящено всего несколько работ. Лишь единичные лаборатории вводят определение солей кобальта в свою методологическую базу. Цель данного обзора состоит в том, чтобы обратить внимание научного сообщества на токсичность соединений кобальта, последствия их приема, фармакокинетику, проблематику и способы обнаружения ввиду их доступности на современном рынке и участившихся случаев злоупотребления ими.*

Результаты. *В представленном обзоре рассмотрены основные биологические функции кобальта и клеточные уровни воздействия, токсичность и симптоматика при отравлении его солями. Обобщены и систематизированы литературные данные по основным используемым методам идентификации кобальта как допингового агента. Особое внимание уделено содержанию кобальта в биологически-активных добавках, при приеме которых спортсмен может сдать положительный допинг-тест на кобальт.*

Выводы. *На основе анализа перспективных подходов и методов определения кобальта, сделан вывод о несомненном преимуществе высокоэффективной жидкостной хроматографии в сочетании с масс-спектрометрией с индуктивно-связанной плазмой для детекции кобальта как допингового агента. Отсутствие четких требований к методам идентификации со стороны ВАДА и обязательности определения кобальта, несомненно, делает привлекательным прием его солей недобросовестными спортсменами. Ввиду этого существует необходимость внедрения вышеуказанного метода в практику антидопинговых лабораторий в ближайшем будущем.*

Ключевые слова: *стимуляторы кроветворения, кобальт, БАД, HIF, антидопинговый контроль, масс-спектрометрия*

Для цитирования: Пронина И.В., Мочалова Е.С., Ефимова Ю.А., Постников П.В. Биологические функции кобальта, токсикология и обнаружение в антидопинговом контроле. *Тонкие химические технологии*. 2021;16(4):318–336. https://doi.org/10.32362/2410-6593-2021-16-4-318-336

INTRODUCTION

For many decades, cobalt(II) chloride has been used effectively to treat various types of anemia. However, cobalt and its compounds are the deadliest inorganic poisons, and they are very toxic in high doses[1]. Cobalt sulfate, e.g., is carcinogenic [1, 2] and mutagenic. Cobalt has been completely excluded from the list of modern clinically significant stimulants of erythropoiesis and its use in experiments has been limited because of the side effects of its preparations that have been discovered over time and the subsequent unambiguous recognition of it as a carcinogen. At the same time, the problem of identifying the use of cobalt as a doping agent arises from the availability of the drug on the pharmaceutical market, a convenient method of oral administration, powerful stimulation of erythropoiesis, and the fact that validated methods for determining soluble cobalt salts in human urine are usually not included in the methodological arsenal of modern anti-doping analysis. The alleged use of cobalt chloride ($CoCl_2$) as a doping agent has already been discussed several times [3–5]. In this case, anti-doping rules promote fair competition in sports and protect athletes from the harmful effects of substances, of which the danger may be underestimated. According to the 2021 World Anti-Doping Agency (WADA) Prohibited List, the use of cobalt salts by athletes is strictly regulated under Article S2 “Peptide hormones, growth factors, related substances, and mimetics,” paragraph 1.2 “hypoxia-inducible factor (HIF) activating agents.”

Biological functions of cobalt as a microelement

Cobalt, a naturally occurring trace mineral with properties similar to those of iron and nickel, induces a noticeable and stable polycythemic response

[1] Normy fiziologicheskikh potrebnostei v energii i pishchevykh veshchestvakh dlya razlichnykh grupp naseleniya Rossiiskoi Federatsii. Metodicheskie rekomendatsii (Norms of physiological needs for energy and nutrients for various groups of the population of the Russian Federation. Guidelines). Moscow: Federal’nyi tsentr gigieny i epidemiologii Rospotrebnadzora; 2009. 36 p. (in Russ).

[6, 7] through a more efficient transcription of the erythropoietin (EPO) gene. When $CoCl_2$ is taken in dosages of 120 or 150 mg/day, it causes a significant increase (up to 20%) in hematocrit and hemoglobin [7]. Cobalt chloride may soon become the most appropriate adjunct or substitute for erythropoiesis-stimulating substances, given the natural propensity of some athletes to experiment with novel, illegal, and potentially harmful doping agents and methods. Nevertheless, $CoCl_2$ administration has unsafe consequences, including toxic effects on the heart, liver, kidneys, and thyroid gland, as well as the development of oncological processes [2, 5].

The main biological function of cobalt is its presence in the vitamin B12 (cyanocobalamin) molecule, where its mass fraction is about 4%. Vitamin B12 is essential for appropriate nervous system function and is involved in the process of hematopoiesis. In humans, cobalt deficiency causes malignant (pernicious) anemia, also known as the Addison–Biermer disease. Cobalt quantification plays an important role in differentiating B12 deficiency anemia from folate deficiency, in which the concentration of cobalt in the blood is within the normal range. However, because cobalt deficiency, according to many scientists, corresponds to vitamin B12 deficiency, the quantitative determination of cobalt in the blood is more typically employed in clinical medicine to detect intoxication rather than deficiency.

To a lesser extent, cobalt is known as a coenzyme that is found in the active center of several vital enzymes in the human body, including ribonucleoside triphosphate reductase (EC 1.4.3.8), methyltransferase (EC 2.1.1.13), methylmalonyl-CoA mutase (EC 5.4.99.2), methylmalonyl-CoAcarboxyltransferase (EC 2.1.3.1), and propionyl-CoAcarboxylase (EC 6.4.1.3) [8]. Cobalt can also act as a coenzyme in some pyrophosphatases, peptidases, and arginases [9]. There is some evidence that cobalt may affect the activity of enzymes, particularly adenylate cyclase and several others [10, 11]. It has a particular effect on heme metabolism enzymes [12].

Cobalt has a variety of physiological and pathophysiological effects. There is evidence that it influences carbohydrate and lipid metabolism, thyroid gland function, and the state of the myocardium. Cobalt is on the carcinogenic agent list of the International Agency for Research on Cancer (IARC) of the World Health Organization (WHO); however, some of its complex compounds have antitumor effects [13]. It is toxic, but because it forms strong bonds with cyan ions, it can be used as an antidote for cyanide intoxication [14]. The epileptogenic effect of cobalt has been documented. Several studies from the first half of the twentieth century have demonstrated the effect of cobalt on blood pressure and vascular tone [15, 16].

Inorganic cobalt is obtained from food. Fish and seafood, liver, kidneys, nuts, mushrooms, vegetables, and fruits all contain sufficient amounts of cobalt required for the body's daily needs. According to studies carried out on healthy people, when 1 μg to 1.2 mg of $CoCl_2$ is administered orally, 5–20% of inorganic cobalt supplied with food is absorbed in the gastrointestinal tract. Women absorb more soluble cobalt than men [17]. The half-life has not yet been established.

According to studies on rats whose drinking water had the $^{57}Co^{2+}$ isotope added to it, the Co^{2+} ion accumulates mostly in the liver, lungs, and kidneys [18], as well as in the pancreas and spleen [10, 19, 20]. In the human blood, the cobalt concentration is an average of 0.238 mg/kg, while in erythrocytes it ranges from 0.059 to 0.13 mg/kg, and in serum from 0.0055 to 0.40 mg/kg. The kidneys eliminate 86% of the excess, whereas the intestines excrete 14%. Additionally, the concentration of cobalt in the blood varies based on the season and time of day, which is linked to human nutritional characteristics.

Cellular exposure to cobalt

The presence or absence of oxygen regulates the EPO gene under the control of the HIF-1 transcription factor. It has been shown that after the signal of a decrease in the oxygen concentration in the cell environment is received, a chain of events begins in the cell, which is the key to the binding of HIF-1 to hypoxiaresponse elements (HREs), which enhance transcription of the EPO gene [21–26]. The HIF-1 is a transcription factor that belongs to the basic helix-loop-helix family, and it consists of two subunits, HIF-1a and HIF-1b [14, 26]. The HIF-1a is a major regulator of cellular and systemic oxygen homeostasis due to an increase in the activity of binding to the DNA sequence of the EPO target gene during hypoxia. Under normoxic conditions, the main mediator, HIF-1a, is rapidly cleaved by the proteasome [26] (see figure). The Fe^{2+} ion, which is reversibly bound to the active center of these metalloenzymes, is known to be a required cofactor for prolyl hydrolase activity in the proteasome [27]. Consequently, a decrease in iron availability caused by competitive substitution with Co^{2+} ions of cobalt inhibits enzyme activity [28, 29]. Hypoxia or $CoCl_2$ introduction, which mimics hypoxia, significantly inhibits HIF-1a degradation. As a result, HIF-1a binds to HIF-1b, penetrates the nuclear membrane, and activates the transcription of the EPO gene as part of the HRE [26].

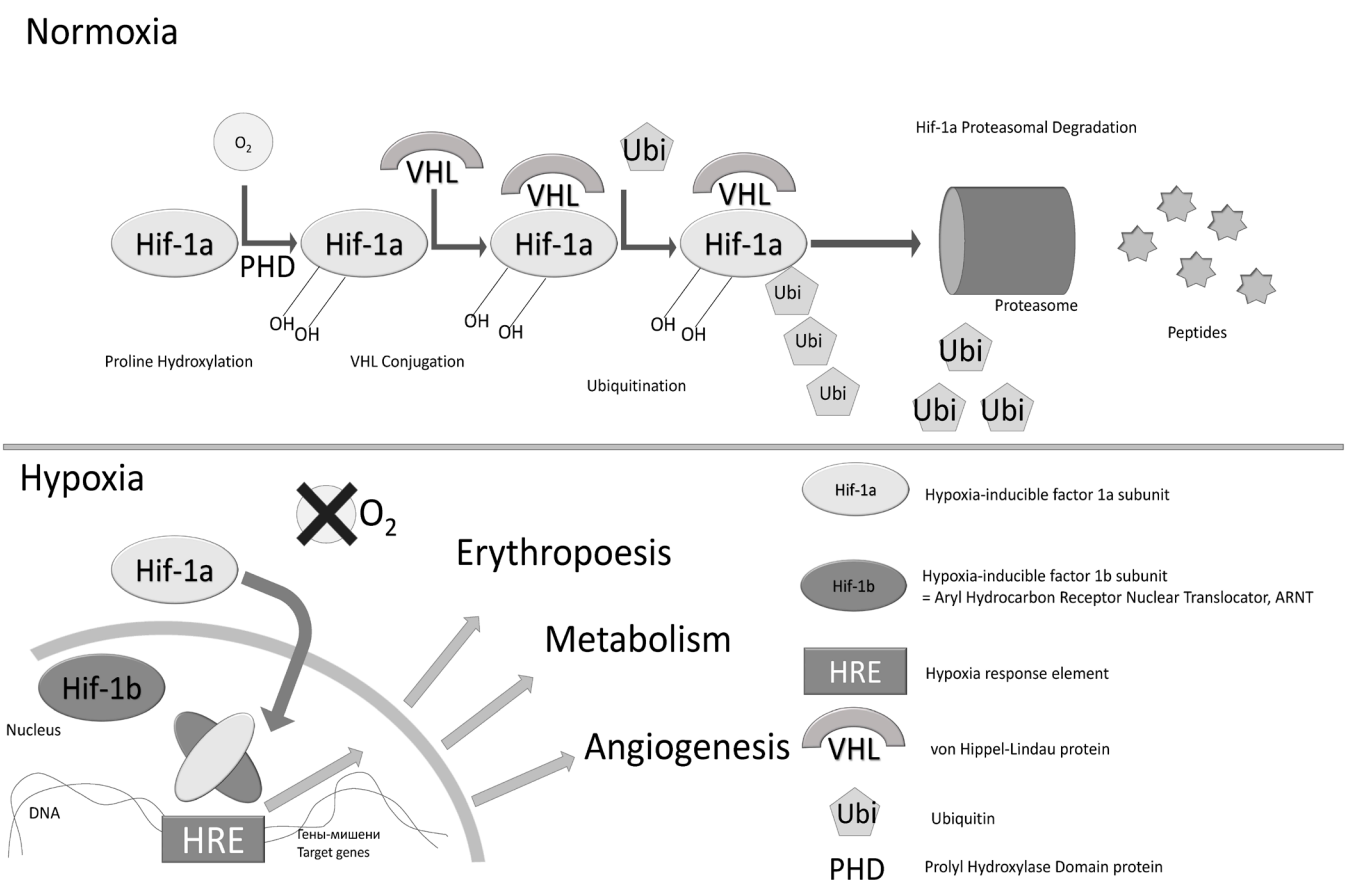

The effect of HIF at normal partial pressure of oxygen is normoxia in the cell and at oxygen deficiency is hypoxia (similar to the effect of cobalt preparations).

The Hep3B and HepG2 human hepatoblastoma cell cultures proved to be appropriate models for *in vitro* examination of the hypoxia induction patterns of EPO gene expression [11]. According to the authors of the hypothesis, a hemoprotein molecule, whose conformation is dependent on the partial pressure of oxygen in the environment where EPO-producing cells are located, serves as an oxygen sensor in cells. When the partial pressure of oxygen is low, the hemoprotein molecule is converted into a deoxy conformation, which triggers a chain of molecular events that eventually result in EPO gene expression. When the partial pressure of oxygenis sufficiently high, the hemoprotein molecule is in an inactive oxy-conformation and does not stimulate the production of EPO. Cobalt chloride, in the context of this hypothesis, appears to work in a similar mechanism; the cobalt atom displaces the iron atom from the heme of the sensory molecule and takes its place, resulting in hemoprotein"locking" in an active deoxyconformation and EPO gene expression, as in hypoxia conditions.

Cobalt is a typical d-element from a chemistry viewpoint, and it has two oxidation states in compounds: +2 (in most compounds) and +3 (mainly in complexes). The characteristic chemical properties of d-elements that are reflected in biology are variable oxidation states, participation in redox reactions, the ability to form complex ions, and catalytic activity. Since the atom and ion of cobalt have similar sizes to those of other micro and macroelements, it can imitate or modify the activity of other elements in addition to providing its biological effects [29, 30–32].

The atomic and electronic structures of metalloporphyrins (MeP) complexes with oxygen ($MeP–O_2$) and water ($MeP–H_2O$) molecules in the presence and absence of imidazole as a second ligand (the imidazole group of histidine is the functional group closest to heme) were studied using quantum chemistry methods [33]. Researchers have evaluated and compared the affinity of iron and cobalt ions for heme under conditions that mimic normoxia ($MeP–O_2$) and hypoxia ($MeP–H_2O$). In summary, the hypothesis is that cobalt ions can displace iron ions

from hemoprotein molecules, including hemoglobin, which changes the heme conformation in the same manner that low oxygen concentrations inside the cell (hypoxia) do. This mechanism explains the universal response of various body cells to excess cobalt [34–36] and the erythropoietic effect of inorganic cobalt action on the body as a whole.

Researchers have determined the energy and characteristics of the chemical bond as well as changes in the spatial configuration of heme under hypoxia conditions and when the iron atom is replaced with a cobalt atom [36]. In complexes of iron and cobalt porphyrins with oxygen (O_2) and water (H_2O) molecules, both molecules occupy the fifth coordination position, whereas the imidazole ring of the amino acid histidine occupies the sixth coordination position. The cobalt ion in a porphyrin complex in the presence of imidazole in the sixth coordination position (imitation of the globin environment) and the addition of oxygen in the fifth coordination position (imitation of normoxia) is displaced in the same manner as the iron ion when water is added in the fifth coordination position (imitation of hypoxia)[2]. These data explain why cells interpret an excess of cobalt in the body as hypoxia and promote the activation of corresponding compensatory processes, such as the activation of EPO gene expression[3].

It is worth noting that the effect of inorganic cobalt on the body is not limited to the stimulation of erythropoiesis. To date, HIF-1 has been demonstrated to cause the expression of diverse proteins in various cells, i.e., the cells and the body universally respond to hypoxia—through the activation of HIF proteins, which are transcription factors for genes. Genes encode proteins that stimulate not only the production of new erythrocytes but also angiogenesis (this may be the basis for the carcinogenic effect of cobalt), i.e., the formation of new blood vessels [2], as well as glycolysis as a method of obtaining energy in the absence or shortage of oxygen [37–42]. The HIF-1 has been demonstrated to stimulate the expression of genes of several glycolysis enzymes [43–46] and regulate angiogenesis and vascular tone [47–49], transferrin and its receptor [50–52], and a protein that binds to insulin-like growth factors [53] under hypoxia conditions. The HIF-1 is estimated to control about 5% of the human genome and genes that regulate cell growth, division, survival, and cell motility in addition to genes that control glycolysis and angiogenesis [37] (see figure).

Some HIF-activated genes encode proteins that can enhance physical performance independent of erythropoiesis (e.g., glycolytic enzymes, glucose transporters, and angiogenic peptides). Currently, reliable data on the effect of cobalt ions on biological processes in the body, which are not associated with the synthesis of erythrocytes but capable of influencing athletic performance, has been accumulated. For ethical reasons, research on this subject is primarily conducted on animals, but the possibility of applying the results to humans is evident even to a layperson. For example, preliminary administration of $CoCl_2$ to rats at a dose of 12.5 mg/kg of body weight has been demonstrated to protect them from high-altitude pulmonary edema that occurs during hypoxia caused by being under high-altitude conditions [54]. In another study, prefeeding rats with $CoCl_2$ supplementation increased mitochondrial biogenesis, glucose uptake, and metabolism by improving aerobic cellular respiration in the skeletal muscle, which improved physical performance [55, 56]. In 2018, a group of scientists from Germany and the United States investigated the effects of low doses of cobalt on the performance of volunteers during aerobic exercises [57]. The scientists discovered that administering 5 mg of cobalt per day to the volunteers for three weeks increased their endurance and maximum strength, even though none of them were involved in professional sports.

Biologically active additives and cobalt

Professional athletes, particularly elite athletes, widely use various nutritional supplements. According to studies in recent years, competitive athletes have been increasingly encountering prohibited compounds in supplements available on the pharmaceutical market to improve training performance, performance level, and overall athletic performance. The problem is that manufacturers of dietary supplements do not always accurately indicate the composition of the product on the packaging, resulting in the detection of prohibited substances in athletes who are sincerely confident that the substances are not present during doping tests. This trend can be found everywhere

[2] Morgulis I.I. Early reaction of the mammalian organism to exposure to cobalt chloride. Cand. Thesis. Krasnoyarsk: Krasnoyarskii nauchnyi tsentr; 2006. 112 p. URL: https://www.dissercat.com/content/rannyaya-reaktsiya-organizma-mlekopitayushchego-na-vozdeistvie-khloridom-kobalta (accessed May 12, 2021) (in Russ.).

[3] Postnikov P.V. Development of a highly sensitive method for the qualitative determination of the hybrid protein erythropoietin fused with the FC-part of human immunoglobulin g (EPO-FC) in blood serum samples for the purpose of anti-doping control. Cand. Thesis. Moscow: Moskovskii tekhnologicheskii universitet; 2017. 152 p. https://www.dissercat.com/content/razrabotka-vysokochuvstvitelnoi-metodiki-kachestvennogo-opredeleniya-gibridnogo-belka-eritro (in Russ.).

[58, 59]. The sensational messages of some anti-doping agencies, including the Russian Anti-Doping Agency and National Anti-Doping Agency of the Republic of Belarus, on the importance of cautiously using the Complivit vitamin complex, which contains inorganic cobalt, are worth remembering. However, erythropoiesis-stimulating agents (e.g., EPO and HIF stabilizers) are not often mentioned as ingredients in such products. Simultaneously, mixtures of a patented and undisclosed composition (including those intended only for veterinary use) have been discovered in the personal environment of elite athletes in recent years [60].

In Geyer's works [61, 62], products that are openly advertised with legitimate properties that assist in improving athletic performance were the subject of research on doping. These mixtures, which were confiscated or purchased for testing from onlinesuppliers by the Center for Preventive Doping Research (Germany) and various anti-doping organizations with allegedly declared properties for improving hematopoiesis, were sent for biochemical analysis to detect EPO and its derivatives; low molecular weight HIF stabilizers or transition metals such as cobalt; growth hormones, which are hormones that stimulate the production of growth hormone-releasing hormones and growth hormone-releasing peptides; low molecular weight organic analytes such as anabolic agents, stimulants, and β2-agonists; and selected trace minerals, including cobalt and nickel, according to established protocols. A total of 19 products were tested using various analytical testing methods, including high-resolution gas and liquid tandem chromatography–mass spectrometry (GC–MS and LC–HRMS–MS), gel electrophoresis, and inductively coupled plasma mass spectrometry (ICP–MS), as described in a previous work [59]. The test results are presented in the table below.

It is worth noting that three of the products had similar labels and the same brand names, but their contents were significantly different. It is assumed that there were fakes, counterfeits, and/or products with different compositions but a quite similar packaging among them [62].

Analysis of the presence of inorganic cobalt in products confiscated and purchased from online suppliers (on data of the Center for Preventive Doping Research, Germany) [62]

Product No.	Advertised effect	Product composition (suggested route of administration)	Components identified in the product relevant to doping control (≥0.1 mg/mL)	Stated on the label (Yes/No)	Note
1	Erythropoiesis stimulation	Water solution (intravenously)	Cobalt (0.1 mg/mL) Nickel (7.5 mg/mL)	No No	Cyanocobalamin is detected (about 2.0 mg/mL), which is about 90 μg/mL of cobalt
2	Erythropoiesis	Water solution (intravenously)	Cobalt (4.8 mg/mL)	No	Cyanocobalamin is detected (about 1.7 mg/mL), which is about 75 μg/mL of cobalt
3	Increases oxygen supply to muscle tissue	Water solution (intravenously)	–	–	Composition is not determined
4	Counteracts fatigue	Water solution (for injection)	–	–	Composition is not determined

Table. Continued

Product No.	Advertised effect	Product composition (suggested route of administration)	Components identified in the product relevant to doping control (≥0.1 mg/mL)	Stated on the label (Yes/No)	Note
5	Anti-inflammatory properties	Gel (intravenously or intramuscularly)	–	–	Composition is not determined
6	–	Water solution	Cobalt (3.4 mg/mL)	No	–
7	–	Water solution	–	–	Composition is not determined
8	Erythropoiesis stimulation	Water Suspension (intravenously)	Cobalt (1.9 mg/mL)	No	Cyanocobalamin is detected (about 2.6 mg/mL), which is about 110 μg/mL of cobalt
9	Erythropoiesis	Water Suspension (intravenously)	Cobalt (2.2 mg/mL)	No	–
10	Erythropoiesis	Water solution (intravenously)	Cobalt (3.3 mg/mL)	No	Cyanocobalamin is detected (about 3.0 mg/mL), which is about 270 μg/mL of cobalt
11	Increased competitiveness	Water solution (intravenously)	–	–	Composition is not determined
12	Counteracts fatigue	Water Suspension (intravenously)	–	–	Composition is not determined
13	Increases oxygen transport	Water solution (intravenously)	–	–	Composition is not determined

Table. Continued

Product No.	Advertised effect	Product composition (suggested route of administration)	Components identified in the product relevant to doping control (≥0.1 mg/mL)	Stated on the label (Yes/No)	Note
14	Increases oxygen transport	Water solution (intravenously)	–	–	Composition is not determined
15	Erythropoiesis	Water Suspension (intravenously or intramuscularly	Cobalt (3.3 mg/mL)	Yes	The label indicates the presence of cobalt gluconate (2.0 mg/mL), which is about 260 μg/mL of cobalt, cyanocobalamin (0.25 mg/mL), which is about 10 μg/mL of cobalt
16	Erythropoiesis stimulation	Water Suspension (intravenously or intramuscularly	Cobalt (0.2 mg/mL)	Yes	The label indicates the presence of cobalt gluconate (0.7 mg/mL), which is about 90 μg/mL of cobalt, cyanocobalamin (0.15 mg/mL), which is about 7 μg/mL of cobal
17	Erythropoiesis	Water solution (intravenously)	Cobalt (0.1 mg/mL)	No	Cyanocobalamin is detected (about 4.0 mg/mL), which is about 175 μg/mL of cobalt
18	Erythropoiesis	Water solution (intravenously)	Cobalt (0.1 mg/mL)	No	Cyanocobalamin is detected (about 3.3 mg/mL), which is about 140 μg/mL of cobalt
19	–	Water solution in confiscated syringe	Cobalt (5.5 mg/mL)	Unknown	Cyanocobalamin is detected (about 5.3 mg/mL), which is about 230 μg/mL of cobalt

In the case of veterinary drugs, interesting studies were conducted jointly by the Hong Kong Jockey Club and the United Arab Emirates Racing Society based on the Racing Laboratory of the Hong Kong Jockey Club [63], as well as independently by the British Racing Society based on the School of Veterinary Medicine and Science of the University of Nottingham [64]. They investigated widely used vitamin preparations, some of which can be purchased without a prescription in veterinary pharmacies in Russia (for example, Hemo-15 or VAM® Injection). Laboratory analysis of blood samples from horses that received these drugs strictly according to the manufacturer's instructions and under the supervision of veterinarians revealed that the cobalt threshold was exceeded within 3–5 days after drug administration.

The results of Geyer's research [61, 62] lead us to believe that additional explanation and educational work on the usage of vitamin–mineral supplements and other biologically active supplements among athletes are necessary. The National Anti-Doping Laboratory of Moscow State University has begun research on developing methods for detecting prohibited substances not only in the blood samples of athletes but also in dietary supplements on the market.

Use of cobalt preparations in clinics and as a doping agent

Over the last ten years, advances in the understanding of the physiological regulation of the erythropoietic system have revealed new anchor points for pharmacological manipulation. The aerobic capacity of the blood correlates with the total hemoglobin mass in erythrocytes and the number of erythrocytes. Since muscle performance is directly dependent on the amount of oxygen supplied through the bloodstream, an increase in red blood cell mass results in an increase in aerobic endurance [65]. This phenomenon prompts dishonest athletes to artificially stimulate erythropoiesis. Recombinant human EPO (rhEPO) and its analogs are commonly used for these purposes, but they can be easily detected through doping tests[4] [66, 67], they are quite expensive, and their use is associated with certain difficulties (e.g., rhEPO exists only in injection forms). In terms of doping control, cobalt(II) chloride is particularly interesting because it is an inexpensive and readily available drug. Cobalt ions activate hypoxia-induced transcription factors that increase EPO expression [68].

The erythropoiesis-stimulating activity of inorganic cobalt was first discovered in the 1940s. Cobalt chloride was used to treat anemic patients from the late 1940s to the late 1970s. The medication drug was normally administered as tablets in divided doses with meals. Cobalt chloride is a reference substance for *in vivo* calibration of the rhEPO drug substance; 5 μmol of $CoCl_2$ has the same erythropoiesis-stimulating activity as one international unit of rhEPO [69].

Jefferson [70] discovered that about 50% of highland residents with excessive erythrocytosis had elevated cobalt levels. The percentage of free cobalt ions is only 5–12% of the total cobalt concentration in the blood plasma, of which the main part is associated with albumin [71]. Cobalt is mainly excreted in the urine, and a small amount is excreted in the bile via the gastrointestinal tract. Normal urinary cobalt concentrations are less than 2 μg/L in individuals who do not use any supplements or are unexposed to a cobalt-rich environment. Women have a higher cobalt concentration in urine (median: 109.7 nmol/mmol creatinine) than men (median: 38.4 nmol/mmol creatinine) when they consume $CoCl_2$. After a single intravenous injection of inorganic cobalt in adult men, 40% of cobalt is excreted from the body within the first 24 h, 70% within one week, and 80% within one month, with approximately 10% remaining after a year.

Cobalt salts are assumed to be used as an alternative to other erythropoiesis-stimulating agents (rhEPO injections) or blood doping drugs in the form of autologous blood transfusion or erythrocyte transfusion by athletes [5]. Indeed, $CoCl_2$ is readily available, inexpensive, easy to administer, and highly effective. It is available as a pill or as an ingredient in sports drinks (electrolytes, protein shakes, and energy drinks). Since the parenteral route prevents the development of unwanted gastrointestinal effects, only a few trials of intravenous or intramuscular administration of $CoCl_2$ have been conducted, but the specific toxicity of intravenous administration is not fully known. Intramuscular administration of $CoCl_2$ can be painful and cause tissue necrosis.

The potential abuse of cobalt deserves special attention from anti-doping organizations. Unscrupulous athletes and trainers who use $CoCl_2$ to improve their athletic performance ignore its cumulative toxic effects and the many side effects

[4] Postnikov P.V. Development of a highly sensitive method for the qualitative determination of the hybrid protein erythropoietin fused with the FC-part of human immunoglobulin g (EPO-FC) in blood serum samples for the purpose of anti-doping control. Cand. Thesis. Moscow: Moskovskii tekhnologicheskii universitet; 2017. 152 p. https://www.dissercat.com/content/razrabotka-vysokochuvstvitelnoi-metodiki-kachestvennogo-opredeleniya-gibridnogo-belka-eritro (in Russ.).

that have resulted in its medical abandonment. Although $CoCl_2$ therapy has been shown to effectively stimulate erythropoiesis in both extrarenal and renal anemia, septic infection, myeloid hypoplasia, sickle cell anemia, rheumatoid arthritis, and chronic kidney disease, the accumulation of the element resulting from long-term use makes it toxic.

Toxic effects of cobalt

Although cobalt is not a highly toxic metal, it can have undesirable effects and cause serious health problems in high concentrations. Pulmonary edema, nausea, vomiting, bleeding, and renal failure are some of the acute symptoms of cobalt poisoning. Chronic intoxication causes pulmonary pathology, allergic dermatitis, hyperkeratosis, thyroid dysfunction, cardiomyopathy and heart failure (particularly in alcoholics), and neuropathy [72]. The toxic effect of cobalt is amplified by increasing air temperatures. Dust inhalation during cobalt-doped metal processing can cause interstitial lung diseases and asthma.

The first reports on cobalt toxicity appeared in the 19th century; however, researchers focused their attention on the study of this issue when the syndrome of "beer cardiomyopathy" was discovered. In the 1960s, some breweries used cobalt salts (chloride and sulfate at concentrations of 1.2–1.5 mg/L) to stabilize foam. People who consumed more than four liters of beer a day experienced major side effects including heart problems, which might be fatal in some cases. Cardiomegaly, various types of arrhythmias, cyanosis, low cardiac output, pericardial effusion, and hypotensionare all symptoms of the syndrome. From 1964 to 1966, cases of beer-related cobalt cardiomyopathy were reported in Omaha (Nebraska, USA), Quebec (Canada), Leuven (Belgium), and Minneapolis (Minnesota, USA). The disease occurred in humans even though the cobalt dose(up to 10 mg/day) was less than the doses used to treat anemia. Cobalt has not been used for brewing since then, and it is now illegal. This also influenced the early discontinuation of its use for the treatment of anemia.

Cardiomyopathies have also been observed in hard metal workers who inhaled cobalt in concentrations exceeding 100 μg/m^3 air. Intravenous or intramuscular administration of $CoCl_2$ can also cause heart failure. For example, a 17-year-old woman with chronic kidney disease died of rapidly progressing dilated cardiomyopathy after nine months of $CoCl_2$ therapy (25 mg per day). According to the postmortem examination, the cobalt concentration in the myocardium was 8.9 μg/g (dry tissue) (norm 0.2 μg/g). Weißbecker [73, 74] observed an increase in the systolic blood pressure in all patients treated with $CoCl_2$. This is consistent with the findings, which revealed that treatment with recombinant epoetin may also be associated with an increase in blood pressure, although the mechanisms of this increase are not fully understood.

Curtis [75] administered 50 mg of $CoCl_2$ daily for three months to 23 hemodialysis patients with chronic kidney disease. As expected, this treatment resulted in a 10 g/L increase in the hemoglobin concentration in about 50% of the patients. However, one patient died three months after completing the cobalt therapy, and histological examination of the myocardial tissue indicated that he developed cardiomyopathy. In the postmortem period, the cobalt concentration in the myocardium was 1.65 μg/g, which is approximately 25–80 times higher than that in the control samples. Curtis [75] conducted a prospective study on blood cobalt concentrations in healthy individuals and hemodialysis patients after two weeks of administration of $CoCl_2$. In both groups, there was a long-term increase in the blood cobalt concentration, which returned to normal six weeks after discontinuation of $CoCl_2$ administration.

Schirrmacher [76] described the case of a 35-year-old woman who was treated for renal anemia with 100 mg of $CoCl_2$ daily. After six months,the intake of cobalt(II) chloride was discontinued because of the development of neurological disease. On examination, the patient had bilateral sensorineural hearing loss, loss of vibration sensitivity in both legs, and disturbances during the calcaneal-knee test, as well as extensive thyroid gland enlargement. Hearing loss has also been reported as a side effect of $CoCl_2$ therapy. Gardner [15] orally administered 50–150 mg of $CoCl_2$ daily to 17 patients with chronic kidney disease, and four of them complained of tinnitus after 4–16 weeks. The audiogram revealed a hearing loss of over 1000 Hz. When the therapy was discontinued, the hearing returned. Hearing loss caused by $CoCl_2$ therapy and its reversibility when treatment is discontinued has also been confirmed by other researchers. Licht [77] observed optic atrophy in a 32-year-old patient who was treated for pancytopenia with up to 200 mg of cobalt(II) chloride per day in four treatment intervals, each lasting three to four months, for three years. The patient developed choroidal perfusion and optic nerve atrophy, which affected visual acuity, as well as nausea and vomiting, which often accompanied the state of chronic intoxication of the body.

Cobalt prevents the thyroid gland from absorbing iodine. Thus, myxedema and thyroid hyperplasia are relatively common side effects of cobalt salt

treatment. During cobalt therapy, Kriss [78] observed thyroid abnormalities in five patients. Among them were four children with sickle cell disease who received 30–100 mg of $CoCl_2$ daily for 14–30 weeks. A few weeks after the therapy was stopped, goiter and thyroid dysfunction decreased. Since the undesirable effects were associated with cobalt treatment, the author criticized its careless use as a therapeutic agent.

Oral administration of 500 mg of $CoCl_2$ can cause gastrointestinal diseases, nausea, vomiting, and weight loss. Mucklow [37] reported the case of a 6-year-old boy who developed abdominal pain and vomiting after taking a drink containing 2.5 g of $CoCl_2$. The cobalt concentration in his blood plasma was 7.23 μM (normal value <0.02 μM) 7 h after ingestion and 0.09 μM one month later. According to Jacobziner and Raybin [79], the worst case was that of a 19-month-old boy who died about 7 h after swallowing about 30 mL of $CoCl_2$ solution. Autopsy results revealed necrosis of the gastric mucosa, and the liver, kidneys, and spleen were overloaded with cobalt.

Various works have described some aspects of the biochemical properties of inorganic cobalt in relation to its bioavailability and the potential hazard of usage [27, 37, 38]. Later, a staff of the Birmingham Center for the National Poison Information Service of Great Britain compiled a monograph on the toxic effects of $CoCl_2$ [39]. Cobalt and its compounds can enter the human body through various routes (oral, dermal, inhalation, intravenous, and subcutaneous). Cobalt toxicity, body tissue or organ, and the extent of damage will vary depending on the route of ingestion. In addition, the exposure time and the amount of cobalt consumed are critical. There is a risk of intolerance and organ damage at high dosages (>25 mg/day) [40].

Even though the toxic effect of cobalt has been proven many times, the molecular mechanisms of its toxicity remain unidentified. When high concentrations of cobalt are used, it causes harmful effects that are associated with the effect of hypoxia or the "sensation" of a lack of oxygen by the cell. Moreover, oxygen is necessary for the proper functioning of all the cells in any organism. Cobalt is a genotoxic metal [52, 80] that induces oxidative stress [53] and apoptosis [81]. By stabilizing HIF, cobalt ions can activate genes that encode proteins involved in tumor growth (e.g., vascular endothelial growth factor [56] and multidrug-resistant P-glycoprotein transporter). Cobalt salts were discovered to promote the development of carcinoma when introduced in experimental animals. Furthermore, inorganic cobalt was discovered to induce DNA strand breaks, DNA-protein cross-linking, exchanges of sister chromatids, and the formation of micronuclei in mammalian cell cultures. Soluble cobalt(II) salts are classified by the IARC of WHO as group 2B carcinogens (possibly carcinogenic to humans) [22]. Their usage as hypoxia mimetics is currently limited to laboratory experiments because of their toxic side effects [23].

The risk of adverse events increases as the dose and duration of treatment increase. The duration of the therapeutic administration of $CoCl_2$ averages approximately 10 weeks. A daily cobalt dose of 0.03 mg/kg of body weight for oral administration is considered safe in terms of toxic health effects in the general population. This dose is much lower than the therapeutic doses used to stimulate erythropoiesis in clinics. Unfortunately, many athletes are either unaware of or unconcerned about the possible health risks associated with using cobalt as a doping agent.

Determination of cobalt in biological samples

The first attempts to develop strategies for detecting cobalt salt doping in athletes were made earlier. The cobalt content in erythrocytes was proposed as a parameter because the absorption of inorganic cobalt by erythrocytes is practically irreversible and reflects the concentration of cobalt in the plasma [43]. Unice [44] used a biokinetic model to estimate the cobalt levels in the blood and urine as a result of oral ingestion of cobalt amounts that exceeded typical dietary intake. The expected cobalt concentrations after 10 days of ingesting cobalt in a daily dose of 0.4–1.0 mg ranged from 1.7 to 10 μg/L in the blood and 20–120 μg/L in the urine. It was expected that using inorganic cobalt preparations at a rate of 1.0 mg of cobalt per day for a year or more would result in the determination of cobalt concentrations of 5.7–13 μg/L in the blood and 65–150 μg/L in the urine.

The concentration of cobalt was also established using atomic absorption spectroscopy with a graphite cell, and according to the findings of the IARC WHO working group, it was 0.1–0.5 μg/L in the human blood plasma in experimental samples [22].

The GC–MS [82] and a validated quantitative tandem electrospray ionization MS method with a low detection limit of 50 pg/mL [83] are two methods that are compatible with routine doping control procedures for determining cobalt in human urine. Other widely used sensitive methods of quantitative determination include ICP–MS, ICP atomic emission spectrometry, and electrothermal atomic absorption spectroscopy [84]. Since cobalt is a natural and essential trace element [50] that can be found in the urine of healthy people in concentrations ranging

from 40 to 810 pg/mL [85], control and threshold values must be determined to confirm an unfavorable analytical conclusion. The highly sensitive LC–ICP–MS method with detection limits of up to 0.8 pg/mL is the best analytical approach for solving this problem.

The use of only plastic laboratory glassware made of polypropylene is regulated in modern anti-doping methods for determining inorganic cobalt because glassware may contain trace amounts of cobalt as a result of the manufacturing process, which may affect the analysis result [63, 86].

Urine, plasma, or blood serum can be used for analysis. Additionally, a method for determining and comparing the cobalt concentration in erythrocytes to the cobalt concentration in the plasma is being developed to distinguish the source of cobalt ingestion in the body (various forms of vitamin B12 or inorganic cobalt) [76]. Blood is collected in tubes containing Li-heparin (lithium heparin salt) or the potassium or sodium salt of ethylenediaminetetraacetic acid and centrifuged to separate the plasma. The urine is collected in clean plastic containers. Samples are kept frozen at −20°C until analysis.

Screening analysis is usually performed with the ICP–MS method [59, 63, 86–88] using standard solutions of cobalt and germanium with certified values that correspond to standard reference materials 3113 and 3120a of the National Institute of Standards and Technology, which are used to construct a calibration curve (cobalt solutions) and as an internal standard (germanium solutions). Working standard solutions of cobalt and germanium are prepared by diluting the corresponding standard solutions with 3.25% (v/v) nitric acid. For the ICP–MS analysis and construction of calibration curves, European laboratories often use the standard solution of cobalt CertiPUR® (1 mg/mL) from *Merck*, Germany, as an internal standard, the indium plasma emission standard (1 mg/mL) from VWR *International GmbH* (Bruchsal, Germany), and a standard solution containing 10 μg/mL of germanium, cobalt, lithium, titanium, and yttrium in 2% nitric acid from *Agilent Technologies* (Waldbronn, Germany).

Calibration mixtures, quality control (QC) samples, and corresponding blanks are analyzed along with each batch of the test samples. Calibration mixtures and QC samples are prepared using standard working cobalt solutions. To obtain a calibration curve, the ratios of the area of cobalt peaks to the internal standard (germanium) versus the added cobalt concentrations are fitted using linear regression. The total cobalt concentrations in the test samples are interpolated using a calibration dependence. For the QC samples, the recovered cobalt concentration is obtained by subtracting the concentration of the corresponding empty matrix from the total determined concentration. At the discretion of the laboratory, calibration mixtures can be prepared in ultrapure water, plasma, or urine depending on the samples that are being analyzed. At least six points in the range of 0–25 ng/mL or more in the plasma and 0–500 ng/mL or more in the urine are plotted on the calibration curves. Each batch includes one or two QC samples and/or a Certified Reference Material. The QC samples are prepared by adding cobalt standard solutions to the purified plasma and urine.

The internal standard (germanium solution) is added to the urine sample before it is diluted 5–50 times with 3.25% nitric acid for screening analysis. After adding an internal standard, blood plasma (serum) samples are deproteinized with a trichloroacetic acid (TCA) solution (10 g of TCA and 120 mg of NaCl per 100 mL of ultrapure water) followed by the addition of 3.25% nitric acid and centrifugation. The plasma sample should be finally diluted 5–50 times. For analysis, 80–100 μL of the original sample is usually used. The diluted sample is injected into the ICP–MS spectrometer through an autosampler. Argon is used as a plasma-forming gas, and helium is used as a target gas. Detected isotopes: m/z 59 for cobalt and m/z 72 for germanium [55]. Three parallel determinations were used to collect all data. To minimize carryover, the autosampler needle is flushed with deionized water for 5 s in the rinse port and 5 s in the rinse bottle after each sample injection, followed by a 0.07% Triton-X rinse for a maximum of 100 s. Finally, the autosampler probe is flushed again with deionized water for 20 s before the next infusion.

Confirmatory analysis for cobalt doping is usually performed using LC–MS [63, 86, 87]. The internal standard is usually not used in this case. Before plasma or serum analysis, protein precipitation is performed. Inorganic cobalt is determined using diethyl thiocarbamate (DDC), which requires additional sample preparation. The Co-DDC complex is detected in a one-time interval in a positive electrospray ionization mode using the selected reaction monitoring. The selected ion-precursor of the Co-DDC complex has an m/z of 355 [63].

Routine doping tests require fast and simple protocols for preparing samples for analysis. In this regard, Knoop's work [87] is interesting because it describes in detail the method of high-performance LC in combination with ICP–MS (HPLC–ICP–MS), which allows chromatographic peaks to distinguish the cobalt prohibited for use (inorganic cobalt) from endogenous cobalt, which is a component

of cyanocobalamin which is extremely important for doping control. This method also has high sensitivity and the ability to detect one cobalt particle out of 10^{12} other particles and analyze the isotopic composition of the ion of interest, making it the method of choice for modern doping control.

Additional testing strategies based on the identification of indirect biological effects of $CoCl_2$ administration, such as activation of vascular endothelial growth factor gene transcription [45], altered microRNA marker profiles, or enhanced synthesis of delta-aminolevulinate [46], could be reliable alternatives. However, they require a lengthy and complex process of clinical and analytical validation.

CONCLUSIONS

The use of cobalt as a doping agent to improve athletic performance has been and will continue to be a relevant topic of discussion. This article discusses in detail its main biological effects on the body in comparison to the use of erythropoiesis-stimulating agents such as recombinant EPOs or inhibitors of HIF-prolyl hydroxylases. The absence of a clear WADA-approved technical document on the detection of cobalt or the analysis method and the obligation for all anti-doping laboratories in the world to determine it makes its use even more appealing to unscrupulous athletes. More focus is placed on the problem of using cobalt salts for medical purposes and as biologically active supplements, the potential harm of their use due to their toxic effects on the human body, and the possible sanctions for athletes who use such dietary supplements.

The data from the literature on the main methods for detecting cobalt were collected and summarized. The HPLC–ICP–MS method, which distinguishes endogenous cobalt (a part of vitamin B12) from the cobalt prohibited for use (inorganic cobalt), is the most promising and highly sensitive of all the methods considered in the review.

Currently, anti-doping laboratories are tasked with the primary responsibility of introducing the abovementioned method into their methodological base for the unambiguous determination of the abuse of cobalt salts by athletes. This will reduce the number of disqualifications associated with their use and prevent possible cases of potential poisoning by them.

The authors declare no conflicts of interest.

REFERENCES

1. Nieboer E., Sanford W.E. Essential, toxic and therapeutic functions of metals (including determinant of reactivity). In: *Rev. Biochem. Toxicol*. New York: Elsevier; 1985;7:205–245

2. Salnikow K., Donald S.P., Bruick R.K., Zhitkovich A., Phang J.M., Kasprzak K.S. Depletion of intracellular ascorbate by the carcinogenic metals nickel and cobalt results in the induction of hypoxic stress. *J. Biol. Chem.* 2004;279(39):40337–40344. https://doi.org/10.1074/jbc.m4030572003

3. Lippi G., Franchini M., Guidi G.C. Cobalt chloride administration in athletes: a new perspective in blood doping? *Br. J. Sports Med.* 2005;39(11):872–873. https://doi.org/10.1136/bjsm.2005.019232

4. Jelkmann W. Erythropoiesis stimulating agents and techniques: a challenge for doping analysts. *Curr. Med. Chem.* 2009;16(10):1236–1247. https://doi.org/10.2174/092986709787846668

5. Lippi G., Franchini M., Guidi G.C. Blood doping by cobalt. Should we measure cobalt in athletes? *J. Occup. Med. Toxicol.* 2006;1:18. https://doi.org/10.1186/1745-6673-1-18

6. Lippi G., Montagnana M., Guidi G.C. Albumin cobalt binding and ischemia modified albumin generation: an endogenous response to ischemia? *Int. J. Cardiol*. 2006;108(3):410–411. https://doi.org/10.1016/j.ijcard.2005.03.040

7. Davis J.E., Fields J.P. Experimental production of polycythemia in humans by administration of cobalt chloride. *Proc. Soc. Exp. Biol. Med.* 1958;99(2):493–495. https://doi.org/10.3181/00379727-99-24395

8. Morgulis I.I., Khlebopros R.G. *Biologicheskaya rol' kobal'ta* (*The biological role of cobalt*). Krasnoyarsk: Krasnoyarskii nauchnyi tsentr Sib. Otd. Ros. Akad. Nauk; 2005. 24 p. URL: http://modernproblems.org.ru/ecology/25-hlebopos10.html (accessed May 12, 2021) (in Russ.).

9. Kudrin A.V. Metals and proteolytic enzymes. *Vopr. biol., med. i farm. khimii = Probl. of Biol., Med. and Pharm. Chemistry.* 1999;(3):19–24 (in Russ.)

10. Taylor A., Marks V. Cobalt: a review. *J. Hum. Nutr.* 1978;32(3):165–177. https://doi.org/10.3109/09637487809144525

11. Ueno M., Seferynska J., Beckman B., Brookins J., Nakashima J., Fisher J. W. Enhanced erythropoietin secretion in hepatoblastoma cells in response to hypoxia. *Am. J. Physiol.* 1989;257:(4Pt. 1):C743–C749. https://doi.org/10.1152/ajpcell.1989.257.4.c743

12. Kaliman P.A., Belovetskaya I.V. Effect of cobalt chloride on the activity of key enzymes of heme metabolism in rat liver. *Biokhimiya = Biochemistry*. 1986;51(8):1307–1308 (in Russ.).

13. Osinskii S., Levitin I., Bubnovskaya L. Selectivity of the action of redox-active complexes of cobalt(III) on tumor tissue. *Eksperimental'naya onkologiya = Experimental Oncology.* 2004;26(2):18–24 (in Russ.).

14. Izom G.E., Way J.L. Cyanide intoxication: protection with cobaltous chloride. *Toxicol. Appl. Pharmacol.* 1973;24(3):449–456. https://doi.org/10.1016/0041-008x(73)90051-3

15. Gardner F.H. The use of cobaltous chloride in the anemia associated with chronic renal disease. *J. Lab. Clin. Med.* 1953;41(1):56–64.

16. Wintrobe M.M., Grinstein M., Dubash J.J., Humphreys S.R., Ashenbrucker H., Worth W. The anemia of infection, VI. The influence of cobalt on the anemia associated with inflammation. *Blood.* 1947;2(4):323–331. https://doi.org/10.1182/blood.v2.4.323.323

17. Christensen J.M., Poulsen O.M., Thomsen M. A short-term cross-over study on oral administration of soluble and insoluble cobalt compounds: sex differences in biological levels. *Int. Arch. Occup. Environ. Health.* 1993;65(4):233. https://doi.org/10.1007/bf00381196

18. Edel J., Pozzi G., Sabbioni E., Pietra R., Devos S. Metabolic and toxicological studies on cobalt. *Sci. Total Environ.* 1994;150(1–3):233–244. https://doi.org/10.1016/0048-9697(94)90159-7

19. Young R.S. Cobalt. In: Frieden E. (Ed.). *Biochemistry of the Essential Ultratrace Elements*. UK: Springer; 1985;3:133–147. URL: https://link.springer.com/chapter/10.1007/978-1-4684-4775-0_6

20. Taylor A. Detection and monitoring of disorders of essential trace elements. *Ann. Clin. Biochem*. 1996;33(Pt 6):486–510. https://doi.org/10.1177/000456329603300603

21. Barceloux D.G. Cobalt. *J. Toxicol. Clin. Toxicol.* 1999;37(2):201–206. https://doi.org/10.1081/clt-100102420

22. Cobalt in Hard Metals and Cobalt Sulfate, Gallium Arsenide, Indium Phosphide and Vanadium Pentoxide. IARC Working Group on the Evaluation of Carcinogenic Risks to Humans. Lyon, France: 2006. V. 86. 353 p. URL: http://monographs.iarc.fr/ENG/Monographs/vol86/mono86.pdf (accessed May 12, 2021).

23. Beuck S., Schänzer W., Thevis M. Hypoxia-inducible factor stabilizers and other small-molecule erythropoiesis-stimulating agents in current and preventive doping analysis. *Drug Test. Analysis.* 2012;4(11):830–845. https://doi.org/10.1002/dta.390

24. Ebert B, Jelkmann W. Intolerability of cobalt salt as erythropoietic agent. *Drug Test Anal.* 2014;6(3):185–189. https://doi.org/10.1002/dta.1528

25. Jelkmann W. The disparate roles of cobalt in erythropoiesis, and doping relevance. *Open J. Hematol.* 2012;3(1):1–9.

26. Zang Q., Yan Q., Yang H., Wei W. Oxygen sensing and adaptability won the 2019 Nobel Prize in Physiology or medicine. *Genes & Diseases*. 2019;6(4):328–332. https://doi.org/10.1016/j.gendis.2019.10.006

27. Stolze I.P., Mole D.R., Ratcliffe P.J. Regulation of HIF: prolyl hydroxylases. *Novartis Found. Symp.* 2006;272:15–25. https://doi.org/10.1002/9780470035009.ch3

28. Epstein A.C., Gleadle J.M., McNeill L.A., Hewitson K.S., O'Rourke J., Mole D.R., Mukherji M., Metzen E., Wilson M.I., Dhanda A., Tian Y.M., Masson N., Hamilton D.L., Jaakkola P., Barstead R., Hodgkin J., Maxwell P.H., Pugh C.W., Schofield C.J., Ratcliffe P.J. C. elegans EGL-9 and mammalian homologs define a family of dioxygenases that regulate HIF by prolyl hydroxylation. *Cell.* 2001;107(1):43–54. https://doi.org/10.1016/s0092-8674(01)00507-4

29. Kolomeitsev A.V., Tararina L.I., Morgulis I.I. The effect of cobalt chloride on hematopoiesis in mice early after exposure. *Vestnik KrasGAU = The Bulletin of KrasGAU*. 2003;2:101–103 (in Russ.).]

30. Goncharevskaya O.A., Monin Yu.G., Natochin Yu.V. Regulation of the rate of proximal and distal reabsorption with intratubular administration of cobalt. *Fiziologicheskii zhurnal SSSR = J. Physiology USSR.* 1985;71(10):1287–1292 (in Russ.).

31. Yamagami K., Nishimura S., Sorimachi M. Cd^{2+} and Co^{2+} at micromolar concentrations mobilize intracellular Ca^{2+} via the generation of inositol 1,4,5-triphosphate in bovine chromaffin cells. *Brain Res.* 1998;798(1–2):316–319. https://doi.org/10.1016/s0006-8993(98)00445-4

32. Comhaire S., Blust R., Van Ginneken L., Vanderborght, O.L.J. Branchial cobalt uptake in the carp, Cyprinus carpio: effect of calcium channel blockers and calcium injection. *Fish Physiol. Biochem.* 1998;18(1):1–13. https://doi.org/10.1023/A:1007746117932

33. Goldberg M.A., Imagawa S., Dunning S.P., Bunn H.F. Oxygen sensing and erythropoietin gene regulation. In: Baldamus C.A., Koch K.M., Scigalla P., Wieczorek L. (Eds.). *Erythropoietin: From Molecular Structure to Clinical Application*; *Contrib. Nephrol*. Basel: Karger; 1989;76:39–56. https://doi.org/10.1159/000417880

34. Bruick R.K. Oxygen sensing in the hypoxic response pathway: regulation of the hypoxia-inducible transcription factor. *Genes Dev.* 2003;17(21):2614–2623. https://doi.org/10.1101/gad.1145503

35. Malard V., Berenguer F., Pratt O., Ruat S., Steinmerz G., Quemeneur E. Global gene expression profiling in human lung cells exposed to cobalt. *BMS Genomics*. 2007;8:147–164. https://doi.org/10.1186/1471-2164-8-147

36. Romanova T.A., Kravchenko O.V., Morgulis I.I., Kuzubov A.A., Krasnov P.O., Avramov P.V. Hypothesis of hemoprotein sensor confirmed by *ab initio* quantum-chemical method. *Russ. J. Coord. Chem*. 2004;30(6):403–406. https://doi.org/10.1023/B:RUCO.0000030160.11788.20

37. Mucklow E.S., Griffin S.J., Delves H.T., Suchak B. Cobalt poisoning in a 6-year-old. *Lancet*. 1990;335(8695):981. https://doi.org/10.1016/0140-6736(90)91053-d

38. Simonsen L.O., Harbak H., Bennekou P. Cobalt metabolism and toxicology–a brief update. *Sci. Total Environ.* 2012;432:210–215. https://doi.org/10.1016/j.scitotenv.2012.06.009

39. Bradberry S., Sabatta M., Vale J. Cobalt Chloride. UKPID Monograph. URL: www.inchem.org/documents/ukpids/ukpids/ukpid50.htm (accessed May 12, 2021).

40. Finley B.L., Monnot A.D., Paustenbach D.J., Gaffney S.H. Derivation of a chronic oral reference dose for cobalt. *Regul. Toxicol. Pharm.* 2012;64(3):491–503. https://doi.org/10.1016/j.yrtph.2012.08.022

41. Linna A., Oksa P., Groundstroem K., Halkosaari M., Palmroos P., Huikko S., Uitti J. Exposure to cobalt in the production of cobalt and cobalt compounds and its effect on the heart. *Occup. Environ. Med.* 2004;61(11):877–885. https://doi.org/10.1136/oem.2003.009605

42. Yuan Y., Hilliard G., Ferguson T., Millhorn D.E. Cobalt inhibits the interaction between hypoxia-inducible factor-alpha and von Hippel-Lindau protein by direct binding to hypoxia-inducible factor-alpha. *J. Biol. Chem.* 2003;278(18):15911–15916. https://doi.org/10.1074/jbc.m300463200

43. Simonsen L.O., Brown A.M., Harbak H., Kristensen B.I., Bennekou P. Cobalt uptake and binding in human red blood cells. *Blood Cell Mol. Dis.* 2011;46(4):266–276. https://doi.org/10.1016/j.bcmd.2011.02.009

44. Unice K.M., Monnot A.D., Gaffney S.H., Tvermoes B.E., Thuett K.A., Paustenbach D.J., Finley B.L. Inorganic cobalt supplementation: Prediction of cobalt levels in whole blood and urine using a biokinetic model. *Food Chem. Toxicol.* 2012;50(7):2456–2461. https://doi.org/10.1016/j.fct.2012.04.009

45. Gray M.J., Zhang J., Ellis L.M., Semenza G.L., Evans D.B., Watowich S.S., Gallick G.E. HIF-1alpha, STAT3, CBP/p300 and Ref-1/APE are components of a transcriptional complex that regulates Src-dependent hypoxia-induced expression of VEGF in pancreatic and prostate carcinomas. *Oncogene.* 2005;24(19):3110–3120. https://doi.org/10.1038/sj.onc.1208513

46. Singh N.K., Chhabra R., Datta K. Nonenzymatic synthesis of delta-aminolevulinate (ALA) by cobalt (Co++). *Biochem. Biophys. Res. Commun.* 1987;143(2):439–446. https://doi.org/10.1016/0006-291x(87)91373-8

47. Chai Y.C., Mendes L.F., van Gastel N., Carmeliet G., Luyten F.P. Fine-tuning pro-angiogenic effects of cobalt for simultaneous enhancement of vascular endothelial growth factor secretion and implant neovascularization. *Acta Biomater.* 2018;72:447–460. https://doi.org/10.1016/j.actbio.2018.03.048

48. Peters K., Schmidt H., Unger R.E., Kamp G., Pröls F., Berger B.G., Kirkpatrick C.J. Paradoxical effects of hypoxia-mimicking divalent cobalt ions in human endothelial cells *in vitro*. *Mol. Cell. Biochem.* 2005;270(1–2):157–166. https://doi.org/10.1007/s11010-005-4504-z

49. De Laia A.G.S., Valverde T.M., Barrioni B.R., da Silva Cunha P., de Goes A.M., de Miranda M.C., Gomes D.A., Gueiros-Junior C.M., de Sa M.A., de Magalhães Pereira M. Cobalt-containing bioactive glass mimics vascular endothelial growth factor A and hypoxia inducible factor 1 function. *J. Biomed. Mater. Res. A*. 2021;109(7):1051–1064. https://doi.org/10.1002/jbm.a.37095

50. Okamoto S., Eltis L.D. The biological occurrence and trafficking of cobalt. *Metallomics.* 2011;3(10):963–970. https://doi.org/10.1039/c1mt00056j

51. Gluhcheva Y., Pavlova E., Petrova E., Tinkov A.A., Ajsuvakova O.P., Skalnaya M.G., Vladov I., Skalny A.V. The Impact of Perinatal Cobalt Chloride Exposure on Extramedullary Erythropoiesis, Tissue Iron Levels, and Transferrin Receptor Expression in Mice. *Biol. Trace Elem. Res.* 2020;194(2):423–431. https://doi.org/10.1007/s12011-019-01790-8

52. Xu X., Liu T., Wu J., Wang Y., Hong Y., Zhou H. Transferrin receptor-involved HIF-1 signaling pathway in cervical cancer. *Cancer Gene Ther.* 2019;26(11–12):356–365. https://doi.org/10.1038/s41417-019-0078-x

53. De Boeck M., Kirsch-Volders M., Lison D. Cobalt and antimony: genotoxicity and carcinogenicity. *Mutat. Res.* 2003;533(1–2):135–152. https://doi.org/10.1016/j.mrfmmm.2003.07.012

54. Shukla D., Saxena S., Purushothaman J., Shrivastava K., Singh M., Shukla S., Malhotra V.K., Mustoori S., Bansal A. Hypoxic preconditioning with cobalt ameliorates hypobaric hypoxia induced pulmonary edema in rat. *Eur. J. Pharmacol.* 2011;656(1–3):101–109. https://doi.org/10.1016/j.ejphar.2011.01.038

55. Saxena S., Shukla D., Bansal A. Augmentation of aerobic respiration and mitochondrial biogenesis in skeletal muscle by hypoxia preconditioning with cobalt chloride. *Toxicol. Appl. Pharmacol.* 2012;264(3):324–334. https://doi.org/10.1016/j.taap.2012.08.033

56. Suzuki J. Time-course changes in VEGF expression and capillarity in the early stage of exercise training with Co treatment in rat skeletal muscles. *Acta Physiol. Scand*. 2004;181(2):225–232. https://doi.org/10.1111/j.1365-201x.2004.01279.x

57. Hoffmeister T., Schwenke D., Krug O., Wachsmuth N., Geyer H., Thevis M., Byrnes W.C., Schmidt W.F.J. Effects of 3 Weeks of Oral Low-Dose Cobalt on Hemoglobin Mass and Aerobic Performance. *Front. Physiol.* 2018;9:1289. https://doi.org/10.3389/fphys.2018.01289

58. da Justa Neves D.B., Caldas E.D. Dietary supplements: International legal framework and adulteration profiles, and characteristics of products on the Brazilian clandestine market. Regul. *Toxicol. Pharmacol*. 2015;73(1):93–104. https://doi.org/10.1016/j.yrtph.2015.06.013

59. Krug O., Thomas A., Walpurgis K., Piper T., Sigmund G., Schänzer W., Laussmann T., Thevis M. Identification of black market products and potential doping agents in Germany 2010–2013. *Eur. J. Clin. Pharmacol*. 2014;70(11):1303–1311. https://doi.org/10.1007/s00228-014-1743-5

60. Thevis M., Krug O., Piper T., Geyer H., Schänzer W. Solutions Advertised as Erythropoiesis-stimulating Products were Found to Contain Undeclared Cobalt and Nickel Species. *Int. J. Sports Med*. 2015;37(1):82–84. https://doi.org/10.1055/s-0035-1569350

61. Geyer H., Braun H., Burke L.M., Stear S.J., Castell L.M. A-Z of nutritional supplements: dietary supplements, sports nutrition foods and ergogenic aids for health and performance-Part 22. *Br. J. Sports Med.* 2011;45(9):752–754. https://doi.org/10.1136/bjsports-2011-090180

62. Geyer H., Parr M.K., Koehler K., Mareck U., Schänzer W., Thevis M. Nutritional supplements cross-contaminated and faked with doping substances. *J. Mass Spectrom*. 2008;43(7):892–902. https://doi.org/10.1002/jms.1452

63. Ho E.N.M., Chan G.H.M., Wan T.S.M., Curl P., Riggs C.M., Hurley M.J., Sykes D. Controlling the misuse of cobalt in horses. *Drug Test. Anal.* 2015;7(1):21–30. https://doi.org/10.1002/dta.1719

64. Hillyer L.L., Ridd Z., Fenwick S., Hincks P., Paine S.W. Pharmacokinetics of inorganic cobalt and a vitamin B12 supplement in the Thoroughbred horse: Differentiating cobalt abuse from supplementation. *Equine Vet. J.* 2018;50(3):343–349. https://doi.org/10.1111/evj.12774

65. Calbet J.A., Lundby C., Koskolou M., Boushel R. Importance of hemoglobin concentration to exercise: acute manipulations. *Respir. Physiol. Neurobiol*. 2006;151(2–3):132–140. https://doi.org/10.1016/j.resp.2006.01.014

66. Reichel C., Gmeiner G. Erythropoietin and analogs. In: Thieme D., Hemmersbach P. (Eds.). *Doping in Sports: Biochemical Principles, Effects and Analysis. Handbook of Experimental Pharmacology*. Berlin, Heidelberg: Springer; 2010;195:251–294. https://doi.org/10.1007/978-3-540-79088-4_12

67. Okano M., Sato M., Kaneko E., Kageyama S. Doping control of biosimilar epoetin kappa and other recombinant erythropoietins after intravenous application. *Drug Test. Anal.* 2011;3(11–12):798–805. https://doi.org/10.1002/dta.369

68. Rodriguez-Jimenez F.J., Moreno-Manzano V. Modulation of hypoxia-inducible factors (HIF) from an integrative pharmacological perspective. *Cell. Mol. Life Sci.* 2012;69(4):519–534. https://doi.org/10.1007/s00018-011-0813-4

69. Jelkmann W. Efficacy of recombinant erythropoietins: is there unity of international units? *Nephrol. Dial. Transpl.* 2009;24(5):1366–1368. https://doi.org/10.1093/ndt/gfp058

70. Jefferson J.A., Escudero E., Hurtado M.E., Pando J., Tapia R., Swenson E. R., Prchal J., Schreiner G.F., Schoene R.B., Hurtado A., Johnson R.J. Excessive erythrocytosis, chronic mountain sickness, and serum cobalt levels. *Lancet.* 2002;359(9304):407–408. https://doi.org/10.1016/s0140-6736(02)07594-3

71. Jansen H.M., Knollema S., van der Duin L.V., Willemsen A.T., Wiersma A., Franssen E.J., Russel F.G., Korf J., Paans A.M. Pharmacokinetics and dosimetry of cobalt-55 and cobalt-57. *J. Nucl. Med*. 1996;37(12):2082–2086.

72. Ebert B., Jelkmann W. Intolerability of cobalt salt as erythropoietic agent. *Drug Test Anal.* 2014;6(3):185–189. https://doi.org/10.1002/dta.1528

73. Weißbecker L. Die Kobalttherapie. Deutsch. Med. Wochenschr. 1950;75:116–118.

74. Weissbecker L. Neue Möglichkeiten der Kobalttherapie. *Klin.Wochenschr.* 1951;29:80–82. https://doi.org/10.1007/BF01480495

75. Curtis J.R., Goode G.C., Herrington J., Urdaneta L.E. Possible cobalt toxicity in maintenance hemodialysis patients after treatment with cobaltous chloride: a study of blood and tissue cobalt concentrations in normal subjects and patients with terminal and renal failure. *Clin. Nephrol.* 1976;5(2):61–65.

76. Schirrmacher U.O. Case of cobalt poisoning. *Brit. Med. J.* 1967;1(5539):544–545. https://doi.org/10.1136/bmj.1.5539.544

77. Licht A., Oliver M., Rachmilewitz E.A. Optic atrophy following treatment with cobalt chloride in a patient with pancytopenia and hypercellular marrow. *Isr. J. Med. Sci.* 1972;8(1):61–66.

78. Kriss J. P., Carnes W. H., Gross R. T. Hypothyroidism and thyroid hyperplasia in patients treated with cobalt. *J. Am. Med. Assoc.* 1955;157(2):117–121. https://doi.org/10.1001/jama.1955.02950190017004

79. Jacobziner H., Raybin H.W. Poison control...accidental cobalt poisoning. *Arch. Pediatr.* 1961;78:200–205.

80. Lison D., De Boeck M., Verougstraete V., Kirsch-Volders M. Update on the genotoxicity and carcinogenicity of cobalt compounds. *Occup Environ Med.* 2001;58(10):619–625. https://doi.org/10.1136/oem.58.10.619

81. Pulido M.D., Parrish A.R. Metal-induced apoptosis: mechanisms. *Mutat Res.* 2003;533(1–2):227–241. https://doi.org/10.1016/j.mrfmmm.2003.07.015

82. Aggarwal S.K., Kinter M., Herold D.A. Determination of cobalt in urine by gas chromatography-mass spectrometry employing nickel as an internal standard. *J. Chromatogr. B.* 1992;576(2):297–304. https://doi.org/10.1016/0378-4347(92)80203-3

83. Minakata K., Suzuki M., Suzuki O. Application of electrospray ionization tandem mass spectrometry for the rapid and sensitive determination of cobalt in urine. *Anal. Chim. Acta* 2008;614(2):161–164. https://doi.org/10.1016/j.aca.2008.03.043

84. Todorovska N., Karadjova I., Arpadjan S., Stafilov T. Electrothermal atomic absorption spectrometric-determination of cobalt in human serum and urine. *Acta Pharm*. 2003;53(2):83–90.

85. Sarmiento-Gonzalez A., Marchante-Gayon J.M., Tejerina-Lobo J.M., Paz-Jimenez J., Sanz-Medel A. High-resolution ICP-MS determination of Ti, V, Cr, Co, Ni, and Mo in human blood and urine of patients implanted with a hip or knee prosthesis. *Anal. Bioanal. Chem.* 2008;391(1):2583–2589. https://doi.org/10.1007/s00216-008-2188-4

86. Popot M.-A., Ho E.N.M., Stojiljkovic N., Bagilet F., Remy P., Maciejewski P., Loup B., Chan G.H.M., Hargrave S., Arthur R.M., Russo C., White J., Hincks P., Pearce C., Ganio G., Zahra P., Batty D, Jarrett M., Brooks L., Prescott L.-A., Bailly-Chouriberry L., Bonnaire Y. and Wan T.S.M. Interlaboratory trial for the measurement of total cobalt in equine urine and plasma by ICP-MS. *Drug Test Anal.* 2017;9(9):1400–1406. https://doi.org/10.1002/dta.2191

87. Knoop A., Planitz P., Wüst B., Thevis M. Analysis of cobalt for human sports drug testing purposes using ICP- and LC-ICP-MS. *Drug Test Anal.* 2020;12(11–12):1666–1672. https://doi.org/10.1002/dta.2962

88. Galay E.Ph., Dorogin R.V., Temerdashev A.Z. Quantification of cobalt and nickel in urine using inductively coupled plasma atomic emission spectroscopy. *Heliyon.* 2021;7(1):e06046. https://doi.org/10.1016/j.heliyon.2021.e06046

About the authors:

Irina V. Pronina, Cand. Sci. (Biol.), Main Specialist, Doping Control Department, National Anti-Doping Laboratory (Institute), Lomonosov Moscow State University (10-1, Elizavetinskii per., Moscow, 105005, Russia); Senior Researcher, Pathogenomics and Transcriptomics Laboratory, Institute of General Pathology and Pathophysiology (8, ul. Baltiiskaya, Moscow, 125315, Russia). E-mail: pronina@dopingtest.ru. Scopus Author ID 8161867200, ResearcherID G-3951-2014, https://orcid.org/0000-0002-0423-7801

Elena S. Mochalova, Acting Director, National Anti-Doping Laboratory (Institute), Lomonosov Moscow State University (10-1, Elizavetinskii per., Moscow, 105005, Russia). E-mail: mochalova@dopingtest.ru.

Yuliya A. Efimova, Cand. Sci. (Chem.), Assistant Professor, I.P. Alimarin Department of Analitical Chemistry, M.V. Lomonosov Institute of Fine Chemical Technologies, MIREA – Russian Technological University (86, Vernadskogo pr., Moscow, 119571, Russia). E-mail: efimova_yulia@bk.ru. https://orcid.org/0000-0002-3582-0012

Pavel V. Postnikov, Cand. Sci. (Chem.), Head of the Doping Control Department, National Anti-Doping Laboratory (Institute), Lomonosov Moscow State University (10-1, Elizavetinskii per., Moscow, 105005, Russia). E-mail: postnikov@dopingtest.ru. eLibrary Index 7251-9937, https://orcid.org/0000-0003-3424-0582

Об авторах:

Пронина Ирина Валерьевна, к.б.н., главный специалист отдела допингового контроля Национальной антидопинговой лаборатории (Института) Московского государственного университета им. М.В. Ломоносова (Россия, 105005, Москва, Елизаветинский переулок, дом 10, стр. 1); старший научный сотрудник лаборатории патогеномики и транскриптомики Федерального государственного бюджетного учреждения «Научно-исследовательский институт общей патологии и патофизиологии» (Россия, 125315, Москва, ул. Балтийская, д. 8). E-mail: pronina@dopingtest.ru. Scopus Author ID 8161867200, ResearcherID G-3951-2014, https://orcid.org/0000-0002-0423-7801

Мочалова Елена Сергеевна, исполняющий обязанности директора Национальной антидопинговой лаборатории (Института) Московского государственного университета им. М.В. Ломоносова (Россия, 105005, Москва, Елизаветинский переулок, д. 10, стр. 1). E-mail: mochalova@dopingtest.ru.

Ефимова Юлия Александровна, к.х.н., доцент, кафедра аналитической химии им. Алимарина И.П. Института тонких химических технологий им. М.В. Ломоносова, ФГБОУ ВО «МИРЭА – Российский технологический университет» (119571, Россия, Москва, пр. Вернадского, д. 86). E-mail: efimova_yulia@bk.ru. https://orcid.org/0000-0002-3582-0012

Постников Павел Викторович, к.х.н., начальник отдела допингового контроля Национальной антидопинговой лаборатории (Института) Московского государственного университета им. М.В. Ломоносова (Россия, 105005, Москва, Елизаветинский переулок, д. 10, стр. 1). E-mail: postnikov@dopingtest.ru. eLibrary Index 7251-9937, https://orcid.org/0000-0003-3424-0582

The article was submitted: May 17, 2021; approved after reviewing: June 08, 2021; accepted for publication: July 23, 2021.

Translated from Russian into English by H. Moshkov
Edited for English language and spelling by Enago, an editing brand of Crimson Interactive Inc.

SYNTHESIS AND PROCESSING OF POLYMERS AND POLYMERIC COMPOSITES

СИНТЕЗ И ПЕРЕРАБОТКА ПОЛИМЕРОВ И КОМПОЗИТОВ НА ИХ ОСНОВЕ

ISSN 2686-7575 (Online)
https://doi.org/10.32362/2410-6593-2021-16-4-337-344
UDC 678. 541.6

RESEARCH ARTICLE

Aqueous polyvinyl alcohol solution foaming at different molecular masses

Anastasiya A. Akimova[1,@], Viktor A. Lomovskoy[1,2], Igor D. Simonov-Emel'yanov[1]

[1]MIREA – Russian Technological University (M.V. Lomonosov Institute of Fine Chemical Technologies), Moscow, 119571 Russia
[2]A.N. Frumkin Institute of Physical Chemistry and Electrochemistry, Russian Academy of Sciences, Moscow, 119071 Russia
[@]Corresponding author, e-mail: akimova@mirea.ru

Abstract

Objectives. *Investigation of aqueous polyvinyl alcohol (PVA) foaming process and the influence of its water solution structure, when possessed of different molecular weights and concentrations, on foaming multiplicity.*
Methods. *Solution foaming analysis was performed on the data of dynamic light scattering obtained on the Zetasizer Nano particle analyzer.*
Results. *In this work, the foaming ability and foaming multiplicity of aqueous PVA solutions (as a main component for obtaining special-purpose foams) have been studied. It is shown that PVA solutions in water are colloidal dispersed systems consisting of different-sized associates (from 4.8 to 68.1 nm), depending on the molecular weight of PVA. Dependencies of aqueous PVA solution foaming multiplicities on the concentration, molecular weight, and solution temperature were given. Optimal values of concentration and molecular PVA weight, as well as optimal foaming process conditions from aqueous PVA solutions, were established.*
Conclusions. *Increasing PVA concentrations in aqueous solutions cause foaming multiplicity to decrease for all molecular weights by 1.5 times, and increasing molecular weight increases foaming multiplicity by 2 times. The foaming ratio of aqueous PVA solutions with different concentrations and molecular weights (depending on a solution temperature characterized by a maximum of 30°C) is associated with decreased viscosity and surface tension.*

Keywords: *polyvinyl alcohol, molecular weight, aqueous solution, solution concentration, foaming multiplicity*

For citation: Akimova A.A., Lomovskoy V.A., Simonov-Emel'yanov I.D. Aqueous polyvinyl alcohol solution foaming at different molecular masses. *Tonk. Khim. Tekhnol. = Fine Chem. Technol.* 2021;16(4):337–344 (Russ., Eng.). https://doi.org/10.32362/2410-6593-2021-16-4-337-344

НАУЧНАЯ СТАТЬЯ

Пенообразование растворов поливинилового спирта с разной молекулярной массой в воде

А.А. Акимова[1,@], В.А. Ломовской[1,2], И.Д. Симонов-Емельянов[1]

[1]МИРЭА – Российский технологический университет (Институт тонких химических технологий им. М.В. Ломоносова), Москва, 119571 Россия
[2]Институт физической химии и электрохимии им. А.Н. Фрумкина Российской академии наук, Москва, 119071 Россия
[@]Автор для переписки, e-mail: akimova@mirea.ru

Аннотация

Цели. *Исследовать процесс пенообразования водных растворов поливинилового спирта (ПВС) с различной молекулярной массой и концентрацией и влияние их структуры на кратность их вспенивания.*
Методы. *Анализ пенообразования растворов проводили по данным динамического светорассеяния, полученным на анализаторе частиц Zetasizer Nano.*
Результаты. *В работе изучена пенообразующая способность и кратность вспенивания водных растворов ПВС как одного из основных компонентов получения пен специального назначения. Показано, что растворы ПВС в воде представляют собой коллоидные дисперсные системы, состоящие из ассоциатов с разными размерами (от 4.8 до 68.1 нм) в зависимости от молекулярной массы ПВС. Приведены зависимости кратности вспенивания водных растворов ПВС от концентрации, молекулярной массы и температуры раствора. Приведены значения оптимальной концентрации и молекулярной массы ПВС, а также установлены оптимальные условия процесса пенообразования из водных растворов ПВС.*
Выводы. *Установлено, что с ростом концентрации водных растворов ПВС кратность вспенивания снижается для всех молекулярных масс приблизительно в 1.5 раза, а с увеличением молекулярной массы она возрастает примерно в 2 раза. Кратность вспенивания водных растворов ПВС с разной концентрацией и молекулярной массой в зависимости от температуры раствора характеризуется максимумом при 30 °C, что связано с уменьшением вязкости и снижением поверхностного натяжения растворов.*

Ключевые слова: *поливиниловый спирт, молекулярная масса, водные растворы, концентрация растворов, кратность вспенивания*

Для цитирования: Акимова А.А., Ломовской В.А., Симонов-Емельянов И.Д. Пенообразование растворов поливинилового спирта с разной молекулярной массой в воде. *Тонкие химические технологии*. 2021;16(4):337–344. https://doi.org/10.32362/2410-6593-2021-16-4-337-344

When creating highly porous filters for separating water from hydrocarbon fuels (kerosene, gasoline, etc.), polyvinyl alcohol (PVA) is used as the initial component, as it selectively absorbs water from hydrocarbon organic matter [1]. The filter technology includes a stage of obtaining foams from aqueous PVA solutions [2–4]. The structure and parameters of formed foams, foaming multiplicity, and foam stability over time are determined primarily by PVA molecular weight, the concentration of aqueous PVA solutions, and the technological parameters of solution production processes [5–9].[1]

Of undoubted interest is the establishment of main regularities when forming foams with adjustable structure parameters and properties. The purpose of this work is to study the foaming process of aqueous PVA solutions and the influence of their structures (with different molecular weights and concentrations) as well as the power-speed and temperature parameters of foaming on their properties.

EXPERIMENTAL

PVA produced by *Mowiol* (Taiwan) with different molecular weights (M_w) was used as the object of this study: Mowiol 5-88 with M_w = 22000, Mowiol 18-88 with M_w = 55000, Mowiol 26-88 with M_w = 68000 and Mowiol 47-88 with M_w = 81000 with a 99.95% share of the base substance. It is impractical to take PVA with a M_w greater than 81000, since in the process of its dissolution in water, the partial flocculation of dissolved PVA particles occurs and forms large associates that cannot be separated [10, 11].

PVA solutions with given concentrations in water were prepared in a measuring flask with a volume of 1000 mL. PVA suspensions were placed and 800 mL of deionized water was poured. Deionized water was obtained using a Type 1 high water purification system, Milli-Q Integral 5 (*Merck Millipore*, Burlington, Massachusetts, USA), with a resistivity of 18.0 mOhm·cm. The flask was then placed in a thermostat at 80°C and the liquid was stirred constantly until the PVA was completely dissolved. The solution was then evaluated visually before being cooled to 25°C. The quality of complete dissolution and solution heterogeneity at different PVA concentrations in water was judged by the data of dynamic light scattering obtained using a Zetasizer Nano particle analyzer (*Malvern Instruments*, USA).

The method is based on the registration of scattered light fluctuations from particles in continuous Brownian motion [12]. A laser beam is passed through the analyzed sample and the intensity of light scattering by particles over time is recorded. When particles are irradiated with a laser, light is scattered in all directions. Observed scattered light comes from a set of scattering elements in a certain volume, depending on the angles at which registration is performed and the aperture characteristics. The observed intensity of scattered light under any conditions will be the result of light superposition scattered by each element, and thus depend on the relative positions of these elements. When the particles move, their relative positions change and fluctuations in scattered light intensity are observed. Since the particles move randomly under the influence of Brownian force and scattered light intensity fluctuations are random. For small fast-moving particles, fast fluctuations are observed, while larger and slower particles show slower fluctuations.

Analysis of intensity fluctuations makes it possible to determine the speed of Brownian motion and calculate the particle size using the Stokes-Einstein equation. The Zetasizer Nano photonic particle analyzer has a particle measurement range of 0.3 to 10000 nm. The operating temperature range is 2–120°C, the scattered light detection angle is 173°, a helium-neon laser with a wavelength of 633 nm is used as a light source, and the light source power is 5 MW. The device determines the particle size by measuring the rate of scattered light fluctuation by particles. Measurement is carried out in automatic mode according to the standard method.

Foams from aqueous PVA solutions with different Mw and concentrations were obtained via mechanical foaming [13] at different temperatures. A 250 mL measure of PVA solution in water was poured into a 500 mL measuring cylinder with a diameter of 50 mm and a height of 350 mm. A three-bladed rotor of an upper-drive laboratory agitator was placed in the cylinder in such a way that it did not touch the bottom of the cylinder (the distance to the bottom is ~50 mm) and the height of the liquid column was measured with a Vernier height gage before mixing. Depending on the experiment temperature, the cylinder with the solution was placed in a thermostat at a given temperature and thermostated for 30 min. The agitator was turned on and the foaming process was carried out at a speed of 1000 rpm for 5 min (it was experimentally determined that this amount of time is necessary to achieve maximum foaming multiplicity), after which the agitator was turned off and the column of liquid with foam was measured again.

[1] Vilkova N.G. Colloidal-chemical properties of polyhedral foams and emulsions. Cand. Thesis (Chem.). Moscow: M.V. Lomonosov Moscow State University; 2007. 285 p. (in Russ.).

The foaming multiplicity (β) was calculated by

$$\beta = \frac{V_f}{V_w},$$

where V_f is the volume of the resulting foam; V_w is the volume of the initial PVA liquid solution.

RESULTS AND DISCUSSION

The homogeneity of aqueous PVA solutions was determined using the method of dynamic light scattering on the Zetasizer Nano particle analyzer. As an example, Fig. 1 shows the dependences of light scattering intensity for 4 vol % of aqueous PVA solutions of with minimum (1) and maximum (2) M_w of the associate diameters.

It has been established that PVA solutions in water are colloidal dispersed systems consisting of PVA associates in water, and the average associate diameter depends on M_w: for M_w = 22000, diameters ranged from 4.8 to 50.8 nm, and for M_w = 81000, diameters ranged from 5.6 to 68.1 nm. The associative structure of aqueous PVA solutions influenced the foaming process.

Figure 2 shows the β dependences for aqueous PVA solutions based on concentration and M_w.

With a concentration increase from 4 to 24 vol %, β decreased from 6.4–3.7 to 4.9–1.8 (i.e., by ~1.5 times) due to an increase in solution viscosity. On the curves of Fig. 2a, there is an inflection at a solution concentration of ~12 vol %; therefore, the dependence of β on M_w for solutions of 12 vol % concentration is of interest. The influence of PVA M_w on foaming is manifested to a lesser extent than the change in solution concentration (Fig. 2b), and an inflection is observed on the curve $\beta = f(M_w)$ at M_w = 55000, indicating an increase in the foaming efficiency when using PVA with a M_w greater than 60000. The maximum β (≈ 5.5) was achieved with PVA water solutions of 81000 M_w and a solution concentration of 4 vol %.

Temperature had a significant influence on the foaming process of aqueous PVA solutions, since temperature increases caused solution viscosity

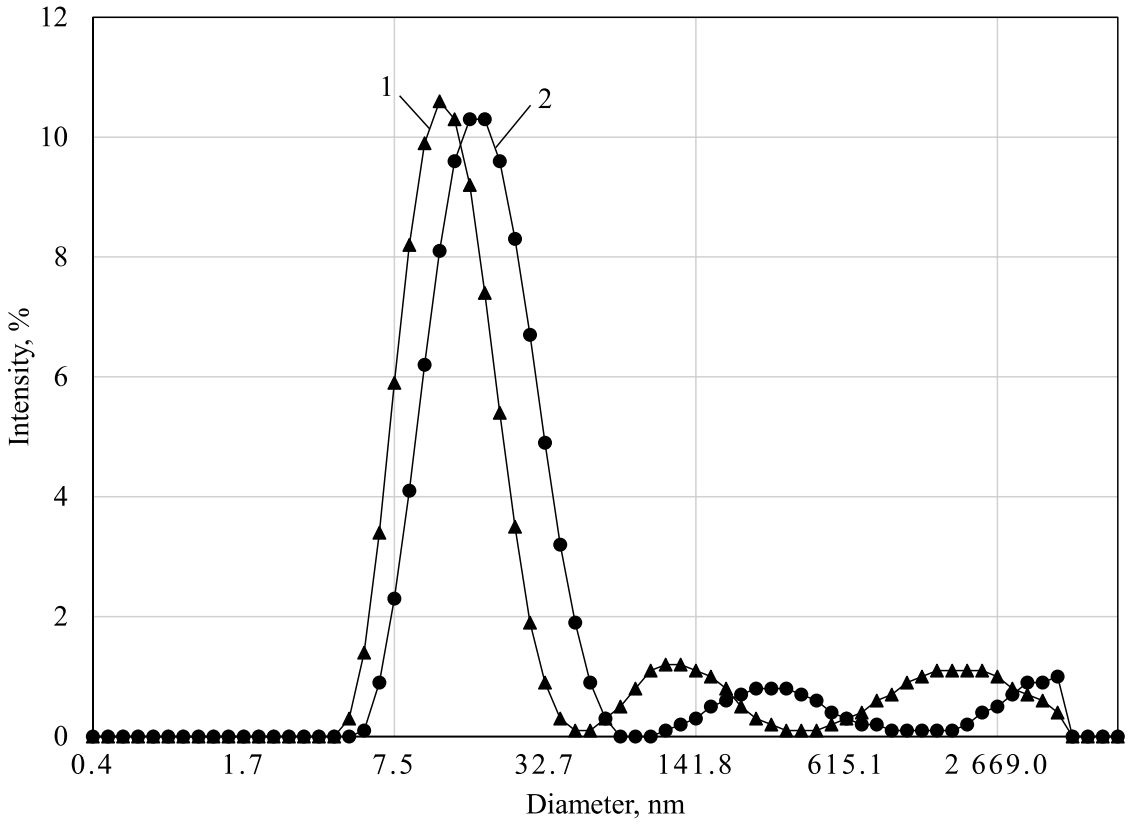

Fig. 1. Dependence of associate distributions by size in 4 vol % aqueous PVA solutions with different molecular weights (M_w): (1) M_w = 22000, (2) M_w = 81000.

to decrease, an equivalent to a lower solution concentration. Figure 3 shows the dependences of β for aqueous PVA solutions at a 4 vol % concentration with measured M_w and temperature.

Figure 3 shows that as M_w increases from 22000 to 81000, the β of the aqueous PVA solutions increases at almost all temperatures (10–60°C) by approximately 2 times. In Fig. 3a, the dependences of β are close to each other at temperatures of 10°C and 60°C (they show the lowest β), yet there is also a sharp decrease in β at 60°C caused by decreased solution viscosity [13]. In Fig. 3b, it is possible to trace the influence of temperature on β, establishing that the maximum β is achieved at 30°C for almost all M_w values. As temperature continued to increase, β decreased.

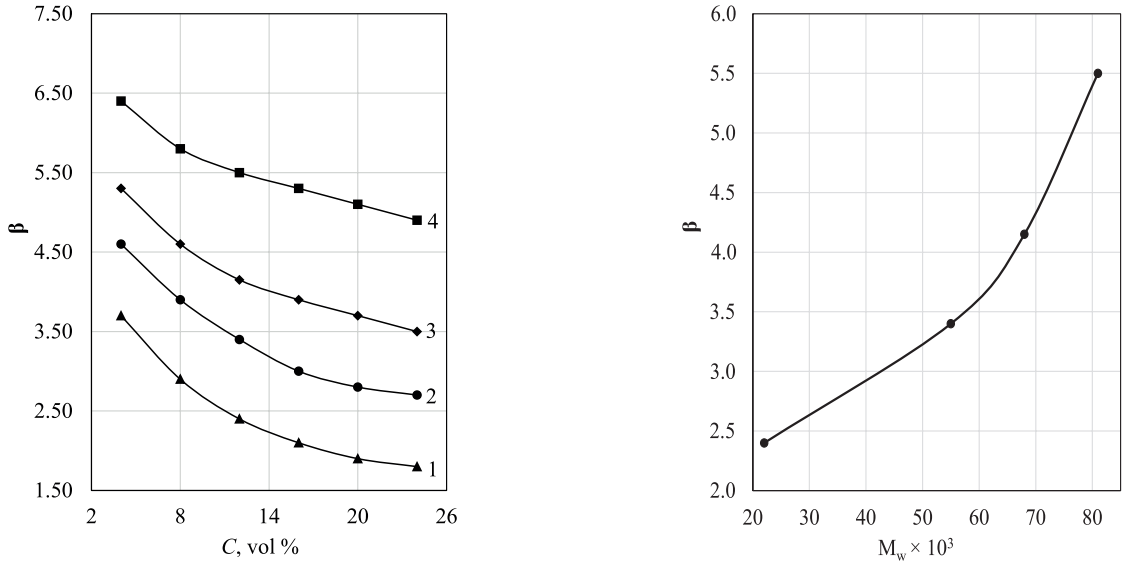

Fig. 2. Dependence of β for aqueous PVA solutions with different M_w at 20°C: (1) M_w = 22000, (2) M_w = 55000, (3) M_w = 68000, (4) M_w = 81000; (a) concentrations, (b) M_w for a concentration of about 12 vol %.

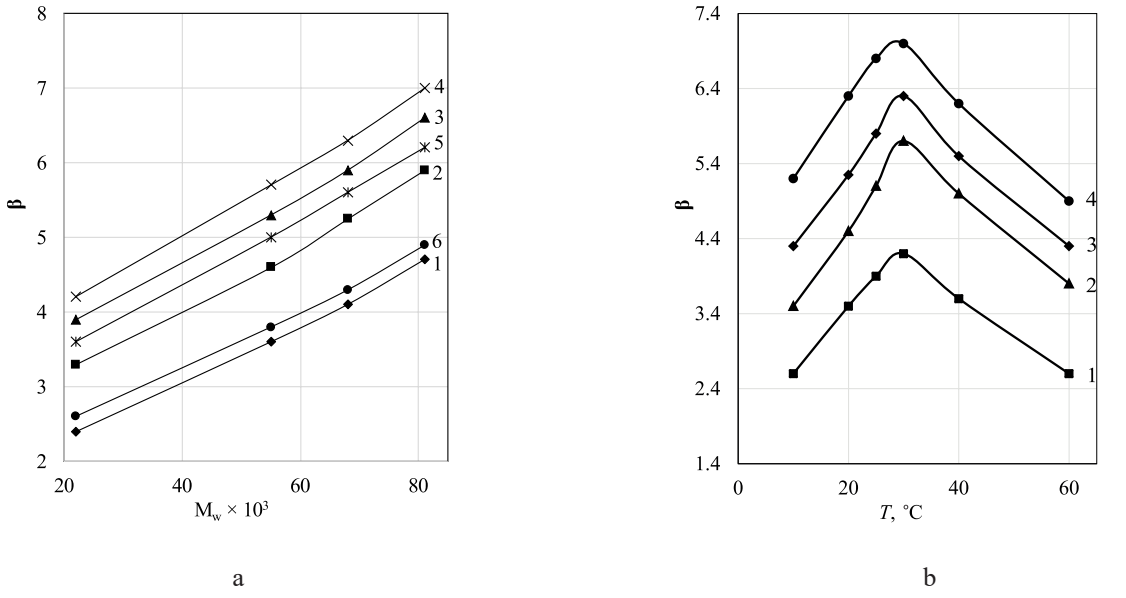

Fig. 3. Dependence of β for aqueous PVA solutions at a concentration of 4 vol %: (a) on the M_w at different temperatures: (1) 10°C, (2) 20°C, (3) 25°C, (4) 30°C, (5) 40°C, and (6) 60°C; and (b) on temperature at different M_w: (1) M_w = 22000, (2) M_w = 55000, (3) M_w = 68000, (4) M_w = 81000.

CONCLUSIONS

This study obtained data on the processes of mechanical foaming from aqueous PVA solutions with different M_w (from 22000 to 81000) and solution concentrations (from 4 to 24 vol %) at different temperatures (10–60°C). It was found that the maximum foaming ability was possessed by PVA solutions with a M_w of 81000 and a concentration of 4 vol %. However, to increase the PVA concentration in aqueous solutions and obtain more stable foams (i.e., the ability to maintain initial structure parameters, since foam is a structured dispersed system), foaming can be carried out at an optimal temperature of 30°C and a PVA concentration equal to 12 vol %. In such cases, the maximum $\beta = 4.2$ is achieved, which was previously obtained at 4 vol %. The β of aqueous PVA solutions with different concentrations and M_w, depending on solution temperature, is characterized by a maximum at 30°C, which is associated with decreased viscosity and solution surface tension.

Authors' contribution

A.A. Akimova – planning and conducting research, processing research materials, writing the text of the article;

V.A. Lomovskoy – scientific consulting and assistance in processing the results obtained;

I.D. Simonov-Emel'yanov – general management of research processes and preparation of material for publication.

The authors declare no conflicts of interest.

REFERENCES

1. Ushakov S.N. *Polivinilovyi spirt i ego proizvodnye: v 2 t.* (*Polyvinyl alcohol and its derivatives: in 2 v.*). Moscow, Leningrad: Izd. Akad. Nauk SSSR; 1960.V. 1. 552 p. (in Russ.).

2. Panov Yu.T. *Nauchnye osnovy sozdaniya penoplastov vtorogo pokoleniya: monografiya* (*Scientific basis for the creation of second-generation foams*). Vladimir: Vladimir Gos. Univ. 2003. 176 p. (in Russ.). ISBN 5-89368-379-X.

3. Lysakov V.N., Sedunov S.G., Taraskin K.A., Spiridonova M.P. Methods of obtaining and studying the properties of foam compositions, promising for creation sound-proof coatings. *Molekul. Tekhnol. = Molecul. Technol.* 2008;2:61–79 (in Russ.).

4. Lomovskoy V. A., Abaturova N. A., Lomovskaya N. Yu., Khlebnikova O. A., Sakov D. M., Galushko T. B., Barteneva A. G. Influence of the porosity of the polyvinylformal structure on its sorption characteristics. 5th Scientific Conference "Physical Chemistry of surface phenomena and adsorption." July 1–6, 2013 Ples: Proceedings of the conference. FGBOU VPO Ivan. Gos. Khim.-Tekhnol. Univ. Ivanovo, 2014. p. 52. (in Russ.)

5. Vilkova N.G., Mishina S.I., Dorchina O.V. Stability of foams containing diesel fuel. *Izv. Vyssh. Uchebn. Zaved. Khim. Khim. Tekhnol*. 2018;61(6):48–53 (in Russ.). https://doi.org/10.6060/tcct.20186106.5361

6. Manzhai V.N., Fufaeva M.S. Dispersity and stability of foams obtained from poly(vinyl alcohol) solution and the properties of resulting formed foams cryogels. *Colloid J.* 2014;76(4):495–499. https://doi.org/10.1134/S1061933X14040097

7. Tikhomirov V.K. *Peny: teoriya i praktika ikh polucheniya i razrusheniya* (*Foams: theory and practice of their production and destruction*). Moscow: Khimiya; 1983. 265 p. (in Russ.).

СПИСОК ЛИТЕРАТУРЫ

1. Ушаков С.Н. *Поливиниловый спирт и его производные: в 2 т*. М.-Л.: Изд. АН СССР; 1960. Т. 1. 552 с.

2. Панов Ю.Т. *Научные основы создания пенопластов второго поколения: монография.* Владимир: Ред.-издат. комплекс ВлГУ; 2003. 176 с. ISBN 5-89368-379-X.

3. Лысаков В.Н., Седунов С.Г., Тараскин К.А., Спиридонова М.П. Методы получения и исследования свойств пенных составов, перспективных для создания звукоизоляционных покрытий. *Молекулярные технологии*. 2008;2:61–79.

4. Ломовской В.А., Абатурова Н.А., Ломовская Н.Ю., Хлебникова О.А., Саков Д.М., Галушко Т.Б., Бартенева А.Г. Влияние пористости структуры поливинилформаля на его сорбционные характеристики. 5-ая Научная конференция «Физическая химия поверхностных явлений и адсорбции». 1–6 июля 2013 г. Плес: Труды конференции. ФБГОУ ВПО Иван.гос.хим.-технол. ун-т. Иваново, 2014. с.52.

5. Вилкова Н.Г., Мишина С.И., Дорчина О.В. Устойчивость пен, содержащих дизельное топливо. *Изв. ВУЗов. Серия: Химия и химическая технология.* 2018;61(6):48–53. https://doi.org/10.6060/tcct.20186106.5361

6. Манжай В.Н., Фуфаева М.С. Дисперсность и устойчивость пены, полученной из раствора поливинилового спирта, и свойства сформированных пенокриогелей. *Коллоидный журнал.* 2014;76(4):495–499. https://doi.org/10.7868/S0023291214040090

7. Тихомиров В.К. *Пены: теория и практика их получения и разрушения*. М.: Химия; 1983. 265 с.

8. Özarmud Ö., Steeb H. Rheology properties of liquid and particle stabilized foam. *J. Phis.: Conf. Ser.* 2015;602(1):012031. https://doi.org/10.1088/1742-6596/602/1/012031

8. Özarmud Ö., Steeb H. Rheology properties of liquid and particle stabilized foam. *J. Phis.: Conf. Ser.* 2015;602(1):012031. https://doi.org/10.1088/1742-6596/602/1/012031

9. Bondarenko Zh. V., Adamtsevich N. Yu., Brutskaya I. O. Foaming in aqueous solutions of binary mixtures of anionic and nonionic surfactants. *Trudy BGTU. Ser. 2. Khimicheskie tekhnologii, biotekhnologiya, geoekologiya = Proceedings of BSTU. Ser. 2. Chemical technologies. Biotechnology. Geoecology.* 2017;2(199):127–131 (in Russ.).

10. Nagarkar R., Patel J. Polyvinyl Alcohol: A Comprehensive Study. *Acta Scientific Pharmaceutical Sciences.* 2019;3(4):34–44.

11. Muppalaneni S., Omidian H. Polyvinyl Alcohol in Medicine and Pharmacy: A Perspective. *J. Develop. Drugs.* 2013;2:112. http://dx.doi.org/10.4172/2329-6631.1000112

12. Khlebtsov B.N., Khanadeev V.A., Pylaev T.E., Khlebtsov N.G. Dynamic light scattering in studies of silicate and gold nanoparticles. *Izvestiya Saratovskogo universiteta. Novaya seriya. Seriya: Fizika = Izv. Saratov Univ. (N.S.). Ser.: Physics.* 2017;17(2):71–84 (in Russ.). https://doi.org/10.18500/1817-3020-2017-17-2-71-84

13. Tager A.A. *Fiziko-khimiya polimerov* (*Physical chemistry of polymers*). Moscow: Nauchnyi mir; 2007. 575 p. (in Russ.). ISBN 978-589-176-437-8

9. Бондаренко Ж. В., Адамцевич Н. Ю., Бруцкая И. О. Пенообразование в водных растворах бинарных смесей анионного и неионогенного поверхностно-активных веществ. *Труды БГТУ. Сер. 2. Химические технологии, биотехнология, геоэкология.* 2017;2(199):127–131.

10. Nagarkar R., Patel J. Polyvinyl Alcohol: A Comprehensive Study. *Acta Scientific Pharmaceutical Sciences.* 2019;3(4):34–44.

11. Muppalaneni S., Omidian H. Polyvinyl Alcohol in Medicine and Pharmacy: A Perspective. *J. Develop. Drugs.* 2013;2:112. http://dx.doi.org/10.4172/2329-6631.1000112

12. Хлебцов Б.Н., Ханадеев В.А., Пылаев Т.Е., Хлебцов Н.Г. Метод динамического рассеяния света в исследованиях силикатных и золотых наночастиц. *Изв. Сарат. ун-та. Нов. сер. Сер.: Физика.* 2017;17(2):71–84. https://doi.org/10.18500/1817-3020-2017-17-2-71-84

13. Тагер А.А. *Физико-химия полимеров*. М.: Научный мир; 2007. 575 с. ISBN 978-589-176-437-8.

About the authors:

Anastasiya A. Akimova, Senior Lecturer, Department of Management Issues Institute of Cybernetics, MIREA – Russian Technological University (78, Vernadskogo pr., Moscow, 119454, Russia). E-mail: akimova@mirea.ru. https://orcid.org/0000-0001-9882-4005

Viktor A. Lomovskoy, Dr. Sci. (Phys. and Math.), Professor, Department of Chemistry and Technology of Plastics and Polymer Composites Processing, M.V. Lomonosov Institute of Fine Chemical Technologies, MIREA – Russian Technological University (86, Vernadskogo pr., Moscow, 119571, Russia); Head of the Laboratory of Structure Formation in Dispersed Systems, A.N. Frumkin Institute of Physical Chemistry and Electrochemistry, Russian Academy of Sciences (31, Leninskii pr., Moscow, 119071, Russia). E-mail: lomovskoy49@gmail.com. Scopus Author ID 38361576700, ResearcherID J-5229-2018, https://orcid.org/0000-0002-6116-1209

Igor D. Simonov-Emel'yanov, Dr. Sci. (Eng.), Professor, Head of the Department of Chemistry and Technology of Plastics and Polymer Composites Processing, M.V. Lomonosov Institute of Fine Chemical Technologies, MIREA – Russian Technological University (86, Vernadskogo pr., Moscow, 119571, Russia). E-mail: simonov@mitht.ru. Scopus Author ID 6603181099.

Об авторах:

Акимова Анастасия Александровна, старший преподаватель кафедры проблем управления Института кибернетики ФГБОУ ВО «МИРЭА – Российский технологический университет» (119454, Россия, Москва, пр-т Вернадского, д. 78). E-mail: akimova@mirea.ru. https://orcid.org/0000-0001-9882-4005

Ломовской Виктор Андреевич, д.ф.-м.н., профессор кафедры химии и технологии переработки пластмасс и полимерных композитов Института тонких химических технологий им. М.В. Ломоносова ФГБОУ ВО «МИРЭА – Российский технологический университет» (119571, Россия, Москва, пр-т Вернадского, д. 86); заведующий лабораторией структурообразования в дисперсных системах, Институт физической химии и электрохимии им. А.Н. Фрумкина Российской академии наук (119071, Россия, Москва, Ленинский проспект, 31, корп. 4). E-mail: lomovskoy49@gmail.com. Scopus Author ID 38361576700. ResearcherID J-5229-2018. https://orcid.org/0000-0002-6116-1209

Симонов-Емельянов Игорь Дмитриевич, д.т.н., профессор, заведующий кафедрой химии и технологии переработки пластмасс и полимерных композитов Института тонких химических технологий им. М.В. Ломоносова ФГБОУ ВО «МИРЭА – Российский технологический университет» (119571, Россия, Москва, пр-т Вернадского, д. 86). E-mail: simonov@mitht.ru. Scopus Author ID 6603181099.

The article was submitted: July 03, 2020; approved after reviewed: September 25, 2020; accepted for publication: August 07, 2021.

Translated from Russian into English by N. Isaeva
Edited for English language and spelling by Enago, an editing brand of Crimson Interactive Inc.

SYNTHESIS AND PROCESSING OF POLYMERS AND POLYMERIC COMPOSITES

СИНТЕЗ И ПЕРЕРАБОТКА ПОЛИМЕРОВ И КОМПОЗИТОВ НА ИХ ОСНОВЕ

ISSN 2686-7575 (Online)
https://doi.org/10.32362/2410-6593-2021-16-4-345-351
UDC 678.5.046

RESEARCH ARTICLE

Effect of relaxation processes during deformation on electrical resistivity of carbon black polypropylene composites

Anatoly V. Markov[@], Katerina S. Tarasova, Vasily A. Markov

MIREA – Russian Technological University (M.V. Lomonosov Institute of Fine Chemical Technologies), Moscow, 119571 Russia
[@]Corresponding author, e-mail: markovan@bk.ru

Abstract

Objectives. *To study the relationship between bending deformation and the change in the electrical resistance of carbon black polypropylene composites.*
Methods. *Conductive polypropylene composites filled with carbon black UM-76 were investigated. The samples were deformed and kept under constant bending at temperatures of 20–155°C.*
Results. *The deformation of the samples led to a reversible increase in their electrical resistance, while subsequent holding of the samples in the deformed state was accompanied by an exponential drop in their electrical resistance. The average times and activation energies of the electrical relaxation of the deformed polypropylene composites were calculated (30–32 kJ/mol) and compared with similar characteristics of polyethylene composites (15–16 kJ/mol).*
Conclusions. *The electrical resistance relaxation of deformed carbon black polypropylene composites at elevated temperatures is similar to their stress relaxation. The average times and activation energies of the electrical relaxation of deformed polypropylene composites are comparable with similar data on their mechanical relaxation. It was found that these electrical and mechanical phenomena are based on the same underlying physical processes.*

Keywords: *conductive polypropylene composites, carbon black, electrical resistivity, deformation, relaxation, PTC effect*

For citation: Markov A.V., Tarasova K.S., Markov V.A. Effect of relaxation processes during deformation on electrical resistivity of carbon black polypropylene composites. *Tonk. Khim. Tekhnol. = Fine Chem. Technol.* 2021;16(4):345–351 (Russ., Eng.). https://doi.org/10.32362/2410-6593-2021-16-4-345-351

НАУЧНАЯ СТАТЬЯ

Влияние релаксационных процессов при деформировании на электрическое сопротивление полипропиленовых композитов с техническим углеродом

А.В. Марков[@], К.С. Тарасова, В.А. Марков

МИРЭА – Российский технологический университет (Институт тонких химических технологий им. М.В. Ломоносова), Москва, 119571 Россия
[@]Автор для переписки, e-mail: markovan@bk.ru

Аннотация

Цели. *Работа посвящена изучению влияния деформации изгиба при повышенных температурах на изменение электрического сопротивления электропроводящих полипропиленовых композитов, наполненных техническим углеродом.*
Методы. *Исследовались полипропиленовые композиты с техническим углеродом УМ-76. Образцы изгибались и выдерживались при заданном прогибе в интервале 20–155 °C.*
Результаты. *При деформировании образцов наблюдался обратимый рост электрического сопротивления. Последующая выдержка образцов в деформированном состоянии сопровождалась экспоненциальным падением их электрического сопротивления. Были рассчитаны средние времена и энергия активации электрической релаксации деформированных полипропиленовых композитов (30–32 кДж/моль), а также проведено их сравнение с аналогичными характеристиками полиэтиленовых композитов (около 14–16 кДж/моль).*
Выводы. *При механическом деформировании электропроводящих полипропиленовых композитов с техническим углеродом, в том числе при повышенных температурах, характер релаксации электрического сопротивления аналогичен характеру релаксации механического напряжения. Средние времена и энергия активации электрической релаксации деформированных полипропиленовых композитов сопоставимы с аналогичными показателями для механической релаксации. Это указывает на общий механизм этих процессов.*
Ключевые слова: *электропроводящий полипропилен, технический углерод, электрическое сопротивление, деформация, релаксация, эффект ПТК*

Для цитирования: Марков А.В., Тарасова К.С., Марков В.А. Влияние релаксационных процессов при деформировании на электрическое сопротивление полипропиленовых композитов с техническим углеродом. *Тонкие химические технологии.* 2021;16(4):345–351. https://doi.org/10.32362/2410-6593-2021-16-4-345-351

INTRODUCTION

Self-regulating heating cables, thermostatic heating elements, thermostatic devices, and self-disconnecting electrical fuses are made based on electrically conductive polymer composites containing carbon black (CB) [1]. The ability of these materials to change their electrical resistance during mechanical deformation [2] has opened up new possibilities for their use, e.g., as internal mechanical stress sensors and damage indicators [3]. Regardless of the shape and size of the electrically conductive fillers, the change in the electrical conductivity of the composites during macroscopic deformation is usually explained by the change in the distances between the conductive particles [4]. The change in electrical resistance during the deformation of electrically conductive composites is associated with the restructuring processes of the system of electrically conductive channels, i.e., the destruction of existing channels or the emergence of new channels [5, 6]. The prevalence of a particular process and, consequently, the increase or decrease in the electrical resistance depends on the nature of the polymer matrix and the content of the electrically conductive filler [7, 8]. The formation of electrically conductive channels during the deformation of a composite is also influenced by the orientation phenomena in the polymer matrix. This effect in particular manifests in the anisotropy of electrical properties during the stretching of an electrically conductive composite due to the appearance of anisotropy of the composite structure when deforming polymer macromolecules [7]. In the case of polymeric electrically conductive composites filled with CB, the mechanical and electrical characteristics change interdependently. This opens up the possibility of studying relaxation phenomena based on data on electrical conductivity changes in a material that cannot be studied with other methods [9]. During cyclic deformation, electrically conductive polymer composites show a hysteresis of electrical resistance similar to the hysteresis of mechanical stress [4]. The highest sensitivity of electrical resistance to temperature change (positive temperature coefficient [PTC]) and tensile deformation is observed when the content of the electrically conductive filler corresponds to the percolation threshold region [10–12]. It is with this content that the electrically conductive polymer composite material is suitable for use in thermostatic heating elements. Simultaneously, the presence of a negative temperature coefficient (NTC effect) is an undesirable effect because it can lead to failure of the polymer composite heater. This effect can be eliminated by radiation crosslinking or chemical crosslinking of the polymer matrix of an electrically conductive composite or by using an electrically conductive composite polymer matrix of a mixture of polyethylene (PE) with a more heat-resistant polymer, e.g., polypropylene (PP) [13, 14]. Note that the influence of various types of deformation, such as tension, compression, and shifting, on the electrical resistance of electrically conductive polymer composites is currently being studied in detail [6, 15, 16]. However, there is practically no data in the scientific and technical literature on the effect of bending deformation on electrical resistance. This phenomenon is especially important for self-regulating heating cables, as these composite materials are used in their manufacturing. This is the main deformation type for heating cables.

The purpose of this work is to study the relationship between deformation and the magnitude of the electrical resistance of PP composites with CB.

EXPERIMENTAL

We studied PP composites (PPG 1120-16 grade, *Stavrolen*, Budenovsk, Russia, TU 2211-008-50236110-2006) with an optimal content of conductive UM-76 CB for heating elements (*Omsk Carbon Group*, Omsk, Russia, TU 38-10001-94) at 20 wt % (11.7 vol %).

The compositions were prepared on a Brabender plastograph (*Brabender GmbH*, Duisburg, Germany) at 200°C, as in [17]. The samples were prepared by pressing at 200 ± 2°C, with the contact lamination made of L-80 brass mesh (GOST 6613-86[1]), as described in [17]. The electrical resistance of the samples was measured with a DT9208A ohmmeter.

The study of the effects of the bending deformation was carried out from 20 to 155°C in a SNOL 3.5 oven (*ThermIKS*, Russia), as described in [18]. In this case, the samples were deformed at a constant injector movement speed of 5 mm/s to a fixed depth of deflection to attain a deformation of 0.1 ± 0.01%. At larger deformations, the samples broke at temperatures below 100°C.

RESULTS AND DISCUSSION

The materials under study were characterized by a sharp increase in electrical resistance due to the rearrangement of the polymer crystal structure in the melting temperature range as well as the intense destruction of the conductive channels formed by the CB particles [17]. The temperature range in the region of the peak in the dependence of the electrical resistance

[1] GOST 6613-86. Square meshed woven wire cloths. Specifications. Moscow: Standartinform, 2006.

on the test temperature practically coincided with the temperature range of PP melting. Figure 1 shows how the samples' temperature affected the change in the electrical resistance of the investigated PP composite.

The effect of the tripping "barrier" resistance (PTC) was also retained for the deformed samples. Figure 2 shows the kinetic dependences of the changes in the electrical resistance of the samples at different temperatures.

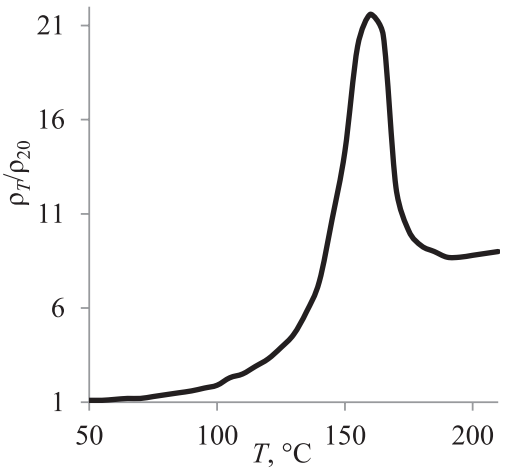

Fig. 1. Dependence of the relative electric volume resistance (ρ_T/ρ_{20}) of the polypropylene samples on temperature.

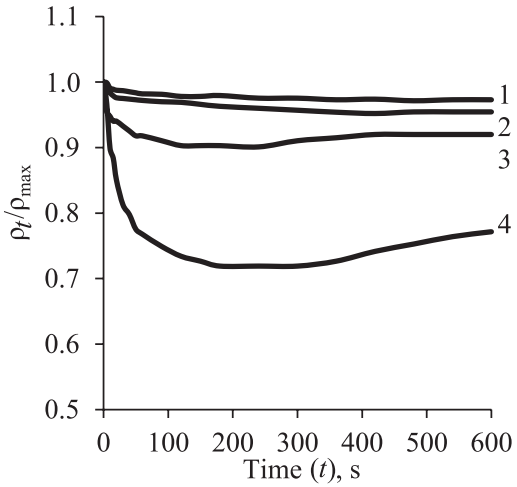

Fig. 2. Change in the relative (ρ_t/ρ_{max}) specific volume electric resistivity during and after bending (f = 0.11) at various temperatures: (1) 90°C, (2) 125°C, (3) 140°C, (4) 155°C.

The obtained time dependences of the changes in electrical resistivity were similar to the well-studied dependences of mechanical stress relaxation [19]. It can be seen in Fig. 2 that during the sample deformation, a jump of electrical resistance was observed from the value of electrical resistance (ρ_T; resistance of an undeformed sample at the test temperature) to the maximum value (ρ_{max}) corresponding to a given deformation (ρ_0 at heat treatment time t = 0). Furthermore, the electrical resistivity at all temperatures exponentially decreased within 4–5 min at a constant bending strain. At longer times (in Fig. 2, the relaxation times are limited to 10 min) and at 140°C and higher temperatures approaching the melting points of the PP matrix, the resistance began to increase (Fig. 2, curves 3 and 4).

It became apparent that the value of the maximum resistance at the same relative deformation at the moment of deformation (as in [20]) depended little on temperature up to 140°C because the effect of the deformation at low temperatures (in the forced highly elastic state of the polymer) on the deformed PP structure also depended little on the temperature. A noticeable increase was observed only at temperatures close to the PP melting point. This effect was similar to that of the increase in the electrical resistance of undeformed samples at the temperatures of the onset of polymer melting in Fig. 1 and was probably of the same nature [20]. As assumed in [20], the relaxational decrease in the electrical resistance at higher temperatures was associated with the restoration of the conductive channels formed by the CB particles. The higher the sample temperature, the greater this decrease in electrical resistance [20]. Isometric heat treatment of a deformed PP composite under isometric conditions also led to the restoration of the conductive channel system [20]. Once again, we could say that this relaxation phenomenon was similar to the NTC effect characterized by decrease in the height of the electrical resistance "barrier" peak upon heating non-deformed samples at high temperatures in Fig. 1. When deformed at higher temperatures (close to the PP melting point), the abovementioned destruction of the conductive channels formed by the CB particles occurred more intensively, possibly due to the recrystallization of the composite's PP matrix [17].

To study the mechanism of electrical resistance relaxation, we could use the concept of average relaxation time, as in the case of mechanical stress relaxation. We used Eq. (1) to calculate the relaxation times [9]:

$$\ln\frac{\rho_t-\rho_{min}}{\rho_{max}-\rho_{min}}=\frac{t}{\tau} \quad (1)$$

where ρ_t, ρ_{max}, and ρ_{min} are the current (at time point t), maximum (at the beginning of the relaxation process),

and minimum (equilibrium) values, respectively, of the specific volumetric electrical resistance (Ohm·m) and τ is the average relaxation time (s). Using these relations, we could calculate the average times of electrical resistance relaxation at the studied temperatures[2]. The obtained relaxation times made it possible to calculate the activation energies of the electrical relaxation by analogy with the activation energy of mechanical relaxation [19]:

$$\ln\tau = \ln\tau_0 + \frac{U_{el}}{RT}, \quad (2)$$

where τ is the average relaxation time (s) at temperature T (K), τ_o is a constant with the dimension of time (s), R is the universal gas constant equal to 8.31 J/(mol·K), and U_{el} is a coefficient independent of temperature (J/mol). The value of U depended on the average size of a kinetic unit (a molecule or part of a molecule) that participated in the thermal motion (relaxation process), as in the case of PE composites [18]. It is known [19] that the activation energy of viscous flow ($U_{vis.flow}$; the motion of segments upon melt shear) for PP and PE is 45–50 and 30–35 kJ/mol, respectively. Relaxation times (τ) linearly depend on the reciprocal of temperature (1/T, K) in a wide temperature range (see Fig. 3).

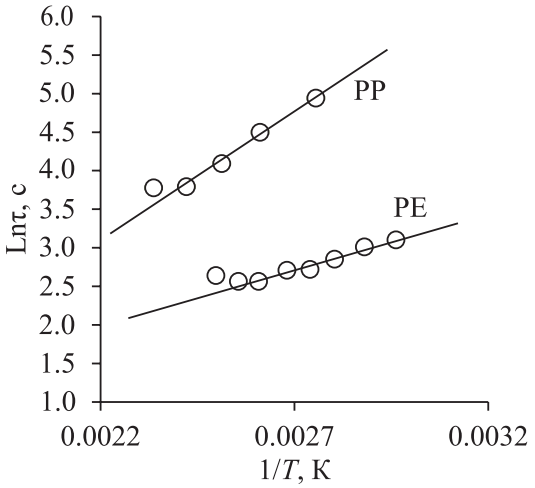

Fig. 3. Dependence of the relaxation time of the electrical resistance of polyethylene (PE) [20] and polypropylene (PP) on the test temperature.

[2] Markov V.A. Electrically conductive polymer composites with an increased positive temperature coefficient of electrical resistance for self-regulating heaters. Cand. Thesis. Moscow: M.V. Lomonosov MITHT; 2014. 120 p. (in Russ.).

The calculated values of the "electrical" activation energies of the studied processes (U) were U_{PP} = 30–32 kJ/mol and U_{PE} = 15–16 kJ/mol. Note that for PP, the value of the "mechanical" activation energy (U) decreased from $U_{vis.flow}$ ~45 kJ/mol in the viscous fluid state to $U_{high.elastic}$ ~32 kJ/mol at temperatures below the temperatures of the onset of PP melting upon its transition to the forced highly elastic state [19]. In linear high-density PE, a corresponding decrease occurred from $U_{vis.flow}$ ~30 kJ/mol to $U_{high.elastic}$ ~17 kJ/mol [18, 19]. In our case, the temperature coefficient (U_{el}) for the electrical relaxation of PP and, as shown earlier, high-density PE [20] in the solid state practically coincided with the above values. Our results indicated a direct relationship between electrical relaxation and mechanical relaxation due to the segmental mobility of the polymer macromolecules.

CONCLUSIONS

This study showed that during the mechanical deformation of electrically conductive PP composites with CB at elevated temperatures the nature of electrical resistance relaxation is similar to the nature of mechanical stress relaxation. The average times and activation energies for the electrical relaxation of deformed PP composites are comparable to those for mechanical relaxation, which indicates the general nature of these processes.

Acknowledgments

This work was supported by the state subsidy (basic part) No. 496332017/54 dated 01.02.2017.

Authors' contribution

A.V. Markov – design of the research concept, development of the experiment, discussion and analysis of the results, writing the text of the article;

K.S. Tarasova – studying the properties of samples, processing and analysis of the data obtained, discussion of the results;

V.A. Markov – studying the properties of samples, data collection and processing, discussion of the results, formatting the text of the article.

The authors declare no conflicts of interest.

REFERENCES

1. Zhang W., Dehghani-Sanij A.A., Blackburn. R.S. Carbon based conductive polymer composites. *J. Mater. Sci.* 2007;42(10):3408–3418. https://doi.org/10.1007/s10853-007-1688-5

2. Carmona F., Canet R., Delhaes P. Piezoresistivity of heterogeneous solids. *J. Appl. Phys.* 1987;61(7):2550–2558. https://doi.org/10.1063/1.337932

3. Flandin L., Cavaille J., Brechet Y., Dendievel R. Characterization of the damage in nanocomposite materials by a.c. electrical properties: experiment and simulation. *J. Mater. Sci.* 1999;34:1753–1759. https://doi.org/10.1023/A:1004546806226

4. De Focatiis D.S.A., Hull D., Sánchez-Valencia A. Roles of prestrain and hysteresis on piezoresistance in conductive elastomers for strain sensor applications. *Plastics, Rubber and Composites.* 2012;41(7):301–309. https://doi.org/10.1179/1743289812Y.0000000022

5. Chodák I., Podhradská S., Jarcusková J., Jurciová J. Changes in Electrical Conductivity During Mechanical Deformation of Carbon Black Filled Elastomeric Matrix. *Open Macromol. J.* 2010;4:32–36.

6. Krückel J., Starý Z., Schubert D.W. Oscillations of the electrical resistance induced by shear deformation in molten carbon black composites. *Polymer.* 2013;54(3):1106–1113. https://doi.org/10.1016/j.polymer.2012.12.051

7. Vigueras-Santiago E., Hernández-López S., Camacho-López M.A., Lara-Sanjuan O. Electric anisotropy in high density polyethylene + carbon black composites induced by mechanical deformation. *J. Phys.: Conf. Ser.* 2009;167(1):012039. https://doi.org/10.1088/1742-6596/167/1/012039

8. Chen Y., Song Y., Zhou J., Zheng Q. Effect of uniaxial pressure on conduction behavior of carbon black filled poly(methyl vinyl siloxane) composites. *Chin. Sci. Bull.* 2005;50(2):101–107. https://doi.org/10.1007/BF02897510

9. Aneli J.N., Zaikov G.E., Mukbaniani O.V. Electric Conductivity of Polymer Composites at Mechanical Relaxation. *Chem. Chem. Technol.* 2011;5(2):187–190. https://doi.org/10.23939/chcht05.02.187

10. Knite M., Teteris V., Kiploka A. Polyisoprene-carbon black nanocomposites as tensile strain and pressure sensor materials. *Sensors and Actuators A: Physical.* 2004;110(1–3):142–149. Part of special issue: Selected Papers from: *The 16th European Conference on Solid-State Transducers*. Prague: 2002; 116–119. https://doi.org/10.1016/j.sna.2003.08.006

11. Starý Z., Krückel J., Schubert D., Münstedt H. Behavior of Conductive Particle Networks in Polymer Melts under Deformation. *AIP Conf. Proc.* 2011;1375(1):232–239. https://doi.org/10.1063/1.3604483

12. Hatami K., Grady B.P., Ulmer M.C. Sensor-Enabled Geosynthetics: Use of Conducting Carbon Networks as Geosynthetic Sensors. *J. Geotch. Geoenv. Eng.* 2009;135(7):863–874. https://doi.org/10.1061/(ASCE)GT.1943-5606.0000062

13. Markov V.A. Kandyrin L.B. Markov A.V., Sorokina E.A. Effect of silane-crosslinking on electrical properties and heat resistance of carbon black-filled polyethylene composites. *Plasticheskie massy*. 2013;(10):21–24 (in Russ.).

14. Markov V.A., Markov A.V., Poldushov M.A., Abysov E.Y. The influence of the method used to prepare electrically conductive composites based on polyethylene, polypropylene, and carbon black on their properties at elevated temperatures. *Int. Polym. Sci. Technol.* 2016;43(3):T13–T18. https://doi.org/10.1177/0307174x1604300303

15. Rogers N., Khan F. Characterization of deformation induced changes to conductivity in an electrically triggered shape memory polymer. *Polym. Test.* 2013;32(1):71–77. https://doi.org/10.1016/j.polymertesting.2012.10.001

16. Wang P., Ding T. Conductivity and piezoresistivity of conductive carbon black filled polymer composite. *J. App. Polym. Sci.* 2010;116(4):2035–2039. https://doi.org/10.1002/app.31693

17. Markov V.A., Kandyrin L.B., Markov A.V. The influence of technological additives on electrical properties of carbon black-filled polyethylene composites. *Fine Chemical Technologies.* 2013;8(6):103–107 (in Russ.).

18. Markov V.A., Kandyrin L.B., Markov A.V. Effect of strain on electrical resistivity of carbon black filled polyethylene composites. *Konstruktsii iz kompozitsionnykh materialov = Composite materials constructions*. 2013;4(132):40–44 (in Russ.).

19. Gul' V.E., Kuleznev V.N. *Struktura i mekhanicheskie svoistva polimerov* (*The structure and mechanical properties of polymers*). Moscow: Labirint; 1994. 367 p. (in Russ.).

20. Markov V.A., Markov A.V., Tahseen A.Saki. Effect of relaxation processes during deformation on electrical resistivity of polyethylene composites filled with carbon black. *J. Polym. Res.* 2016;23(9):191. https://doi.org/10.1007/s10965-016-1088-0

About the authors:

Anatoly V. Markov, Dr. Sci. (Eng.), Professor, Department of Chemistry and Technology of Plastic Processing and Polymer Composites, M.V. Lomonosov Institute of Fine Chemical Technologies, MIREA – Russian Technological University (86, Vernadskogo pr., Moscow 119571, Russia). E-mail: markovan@bk.ru. https://orcid.org/0000-0001-7952-7419

Kristina S. Tarasova, Master, Department of Chemistry and Technology of Plastic Processing and Polymer Composites, M.V. Lomonosov Institute of Fine Chemical Technologies, MIREA – Russian Technological University (86, Vernadskogo pr., Moscow, 119571, Russia). E-mail: shkarypa-kristina1992@ya.ru.

Vasily A. Markov, Postgraduate Student, Department of Chemistry and Technology of Plastic Processing and Polymer Composites, M.V. Lomonosov Institute of Fine Chemical Technologies, MIREA – Russian Technological University (86, Vernadskogo pr., Moscow, 119571, Russia). E-mail: vasily@markov.biz. https://orcid.org/0000-0002-5768-9107

Об авторах:

Марков Анатолий Викторович, д.т.н., профессор кафедры химии и технологии переработки пластмасс и полимерных композитов Института тонких химических технологий им. М.В. Ломоносова, ФГБОУ ВО «МИРЭА – Российский технологический университет» (119571, Россия, Москва, пр-т Вернадского, д. 86). E-mail: markovan@bk.ru. https://orcid.org/0000-0001-7952-7419

Тарасова Кристина Сергеевна, магистр кафедры химии и технологии переработки пластмасс и полимерных композитов Института тонких химических технологий им. М.В. Ломоносова, ФГБОУ ВО «МИРЭА – Российский технологический университет» (119571, Россия, Москва, пр-т Вернадского, д. 86). E-mail: shkarypa-kristina1992@ya.ru.

Марков Василий Анатольевич, аспирант кафедры химии и технологии переработки пластмасс и полимерных композитов, Института тонких химических технологий им. М.В. Ломоносова, ФГБОУ ВО «МИРЭА – Российский технологический университет» (119571, Россия, Москва, пр-т Вернадского, д. 86). E-mail: vasily@markov.biz. https://orcid.org/0000-0002-5768-9107

The article was submitted: May 06, 2020; approved after reviewed: December 28, 2020; accepted for publication: August 02, 2021.

Translated from Russian into English by M. Povorin
Edited for English language and spelling by Enago, an editing brand of Crimson Interactive Inc.

CHEMISTRY AND TECHNOLOGY OF INORGANIC MATERIALS
ХИМИЯ И ТЕХНОЛОГИЯ НЕОРГАНИЧЕСКИХ МАТЕРИАЛОВ

ISSN 2686-7575 (Online)

https://doi.org/10.32362/2410-6593-2021-16-4-352-362

UDC 546.41:54.022.384.057

RESEARCH ARTICLE

A novel calcium trifluoroacetate structure

Alexandra A. Vasilyeva[1], Tatyana Yu. Glazunova[1,@], Denis S. Tereshchenko[1], Elmira Kh. Lermontova[2]

[1]Faculty of Chemistry, Lomonosov Moscow State University, Moscow, 119991 Russia
[2]N.S. Kurnakov Institute of General and Inorganic Chemistry, Moscow, 119071 Russia
[@]Corresponding author, e-mail: ctpayc@mail.ru

Abstract

Objectives. *The study was devoted to considering the features of the synthesis and crystal structure of calcium trifluoroacetate $Ca_2(CF_3COO)_4 \cdot 8CF_3COOH$ and investigating the products of its thermal behavior.*

Methods. *The compositions of the proposed structural form were characterized by various physicochemical methods (X-ray diffraction, IR spectroscopy), and the products of thermal decomposition were determined under dynamic vacuum conditions.*

Results. *The reaction between calcium carbonate and 99% trifluoroacetic acid yielded a new structural type of calcium trifluoroacetate $Ca_2(CF_3COO)_4 \cdot 8CF_3COOH$ (I) in the form of colorless prismatic crystals unstable air. X-ray diffraction results confirmed the composition **I**: space group $P2_1$, with unit cell parameters: a = 10.0193(5) Å, b = 15.2612(7) Å, c = 16.3342(8) Å, β = 106.106(2)°, V = 2399.6(2) Å^3, Z = 2. The structure is molecular, constructed from $Ca_2(CF_3COO)4 \cdot 8CF_3COOH$ dimers. The end molecules of the trifluoroacetic acid were involved in the formation of intramolecular hydrogen bonds with oxygen atoms of the bidentate bridging anions CF_3COO^-. There were strongly pronouncedsymmetric and asymmetric absorption bands of COO and CF_3-groups in the IR spectrum of the resulting compound in the range of 1200–1800 cm^{-1}. The definite peak of the oscillation of the OH-group at 3683 cm^{-1} corresponds to the trifluoroacetic acid molecules present in the structure. The broadpeak of the valence oscillations in the range of 3300–3500 cm^{-1} is caused by the presence of intramolecular hydrogen bonds. Decomposition began at 250°C and 10^{-2} mm Hg with calcium fluoride CaF_2 as the final decomposition product.*

Conclusions. *We obtained a previously undescribed calcium–trifluoroacetic acid complex whose composition can be represented by $Ca_2(CF_3COO)_4 \cdot 8CF_3COOH$. The crystal island structure is a dimeric molecule where the calcium atoms are bound into dimers by four trifluoroacetate groups. The complex was deposited in the Cambridge Structural Data Bank with a deposit number CCDC 2081186. Although the compound has a molecular structure, thermal decomposition leads to the formation of calcium fluoride characterized by a small particle size, which may further determine its applications.*

Keywords: *trifluoroacetate complexes, alkaline earth metals, crystal structure, IR spectroscopy, thermal properties, calcium fluoride*

For citation: Vasilyeva A.A., Glazunova T.Yu., Tereshchenko D.S., Lermontova E.Kh. A novel calcium trifluoroacetate structure. *Tonk. Khim. Tekhnol. = Fine Chem. Technol.* 2021;16(4):352–362 (Russ., Eng.). https://doi.org/10.32362/2410-6593-2021-16-4-352-362

НАУЧНАЯ СТАТЬЯ

Трифторацетат кальция: новый структурный тип

А.А. Васильева[1], Т.Ю. Глазунова[1,@], Д.С. Терещенко[1], Э.Х. Лермонтова[2]

[1]Химический факультет, Московский государственный университет им. М.В. Ломоносова, Москва, 119991 Россия
[2]Институт общей и неорганической химии им. Н.С. Курнакова, Москва, 119071 Россия
[@]Автор для переписки, e-mail: ctpayc@mail.ru

Аннотация

Цели. *Работа посвящена рассмотрению особенностей синтеза и кристаллического строения трифторацетата кальция $Ca_2(CF_3COO)_4 \cdot 8CF_3COOH$, а также изучению продуктов его термического поведения.*

Методы. *Соединение охарактеризовано различными физико-химическими методами (рентгеноструктурный анализ, ИК-спектроскопия), установлены продукты термического разложения в условиях динамического вакуума.*

Результаты. *Взаимодействием карбоната кальция с 99% трифторуксусной кислотой синтезирован новый структурный тип трифторацетата кальция $Ca_2(CF_3COO)_4 \cdot 8CF_3COOH$ (I) в виде неустойчивых на воздухе бесцветных призматических кристаллов. Строение **I** установлено по результатам рентгеноструктурного анализа: пространственная группа $P2_1$, параметры элементарной ячейки: a = 10.0193(5) Å, b = 15.2612(7) Å, c = 16.3342(8) Å, β = 106.106(2)°, V = 2399.6(2) Å^3, Z = 2. Структура молекулярная, построена из димеров $Ca_2(CF_3COO)_4 \cdot 8CF_3COOH$. Торцевые молекулы трифторуксусной кислоты участвуют в образовании внутримолекулярных водородных связей с атомами кислорода бидентатных мостиковых анионов CF_3COO^-. На ИК-спектре полученного соединения в диапазоне 1200–1800 см$^{-1}$ присутствуют ярко выраженные симметричные и асимметричные полосы поглощения COO и CF_3-групп. Четкий пик колебания OH-группы на 3683 см$^{-1}$ соответствует присутствующим в структуре молекулам трифторуксусной кислоты. Широкий пик валентных колебаний в области 3300–3500 см$^{-1}$ обусловлен наличием внутримолекулярных водородных связей. При давлении 10^{-2} мм рт.ст. разложение начинается при 250 °C, конечным продуктом разложения является фторид кальция CaF_2.*

Выводы. *Нами получен ранее не описанный комплекс кальция с трифторуксусной кислотой, состав которого может быть представлен формулой $Ca_2(CF_3COO)_4 \cdot 8CF_3COOH$, кристаллическая островная структура которого представляет собой димерную молекулу, а атомы кальция связаны в димеры четырьмя трифторацетатными группами. Комплекс задепонирован в Кембриджском банке структурных данных, номер депонирования – CCDC 2081186. Соединение имеет молекулярное строение, термическое разложение приводит к образованию фторида кальция, характеризующегося небольшим размером частиц, что может в дальнейшем обусловить его применение.*

Ключевые слова: *трифторацетатные комплексы, щелочноземельные металлы, кристаллическая структура, ИК-спектроскопия, термические свойства, фторид кальция*

Для цитирования: Васильева А.А., Глазунова Т.Ю., Терещенко Д.С., Лермонтова Э.Х. Трифторацетат кальция: новый структурный тип. *Тонкие химические технологии*. 2021;16(4):352–362. https://doi.org/10.32362/2410-6593-2021-16-4-352-362

INTRODUCTION

Trifluoroacetic acid CF_3COOH (dissociation constant 0.69 [1]) is considered a strong acid due to the influence of the trifluoromethyl group on the carboxyl group. The bond between the trifluoroacetate anion and the complexing atom exhibits a more ionic character and is weaker than the coordination bond in most carboxylates. As a consequence, the coordination chemistry of trifluoroacetate complexes often differs from most carboxylates. At the same time, trifluoroacetic acid performs various structural functions depending on the conditions of the synthesis, leading to the appearance of certain characteristic features in the composition and structure of the resulting trifluoroacetate metal complexes. A review of trifluoroacetate complexes of 3d metals was provided in [2].

Interest in the study of trifluoroacetate complexes of various metals is primarily associated with the possibility of obtaining simple and complex fluorides during their thermal decomposition [3–6] in the form of nanoparticles, solid fluoride solutions [7], and fluoride glasses of various compositions [8–10].

The study aims at synthesizing a calcium trifluoroacetate complex not previously described, investigate its crystal structure by X-ray diffraction and IR spectroscopy, compare the features of the crystal structure of trifluoroacetate complexes of various alkaline-earth metals based on their synthesis conditions, and analyze the product of thermal decomposition of the resulting compound.

MATERIALS AND METHODS

The starting materials for the synthesis were calcium carbonate, $CaCO_3$ (analytical grade, *Vecton*, Russia), and trifluoroacetic acid, CF_3COOH (99% chemically pure, *Argentum 107*, Russia).

*Synthesis of $Ca_2(CF_3COO)_4 \cdot 8CF_3COOH$ (complex **I**):*

A sample of 90.0 mg of $CaCO_3$ (1.0714 mmol) was dissolved by heating in 5.0 mL of 99% CF_3COOH. Concentrating the resulting solution in a desiccator over phosphorus pentoxide (P_2O_5, pure, *Vecton*, Russia) produced isolated colorless and air-unstable crystals, filtered and dried in an argon atmosphere with the yield of 630 mg (81%). Complex **I** is soluble in concentrated trifluoroacetic acid but decomposes in moist air and aqueous solutions with the formation of calcium trifluoroacetate hydrate.

Compound **I** was characterized by IR spectroscopy and X-ray diffraction. IR spectra were recorded on the FTIR Spectrum using One Perkin-Elmer spectrometer (*SpectraLab Scientific Incorporation*, Canada) in KBr tablets in the region of 400–4000 cm^{-1} with a resolution of 0.5 cm^{-1}. The assignment of bands in the IR absorption spectrum of the complex is given in Table 1. The observed spectrum is shown in Fig. 1.

The shift in the absorption bands of the COO groups of compound **I** relative to similar data for the calcium trifluoroacetate complex described in [11] indicated an attenuation of the interaction and an increase in the Ca–O bond length, consistent with an increase in the coordination number of the calcium atom to 8 in compound **I**.

The study of the thermal behavior of the sample $Ca_2(CF_3COO)_4 \cdot 8CF_3COOH$ under dynamic vacuum conditions was carried out by heating the sample in a glass ampoule using a tubular furnace. Under dynamic vacuum conditions (at 10^{-2} mm Hg), compound **I** was stable up to a temperature of 250°C, after which it began to decompose, resulting in a sharp decrease in pressure up to 10^{-1} mm Hg. However, as the temperature increased to 270°C, the pressure became stabilized at 10^{-2} mm Hg.

Experimental and theoretical values of mass loss are given in Table 2.

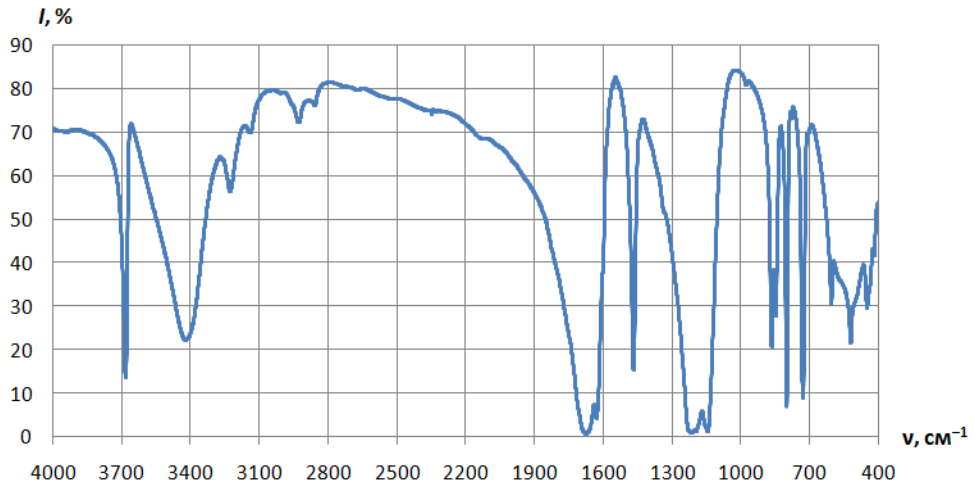

Fig. 1. IR absorption spectrum of the compound **I** $Ca_2(CF_3COO)_4 \cdot 8CF_3COOH$.

Table 1. Assignment of the peaks of the IR spectrum of the compound **I** $Ca_2(CF_3COO)_4 \cdot 8CF_3COOH$

Wavenumber, cm^{-1}	Assignment	Notes/references
3683	υ(OH)	–
3419.5	υ(O–H…O)	3431 [12]
3226.3	υ(O–H…O)	–
1677.7	$υ_{as}$(COO)	1660 [11]
1469.3	$υ_s$(COO)	1444 [11]
1215.2	$υ_s(CF_3)$	1210 [11]
1145.9	$υ_{as}(CF_3)$	1142 [11]
867.33	υ(C–C) υ(C–O)	850 [11]
801.35	CF_3 symmetric stretch	800 [11]
729.95	δ(COO) (C–CO_2 in-planebend)	728 [11]
606.41	$δ_s(CF_3)$	605 [11]
522.09	$δ_{as}(CF_3)$	520 [11]
450.08	δ(CCF_3) (C–CF_3 planerock)	υ(Ca–O), 430 [12]

Table 2. Experimental and theoretical mass loss values for the formation of CaF_2 from compound **I** $Ca_2(CF_3COO)_4 \cdot 8CF_3COOH$

Compound	$\Delta m_{exper.}$, %	$\Delta m_{theor.}$, %
$Ca_2(CF_3COO)_4 \cdot 8CF_3COOH$	89.26	89.20
CaF_2		

X-ray phase analysis of the decomposition products of the sample $Ca_2(CF_3COO)_4 \cdot 8CF_3COOH$ was performed on the STOE STADI IP device (*Stoe*, Germany) (Ge (111) monochromator, Cu Ka1). In addition, measurement and indexing of radiographs were carried out by the STOE WinXPow and Powder2 software package[1].

[1] STOE WinXPow, Jana, 2006; Powder2, Laboratory of Inorganic Crystallochemistry, MSU by Oleynikov Peter, 1998.

The product of thermal decomposition is a cubic modification of calcium fluoride CaF_2 (a = 5.4626 Å, Z = 4, space group $Fm3m$). The X-ray diffraction pattern is shown in Fig. 2, where the peaks were indicated according to the data of the powder data bank[2] [00-077-2093], with the results of indexing presented in Table 3.

The relatively large half-width of the peaks on the radiograph indirectly indicated the formation of calcium fluoride, characterized by small particle size.

For the X-ray analysis, $Ca_2(CF_3COO)_4 \cdot 8CF_3COOH$ crystals were selected under a layer of vaseline oil in a Meiji Techno EMZ-8TRD polarization microscope (Japan) and were quickly (in less than 1 min) transferred to a diffractometer, where a stream of dry nitrogen gas was used to cool them. The analysis was carried out in an automatic diffractometer, Bruker SMART APEX II, *Bruker AXS GmbH* (Germany) at a temperature of 100K using MoKα radiation (λ = 0.71073 Å, graphite monochromator). Absorption was calculated by measuring the intensities of equivalent reflections [13]. The structures were solved by the direct method and refined by the full-matrix anisotropic least-squares method in F^2 for all non-hydrogen atoms (SHELXTL-Plus [14]). The hydrogen atoms were placed in the calculated positions and refined using the "riding" scheme. The crystallographic data, the experimental details, and the $Ca_2(CF_3COO)_4 \cdot 8CF_3COOH$ structure refinement data are given in Table 4. Tables of atomic coordinates, bond lengths, valence and torsion angles, and anisotropic temperature parameters for the compound **I** are available in the Cambridge Structural Data Bank,[3] with the deposit number CCDC 2081186.

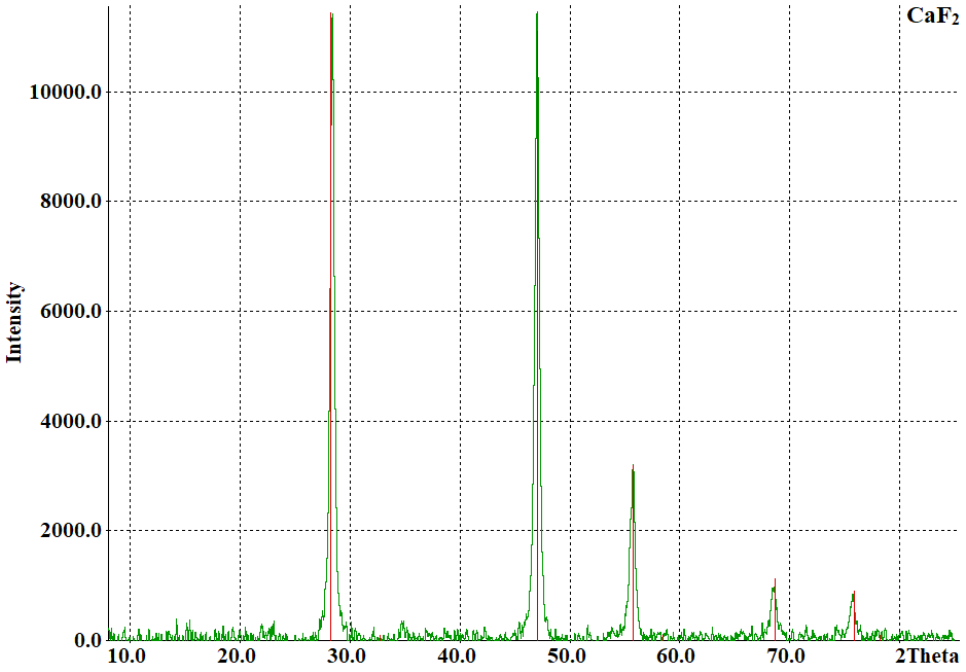

Fig. 2. Radiograph of the decomposition product of compound **I** $Ca_2(CF_3COO)_4 \cdot 8CF_3COOH$. The assignment was made with the powder database [00-077-2093].

Table 3. CaF_2 indexing results

Cubic F-centered cell parameters: a = 5.471(2), Volume = 163.8(2), $F(5)$ = 17.1(0.0488, 6) $M(5)$ = 114.6(4.62, 6)									
No.	**2θ(obs)**	***D*(obs)**	***Q*(obs)**	***I*/*I*o**	***h***	***k***	***l***	***Q*(calc)**	**Δ*Q***
1	28.364	3.1440	1011.66	100	1	1	1	1002.25	9.41
2	46.998	1.9319	2679.36	98	2	2	0	2672.68	6.68
3	55.685	1.6493	3676.21	27	3	1	1	3674.93	1.28
4	68.524	1.3683	5341.18	8	4	0	0	5345.35	−4.17
5	75.708	1.2553	6346.07	6	3	3	1	6347.60	−1.53

[2] ICDD PDF-2 (Database), International Centre for Diffraction Data, Newtown Square, PA, USA. № 00-077-2093.
[3] The Cambridge Crystallographic Data Center, www.ccdc.cam.ac.ukn. Accessed April 30, 2021.

Table 4. Crystallographic data for $Ca_2(CF_3COO)_4 \cdot 8CF_3COOH$

Parameter	Value
Empirical formula	$C_{24}H_8Ca_2F_{36}O_{24}$
Formula weight	1444.46
Crystal size, mm	0.30 × 0.25 × 0.21
Syngonia	Monoclinic
Space group	$P2_1$
a, Å	10.0193(5)
b, Å	15.2612(7)
c, Å	16.3342(8)
α, °	90
β, °	106.106(2)
γ, °	90
V, Å^3	2399.6(2)
Z	2
ρ_{calc}, g/cm^3	1.999
μ(MoKα), mm^{-1}	0.458
F(000)	1416
Interval of θ, °	2.533–25.717
Intervals of indexes	$-12 \le h \le 12$ $-19 \le k \le 17$ $-20 \le l \le 17$
Total reflections	17553
Independent reflections	8795 (R_{int} = 0.1084)
Number of parameters	783
R_1 for $I > 2\sigma(I)$	0.0607
wR_2 (all data)	0.0862
Q factor according to F^2 (GOF)	1.045
$\Delta\rho_{min}/\Delta\rho_{max}$, e/Å^3	−0.500/0.608

RESULTS AND DISCUSSION

The reviewed literature allowed us to establish the relationship between the synthesis conditions (the ratio of solvent and trifluoroacetic acid) and the cation size on the structure of the resulting trifluoroacetate complexes of alkaline-earth metals.

With an excess of a donor solvent, such as water, mononuclear tetraaquacomplexes were formed. Thus, for magnesium, island structures $Mg(CF_3COO)_2 \cdot (H_2O)_4$ were previously obtained, in which the trifluoroacetate anion is a monodentate ligand with a magnesium coordination number (c.n.) of 6 [2].

In the absence of a donor solvent, trifluoroacetic acid exhibited a bridging function. For example, in the presence of tetrahydrofuran (THF), the formation of chain-bounded $Ca_2(CF_3COO)_4 \cdot (THF)_4$ dimers with the help of trifluoroacetate groups (c.n. Ca = 6) [12].

In the absence of trifluoroacetic acid, the trifluoroacetate anion was either a tri- or tetradentate. CF_3-group fluorine atoms can complete the metal environment, shown by the example of crystal structures of polymer trifluoroacetate obtained from calcium ($Ca_3(CF_3COO)_6 \cdot (H_2O)_4$, c.n. Ca = 6) [15] and strontium ($Sr_3(CF_3COO)_6 \cdot (THF)$, c.n. Sr = 8–9) [16].

In the complete absence of a donor solvent, the synthesis between a trifluoroacetic acid and excess alkaline-earth metal carbonates as precursors lead to the formation of strontium trifluoroacetate $Sr(CF_3COO)_2$ and barium $Ba(CF_3COO)_2$, in which the trifluoroacetic acid anion was bridged and tridentate [17].

The synthesis in excess trifluoroacetic acid also lead to the manifestation of bridge functions by the trifluoroacetate anion. The primary factor responsible for forming the crystal structure is the size of the metal ion—the complexing agent. For small-sized ions such as magnesium, infinite chains were obtained $[Md(CF_3COO)_2(CF_3COOH)_2]_n$ [2], c.n. Mg = 6.

In this work, the synthesis was carried out in a trifluoroacetic acid medium that acted as the reagent and solvent, making it possible to stabilize a new structural type of acidic calcium trifluoroacetate $Ca_2(CF_3COO)_4 \cdot 8CF_3COOH$ (c.n. Ca = 8). Dimeric molecules formed the resulting structure, which is island and coordination saturated (c.n. Ca = 8).

Previously, such a method of metal atoms coordination and the type of crystal structure was not described for trifluoroacetate complexes. Of all the known carboxylates, such coordination was represented by a single example of a strontium salt of dimethylbutanoic acid and several rare-earth elements with dimethylbutanoic and pivalic acids [18].

Description of the crystal structure of $Ca_2(CF_3COO)_4 \cdot 8CF_3COOH$

The structure of compound **I** contains two independent crystallographic calcium atoms connected by four trifluoroacetate bidentate groups (Fig. 3). The coordination environment of each calcium atom is formed by four oxygen atoms of the bridge trifluoroacetate groups and four carbonyl oxygen atoms of trifluoroacetic acid molecules, producing a coordination polyhedron in the form of a quadrangular antiprism (Fig. 4). Thus, the structure of compound **I** is constructed from dimers

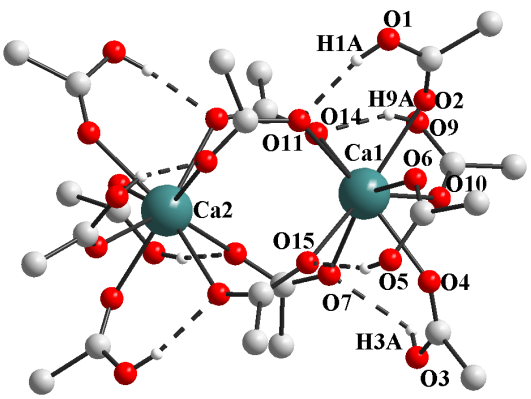

Fig. 3. Fragment of the crystal structure of $Ca_2(CF_3COO)_4 \cdot 8CF_3COOH$.

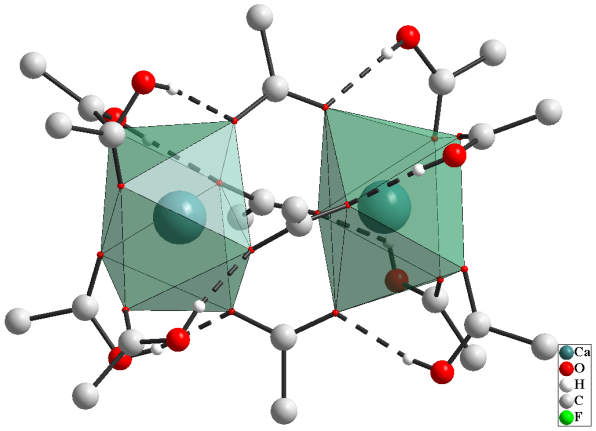

Fig. 4. The surrounding of calcium atoms in the crystal structure of $Ca_2(CF_3COO)_4 \cdot 8CF_3COOH$ is a quadrilateral antiprism.

$Ca_2(CF_3COO)_4 \cdot 8CF_3COOH$. Eight trifluoroacetic acid molecules formed eight intramolecular hydrogen bonds between the hydrogen atoms of the trifluoroacetic acids and the oxygen atoms of the bridged trifluoroacetate groups (Fig. 3).

The molecules in the structure are held together by Van der Waals interactions and are arranged in a staggered order (Fig. 5).

The Ca–O bond lengths and O–Ca–O angles are presented in Table 5. The distances between the calcium and the oxygen atoms of the bidentate trifluoroacetate groups (the average value: 2.456 Å) are less than between the calcium atoms and the carbonyl oxygen atoms of the trifluoroacetic acid molecules (2.462 Å). When the O atoms are oxygen

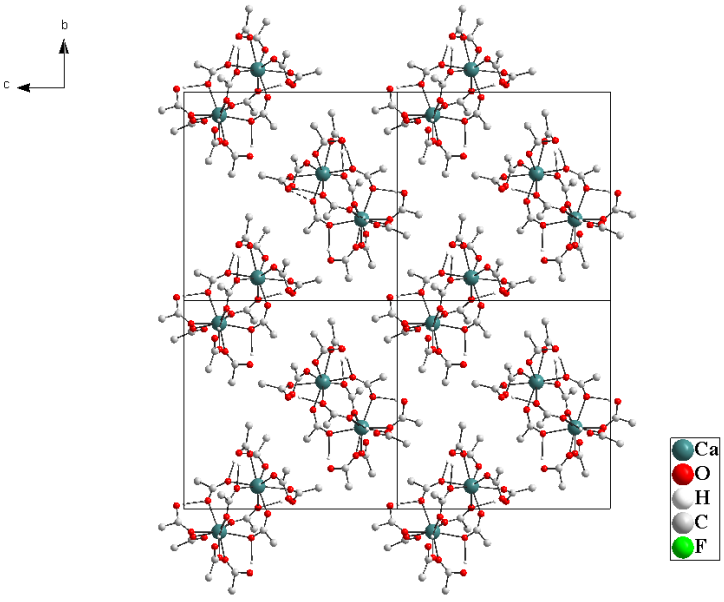

Fig. 5. The arrangement of molecules in the structure of $Ca_2(CF_3COO)_4 \cdot 8CF_3COOH$ along the *a*-axis.

Table 5. The lengths of the Ca–O bonds and O–Ca–O angles in the structure of $Ca_2(CF_3COO)_4 \cdot 8CF_3COOH$

Bond	Length of the bond, Å
$Ca–O14_{CF3COO}$	2.471 (5)
$Ca–O11_{CF3COO}$	2.434 (5)
$Ca–O15_{CF3COO}$	2.466 (5)
$Ca–O17_{CF3COO}$	2.454 (5)
$Ca–O4_{CF3COOH}$	2.448 (5)
$Ca–O6_{CF3COOH}$	2.473 (5)
$Ca–O10_{CF3COOH}$	2.481 (5)
$Ca–O2_{CF3COOH}$	2.447 (5)
Angle	**Value, °**
$O14_{CF3COO}–Ca–O11_{CF3COO}$	76.736 (2)
$O14_{CF3COO}–Ca–O15_{CF3COO}$	78.782 (2)
$O11_{CF3COO}–Ca–O15_{CF3COO}$	125.976 (2)
$O14_{CF3COO}–Ca–O17_{CF3COO}$	123.747 (2)
$O11_{CF3COO}–Ca–O17_{CF3COO}$	78.965 (2)
$O15_{CF3COO}–Ca–O17_{CF3COO}$	76.054 (2)
$O4_{CF3COOH}–Ca–O6_{CF3COOH}$	70.925 (2)
$O4_{CF3COOH}–Ca–O10_{CF3COOH}$	69.345 (2)
$O4_{CF3COOH}–Ca–O2_{CF3COOH}$	110.010 (2)
$O6_{CF3COOH}–Ca–O10_{CF3COOH}$	111.356 (2)
$O6_{CF3COOH}–Ca–O2_{CF3COOH}$	74.716 (2)
$O10_{CF3COOH}–Ca–O2_{CF3COOH}$	69.676 (2)

atoms of trifluoroacetic acid molecules, the O–Ca–O angles are smaller than in the case of oxygen atoms of bidentate trifluoroacetate groups.

Length relations of Ca–O of 0.1–0.2 Å exceeded the length relations of Ca–O in the previously described structures of $Ca_2(CF_3COO)_4 \cdot (TGF)_4$ [12] and $Ca_3(CF_3COO)_6 \cdot (H_2O)_4$ [15], which is associated with an increase in c.n. of calcium from 6 [12, 15] to 8 (compound **I**). This correlates with the interpretation of the absorption bands of the IR spectrum of compound **I**.

CONCLUSIONS

We have obtained a previously unknown calcium complex with trifluoroacetic acid whose composition can be represented as $Ca_2(CF_3COO)_4 \cdot 8CF_3COOH$. The crystal island structure is a dimeric molecule whose calcium atoms are linked in dimers by four trifluoroacetate groups. The complex was characterized by X-ray diffraction and IR spectroscopy. The crystallografic data of the complex was deposited in the Cambridge Structural Data Bank with deposit number CCDC 2081186. Although the compound has a molecular structure, thermal decomposition lead to calcium fluoride formation characterized by a small particle size, which may further determine its application.

Acknowledgments

The study was supported by the Russian Foundation for Basic Research, grant No. 19-03-01059. X-ray diffraction studies were performed at the User Facilities Center of the Kurnakov Institute of General and Inorganic Chemistry, Russian Academy of Sciences, within the State Assignment on Fundamental Research for the Kurnakov Institute of General and Inorganic Chemistry.

Authors' contribution

A.A. Vasilyeva – conducting synthesis, working with literary data, writing the text of the article;

T.Yu. Glazunova – conducting thermal analysis, working with literary data, writing the text of the article;

D.S. Tereshchenko – conducting physicochemical analyses;

E.Kh. Lermontova – X-ray diffraction analysis, solution of the structure.

The authors declare no conflicts of interest.

REFERENCES

1. Milne J.B., Parker T.J. Dissociation constant of aqueous trifluoroacetic acid by cryoscopy and conductivity. *J. Solution Chem.* 1981;10(7):479–487. https://doi.org/10.1007/BF00652082

2. Morozov I.V., Karpova E.V., Glazunova T.Yu., Boltalin A.I., Zakharov M.A., Tereshchenko D.S., Fedorova A.A., Troyanov S.I. Trifluoroacetate complexes of 3d-elements: specific features of synthesis and structures. *Russ. J. Coord. Chem.* 2016;42(10):647–661. https://doi.org/10.1134/S107032841610002X

[Original Russian Text: Morozov I.V., Karpova E.V., Glazunova T.Yu., Boltalin A.I., Zakharov M.A., Tereshchenko D.S., Fedorova A.A, Troyanov S.I. Trifluoroacetate complexes of 3d-elements: specific features of synthesis and structures. *Koordinatsionnaya Khimiya.* 2016;42(10):609–623 (in Russ.). https://doi.org/10.7868/S0132344X16100029]

3. Mishra S., Daniele S. Metal–Organic Derivatives with Fluorinated Ligands as Precursors for Inorganic Nanomaterials. *Chem. Rev.* 2015;115(16):8379–8448. https://doi.org/10.1021/cr400637c

4. Mai H.-X., ZhangYa-W., Sun L.-D., Yan Ch.-H. Highly Efficient Multicolor Up-Conversion Emissions and Their Mechanisms of Monodisperse $NaYF_4$:Yb,Er Core and Core/Shell-Structured Nanocrystals. *J. Phys. Chem.* 2007;111(37):13721–13729. https://doi.org/10.1021/jp073920d

5. Fedorova A.A., Arkhipenko S.Yu., Fatula E.R. Chikov N.P., Sorokina N.M., Morozov I.V. The novel method of synthesis of solid solutions $Ln_xCa_{1-x}F_{2+x}$ (Ln=Yb,Nd) using beta-cyclodextrin. *Procedia Chem.* 2014;11:20–25. https://doi.org/10.1016/j.proche.2014.11.005

6. Fedorova A.A., Fedulin A.I., Morozov I.V. New method of beta-$NaYF_4$: Yb^{3+}, Er^{3+} synthesis by using beta-cyclodextrin. *J. Fluorine Chem*. 2015;178:173–177. https://doi.org/10.1016/j.jfluchem.2015.07.003

7. Glazunova T.Yu., Boltalin A.I., Fedorov P.P. Synthesis of calcium, strontium and barium fluorides by thermal decomposition of trifluoroacetates. *J. Inorg. Chem.* 2006;51(7):983–987. https://doi.org/10.1134/S0036023606070011

[Original Russian Text: Glazunova T.Yu., Boltalin A.I., Fedorov P.P. Synthesis of calcium, strontium and barium fluorides by thermal decomposition of trifluoroacetates. *Zhurnal Neorganicheskoi Khimii.* 2006;51(7):1061–1065 (in Russ.).]

8. Sorokin N.I., Fedorov P.P., Zakalyukin R.M. Electrical conductivity of fluoride glasses based on PbF_2 and InF_3. *Neorganicheskie materialy = Inorg. Mater.* 1999;35(1):88–93 (in Russ.).

9. Zakalyukin R.M., Boltalin A.I., Fedorov P.P., Sobolev B.P. Synthesis and electrical conductivity of multicomponent fluoride glasses. *Fizika i khimiya stekla = Glass Phys. Chem.* 1999;25(3):355–362 (in Russ.).

10. Sorokin N.I., Zakalyukin R.M., Glazunova T.Yu., Boltalin A.I., Fedorov P.P., Sobolev B.P. Ionic conductivity of fluoroaluminate glasses. *Neorganicheskie materialy = Inorg. Mater.* 2000;36(8):1008–1010 (in Russ.).

11. Faniran J.A., Patel K.S. Physicochemical studies of metal haloacetates-VI Infrared spectra of alkaline-earth metals and lead trifluoroacetates. *Spectrochimica Acta. Part A.* 1976;32(6):1351–1354. https://doi.org/10.1016/0584-8539(76)80180-8

СПИСОК ЛИТЕРАТУРЫ

1. Milne J.B., Parker T.J. Dissociation constant of aqueous trifluoroacetic acid by cryoscopy and conductivity. *J. Solution Chem.* 1981;10(7):479–487. https://doi.org/10.1007/BF00652082

2. Морозов И.В., Карпова Е.В., Глазунова Т.Ю., Болталин А.И., Захаров М.А., Терещенко Д.С., Федорова А.А., Троянов С.И. Трифторацетатные комплексы 3d-элементов: особенности синтеза и строения. *Коорд. химия.* 2016;42(10):609–623. https://doi.org/10.7868/S0132344X16100029

3. Mishra S., Daniele S. Metal–Organic Derivatives with Fluorinated Ligands as Precursors for Inorganic Nanomaterials. *Chem. Rev.* 2015;115(16):8379–8448. https://doi.org/10.1021/cr400637c

4. Mai H.-X., ZhangYa-W., Sun L.-D., Yan Ch.-H. Highly Efficient Multicolor Up-Conversion Emissions and Their Mechanisms of Monodisperse $NaYF_4$:Yb,Er Core and Core/Shell-Structured Nanocrystals. *J. Phys. Chem.* 2007;111(37):13721–13729. https://doi.org/10.1021/jp073920d

5. Fedorova A.A., Arkhipenko S.Yu., Fatula E.R. Chikov N.P., Sorokina N.M., Morozov I.V. The novel method of synthesis of solid solutions $Ln_xCa_{1-x}F_{2+x}$ (Ln=Yb,Nd) using beta-cyclodextrin. *Procedia Chem*. 2014;11:20–25. https://doi.org/10.1016/j.proche.2014.11.005

6. Fedorova A.A., Fedulin A.I., Morozov I.V. New method of beta-$NaYF_4$: Yb^{3+}, Er^{3+} synthesis by using beta-cyclodextrin. *J. Fluorine Chem.* 2015;178:173–177. https://doi.org/10.1016/j.jfluchem.2015.07.003

7. Глазунова Т.Ю., Болталин А.И., Федоров П.П. Синтез фторидов кальция, стронция и бария путем термического разложения трифторацетатов. *Журн. неорган. химии.* 2006;51(7):1061–1065.

8. Сорокин Н.И., Федоров П.П., Закалюкин Р.М. Электропроводность фторидных стекол на основе PbF_2 и InF_3. *Неорг. материалы.* 1999;35(1):88–93.

9. Закалюкин Р.М., Болталин А.И., Федоров П.П., Соболев Б.П. Синтез и электропроводность многокомпонентных фторидных стекол. *Физика и химия стекла.* 1999;25(3):355–362.

10. Сорокин Н.И., Закалюкин Р.М., Глазунова Т.Ю., Болталин А.И., Федоров П.П., Соболев Б.П. Ионная проводимость фтороалюмоиндатных стекол. *Неорг. материалы.* 2000;36(8):1008–1010.

11. Faniran J.A., Patel K.S. Physicochemical studies of metal haloacetates-VI Infrared spectra of alkaline-earth metals and lead trifluoroacetates. *Spectrochimica Acta. Part A.* 1976;32(6):1351–1354. https://doi.org/10.1016/0584-8539(76)80180-8

12. Boyle T.J., Pratt III H.D., Alam T.M., Rodriquez M.A., Clem P.G. Synthesis and characterization of solvated trifluoroacetate alkaline earth derivatives. *Polyhedron*. 2007;26(17):5095–5103. https://doi.org/10.1016/j.poly.2007.07.009

13. Sheldrick G.M. SADABS. Program for scaling and correction of area detector data. Göttingen, Germany: University of Göttingen; 1997.

14. Sheldrick G.M. A short history of SHELX. *Acta Cryst.* 2008;A64(1):112–122. https://doi.org/10.1107/S0108767307043930

15. Khristov M., Peshev P., Angelova O., Petrova R., Macicek J. Preparation, Thermal Behaviour, and Structure of Calcium Trifluoroacetate Monohydrate. *Monatshefte für Chemie.* 1998;129(11):1093–1102. https://doi.org/10.1007/PL00010122

12. Boyle T.J., Pratt III H.D., Alam T.M., Rodriquez M.A., Clem P.G. Synthesis and characterization of solvated trifluoroacetate alkaline earth derivatives. *Polyhedron.* 2007;26(17):5095–5103. https://doi.org/10.1016/j.poly.2007.07.009

13. Sheldrick G.M. SADABS. Program for scaling and correction of area detector data. Göttingen, Germany: University of Göttingen.; 1997.

14. Sheldrick G.M. A short history of SHELX. *Acta Cryst.* 2008;A64(1):112–122. https://doi.org/10.1107/S0108767307043930

15. Khristov M., Peshev P., Angelova O., Petrova R., Macicek J. Preparation, Thermal Behaviour, and Structure of Calcium Trifluoroacetate Monohydrate. *Monatshefte für Chemie.* 1998;129(11):1093–1102. https://doi.org/10.1007/PL00010122

16. Rabuffetti F.A., Suescun L., Munasinghe H.N. Crystal Structure of the Low-Temperature Phase of $Mn(CF_3COO)_2·4H_2O$. *CSD Communications.* 2017. https://doi.org/10.5517/ccdc.csd.cc1nr67v

17. Dissanayake K.T., Mendoza L.M., Martin P.D., Suescun L., Rabuffetti F.A. Open-Framework Structures of Anhydrous $Sr(CF_3COO)_2$ and $Ba(CF_3COO)_2$. *Inorganic Chemistry.* 2016;55:170–176. https://doi.org/10.1021/acs.inorgchem.5b02081

18. Boyle T.J., Tafoya C.J., Scott B.L., Ziller J.W. Coordination Compounds of Strontium: Syntheses, Characterizations, and Crystal Structures of $[Sr(\mu\text{-}ONc)_2(HONc)_4]_2$ and $Sr_5(\mu_4\text{-}O)(\mu_3\text{-}ONep)_4(\mu\text{-}ONep)_4(HONep)(solv)_4$ (ONc = $O_2CCH_2CMe_3$; Nep = CH_2CMe_3; solv = Tetrahydrofuran or 1-Methyl-Imidazole). *Journal of Coordination Chemistry.* 2000;51:361–378. https://doi.org/10.1080/00958970008055141

16. Rabuffetti F.A., Suescun L., Munasinghe H.N. Crystal Structure of the Low-Temperature Phase of $Mn(CF_3COO)_2·4H_2O$. *CSD Communications.* 2017. https://doi.org/10.5517/ccdc.csd.cc1nr67v

17. Dissanayake K.T., Mendoza L.M., Martin P.D., Suescun L., Rabuffetti F.A. Open-Framework Structures of Anhydrous $Sr(CF_3COO)_2$ and $Ba(CF_3COO)_2$. *Inorganic Chemistry.* 2016;55:170–176. https://doi.org/10.1021/acs.inorgchem.5b02081

18. Boyle T.J., Tafoya C.J., Scott B.L., Ziller J.W. Coordination Compounds of Strontium: Syntheses, Characterizations, and Crystal Structures of $[Sr(\mu\text{-}ONc)_2(HONc)_4]_2$ and $Sr_5(\mu_4\text{-}O)(\mu_3\text{-}ONep)_4(\mu\text{-}ONep)_4(HONep)(solv)_4$ (ONc = $O_2CCH_2CMe_3$; Nep = CH_2CMe_3; solv = Tetrahydrofuran or 1-Methyl-Imidazole). *Journal of Coordination Chemistry.* 2000;51:361–378. https://doi.org/10.1080/00958970008055141

About the authors:

Alexandra A. Vasilyeva, Student, Faculty of Chemistry, M.V. Lomonosov Moscow State University (1-3, Leninskie Gory, GSP-1, Moscow, 119991, Russia). E-mail: 6490351@gmail.com. https://orcid.org/0000-0003-4694-2602

Tatyana Yu. Glazunova, Senior Lecturer, Department of Inorganic Chemistry, Faculty of Chemistry, M.V. Lomonosov Moscow State University (1-3, Leninskie Gory, GSP-1, Moscow, 119991, Russia). E-mail: ctpayc@mail.ru. https://orcid.org/0000-0002-7874-4179

Denis S. Tereshchenko, Research Assistant, Faculty of Chemistry, M.V. Lomonosov Moscow State University (1-3, Leninskie Gory, GSP-1, Moscow, 119991, Russia). E-mail: tereschenko_den@mail.ru. https://orcid.org/0000-0001-8972-3325.

Elmira Kh. Lermontova, Researcher, N.S. Kurnakov Institute of General and Inorganic Chemistry, Russian Academy of Sciences (31, Leninskii pr., Moscow, 119071, Russia). E-mail: Elmira.ler@gmail.com. ResearcherID N-9307-2015, https://orcid.org/0000-0003-2579-7960

Об авторах:

Васильева Александра Андреевна, студентка, химический факультет, Московский государственный университет им. М.В. Ломоносова (Россия, 119991, Москва, ГСП-1, Ленинские горы, д. 1, стр. 3). E-mail: 6490351@gmail.com. https://orcid.org/0000-0003-4694-2602

Глазунова Татьяна Юрьевна, старший преподаватель кафедры неорганической химии, химический факультет, Московский государственный университет им. М.В. Ломоносова (Россия, 119991, Москва, ГСП-1, Ленинские горы, д. 1, стр. 3). E-mail: ctpayc@mail.ru. https://orcid.org/0000-0002-7874-4179

Терещенко Денис Сергеевич, младший научный сотрудник, химический факультет, Московский государственный университет им. М.В. Ломоносова (Россия, 119991, Москва, ГСП-1, Ленинские горы, д. 1, стр. 3). E-mail: tereschenko_den@mail.ru. https://orcid.org/0000-0001-8972-3325

Лермонтова Эльмира Харисовна, научный сотрудник, Институт общей и неорганической химии им. Н.С. Курнакова Российской академии наук (Россия, 119991, Москва, Ленинский пр-т, 31). E-mail: Elmira.ler@gmail.com. ResearcherID N-9307-2015, https://orcid.org/0000-0003-2579-7960

The article was submitted: June 03, 2021; approved after reviewing: June 28, 2021; accepted for publication: July 17, 2021.

Translated from Russian into English by N. Isaeva
Edited for English language and spelling by Enago, an editing brand of Crimson Interactive Inc.

CHEMISTRY AND TECHNOLOGY OF INORGANIC MATERIALS

ХИМИЯ И ТЕХНОЛОГИЯ НЕОРГАНИЧЕСКИХ МАТЕРИАЛОВ

ISSN 2686-7575 (Online)

https://doi.org/10.32362/2410-6593-2021-16-4-363-371

UDC 548.736

RESEARCH ARTICLE

Use of a 4-circle goniometer for neutron and X-ray diffractometer in the study of single crystals

Viktor A. Sarin

MIREA – Russian Technological University, Moscow, 119454 Russia
Correspondence author, e-mail: vic.fet@yandex.ru

Abstract

Objectives. *This study described the 4-circle goniometer Syntex P1N and its possible applications in X-ray and neutron structure analysis of single crystals.*

Methods. *The 4-circle goniometer Syntex P1N, due to its high-precision mechanical characteristics and individual components from domestic equipment (sets of DRON type X-ray diffractometers), formed the basis for developing an instrument complex for X-ray and neutron-structure studies.*

Results. *The neutron diffractometer was upgraded based on the Syntex P1N goniometer. Therefore, the $^{10}BF_3$-based end neutron counter, included in the diffractometer kit, was replaced by the ^{3}He-based domestic side counter, SNM-16. Such a significant reduction in the linear dimensions of the detector allowed us to expand the range of measured angles of 2θ from 90° to 140° and increase the accuracy of the measured interplanar distances accordingly. The goniometer was adjusted relative to the primary neutron beam by placing it on a specially designed plate. Highly accurate measured parameters of the unit cell and the intensity of the reflexes were achieved by optimizing the installation geometry and the protection of the goniometer and detector. Based on the Syntex P1N goniometer, an instrument complex for X-ray diffraction studies has also been developed. Both the developed X-ray and the upgraded neutronography facilities were used to perform experiments to measure the unit cell parameters, the coordinates of atoms, and the parameters of their thermal vibrations on several crystals of domestic synthetic samples: diamond C, silicon Si, halite, or rock salt NaCl, and corundum a-Al_2O_3. An excellent correlation was achieved by comparing the data obtained with the corresponding chemical crystals' parameters and reference samples recommended by the International Union of Crystallographers.*

Conclusions. *This paper described a neutron installation and a Syntex P1N neutron diffractometer for the study of single crystals. Based on the latter, an instrument complex for X-ray diffraction studies has also been developed. Experiments on standard samples have shown a high level of accuracy in measuring the lattice parameters, the coordinates of atoms, and the parameters of their thermal vibrations on both the X-ray and neutron diffractometers.*
Keywords: *install neutron diffraction, neutron diffraction, crystal lattice parameters, a goniometer, standard samples, the coordinates of atoms, thermal vibrations*

For citation: Sarin V.A. Use of a 4-circle goniometer for neutron and X-ray diffractometer in the study of single crystals. *Tonk. Khim. Tekhnol. = Fine Chem. Technol.* 2021;16(4):363–371 (Russ., Eng.). https://doi.org/10.32362/2410-6593-2021-16-4-363-371

НАУЧНАЯ СТАТЬЯ

Использование 4-х кружного гониометра для нейтронного и рентгеновского дифрактометра при исследовании монокристаллов

В.А. Сарин

НИИ Материалов твердотельной электроники, МИРЭА – Российский технологический университет, Москва, 105275 Россия
@Автор для переписки, e-mail: vic.fet@yandex.ru

Аннотация

Цели. *Модернизировать нейтронный дифрактометр с помощью 4-х кружного гониометра «Синтекс P1N» и оценить особенности его применения при проведении рентгеноструктурного и нейтроноструктурного анализа монокристаллов с возможностью использования для этих целей аналогичных гониометров.*
Методы. *4-х кружный гониометр «Синтекс P1N» и отдельные узлы российского оборудования из комплектов рентгеновских дифрактометров типа ДРОН легли в основу разработки приборного комплекса для рентгеноструктурных и нейтроноструктурных исследований.*
Результаты. *На основе гониометра «Синтекс P1N» была выполнена модернизация нейтронного дифрактометра. Входивший в комплект дифрактометра торцевой нейтронный счетчик на основе $^{10}BF_3$ был заменен российским боковым счетчиком СНМ-16 на основе ^3He. Существенное уменьшение линейных размеров детектора позволило расширить диапазон измеряемых углов по 2θ с 90° до 140° и, соответственно, повысить точность измеряемых межплоскостных расстояний. Благодаря оптимизации геометрии установки и защиты гониометра и детектора, была достигнута высокая точность измеряемых параметров элементарной ячейки и интенсивностей рефлексов. На основе гониометра «Синтекс P1N» был также разработан приборный комплекс для рентгеноструктурных исследований. Как на разработанной рентгеновской, так и на модернизированной нейтронографической установках были осуществлены эксперименты по измерению параметров элементарной ячейки, координат атомов и параметров их тепловых колебаний на ряде кристаллов: алмаз C, кремний Si, галит NaCl, корунд α-Al_2O_3. Сравнение полученных данных с соответствующими параметрами кристаллов химических веществ и стандартных образцов, рекомендуемых Международным союзом кристаллографов, показало очень хорошее совпадение.*

Выводы. *В настоящей работе дается описание нейтронографической установки и нейтронного дифрактометра «Синтекс P1N» для исследования монокристаллов. На основе последнего разработан приборный комплекс для рентгеноструктурных исследований. Эксперименты на стандартных образцах показали высокий уровень точности измерений параметров решетки, координат атомов и параметров их тепловых колебаний как на рентгеновском, так и на нейтронном дифрактометрах.*

Ключевые слова: *нейтронографическая установка, нейтронный дифрактометр, кристалл, параметры решетки, гониометр, стандартные образцы, координаты атомов, тепловые колебания*

Для цитирования: Сарин В.А. Использование 4-х кружного гониометра для нейтронного и рентгеновского дифрактометра при исследовании монокристаллов. *Тонкие химические технологии*. 2021;16(4):363–371. https://doi.org/10.32362/2410-6593-2021-16-4-363-371

INTRODUCTION

In experimental neutron studies at pre-reactor research facilities, it is sometimes necessary to use the same equipment on different devices, including those not necessarily located in the reactor hall. Such a situation, for example, occurs during annual maintenance or prolonged reactor shutdown. The need for complex equipment usage is usually due to the uniqueness of the neutronographic installation.

EXPERIMENTAL

The neutron diffractometer Syntex P1N (*Syntex*, USA) used for carrying out neutron-structure experiments was included in the neutronography unit for the study of single crystals located on the horizontal channel of the VVR-c nuclear reactor (the water-water reactor, target, was manufactured in N.A. Dollezhal Order of Lenin Research and Design Institute of Power Engineering, Moscow, USSR) in the Branch of L.A. Karpov Research Institute of Physics and Chemistry. By design and function, the neutron diffractometer is analogous to the X-ray diffractometer.

For the diffractometer location in the reactor hall, a geometric scheme of the neutronographic installation (from the primary neutron beam to the crystal monochromator to the secondary neutron beam and finally to the sample) was implemented (Fig. 1), where the secondary neutron beam is oriented relative to the primary beam at an angle of 90° [1].

Based on the function of the diffractometer and the fact that no X-ray source was available, the X-ray detector was replaced with a neutron detector. The diffractometer's goniometer was placed in a special housing protected from the background reactor radiation. The housing walls were double-welded steel sheets, with the cavities between the walls filled with water-diluted boric acid. The selected installation geometry and the diffractometer's goniometer placement increased the area of diffraction reflections, and consequently, the experiment time, making it possible to use standard X-ray programs to clarify the diffraction reflection position in the reciprocal space.

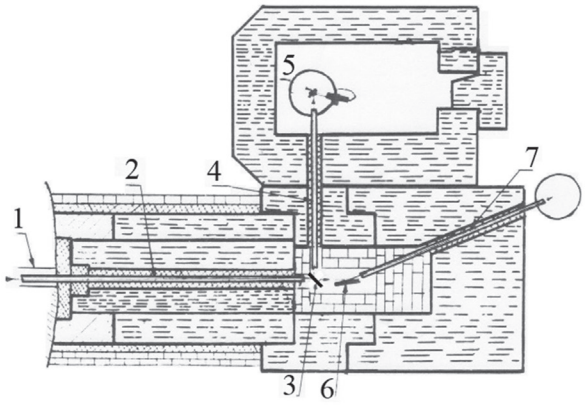

Fig. 1. Layout of the neutron diffractometric installation (cross-section at the level of the horizontal channel of the reactor) [1].
1 – reactor channel; 2, 4, 7 – collimators;
3, 6 – monochromator crystals; 5 – goniometer of the Syntex P1N diffractometer.

The reactor hall neutrons background in the "house" decreased sharply, resulting in several pulses per minute, making it possible to replace the heavy protection of the neutron detector with a thin layer of cadmium that protects the detector from gamma radiation. Later, the $^{10}BF_3$-based end neutron counter, included in the diffractometer kit, was replaced by a Russian ^3He-based side counter. The measured 2θ angles range expanded from 90° to 140° with a corrsponding increase in the accuracy of the measured interplanar distances due to significant reductions in the linear dimensions of the detector. In addition, the goniometer was aligned relative to the primary neutron beam by was placing it on a specially designed plate. In real-world applications, it is common practice to use the unit cell parameters of a crystal previously studied by X-ray diffraction in neutron diffractometers installed directly in the reactor hall with heavy detector protection from background neutrons, having a small range of measured 2θ angles, due to the low accuracy of determining interplanar distances and angles between the crystallographic axes of the crystal. However, by optimizing the installation geometry and goniometer and detector protections, accurately measured unit cell parameters and intensity of reflexes were achieved in the designed neutron diffractometer. In particular, an elementary cell's parameters were successfully determined only from neutron data by selecting a spatial group (sp. gr.), deciphering it using the "direct method," and refining the crystal structure of unknown crystals.

At the same time, to ensure the diffractometer's accuracy, it was required to understand its fundamental characteristics by benchmarking it against crystals recommended by the commission of the International Union of Crystallographers and used in international practice [2]. Such experiments on measuring the parameters of the unit cell were carried out on several crystals of Russian synthetic samples: diamond C, silicon Si, halite, or rock salt NaCl, and corundum α-Al_2O_3. A comparison between the obtained results and the unit cell parameters of crystals of chemicals and standard samples recommended by the International Union of Crystallographers showed an excellent correlation (Table 1).

In the experiments under consideration, the axes parameters and the angles between the axes were refined while studying highly symmetric crystals. In this case, the crystals were considered triclinic. Therefore, the symmetry relations were not superimposed, and the values of the parameters of the equivalent axes were not averaged. The results obtained in Table 1 and a comparison of the parameter values for each of the axes and the angles between the axes further confirmed the accuracy of determining these parameters using the goniometer of the Syntex P1N diffractometer. Furthermore, in the measurements taken from the same batch of quartz samples on the developed Syntex P1N neutron diffractometer and the same type of X-ray diffractometer, a very good agreement between the results of determining the structural parameters of single quartz crystals was achieved [4].

These results further justified with a crystallogfafic viewpoint the need to design a new X-ray instrument complex based on the Syntex P1N neutron diffractometer and consist of a goniometer, a counting rack, a control computer, and a Russian X-ray equipment taken from a DRON type diffractometer configuration and including a high-voltage power source, an X-ray tube with a molybdenum anode, and

Table 1. Comparison of the unit cell parameters of crystals measured on a neutron diffractometer Syntex P1N on synthetic samples with their standard values

Substance	*a*, Å	*b*, Å	*c*, Å	α, °	β, °	γ, °
Diamond, C Adopted in [3]	3.566(2) 3.568	3.568(2) = *a*	3.565(2) = *a*	89.98(4) 90.00	89.98(4) 90.00	89.98(4) 90.00
Silicon, Si Standard SRM* 640c	5.431(2) 5.4312(1)	5.430 (2) = *a*	5.431(2) = *a*	90.02(2) 90.00	89.99(2) 90.00	90.01(2) 90.00
Halite, NaCl Adopted in [3]	5.639(2) 5.640	5.638(2) = *a*	5.638(2) = *a*	89.98(3) 90.00	90.03(3) 90.00	90.02(3) 90.00
Corundum, α-Al_2O_3 Standard SRM 674	4.759(1) 4.7589(1)	4.760(1) = *a*	12.991(4) 12.9917(7)	90.02(2) 90.00	89.99(2) 90.00	119.99(2) 120.00

* SRM – standard reference material.

a desktop for a goniometer. Based on the experiment results performed using the Syntex P1N neutron diffractometer of this neutronographic installation and the X-ray instrument complex, an installation with a HUBER 511/424 goniometer was manufactured and put into operation (Fig. 2).

Fig. 2. HUBER 511/424 goniometer with vertical "side" detector in the "house."

To check the operability and stability of such an X-ray instrument complex, control X-ray diffraction experiments were also carried out on single crystals of Si, NaCl, SiO_2, etc. For comparison, the coordinates of atoms and the individual parameters of the thermal vibrations of the atoms, refining by least squares method, were taken. This was done as not only the value of *R*-factors obtained as a result of the refinement of the coordinates of atoms, but the individual factors of the thermal vibrations of atoms B_j characterize the accuracy of measurements of the intensities of the reflexes in the whole range of values of sinθ/λ. The results of refining the values of the isotropic thermal factors of the NaCl crystal atoms obtained in this study and their comparison with the data of [5] are shown in Table 2.

A somewhat more complex comparison was performed for single crystals of silicon and the α-SiO_2 piezoelectric. The quality of single silicon crystals considered in this study depended on the method of preparing the crystal for the experiment. Initially, the samples were taken from a batch of large crystals grown without dislocation. Cubes with rib sizes of 10 and 2 mm were then cut out of large ingots for neutron and X-ray experiments and then rolled on an air gurney to prepare spherical samples with diameters of 6 and 0.3 mm. After running in, the crystals were polished to remove the disturbed top layer. Finally, several crystals were subjected to deformation by mechanical pressure treatment under a press. In neutronographic and X-ray experiments on a Syntex P1N neutron diffractometer and the X-ray complex, the Si atom's thermal vibration parameter values depend on the method of processing the single crystal before the experiment. The corresponding data are given in Table 3. This allows us to conclude that the absolute values of thermal corrections in diffraction experiments depend on the method of crystal growth, its quality, and the types of pre-processing. Therefore, it was pretty difficult to compare the thermal vibration parameters obtained by different authors on samples with different histories.

In [4], the coordinates of quartz atoms obtained in different laboratories were compared on the different but same types of goniometers in X-ray and neutronographic experiments. However, the parameters of thermal vibrations of atoms were not considered in [4]. In this paper, an attempt was made to evaluate these parameters, given by different authors, from the point of view of the experiment's reliability on the X-ray instrument complex under consideration.

Table 2. Comparison of the parameters of individual isotropic thermal vibrations B_j for NaCl crystals obtained at $T = 296$ K in this study and [5]

Reference	Ion	*x*/*a*	*y*/*b*	*z*/*c*	B_j, Å²	R_w	N_u
This study	Na^+	0	0	0	1.77(1)	0.0088	50
This study	Cl^-	1/2	0	0	1.48(1)	0.0088	50
[5]	Na^+	0	0	0	1.689(24)	0.022	55
[5]	Cl^-	1/2	0	0	1.357(17)	0.022	55

Note: R_w is a weighted confidence factor of the specified structure; N_u is the number of independent reflexes averaged over the intensities.

Table 3. Values of the thermal parameter B_j of the Si atom depending on the type of processing of the single crystal

Si single crystal type of processing	Diffraction method	B_j, Å²	Type of extinction	R_w-factor
Running-in	Neutronographic	0.17	Becker–Coppens (primary)	0.0165
Polishing after running-in	Neutronographic	0.10	Becker–Coppens (primary)	0.0185
Deformation	X-ray	0.52	Becker–Coppens (secondary)	0.0153
Deformation	Neutronographic	0.61	Becker–Coppens (secondary)	0.0079

The α-SiO_2 crystals belong to the space group $P3_121$ (right quartz). Samples for X-ray diffraction experiments on α-SiO_2 crystals were prepared as follows. First, small cubes with an edge of 1.5–2 mm were cut from large quartz plates. Then the cubes were ground in an air gurney into spheres with a radius of ~0.15 mm to prepare samples for the X-ray experiment. The coordinates of the atoms in the α-SiO_2 crystal structure refined after the experiment were compared with the data of [6], where the average values of the coordinates are given after analyzing the results of 18 precision works on the structure of α-SiO_2 crystals.

Data on the comparison of coordinates are shown in Table 4. Plates of natural and synthetic single crystals of α-SiO_2 for further processing and preparation for the experiment were provided by B.N. Kodess, Doctor of Sciences in Physics and Mathematics.

To analyze the values and compare thermal vibrations parameters of the atoms (Table 5), data from [7, 8] were used, in which the most reliable values of thermal vibrations parameters of atoms in the α-SiO_2 crystal structure are given. The * means that the isotropic parameters, B_j were calculated in this study from the root-mean-square displacements of U_{ij} atoms provided in the publication [9]. The ** means that the values of the isotropic root-mean-square displacements of U_j atoms, provided in the publication [10], have been recalculated in this study and incorporated into the parameters of isotropic thermal vibrations B_j (Table 6).

Discrepancies in the parameters of thermal vibrations of atoms (Table 5), obtained by different authors, exceeded 3σ. Nevertheless, similar anisotropic thermal parameters of the ion oscillations were obtained for silicon as a heavier ion. The values for oxygen ions also correctly reflected the relations

Table 4. Comparing the refined coordinates of atoms in the α-SiO_2 crystal structure in this study and those recommended in [6]. Sp. gr. No. 152, $P3_121$, right quartz

Reference	*a*, Å	*c*, Å	Ion	*x*/*a*	*y*/*b*	*z*/*c*
[6]	4.9130(1)	5.4047(1)	Si^{4+}	0.5301(2)	0	1/3
[6]	4.9130(1)	5.4047(1)	O^{2-}	0.4139(5)	0.1466(4)	0.1188(3)
This study^n	4.913(1)	5.404(1)	Si^{4+}	0.5302(2)	0	1/3
This study^n	4.913(1)	5.404(1)	O^{2-}	0.4131(4)	0.1458(4)	0.1192(3)
This study^s	4.913(1)	5.404(1)	Si^{4+}	0.5304(1)	0	1/3
This study^s	4.913(1)	5.404(1)	O^{2-}	0.4131(3)	0.1463(3)	0.1189(2)

Note: The upper index "s" means the results obtained from synthetic crystals, and the upper index "n"—on natural crystals.

Table 5. Comparing the parameters of isotropic thermal vibrations of atoms in α-SiO_2 crystal structure

Reference	Si^{4+}, B_j, Å²	B_j, O^{2-}, Å²	R_w	N_a /N_u
[7][c]	0.50*	1.03*	0.020	383/369
[8][c]	0.36**	0.80**	0.023	1324/279
This study[n]	0.45(1)	0.85(4)	0.0205	1411/318
This study[s]	0.47(1)	0.88(2)	0.0180	1903/439

Note: see Note to Table 4.

Table 6. Comparing the parameters of anisotropic thermal vibrations of atoms in the structure of α-SiO_2 crystal

Reference	Ion	B11	B22	B33	B12	B13	B23
[7][c]	Si^{4+}	0.549	0.428	0.485	1/2B22	0.006	2B13
[7][c]	O^{2-}	1.219	0.873	0.892	0.693	0.238	0.362
This study[n]	Si^{4+}	0.536(9)	0.40(1)	0.439(9)	1/2B22	0.009(6)	2B13
This study[s]	O^{2-}	1.15(3)	0.66(3)	0.88(2)	0.49(2)	0.24(2)	0.12(2)

Note: see Note to Table 4.

of the thermal parameters for both ions. The crystal structure of α-SiO_2 is shown in Fig. 3. It is not trivial to compare the parameters of thermal vibrations for structures obtained by different authors; since the quality of the studied single crystals may be different, the results of studies that are sensitive to the refinement of structural parameters will be different. Such work requires high experimental accuracy and appropriate data processing programs [9]. However, the thermal parameters obtained in this work for natural and synthetic quartz were similar, which may be due to experiments performed with sufficiently high accuracy, good quality of the initial, well prepared single-crystal samples for diffraction study, as well as the same tactics of parameter refinement in the crystallographic calculations.

The close agreements between the specified structural parameters obtained in the control experiments in this work compared to the generally accepted data published in the literature have validated the developed instrument complex for conducting X-ray experiments in the future within the framework of actual problems.

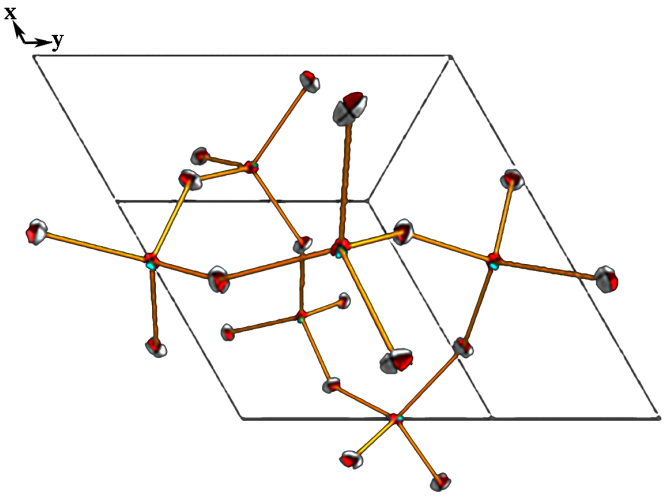

Fig. 3. The crystal structure of α-SiO_2. Viewed along the "c" axis. The image is constructed according to the data of this study[s] (Tables 3–6) using the Diamond graphic program.

CONCLUSIONS

Based on the Syntex P1N goniometer, the neutron diffractometer was upgraded, and an instrument complex for X-ray diffraction studies was developed. Experiments on standard samples have shown a high level of accuracy in measuring the lattice parameters, coordinates of atoms, and parameters of their thermal vibrations on both X-ray and neutron diffractometers.

Acknowledgments

The author is grateful to the leading engineers N.N. Bydanov and E.E. Reader and the adjuster of the instrumentation and control system V.P. Chubykin for the engineering support of all mechanical and electronic work within the framework of this project.

Author's contribution

V.A. Sarin – conducting X-ray and neutron structural experiments, processing results, and writing the text of the article.

The author declares no conflicts of interest.

REFERENCES

1. Datt I.D., Ozerov R.P., Rannev N.V. High-resolution neutron diffraction device with variable wavelength. In: *Apparatura i metody rentgenovskogo analiza = Equipment and methods of X-ray analysis*. Leningrad: Mashinostroenie; 1973. V. 12. P. 16–19 (in Russ.).

2. Prince E. (Ed.). *International Tables for Crystallography.* V. C: *Mathematical, physical and chemical tables.* Dordrecht: Springer; 2006. P. 498–504. https://it.iucr.org/Cb/, https://doi.org/10.1107/97809553602060000103

3. Gorelik S.S., Rastorguev L.N., Skakov Yu.A. *Rentgenograficheskii i elektronnoopticheskii analiz. Prilozheniya* (*X-ray and electron-optical analysis. Applications*). Moscow: Metallurgiya; 1970. 107 p. (in Russ.).

4. Kodess B.N., Sarin V.A. A Neutron Diffractometer for Determining the Structural Characteristics of Single Crystals. *Measurement Techniques.* 2015;57(11):1299–1303. https://doi.org/10.1007/s11018-015-0624-3

5. Abrahams S.C., Bernstein J.L. Accuracy of an Automatic Diffractometer. Measurement of the Sodium Chloride Structure Factors. *Acta Cryst.* 1965;18(5):926–932. https://doi.org/10.1107/S0365110X65002244

6. Baur W.H. In search of the crystal structure of low quartz. *Z. Kristallogr.* 2009;224(12):580–592. http://dx.doi.org/10.1524/zkri.2009.1219

7. Le Page Y., Calvert L.D., Gabe E.J. Parameter variation in low-quartz between 94 and 298K. *J. Phys. Chem. Solids.* 1980;41(7):721–725. https://doi.org/10.1016/0022-3697(80)90078-5

8. Glinnemann J., King H.E. Jr., Schulz H., Hahn Th., La Placa S.J., Dacol F. Crystal structures of the low-temperature quartz-type phases of SiO_2 and GeO_2 at elevated pressure. *Zeitsehrift fur Kristallographic.* 1992;198(3–4):177–212. http://doi.org/10.1524/zkri.1992.198.3-4.177

9. Tsirelson V.G. Chemical bond and thermal motion of atoms in crystals. *Itogi nauki i tekhniki. Ser. Kristallokhimiya.* 1992;27;3–269 (in Russ.).

СПИСОК ЛИТЕРАТУРЫ

1. Датт И.Д., Озеров Р.П., Раннев Н.В. Нейтронографическая установка высокого разрешения с переменной длиной волны. В сб.: *Аппаратура и методы рентгеновского анализа*. Л.: Машиностроение; 1973. Вып. 12. С. 16–19.

2. Prince E. (Ed.). *International Tables for Crystallography.* V. C: *Mathematical, physical and chemical tables.* Dordrecht: Springer; 2006. P. 498–504. https://it.iucr.org/Cb/, https://doi.org/10.1107/97809553602060000103

3. Горелик С.С., Расторгуев Л.Н., Скаков Ю.А. *Рентгенографический и электронно-оптический анализ. Приложения.* М: Металлургия; 1970. 107 с.

4. Кодесс Б.Н., Сарин В.А. Нейтронный дифрактометр для определения структурных характеристик монокристаллов. *Измерительная техника*. 2014;11:51–54.

5. Abrahams S.C., Bernstein J.L. Accuracy of an Automatic Diffractometer. Measurement of the Sodium Chloride Structure Factors. *Acta Cryst.* 1965;18(5):926–932. https://doi.org/10.1107/S0365110X65002244

6. Baur W.H. In search of the crystal structure of low quartz. *Z. Kristallogr.* 2009;224(12):580–592. http://dx.doi.org/10.1524/zkri.2009.1219

7. Le Page Y., Calvert L.D., Gabe E.J. Parameter variation in low-quartz between 94 and 298K. *J. Phys. Chem. Solids.* 1980;41(7):721–725. https://doi.org/10.1016/0022-3697(80)90078-5

8. Glinnemann J., King H.E. Jr., Schulz H., Hahn Th., La Placa S.J., Dacol F. Crystal structures of the low-temperature quartz-type phases of SiO_2 and GeO_2 at elevated pressure. *Zeitsehrift fur Kristallographic.* 1992;198(3–4):177–212. http://doi.org/10.1524/zkri.1992.198.3-4.177

9. Цирельсон В.Г. Химическая связь и тепловое движение атомов в кристаллах. *Итоги науки и техники. Сер. Кристаллохимия.* 1993;27:3–269.

About the author:

Viktor A. Sarin, Cand. Sci. (Phys.-Math.), Leading Engineer, Research Institute of Solid-State Electronics Materials, MIREA – Russian technological University (78, Vernadskogo pr., Moscow, 119454, Russia). E-mail: vic.fet@yandex.ru. Scopus Author ID 7005455400.

Об авторе:

Сарин Виктор Анатольевич, к.ф.-м.н., ведущий инженер НИИ материалов твердотельной электроники ФГБОУ ВО «МИРЭА – Российский технологический университет» (119454, Россия, Москва, пр-т Вернадского, д. 78). E-mail: vic.fet@yandex.ru. Scopus Author ID 7005455400.

The article was submitted: February 11, 2021; approved after reviewing: April 13, 2021; accepted for publication: July 27, 2021.

Translated from Russian into English by N. Isaeva
Edited for English language and spelling by Enago, an editing brand of Crimson Interactive Inc.

MIREA – Russian Technological University
78, Vernadskogo pr., Moscow, 119454, Russian Federation.
Publication date *August 31, 2021.*
Not for sale

МИРЭА – Российский технологический университет
119454, РФ, Москва, пр-кт Вернадского, д. 78.
Дата опубликования *31.08.2021.*
Не для продажи

www.finechem-mirea.ru